

DEVELOPMENT OF PORPHYRIN TWEEZER SYSTEM FOR DETERMINING
ABSOLUTE CONFIGURATION OF CHIRAL MOLECULES VIA ECCD

By

Xiaoyong Li

A DISSERTATION

Submitted to
Michigan State University
In partial fulfillment of the requirements
for the degree of

DOCTOR OF PHILOSOPHY

Chemistry

2010

ABSTRACT

DEVELOPMENT OF PORPHYRIN TWEEZER SYSTEM FOR DETERMINING ABSOLUTE CONFIGURATION OF CHIRAL MOLECULES VIA ECCD

By

Xiaoyong Li

This dissertation focuses on three parts. The first portion introduces the concept of exciton coupled circular dichroism (Chapter I) and the rationale about how we design and prepare electronically tuned porphyrin tweezers with enhanced sensitivity for chirality sensing (Chapter II). A number of porphyrin tweezers with electron deficient or electron rich phenyl rings at the *meso* positions were synthesized and evaluated for chirality sensing of chiral diamines and derivatized chiral carboxylic acids via ECCD protocol. This screening afforded TPFP tweezer which contains three pentafluorophenyl groups at 10,15,20 positions as the best candidate for chirality sensing of chiral molecules.

Chapters III-VI constitute the second portion of this dissertation describing successful applications of TPFP tweezer as a chirality reporter for a wide range of chiral molecules which are difficult subjects for conventional methods. Chirality assignment of acyclic bisfunctionalized molecules has been a tough task due to their flexible skeleton. Erythro substrates are the most difficult ones among those bisfunctionalized molecules. Chapter III describes how we solved this issue using the newly developed TPFP tweezer devoid of chemical derivatization. Upon complexation of the substrates with TPFP tweezer in solution, intense ECCD signals arose and consistent trend was obtained. The proposed binding modes provide unambiguous assignment of substrate chirality in a non-empirical

fashion. Chiral epoxy alcohols are extremely useful building blocks for organic synthesis, however there is no direct method for their absolute stereochemical assignment. In Chapter IV, the TPFP tweezer demonstrated its power again by rendering fairly strong and consistent ECCD signals upon complexation with 20 epoxy alcohols (2,3-disubstituted, 2,2-disubstituted, 2,2,3-trisubstituted and 2,3,3-trisubstituted). The elicited binding mechanism led to a rapid and reliable way for stereochemical determination of epoxy alcohols. In addition, while extending this study to long chain (3,4-, 4,5-, 5,6-, 6,7-, 7,8- substituted) epoxy alcohols, a striking odd-even effect was discovered. Chapter V centers on the chirality assignment of chiral 1,n-glycols with long alkyl chains which are also very tough molecules for chirality analysis using conventional methods. Chapter VI illustrates the natural extension of this project to the ECCD study of chiral aziridinols which also lack an efficient method for chirality determination. Free aziridinols proved to behave the same as epoxy alcohols and to our surprise some *N*-protected aziridinols are also ECCD active.

The last chapter is devoted to further demonstrate the great potential of TPFP tweezer in stereochemical determinations by challenging it with more complex molecules like steroids which contain multiple oxygenated functionalities (hydroxyl, ketone, epoxide, etc.). A number of steroids yielded strong ECCD signals. So did several substrates containing complicated bisTHF ring system. This work will attract not only organic chemists in academic labs but also pharmaceutical companies that are interested in elucidating absolute configurations of functionalities in complex molecules.

Copyright by
Xiaoyong Li
2010

Dedicated to my beloved family, for their love and support

ACKNOWLEDGEMENTS

I would like to express my deepest gratitude to my advisor, Professor Babak Borhan, for his seasoned guidance, continuing encouragement, patience, and providing me with an excellent atmosphere for my graduate research. As a great mentor, Professor Borhan taught me a lot of things beyond the textbooks and things learned from him would certainly benefit me during my whole life.

I am heartily thankful to my committee members, Professor William Wulff, Professor Gregory Baker and Professor Milton Smith, for their help and suggestions during my graduate work.

I also want to thank all the members of the Borhan group for their invaluable help and friendship during the past several years. Specially, I would like to thank Dr. Marina Tanasova, who offered great help when I started research in the lab. The academic arguments between us always drove me to think hard and critically. I am indebted to Dr. Jun Yan, who provided valuable synthetic samples for my project, and Dr. Chrysoula Vasileiou for her help in the ECCD project. I appreciate Dr. Dan Whitehead for his help and patience in proofreading my dissertation. I offer my regards and blessings to all of those who supported me in any respect during the completion of the project. Working and studying with the Borhan group members is a precious experience that I would cherish.

I want to extend my sincere thanks to Professor Patrick Walsh at University of Pennsylvania for kindly providing epoxy alcohol samples, and Professor Dennis Curran at University of Pittsburgh for kindly providing petrocortyne A samples. I also want to

acknowledge Professor William Reusch at Michigan State University for his generous gift of steroids compounds. The collaboration with them highly diversified the ECCD project.

I want to thank Dr. Maozhu Jin who is my best friend. His continued support and encouragement far from China always cheered me up.

Lastly, I want to say thanks to my mom, my dad and my brother, who continuously supported my pursuit over years. My lovely wife Keke Yang is always there cheering me up. This dissertation would not have been possible without the love and support from my family, who gave the strength to be confident, be strong and keep moving forward.

TABLE OF CONTENTS

LIST OF TABLES.....	xi
LIST OF FIGURES.....	xiii
LIST OF SCHEMES.....	xxii
KEY TO SYMBOLS AND ABBREVIATIONS.....	xxv

CHAPTER I

Chiroptical Methods for Determination of Chirality.....	1
I.1 Introduction of chirality.....	1
I.1.1 Chirality.....	1
I.1.2 Conventional methods for determination of chirality.....	4
I.2 Introduction of optical rotatory dispersion and circular dichroism.....	8
I.3 Introduction to of Exiton Coupled Circular Dichroism.....	16
I.3.1 Theoretical background of ECCD.....	16
I.3.2 The application of the ECCD method in stereochemical determination for chiral molecules.....	23
I.4 Research aims for our project using ECCD.....	29
References.....	31

CHAPTER II

Electronically Tuned Porphyrin Tweezers in ECCD Study – Development of Highly Sensitive Chirality Sensor.....	39
II.1 Design and synthesis of electronically tuned porphyrin tweezers.....	39
II.1.1 Stereochemical determination using porphyrin tweezers.....	39
II.1.2 Synthesis of electronically tuned porphyrin tweezers.....	47
II.2 ECCD study using electronically tuned porphyrin tweezers.....	67
Experimental procedures.....	72
References.....	106

CHAPTER III

Determination of Absolute Configurations for <i>erythro</i> and <i>threo</i> Diols, Amino Alcohols, and Diamines using Zn-TPFP Tweezer.....	77
III.1 Background.....	77
III.1.1 The vicinal bisfunctionalized molecules.....	77
III.1.2 Conventional methods for stereochemical determination of vicinal diols and amino alcohols.....	77

III.2	ECCD study of vicinal bisfunctionalized chiral molecules using Zn TPFP tweezer.....	81
III.2.1	Binding affinity of zinc TPFP tweezer.....	81
III.2.2	Determination of chirality for <i>erythro</i> substrates.....	92
III.2.3	Determination of chirality for <i>threo</i> substrates.....	99
III.2.4	NMR for binding studies of Zn-TPFP tweezer system.....	106
III.2.5	Conformational study of Zn-TPFP tweezer complex.....	109
III.2.6	Comparison between Zn-TPFP tweezer and Zn-TPP tweezer.....	113
III.3	ECCD study of 1,2-terminal diols and amino alcohols using Zn-TPFP tweezer	117
III.4	Future work of developing novel zinc porphyrin tweezers for ECCD Study.....	125
	Experimental procedures.....	129
	References.....	133

CHAPTER IV

Determination of Absolute Configurations for Chiral Epoxy Alcohols using

Zn-TPFP Tweezer.....	139
IV.1. Background.....	139
IV.1.1 Conventional methods for stereochemical determination of epoxy alcohols.....	139
IV.2 ECCD study of chiral epoxy alcohols using Zn TPFP tweezer.....	142
IV.2.1 Binding affinity of Zn-TPFP tweezer.....	142
IV.2.2 Determination of chirality for epoxy alcohols.....	144
IV.2.3 Synthesis of chiral epoxy alcohols.....	156
IV.2.4 ECCD study of chiral secondary epoxy alcohols.....	162
IV.2.5 ECCD study of long chain epoxy alcohols - The Odd-Even effect.....	170
IV.2.5.1 Synthesis of long chain epoxy alcohols.....	171
IV.2.5.2 Investigation of ECCD for long chain epoxy alcohols.....	175
Experimental procedures.....	184
References.....	187

CHAPTER V

Absolute Configurations of 1,n Glycols: A Non-empirical Approach for

Remote Stereochemical Determination.....	196
V.1 Background.....	196
V.2 ECCD study of 1,n-glycols.....	199
V.2.1 ECCD study of 1,n-glycols using Zn-TPFP tweezer II-25.....	199
V.2.2 ECCD study of 1,n-glycols using a reengineered tweezer.....	204
V.3 Synthesis of chiral 1,n-glycols.....	220
V.4 A case study of chirality sensing using tweezer V-12	226
Experimental procedures.....	236
References.....	247

CHAPTER VI

Determination of Absolute Configurations of Chiral Aziridines using Zn TPFP

Tweezer	252
VI.1 Background.....	252
VI.2 ECCD study of chiral aziridines.....	253
VI.2.1 ECCD study of <i>cis</i> chiral aziridinols using tweezer II-25.....	253
VI.2.2 ECCD study of <i>trans</i> chiral aziridines using tweezer II-25.....	269
Experimental procedures.....	283
References.....	286

CHAPTER VII

Elucidating the Absolute Configurations for Functionalities in Complex Molecules using TPFP Tweezer: The Case Study in Natural Products.....

VII.1 Background.....	287
VII.2 ECCD study of steroids.....	287
VII.3 ECCD study of hydroxyl tetrahydrofurans.....	302
Experimental procedures.....	306
References.....	310

LIST OF TABLES

Table I-1	Definition of exciton chirality for a binary system.....	21
Table II-1	Effect of solvent in the synthesis of TCP monolinker II-6	48
Table II-2	Effect of solvent in the synthesis of TCP tweezer II-7	51
Table II-3	ECCD data for chiral diamines and derivatized α -chiral carboxylic acids bound with tweezer II-1 and II-13	54
Table II-4	NMR analysis of α -chiral amides in Zn-TPP and Zn-TTFP tweezer complex.....	57
Table II-5	Synthetic yields for synthesis of new porphyrin tweezer.....	58
Table II-6	Solvent & catalyst effect in the synthesis of TMOP monoester II-26 ...	63
Table II-7	Effect of solvent in the synthesis of TMOP monolinker II-34	64
Table II-8	Absorptions and λ_{max} for different zinc porphyrin tweezers.....	65
Table II-9	ECCD data of chiral diamines and derivatized carboxylic acids.....	68
Table II-10	Calculated charge and energetic information for porphyrin monoesters.....	70
Table III-1	Frontier orbital energy and charges of zinc porphyrins.....	85
Table III-2	Binding affinity of ROH and RNH ₂ with III-4 and III-5	86
Table III-3	ECCD data of Zn-TPFP tweezer bound <i>erythro</i> -1,2- diols and amino alcohols.....	96
Table III-4	ECCD data of Zn-TPFP tweezer bound <i>threo</i> - 1,2- diols, amino alcohols and diamines.....	100
Table III-5	ECCD Data for enantiomers of chiral <i>threo</i> substrates in Table III-4....	103
Table III-6	Effect of concentration on ECCD using TPFP tweezer.....	107

Table III-7	Effect of concentration on ECCD using TPFP tweezer in CHCl ₃	108
Table III-8	ECCD data of Zn-TPP tweezer bound <i>erythro</i> and <i>threo</i> 1,2- diols.....	115
Table III-9	ECCD data of Zn-TPFP tweezer bound terminal 1,2- diols.....	118
Table III-10	ECCD data of Zn-TPFP tweezer bound terminal amino diols.....	124
Table IV-1	ECCD data of 2,3- epoxy alcohols bound to Zn-TPFP tweezer in hexane.....	145
Table IV-2	ECCD data of <i>trans</i> - epoxy alcohols bound to Zn-TPFP tweezer in hexane.....	176
Table V-1	ECCD data of 1,n-glycols in hexane bound with tweezer II-25	200
Table V-2	ECCD data of 1,n-glycols in hexane bound with tweezer V-12	207
Table V-S1	Crystal data and structure refinement for diol V-11	239
Table V-S2	Crystal data and structure refinement for diol V-9	241

LIST OF FIGURES

Figure I-1	Molecular chirality of different origins.....	2
Figure I-2	Structures of thalidomide and methorphan.....	4
Figure I-3	Structure of MPA mosher esters of chiral alcohol.....	5
Figure I-4	Structures of MPA mosher esters of chiral cyanohydrins.....	6
Figure I-5	Propagation of light which contains electric field and magnetic field.....	8
Figure I-6	Linearly and circularly polarized light.....	9
Figure I-7	Linear polarized light passes through chiral sample leading to right circular polarized light.....	10
Figure I-8	Positive (left) and negative (right) Cotton effect.....	12
Figure I-9	Electron redistribution upon light excitation for a transition of chiral molecule hexahelicene.....	13
Figure I-10	Schematic representation of a CD spectropolarimeter.....	6
Figure I-11	Splitting of the excited states of isolated chromophores <i>i</i> and <i>j</i> by exciton interaction.....	17
Figure I-12	The UV spectrum (A) and ECCD spectrum (B) upon through space interaction of two degenerate chromophores.....	18
Figure I-13	A qualitative view of ECCD.....	19
Figure I-14	The rationalization of ECCD spectrum for dibenzoate.....	20
Figure I-15	(+)-Absciscic acid and the exciton chirality.....	24
Figure I-16	Periplanone B and the exciton chirality after derivatization.....	24
Figure I-17	Chromophoric derivatization of amino acids for stereochemical determination.....	25
Figure I-18	Trityl ether as molecular bevel gears for assigning chirality of alcohols.....	26

Figure I-19	Determination of chirality for chiral amine through H-bonding with biphenol host.....	27
Figure I-20	Porphyrin tweezer and schematic representation.....	28
Figure II-1	Zn-Porphyrin tweezer for stereochemical determination of chiral diamine.....	40
Figure II-2	Determination of chirality for derivatized α -carboxylic acids.....	42
Figure II-3	Inoue's porphyrin tweezer for stereochemical determination.....	43
Figure II-4	Improving the sensitivity of porphyrin tweezer by tuning sterics.....	45
Figure II-5	Bulky porphyrin tweezers for ECCD study.....	46
Figure II-6	Improving the sensitivity of porphyrin tweezer by tuning electronics.....	47
Figure II-7	The reversed ECCD spectra of II-16 with different tweezers.....	55
Figure II-8	The structure of TPFP monoester II-23	59
Figure II-9	UV-vis titration of Zn-TPFP tweezer (II-25) solution (0.5 μ M in MCH) with L-lysine methyl ester (1 mM in DCM).....	66
Figure III-1	Vicinal bisfunctionalized molecules in organic synthesis and catalysis..	78
Figure III-2	Stereochemical determination of <i>threo</i> diols using dibenzoate method..	79
Figure III-3	Stereochemical determination of <i>threo</i> diols using $M_2(\text{AcO})_4$	80
Figure III-4	Stereochemical determination of <i>threo</i> diols by forming dioxolanes.....	80
Figure III-5	Stereochemical determination of terminal diols by forming cyclic borate.....	81
Figure III-6	a) Structure of Zn-TPP tweezer II-1 . b) Binding of a chiral diamine to II-1 leads to a helical disposition of the porphyrin rings dictated by the sterics at the chiral center. The resultant ECCD is used to assign the absolute stereochemistry of the chiral center. c) A 1,2-diol with two chiral centers can be envisioned as two independent chiral alcohols.....	83
Figure III-7	Electrostatic potential surface of Zn-TPFP-monoester (III-4) and Zn-TPP-monoester (III-5) based on B3LYP/6-31G(d)//PM3 calculation.....	84
Figure III-8a	Titration of Zn-TPFP ester III-4 with <i>i</i> PrNH ₂ (0-30 equiv,	

bathochromic shift from 412 nm to 424 nm) in hexane.....	87
Figure III-8b Titration of Zn-TPFP ester III-4 with <i>i</i> PrOH (0-12,000 equiv, bathochromic shift from 412 nm to 418 nm) in hexane.....	88
Figure III-9 Titration of Zn-TPFP-tweezer II-25 with amino alcohol III-12	89
Figure III-10 Two step binding of amino alcohol with Zn-TPFP tweezer.....	90
Figure III-11 Titration of Zn-TPFP tweezer II-25 with diol III-16 (0-300 equiv) in Hexane.....	92
Figure III-12 Proposed binding conformation between tweezer II-25 and <i>erythro</i> amino alcohol III-12 , yielding a positive ECCD spectrum.....	94
Figure III-13 Increasing concentration of amino alcohol III-12 leads to diminished ECCD signals.....	98
Figure III-14 Proposed conformation of the complex generated between the binding of tweezer II-25 and <i>threo</i> diol III-13 , resulting in a positive ECCD spectrum.....	102
Figure III-15 Proposed conformation of the complex generated between Zn-TPFP tweezer and <i>S,S</i> -1,2-diamino cyclohexane (III-28).....	105
Figure III-16 Front view (left) and side view (right) of the III-12 -tweezer complex...	110
Figure III-17 Front view (left) and side view (right) of the preferred conformation for III-15 -tweezer complex.....	111
Figure III-18 Front view (left) and side view (right) of the preferred conformation for III-27 -tweezer complex.....	112
Figure III-19 Energy profile of diepoxide III-27 at HF/6-31G(d) level.....	112
Figure III-20 Proposed complexation pattern between Zn-TPFP tweezer and diepoxide III-27	113
Figure III-21 ECCD spectrum of diol III-32 (200 eq.) bound with Zn-TPFP tweezer II-25 (2 μ M) in MCH.....	119
Figure III-22 ECCD spectra of diol III-29 (200 eq.) and III-35 (40 eq.) bound with Zn-TPFP tweezer II-25 (1 μ M) in MCH.....	120
Figure III-23 ECCD data of diol III-36 and III-37 bound with Zn-TPFP tweezer	

II-25 (2 μ M).....	121
Figure III-24 ECCD spectra of amino alcohol III-41 (20 eq.) bound with Zn-TPFP tweezer II-25 in MCH (1 μ M, dashed line) and in hexane (2 μ M, solid line).....	122
Figure III-25 ECCD data of III-29-ent and III-42 with tweezer II-25	123
Figure III-26 Proposed zincated porphyrin esters and tweezers for future work.....	126
Figure IV-1 Epoxy alcohols in natural products.....	139
Figure IV-2 Mnemonics for asymmetric epoxidation.....	141
Figure IV-3 (a) UV-Vis spectra change upon titration of TPFP tweezer (1 μ M in hexane) with IV-1 (10 mM in DCM) at different equivalents. (b) Non-linear least square fit of the change in absorption at 426 nm leads to the estimation of K_{assoc}	143
Figure IV-4 Complexation pattern of epoxy alcohol with porphyrin tweezer.....	147
Figure IV-5 a) Proposed complexation pattern between tweezer and epoxy alcohol. Negative ECCD spectrum was obtained for compound IV-4 ; b) enantiomeric ECCD of IV-5 and IV-5-ent (40 eq.) in hexane exhibiting complex CD.....	148
Figure IV-6 (a) ECCD of IV-5 (solid) and IV-5-ent (dashed) with 2 μ M tweezer II-25 in MCH at 0 $^{\circ}$ C; (b) ECCD spectrum of IV-5 in MCH at rt.....	150
Figure IV-7 (a) ECCD signal change at increasing concentration of IV-6 in hexane; (b) ECCD of IV-13 in hexane.....	151
Figure IV-8 Proposed complexation pattern between tweezer II-25 and <i>cis</i> -epoxy alcohol.....	152
Figure IV-9 Proposed complexation pattern between tweezer II-25 and 2,2-epoxy alcohol.....	154
Figure IV-10 The plot of %ee of IV-1 versus ECCD amplitudes of IV-1 / Zn-TPFP tweezer complex.....	155
Figure IV-11 Sharpless kinetic resolution of allylic alcohols.....	163
Figure IV-12 ECCD data of <i>trans</i> secondary epoxy alcohols (40 eq.) with tweezer II-25	

	(2 μM) in hexane at 0 $^{\circ}\text{C}$	165
Figure IV-13	Samples obtained from Professor Walsh's lab.....	165
Figure IV-14	ECCD data of <i>cis</i> secondary epoxy alcohols IV-41~IV-44 (40 eq.) with tweezer II-25 (2 μM) in hexane at 0 $^{\circ}\text{C}$	167
Figure IV-15	Proposed binding model for <i>cis</i> secondary epoxy alcohols with tweezer II-25	167
Figure IV-16	3D models for diastereomers of epoxy alcohol IV-42	168
Figure IV-17	ECCD spectra of <i>cis</i> secondary epoxy alcohols (40 eq.) with Zn-TPFP tweezer II-25 (2 μM) in hexane at 0 $^{\circ}\text{C}$	170
Figure IV-18	The odd-even effect of ECCD spectra of long chain epoxy alcohol-tweezer (II-25) complex.....	171
Figure IV-19	ECCD spectra of IV-54 (solid line) and IV-61 (dashed line) with Zn-TPFP tweezer II-25	177
Figure IV-20	Plot of 1 st Cotton effects (solid line) and 2 nd Cotton effects (dashed line) of (<i>R,R</i>)- <i>trans</i> -Ph-substituted epoxy alcohols vs. number of methylene group.....	178
Figure IV-21	UV-Vis spectra change upon titration of TPFP tweezer (1 μM in hexane) with IV-54 (graph a) and IV-61 (graph b) (10 mM in DCM) at different equivalents.....	180
Figure IV-22	UV-Vis spectra change upon titration of TPFP tweezer (1 μM in hexane) with IV-72 (graph a) and IV-69 (graph b) (10 mM in DCM) at different equivalents.....	181
Figure IV-23	The zig-zag orientation of terminal OH groups in long-chain epoxy alcohols.....	182
Figure V-1	Stereochemical determination of 1,3- <i>syn</i> diols using ECCD method.....	196
Figure V-2	Rosini's method for stereochemical determination of short chain diols..	197
Figure V-3	ECCD spectra of tweezer II-25 (2 μM in hexane) with V-6 (graph a) and V-11 (graph b) at different equivalents.....	201
Figure V-4	UV-Vis spectra change upon titration of tweezer II-25 (1 μM in hexane) with V-6 (graph a) and V-11 (graph b) at different equivalents.....	202

Figure V-5	ECCD spectra of tweezer II-25 (2 μ M in hexane) with 1,12-diol V-11 at -10 °C (graph a) and 25 °C (graph b) at different equivalents.....	203
Figure V-6	Zn-TPFP porphyrin tweezer V-12	204
Figure V-7	Utaka's porphyrin tweezer.....	204
Figure V-8	CD titration for 1,6-diol with tweezer V-12 ; consistent positive signals were obtained at 5—100 eq. of V-6	206
Figure V-9	CD titration for 1,12-diol with tweezer V-12 ; consistent positive signals were obtained at 5—100 eq. of V-11	206
Figure V-10	Side-on binding and head-on binding models.....	208
Figure V-11	Proposed compexation pattern for 1,n-diols (n = even) with tweezer V-12 ; Positive ECCD was obtained for V-6	209
Figure V-12	<i>trans</i> –all staggered conformation of V-6	210
Figure V-13	Crystal structure of 1,12-diol V-11	211
Figure V-14	<i>trans</i> all staggered conformations of 1,7-diol V-7	211
Figure V-15	3D structure of zinc TPFP porphyrin monoester.....	212
Figure V-16	Crystal structures of 1,9-diol V-9	213
Figure V-17	Proposed compexation pattern for 1,n-diols (n = odd) with tweezer V-12 ; Positive ECCD was obtained for V-7	214
Figure V-18	Front view (left) and side view (right) of the 1,6-diol-tweezer V-12 complex.....	215
Figure V-19	Front view (left) and side view (right) of the 1,7-diol-tweezer V-12 complex.....	215
Figure V-20	Front view (left) and side view (right) of the 1,12-diol-tweezer V-12 complex.....	216
Figure V-21	UV-Vis spectra change upon titration of tweezer V-12 (1 μ M in hexane) with V-6 (10 mM in DCM, graph a) and V-11 (10 mM in DCM, graph b).....	217
Figure V-22	Petrocortyne A and its isomers.....	227

Figure V-23	ECCD spectra of diol V-66 with tweezer V-12 in hexane at 0 °C.....	234
Figure V-S1	Crystal structure of diol V-11	239
Figure V-S2	Crystal structure of diol V-9	241
Figure VI-1	Proposed binding mode between tweezer II-25 and <i>cis</i> -aziridinol. Positive ECCD was obtained for <i>cis</i> - (2 <i>R</i> ,3 <i>R</i>) substrate VI-9	256
Figure VI-2	ECCD titration curves of tweezer (II-25)-aziridinol (VI-10) complex in hexane (2 µM tweezer) at 0 °C.....	258
Figure VI-3	UV-vis profile of tweezer II-25 -aziridinol VI-10 complex in hexane (1 µM tweezer).....	258
Figure VI-4	UV-vis profile of tweezer II-25 -aziridinol VI-10 complex in hexane (1 µM tweezer) at 0~1.6 eq. (graph a) and 2~200 eq. (graph b).....	259
Figure VI-5	ECCD spectra of N-benzhydryl aziridinols VI-15 and VI-17 (40 eq.) with tweezer II-25 (2 µM) in hexane at 0 °C.....	262
Figure VI-6	Crystal structure of VI-14	264
Figure VI-7	Proposed binding mode for epoxy alcohol and free aziridinol.....	265
Figure VI-8	Proposed binding model for N-benzhydryl aziridinol with tweezer; Positive ECCD spectrum was obtained for N-benzhydryl aziridinol VI-14 (40 eq.) with tweezer II-25 (2 µM) in hexane at 0 °C.....	266
Figure VI-9	ECCD of aziridinol VI-20 with tweezer II-25 (2 µM) in hexane at 0 °C.....	268
Figure VI-10	Proposed binding mode between tweezer II-25 and <i>trans</i> (2 <i>R</i> ,3 <i>S</i>) unprotected aziridinol.....	273
Figure VI-11	Positive ECCD was obtained for <i>trans</i> (2 <i>S</i> ,3 <i>R</i>) substrate VI-28 (1 eq.) with tweezer II-25 (2 µM) in hexane at 0 °C.....	273
Figure VI-12	ECCD spectra of tweezer II-25 (2 µM in hexane) with <i>trans</i> (2 <i>S</i> ,3 <i>R</i>) substrate VI-28 at 0 °C at different equivalents.....	274
Figure VI-13	ECCD spectrum of <i>trans</i> - (2 <i>R</i> ,3 <i>S</i>) amide VI-32 (5 eq.) with tweezer II-25 (2 µM) in hexane at 0 °C.....	276

Figure VI-14	ECCD spectrum of <i>trans</i> - (2 <i>S</i> ,3 <i>R</i>) amide VI-33 (20 eq.) with tweezer II-25 (2 μ M) in hexane at 0 $^{\circ}$ C.....	277
Figure VI-15	ECCD spectrum of <i>trans</i> - (2 <i>R</i> ,3 <i>S</i>) amide VI-34 (5 eq.) with tweezer II-25 (2 μ M) in hexane at 0 $^{\circ}$ C.....	277
Figure VI-16	Proposed binding mode between tweezer II-25 and <i>trans</i> (2 <i>R</i> ,3 <i>S</i>) N-MEDAM aziridine amide; Negative ECCD was obtained for <i>trans</i> (2 <i>R</i> ,3 <i>S</i>) substrate VI-35 (5 eq.) with tweezer II-25 (2 μ M) in hexane at 0 $^{\circ}$ C.....	280
Figure VII-1	ECCD spectrum of VII-1 (20 eq.) with tweezer II-25 (2 μ M) in MCH at 0 $^{\circ}$ C	288
Figure VII-2	UV-Vis spectra change upon titration of tweezer VII-25 (1 μ M in MCH) with VII-1 (10 mM in DCM).....	289
Figure VII-3	ECCD spectra of VII-2 (40 eq.) and VII-3 (40 eq.) with tweezer II-25 (2 μ M) in MCH at 0 $^{\circ}$ C.....	290
Figure VII-4	Interpretation of ECCD sign for VII-2 -tweezer (top) and VII-3 -tweezer (bottom) complex. The red arrow across the molecule indicated the perspective for looking at the relative orientation of hydroxyl groups.....	291
Figure VII-5	Interpretation of the ECCD sign for VII-1 -tweezer complex	292
Figure VII-6	Complexation of VII-4 (40 eq.) with tweezer II-25 (2 μ M) in MCH at 0 $^{\circ}$ C led to negative ECCD signal	292
Figure VII-7	Exciton chirality of steroidal diol that is derivatized with porphyrin.....	293
Figure VII-8	ECCD data of VII-5~VII-7 (40 eq.) with tweezer II-25 (2 μ M) in MCH at 0 $^{\circ}$ C. The red arrow across the molecule indicated the perspective for looking at the relative orientation of functional groups.....	294
Figure VII-9	Three possible binding modes of VII-8 with tweezer II-25 (dashed arrows indicated the functionalities bound to porphyrins). Mode c is preferred and leads to positive ECCD signal in MCH at 0 $^{\circ}$ C. The red arrow across the molecule indicated the perspective for looking at the relative orientation of functional groups.....	295
Figure VII-10(a)	ECCD data of VII-11 , VII-12 (40 eq.) with tweezer II-25 (2 μ M) in MCH at 0 $^{\circ}$ C. (b) Exciton chirality induced by complexation of VII-11 with tweezer.....	297

Figure VII-11 (a) ECCD spectra of VII-11 (40 eq.) with tweezer II-25 (2 μ M) in MCH at 0 $^{\circ}$ C; (b) UV-Vis spectra change upon titration of tweezer VII-25 (1 μ M in MCH) with VII-11 (10 mM in DCM).....	298
Figure VII-12 ECCD spectra of VII-12 (40 eq.) with tweezer II-25 (2 μ M) in MCH at 0 $^{\circ}$ C.....	299
Figure VII-13 Exciton chirality induced by complexation of VII-15 (40 eq.) with tweezer II-25 (2 μ M) in MCH at 0 $^{\circ}$ C. Positive helicity was observed.....	301
Figure VII-14 UV-Vis spectra change upon titration of tweezer VII-25 (1 μ M in MCH) with VII-20 (10 mM in DCM).....	303
Figure VII-15 ECCD data of VII-21~VII-26 (40 eq.) with tweezer II-25 (2 μ M) MCH at 0 $^{\circ}$ C.....	305

LIST OF SCHEMES

Scheme II-1	Synthesis of porphyrin monoester II-2	47
Scheme II-2	Synthesis of TCP porphyrin monolinker II-6	49
Scheme II-3	Synthesis of TCP porphyrin tweezer II-7	50
Scheme II-4	Synthesis of porphyrin monoester II-9 via direct condensation of aldehyde.....	51
Scheme II-5	Synthesis of porphyrin monoester II-9 via condensation of dipyrromethanes.....	52
Scheme II-6	Synthesis of Zn-TTFP porphyrin tweezer II-13	53
Scheme II-7	Metalation of free TPFP porphyrin tweezer II-24	60
Scheme II-8	Synthesis of TMOP monoester II-26	61
Scheme II-9	Synthesis of TMOP monoacid II-31	62
Scheme II-10	Synthesis of TMOP monolinker II-34	64
Scheme III-1	Synthesis of amino alcohol III-41	122
Scheme III-2	Formation of iminoboronic ester	132
Scheme IV-1	Synthesis of <i>trans</i> and <i>cis</i> disubstituted chiral epoxy alcohols.....	157
Scheme IV-2	Synthesis of <i>cis</i> allylic alcohol IV-24 from propargylic alcohol.....	158
Scheme IV-3	Modified HWE condition for synthesis of Z-allylic ester.....	158
Scheme IV-4	Synthesis of modified ylide IV-26	159
Scheme IV-5	Synthesis of <i>cis</i> epoxy alcohol IV-13	159
Scheme IV-6	Isomerization test of <i>cis</i> allylic alcohol IV-24	160
Scheme IV-7	Synthesis of trisubstituted epoxy alcohols.....	161
Scheme IV-8	Synthesis of 2,2-disubstituted epoxy alcohol IV-19	162

Scheme IV-9	Synthesis of 2,2-disubstituted epoxy alcohol IV-20	162
Scheme IV-10	Sharpless kinetic resolution of allylic alcohols	163
Scheme IV-11	Synthesis of epoxy alcohol IV-36 via Sharpless kinetic resolution.....	164
Scheme IV-11	Synthesis of epoxy alcohol IV-39 via Sharpless kinetic resolution.....	164
Scheme IV-12	Walsh's route for synthesis of <i>cis</i> secondary epoxy alcohols.....	168
Scheme IV-13	Synthesis of aryl substituted <i>trans</i> 3 <i>R</i> ,4 <i>R</i> -epoxy alcohol.....	172
Scheme IV-14	Synthesis of alkyl substituted <i>trans</i> 4 <i>R</i> ,5 <i>R</i> -epoxy alcohol.....	173
Scheme IV-15	Synthesis of aryl substituted <i>trans</i> 4 <i>R</i> ,5 <i>R</i> -epoxy alcohol.....	174
Scheme IV-16	Synthesis of alkyl substituted <i>trans</i> 7 <i>R</i> ,8 <i>R</i> -epoxy alcohol.....	175
Scheme V-1	Jacobsen hydrolytic kinetic resolution (HKR).....	220
Scheme V-2	Jacobsen hydrolytic kinetic resolution (HKR) for bisepoxides.....	221
Scheme V-3	The example for synthesis of even-numbered chiral diol V-6	221
Scheme V-4	The example for synthesis of odd-numbered chiral diol V-7	222
Scheme V-5	Synthesis of long chain chiral diol V-11	223
Scheme V-6	Synthesis of long chain chiral diol V-11 using bis-Grignard reagent.....	223
Scheme V-7	Synthesis of long chain chiral diol V-14 using bis-Grignard reagent.....	224
Scheme V-8	Synthesis of long chain chiral diol V-11	225
Scheme V-9	Synthesis of bis-ynone V-52 from oxidation.....	228
Scheme V-10	Synthesis of diol V-50	229
Scheme V-11	Synthesis of bis-ynone V-52	230
Scheme V-12	Synthesis of diol V-60 by CBS reduction of bis-ynone V-52	231
Scheme V-13	Literature example of CBS reduction of bis-ynone.....	231

Scheme V-14 Determination of optical purity for chiral bisynol.....	232
Scheme V-15 Reduction of bisynol V-60	233
Scheme V-16 Reduction of Petrocortyne A isomer.....	235
Scheme VI-1 Wulff catalytic asymmetric aziridination using VAPOL / VANOL.....	254
Scheme VI-2 Synthesis of free aziridinol from N-benzhydryl aziridine esters.....	255
Scheme VI-3 ECCD data of free aziridinols with tweezer II-25 (2 μ M) in hexane at 0 $^{\circ}$ C.....	255
Scheme VI-4 Binding process of tweezer II-25 with aziridinol VI-10	260
Scheme VI-5 ECCD data of free aziridinols with tweezer II-25 in hexane at 0 $^{\circ}$ C.....	261
Scheme VI-6 Reduction of N-benzhydryl aziridine esters to aziridinols.....	262
Scheme VI-7 ECCD data of N-benzhydryl aziridinols with tweezer II-25 (2 μ M) in hexane at 0 $^{\circ}$ C.....	263
Scheme VI-8 Synthesis of N-Boc-protected aziridinols and their ECCD data with tweezer II-25 (2 μ M) in hexane 0 $^{\circ}$ C.....	269
Scheme VI-9 Synthetic route for <i>trans</i> chiral aziridinol.....	270
Scheme VI-10 Synthesis of <i>trans</i> chiral aziridinol VI-28	271
Scheme VI-11 ECCD data of <i>trans</i> aziridinols (1 eq.) with tweezer II-25 (2 μ M) in hexane 0 $^{\circ}$ C	272
Scheme VI-12 Catalytic asymmetric synthesis of <i>trans</i> aziridines.....	275
Scheme VI-13 ECCD data of <i>trans</i> - (2 <i>R</i> ,3 <i>S</i>) amides (5 eq.) with tweezer II-25 (2 μ M) in hexane at 0 $^{\circ}$ C.....	278
Scheme VII-1 Synthesis of steroids VII-11~VII-13 from cholesterol.....	296
Scheme VII-2 Synthesis of steroid VII-15 from testosterone.....	301
Scheme VII-3 Synthesis of VII-20	302

KEY TO SYMBOLS AND ABBREVIATIONS

α	angle of rotation
$[\alpha]$	specific rotation
Å	angstrom
A	CD amplitude
ACN	acetonitrile
AcOH	acetic acid
Ar	aromatic
BF ₃ •Et ₂ O	boron trifluoride diethyl ether
BINOL	1,1'-Bi-2-naphthol
Bn	Benzyl
BnBr	benzylbromide
Boc	<i>tert</i> -butoxycarbonyl
CD	circular dichroism
CE	cotton effect
<i>p</i> -chloranil	tetrachloro-1,4-benzoquinone
cm	centimeter
d	doublet
DCM	dichloromethane
DDQ	2,3-dichloro-5,6-dicyano-1,4-benzoquinone
DET	diethyl tartrate
DFT	density functional theory

DIBALH	diisobutylaluminum hydride
DIPT	diisopropyl tartrate
DMAP	4-diaminopyridine
DMF	N,N-dimethylformamide
DNA	deoxyribonucleic acid
e.e.	enantiomeric excess
Et ₃ N	triethylamine
EtOH	ethanol
ε	molar absorption coefficient
ECCD	Exciton Coupled Circular Dichroism
EDCI	N-(3-Dimethylaminopropyl)-N'-ethyl-carbodiimide
ESI	electrospray ionization
EtMgBr	ethyl magnesium bromide
Et ₂ O	diethyl ether
EtOAc	ethyl acetate
Eq.	equivalents
FAB	fast atom bombardment
g	gram(s)
h	hour(s)
HKR	hydrolytic kinetic resolution
HPLC	high pressure liquid chromatography
HRMS	high resolution mass spectrometry
Hz	hertz

<i>i</i> Pr	isopropyl
IR	infrared
<i>J</i>	NMR coupling constant
K ₂ CO ₃	potassium carbonate
LDA	lithium diisopropylamine
LAH	lithium aluminum hydride
<i>m</i>	magnetic dipole transition moment
m	multiplet
mCPBA	3-chloroperoxybenzoic acid
MeOH	methanol
min	minute
mg	milligram
MHz	megahertz
M	molar
μM	micromolar
MS	mass spectrometry
<i>m</i> / <i>z</i>	mass to charge ratio
<i>n</i>	refractive index
NaBH ₄	sodium borohydride
NaHMDS	sodium hexamethyldisilylazide
NaOH	sodium hydroxide
NaH	sodium hydride
nm	nanometer

NMR	nuclear magnetic resonance
ORD	optical rotatory dispersion
PCC	pyridinium chlorochromate
Ph	phenyl
$^n\text{PrNH}_2$	propyl amine
q	quartet
s	singlet
R	rotational strength
Rt	room temperature
t	triple
PMB	<i>para</i> -methoxybenzyl
SAD	sharpless asymmetric epoxidation
SAE	sharpless asymmetric dihydroxylation
TBAF	tetrabutylammonium fluoride
TBS	<i>t</i> -butyldimethylsilyl
TEEDA	Tetraethyl ethylenediamine
TES	triethylsilyl
TFA	trifluoroacetic acid
THF	tetrahydrofuran
UV-vis	ultraviolet-visible spectroscopy
Zn-TPP	zinc tetraphenylporphyrin
Zn-TPP-tweezer	zinc 5-(4-carboxyphenyl)-10,15,20-triphenylporphyrin tweezer
Zn(OAc) ₂	zinc acetate

Chapter I

Chiroptical Methods for Determination of Chirality

I.1 Introduction of Chirality

I.1.1 Chirality

Chirality as a fundamental property of molecules is central to the existence and perpetuation of life. Since the word ‘chirality’ was introduced by Lord Kelvin 125 years ago, the phenomenon of chirality has been intriguing generations of scientists in trying to understand its impact on chemistry and life.

Chirality refers to non-superimposable mirror images and originates from the Greek word *cheir*, meaning “hand”.¹ Actually, our two hands are one of the best examples for chirality in nature. In the molecular level, chirality refers to the asymmetric disposition of atoms in a molecule which lead to non-superimposable mirror images of the molecule skeleton. In terms of generating molecular chirality several different scenarios are possible (Figure I-1), but they essentially follow one rule: lacking the plane of symmetry.

A classic example of point chirality was shown in Figure I-1A in which a tetrahedral carbon is attached with four different substituents leading to a chiral carbon center in the molecule. The letters *R* (from Latin “*rectus*”) and *S* (from Latin “*sinister*”) are used to indicate the configuration (arrangement of groups) on the chiral center, based on priorities set in place by Cahn, Ingold and Prelog.² A different example comes from allene and was shown in Figure I-1B.³ This molecule is not

planar since the two π bonds are perpendicular to each other causing the molecule to lack any plane of symmetry when both sides are unsymmetrically substituted. In this case no chiral center exists, but the whole molecule is still chiral and is referred as axial chirality.

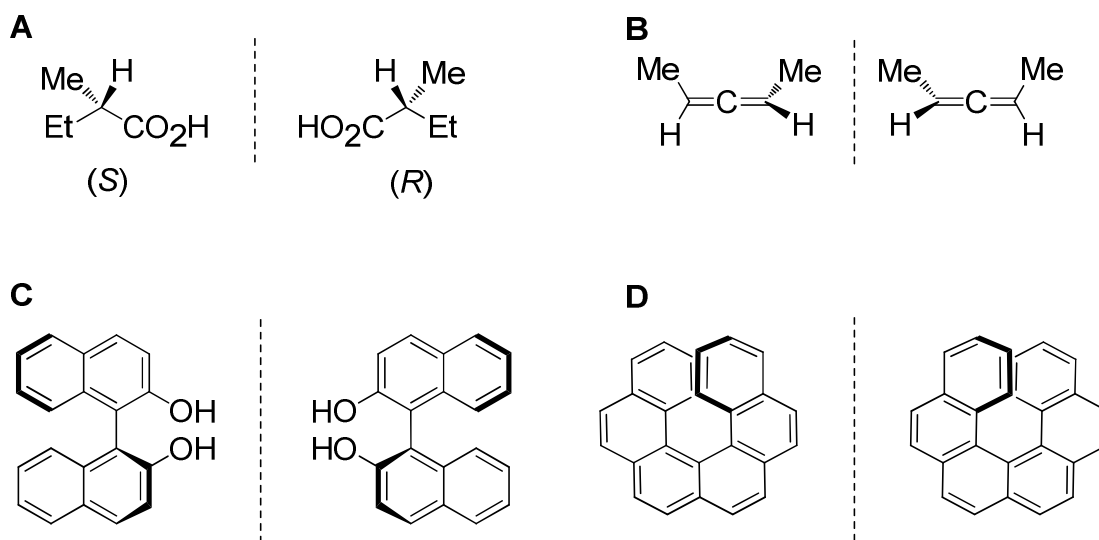


Figure I-1. Molecular chirality of different origins.

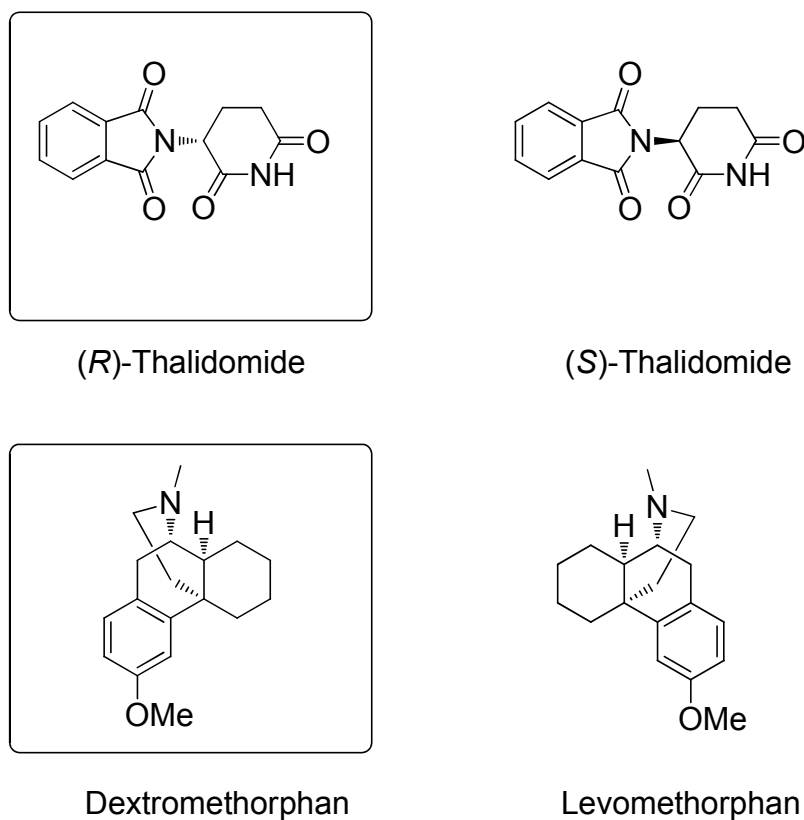
Figure I-2C reveals the structure of binaphthol molecule which is a representative example for axial chirality. The presence of large aryl group each side of the C-C single bond restricts the free rotation around the single bond and the steric hindrance between *ortho*-substituents further prevents bond rotation “locking” the molecule into a chiral conformation. Consequently, two enantiomers are produced, which are referred to as atropisomers since the restriction of rotation is the source of geometric isomerism (atropisomerism). The structures shown in Figure I-21D demonstrate another scenario of molecular chirality which is induced by helical arrangement of molecular skeleton. Hexahelicene contains six continuously fused benzene rings but it is not planar. The skeleton of this molecule traces a helix when one side of the

molecule lies above the other due to steric repulsion of the terminal benzene rings. The defined helix can be either right-handed, (+)-hexahelicene, or left-handed, (-)-hexahelicene and, therefore, non-superimposable on its mirror image.^{4, 5} This molecule is also chiral though it does not have any asymmetric carbons. DNA double helix is another classical example of molecular helicity.

The human body is composed of large amount of chiral molecules and they are present exclusively in one chiral form. For instance, all amino acids in our body are left handed (*L*, stems from Greek word *levorotatory*) and all sugars in our body are right handed (*D*, stems from Greek word *dextrorotatory*). This homochirality not only exists in human body but also virtually in all living organisms. The origin of this homochirality of life is still under debate and is an interesting field being actively pursued.⁶⁻⁹

Structurally speaking, both enantiomers of a chiral molecule share the same feature. However, their chemical, physical as well as biological properties could be significantly different. One historical example addressing the dramatically different property of enantiomers is the drug thalidomide (Figure I-2). In late 1950s, the racemic thalidomide was commercialized as a wonder drug to cure colds, coughs and particularly the morning sickness of pregnant women. Unfortunately, it was soon found out that though (*R*)-thalidomide demonstrated the desired curing effect, (*S*)-thalidomide is highly teratogenic causing birth defect for many babies. This tragedy rang the bell for pharmaceutical industry revealing the great importance of molecular chirality in drug activity.^{10, 11} Many other examples are also known.

Dextromethorphan is a cough suppressant while its enantiomer, levomethorphan is narcotic. Today, drug companies are making great effort to provide enantiomerically pure drugs for better efficiency and safety.



. **Figure I-2.** Structures of thalidomide and methorphan.

Determination of molecular chirality is important for pharmaceutical industry. It is self-evident that organic chemists in academic labs especially those working on natural product synthesis or synthetic methodology also require reliable and rapid methods for stereochemical determination of small molecules.

I.1.2 Conventional methods for determination of chirality

¹H NMR based Mosher method and its revised versions have been the most

extensively applied method for configurational assignment of a variety of chiral compounds, majorly the chiral alcohols and amines.¹²⁻¹⁸ This method involves derivatization of hydroxyl or amino group of the interested compound with both enantiomers of chiral aromatic acid like α -methoxy- α -(trifluoromethyl) phenylacetic acid (MTPA) or α -methoxyphenylacetic acid (MPA) to form two diastereomers.¹⁷ The ^1H NMR spectra of the two diastereomers are compared and the different shielding / deshielding effect from the introduced aryl ring upon the neighboring protons in the chiral center are measured ($\Delta\delta^{R,S}$). This difference is then used to elucidate the absolute stereochemistry. Riguera and coworkers have worked to extend the scope of Mosher ester method and have achieved considerable advances enabling the stereochemical determination of chiral diols and amino alcohols.^{16, 19-23}

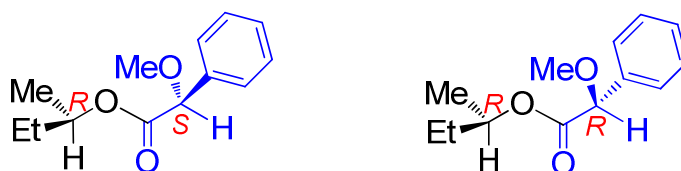


Figure I-3. Structure of MPA Mosher esters of chiral alcohol. (For interpretation of the references to color in this and all other figures, the reader is referred to the electronic version of this dissertation.)

The success of this method relies on an important premise, namely the dominant conformation in NMR experiment should be as the one shown in Figure I-3. The carbinol hydrogen of chiral alcohol, the ester bond, and the carbinol hydrogen of chiral acid should lie in the same plane. In most cases, the premise would hold since

that is usually the most stable conformation. However, when the chiral alcohol resides in a sterically demanding cyclic skeleton the preference of this conformation may change and consequently the NMR analysis is not reliable.^{24, 25} In the latest study by Riguera regarding the application of Mosher ester method for stereochemical determination of chiral ketone cyanohydrins, the presence of highly polar –CN group also led to the preference for a different conformation (Figure I-4).²⁶ In addition, the requirement for chemical derivatization and milligrams of samples is also a major limitation of the Mosher method.

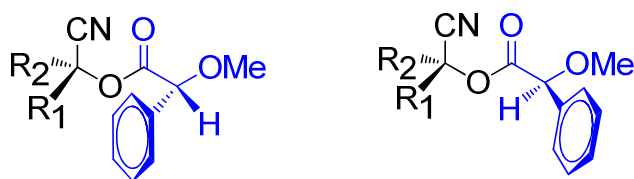


Figure I-4. Structures of MPA Mosher esters of chiral cyanohydrins.

Chiral shift reagents containing Lanthanides are also widely used for chirality sensing via NMR spectroscopy.²⁷⁻²⁹ These chiral reagents complex with chiral substrates and form diastereomeric complexes which could be discriminated by ¹H NMR. However, it requires the use of expensive chiral reagents and line-broadening phenomenon could be a serious problem. This method does not always guaranty well-resolved NMR spectra, thus its application is restricted when high sensitivity is desired.

X-ray crystallography could provide full stereochemical analysis of chiral substrates and is the most unambiguous method for absolute stereochemical determination. However, several shortcomings should be addressed. First,

crystallization is a must. For compounds that can be crystallized, obtaining a high quality single crystal for X-ray analysis can be a challenging task requiring days or weeks of effort. Secondly, due to intrinsic limitation of this technique, in most cases X-ray crystallography can only give *relative* stereochemistry unless there is a heavy atom (Br, I, heavy metal ion, etc.) or a chiral center with known chirality which enables the assignment of absolute configuration for the whole molecule. Finally, even though only a single crystal is required for X-ray analysis, people often need milligrams of substrate for crystal growth.

Measuring optical rotation is also a frequently used empirical method for chirality assignment.³⁰⁻³³ By comparing the specific optical rotation (α_D) measured from polarimeter with the literature reported value for exactly the same compound, one would know the stereochemistry of synthesized compound. Undoubtedly, this method only works for known compounds. Measuring the α_D of a new molecule will tell nothing about its configuration.³⁰⁻³³

In past decades, chiroptical methods based on circular dichroism (CD) spectroscopy have been developed and attracted active attention. Vibrational CD (VCD) and electronic CD (ECD) are the two main categories used for conformational determination. VCD was pioneered in the 1970s by Stephens and Nafie.³⁴ It features the comparison of experimental VCD spectrum of one enantiomer with calculated VCD spectra of both enantiomers.^{35, 36} Since VCD spectra of both enantiomers are opposite, this comparison would reveal the absolute stereochemistry of the test compound. One big advantage of this method is that unlike electronic

circular dichroism it does not require the presence of a chromophore in the molecules. The accuracy of this method relies on the high level quantum chemical computation which is not preferred for large molecules.

The electronic circular dichroism has emerged a powerful tool for elucidating stereochemistry and its principle concepts will be detailed in the following section.

I.2 Introduction to Optical Rotatory Dispersion and Circular Dichroism

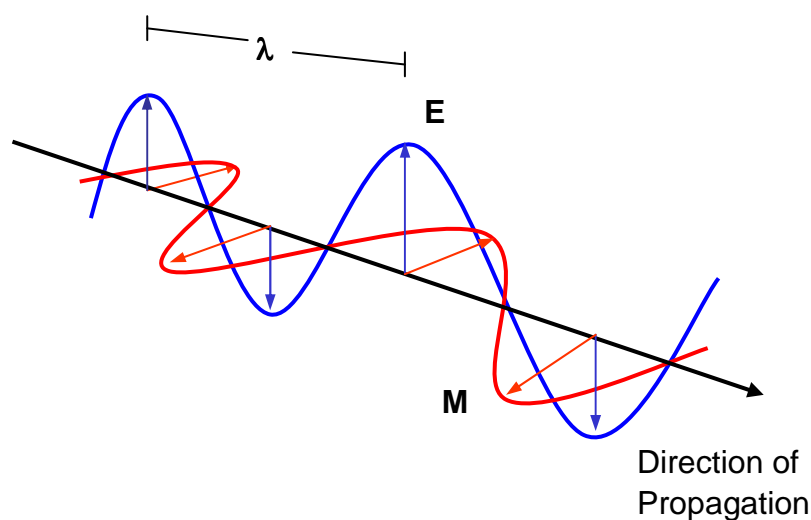


Figure I-5. Propagation of light which contains electric field and magnetic field.

Optical Rotatory Dispersion and Circular Dichroism are two major methods for enantioselective discrimination making use of light and benefiting from the different chiroptical properties of enantiomers. Light consists of both an electric field E and a magnetic field M , which oscillate perpendicular to each other and to the direction of propagation of light forming a right handed coordinate system as depicted in Figure I-5.

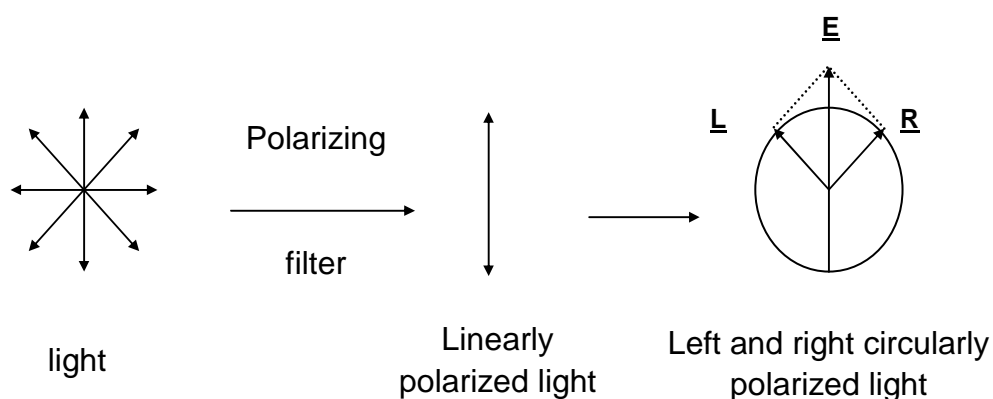


Figure I-6. Linearly and circularly polarized light.

Ordinary light consists of light waves propagating in all directions and shows no preference for a particular plane. Consequently it is unpolarized. However, when the unpolarized light passes through a polarizing filter, only a fraction of light waves whose oscillation parallel to the direction of the filter pass through. The light thus passing through is defined as linearly polarized light since it is aligned in only one oscillation plan. In the specific direction the linearly polarized light oscillates, the electric field (E) remains constant in magnitude, but traces out a helix as a function of time.³⁷ It is composed of two circularly polarized light beams (Figure I-6): a left circular component (L) and a right circular component (R). When both circularly polarized light components pass through an achiral or racemic media, the velocity and absorbance of each circularly polarized light is equally affected. As such, the polarization of light is still the same and the light still oscillates in the same specific plane.

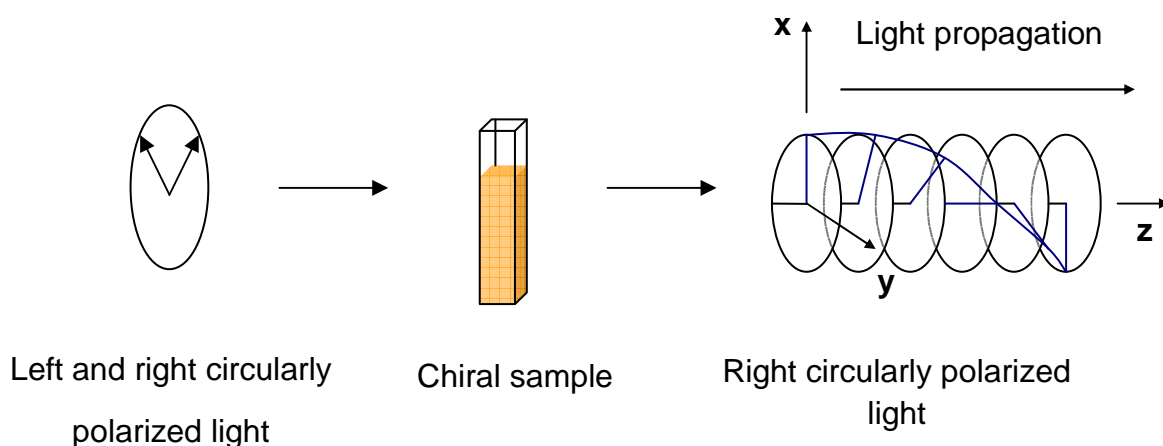


Figure I-7. Linear polarized light passes through chiral sample leading to right circular polarized light.

If the medium is optically active, after the light passes through, the velocity and absorbance of one of the circularly polarized components is changed to a different extent (Figure I-7), leading to a Cotton effect (CE, in honor of French physicist Aimé Cotton, who observed both ORD and CD phenomena). The difference in velocity of the left and right components of circularly polarized light results in ORD. It can be correlated to the differences in the respective refractive indices as shown in equation I-1 where n_L and n_R are the refractive indices for left and right circularly polarized light respectively.³⁸

$$\Delta n = n_L - n_R \neq 0 \quad (\text{I-1})$$

Since the left and right circularly polarized light travels through the optically active medium at different velocities, the two components are out of phase, and the resultant vector will progress as a trace of an ellipse instead of circle and also it will be rotated

by an angle α relative to the original plane of polarization. The relation between α and the difference in refractive indices can be quantitatively described by equation I-2: Where α is the angle of rotation in degrees, n_L and n_R are the refractive indices, l is the path length in decimeters and λ_0 is the wavelength of the light

$$\alpha = (n_L - n_R) 1800l / \lambda_0 \quad (\text{I-2})$$

Specific rotation $[\alpha]$ is commonly determined in ORD spectroscopy and can be derived from the observed angle of rotation α using following equation I-3:

$$[\alpha] = \alpha / cl \quad (\text{I-3})$$

Where α is the angle of rotation (degree units), c is the concentration of the sample (g mL^{-1}), and l is the path length (decimeters).

Since ORD is only based on the difference in the refractive indices, and all chiral molecules exhibit a molecular refraction at almost any wavelength of irradiation, In theory, ORD can be detected over all wavelengths leading to a distribution of optical rotations versus wavelengths. The sodium D-line (589 nm) is commonly used to detect and quantify the optical activity.

As discussed before, both the velocity and the absorbance of light will be altered differently while the circularly polarized lights pass through an optically active medium. The ORD takes advantage of the difference in velocity and determines the specific rotation which is characteristic for the chiral medium. Accordingly, the difference in absorbance of the left and right circularly polarized light results in the development of circular dichroism (CD) in which the absorption change of circular component is used to describe the optical activity of chiral medium. The difference

in molar absorptivity of the left (ϵ_L) and right (ϵ_R) circularly polarized light, $\Delta\epsilon$, is defined as circular dichroism (equation I-4).³⁸

$$\Delta\epsilon = \epsilon_L - \epsilon_R \neq 0 \quad (\text{I-4})$$

Obviously, CD is an absorptive process and hence it only occurs in the vicinity of an absorption band. As a consequence, chiral compounds need to contain a chromophore in order for a CD spectrum to be observed. In terms of shape and appearance, the CD curve shares the same feature as that of the ordinary UV-vis absorption curve. But, there is an important difference between these two. The UV-vis curves can only be positive while the CD curves may be positive or negative as shown in Figure I-8.

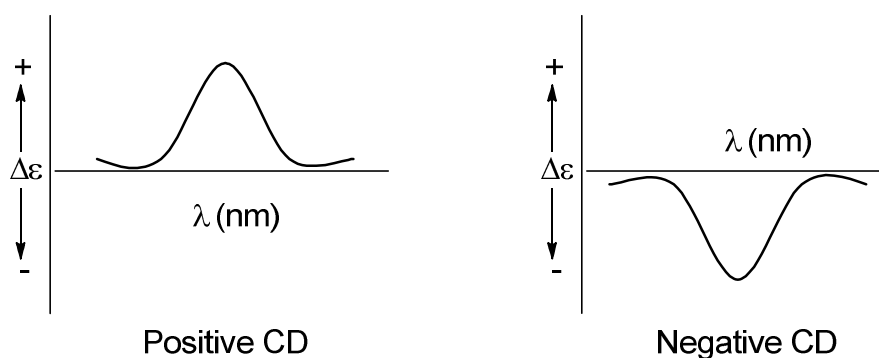


Figure I-8. Positive (left) and negative (right) Cotton effect.

CD and ORD are both manifestations of the same phenomenon and the molar amplitude A of an ORD can be approximately related to the intensity of the CD curve, $\Delta\epsilon$, by equation I-5:³⁹

$$A \approx 40.28 \Delta\epsilon \quad (\text{I-5})$$

When a molecule absorbs light, an electron is promoted from its ground state to an excited state. This is a charge polarization process creating a momentary dipole which is referred to as the electric dipole transition moment and denoted by the vector μ . In a chiral molecule, the electron would redistribute in a *helical* manner generating a magnetic field. The strength and direction of this magnetic field can be described by the magnetic transition dipole moment denoted by the vector m .

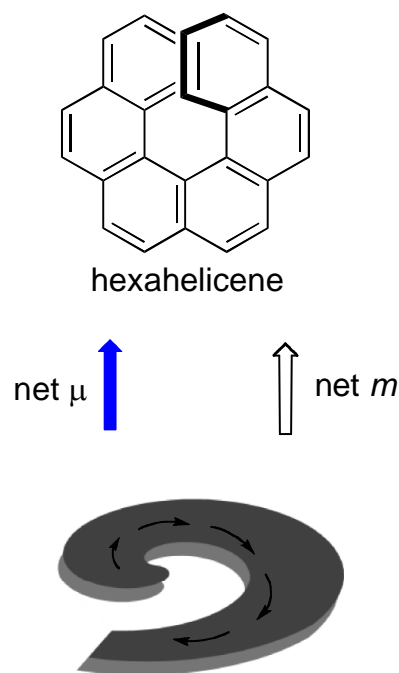


Figure I-9. Electron redistribution upon light excitation for a transition of chiral molecule hexahelicene.

The direction of magnetic transition moment (m) follows the “right hand rule” for the rotation of the charge (circular electric current). Namely, the direction of the magnetic transition dipole moment is defined by direction of the outstretched thumb when the right hand fingers are curved in the direction of electron flow.^{40, 41} Hexahelicene provides a good example for demonstrating the “right hand rule” as well as the interaction of electric and magnetic dipole moments (Figure I-9).

The physical origin of CD can be considered as the helical redistribution of electrons within chiral molecules upon light irradiation. The helical flow of electrons interacts with the left and right circularly polarized light to a different extent

manifested as different absorption and leads to the Cotton effect. Rotational strength, R , is employed to depict the sign and strength of a CD Cotton effect (CE). This theoretical parameter is derived by the scalar product of the electric and magnetic transition moments (equation I-6):¹

$$R = \mu \bullet m = |\mu| |m| \cos \beta \quad (\text{I-6})$$

Where μ and m are the electric and magnetic transition dipole moments, respectively, and β is the angle between the two transition moments. The sign of the CE is positive when the angle is acute ($0^\circ \leq \beta < 90^\circ$) or, in the limiting case, parallel, and it is negative when the angle is obtuse ($90^\circ < \beta \leq 180^\circ$) or, in the limiting case, antiparallel. The right hand rule can be used to determine the direction of magnetic dipole transition moment (m). Dextrorotation results when $R > 0$, together with positive CD, and levorotation is generated when $R < 0$, together with negative CD curve. There is no CE when the electric and magnetic transition dipole moments are perpendicular to each other.

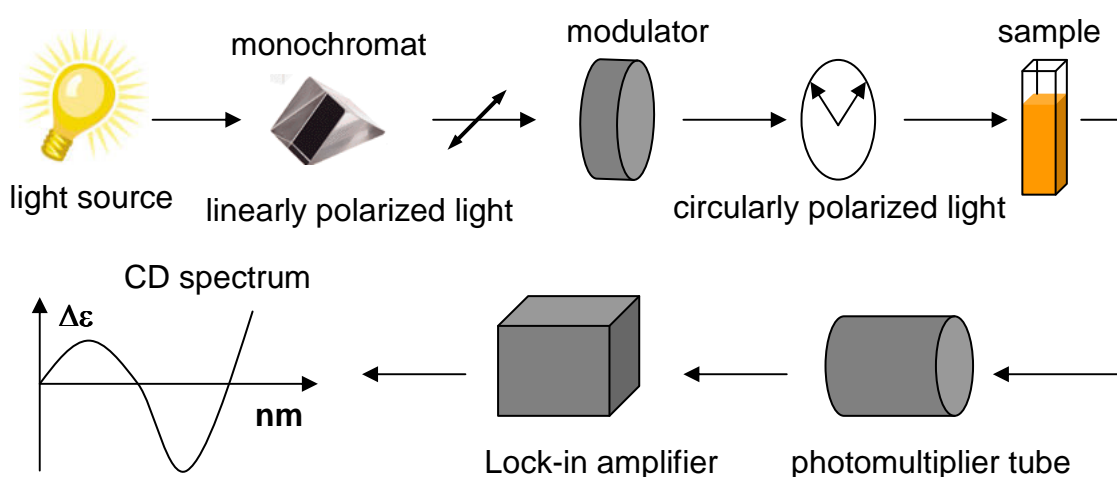


Figure I-10. Schematic representation of a CD spectropolarimeter.

Figure I-10 illustrates the typical composition of CD spectropolarimeter. A Xenon lamp is typically used as the source of light. This light passes through a monochromator consisting of a series of crystal prisms to produce linearly polarized light. In the CD spectropolarimeter, the optical system comprises of two monochromators (a double monochromator), which helps in reducing stray light. The linearly polarized light is then modulated into left and right circularly polarized light. The modulator consists of a thin crystalline plate known as a wave plate. When linearly polarized light is incident on a wave plate at 45° , the light is divided into two equal electric field components, one of which is retarded by a quarter wavelength by the plate. This throws the two components 90° out of phase with each other such that upon emerging, one is always maximum, while the other is always zero and vice versa. The effect is to produce circularly polarized light. The 90° phase shift is produced by a precise thickness d of the birefringent crystal, which, because of the 90° shift, is referred to as a quarter wave plate. This light then passes through the sample chamber. The light transmitted through the sample is measured by a photomultiplier tube, which produces a current whose magnitude depends on the number of incident photons. This current is then detected by a lock-in amplifier and recorded.

CD spectropolarimeters usually measure the differential absorbance (ΔA) between the left and right circularly polarized light, which can then be converted to $\Delta \epsilon$ based on the Beer-Lambert law (equation I-7).¹

$$\Delta A = \Delta \epsilon c l \quad (1-7)$$

where ΔA is the difference in absorbance and $\Delta \epsilon$ is the difference in molar extinction coefficients ($M^{-1}L^{-1}$). Since Optical Rotatory Dispersion (ORD) and Circular Dichroism (CD) are only detected when the system contains chiral substances, they can be used to evaluate the optical activity of the substance examined. However, ORD and CD by themselves do not enable the direct determination of absolute configuration for chiral substrates. To solve this issue, extensive theoretical studies have been conducted to provide empirical and semiempirical rules, which allow the computation of ORD or CD for small molecules with specific stereochemistry. Comparison of the calculated data with experimental ones would permit the prediction of configuration for substrate molecules. However, the empirical nature of these approaches is a big limitation and its accuracy also heavily relies on the careful selection of different computational methods which quite often is a tough task especially for complex molecules.

I.3 Introduction to Exciton Coupled Circular Dichroism

I.3.1 Theoretical background of ECCD

The ECCD method is a non-empirical approach to establish the absolute configuration of chiral compounds pioneered by Harada and Nakanishi.^{39, 42} It is based on the through space exciton coupling between two or more chirally oriented non-conjugated chromophores. The coupling of the chromophores' electric transition dipole moments leads to the observed bisignate CD spectrum, which can be used for the nonempirical determination of their orientation.

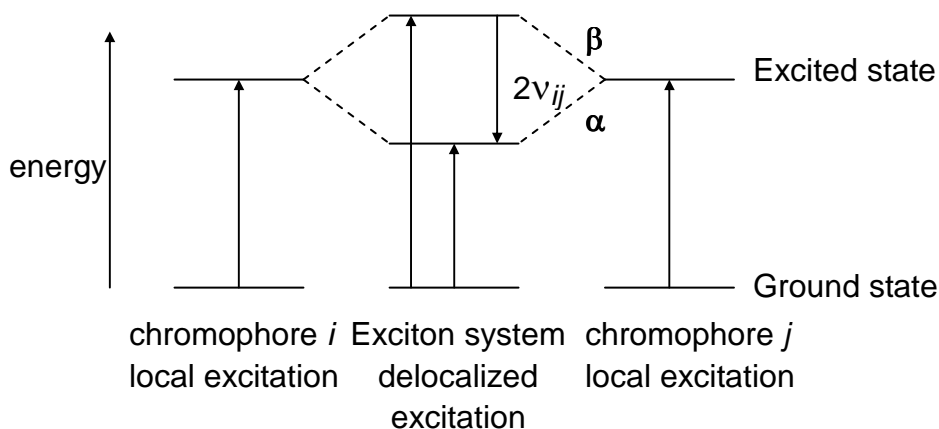


Figure I-11. Splitting of the excited states of isolated chromophores *i* and *j* by exciton interaction. The energy gap $2\nu_{ij}$ is called Davydov splitting.

The ECCD theory is described as follows. After the excitation by light, the through space interaction causes splitting of the energy level of the excited state (exciton) into two states (α and β) by resonance interaction of the local excitations (Figure I-11). The transitions from the ground state to the energetically different α state and β state give rise to the two different UV-vis absorbances. The energy gap between the energy levels of the two states (α and β) corresponds to the difference in the λ_{\max} of the two UV-vis peaks. This difference is referred to as the Davydov splitting and is designated as $2\nu_{ij}$.³⁹ In case of small energy gap, the two separate peaks mostly overlap into one in the spectrum.

In a chiral molecule containing two chromophores, the excitation of electrons results in the interaction between the electric dipole transition moments (edtm) of each chromophore in a helical fashion. Depending on whether the electric dipole transition moments are in phase (symmetric) or out of phase (anti symmetric), a

Cotton effect of different sign is produced, and a CD couplet with two peaks (bisignate curve) is expected. Since the two Cotton effects are out of phase, the Davydov splitting is usually large enough to be captured in the ECCD spectrum (Figure I-12).³⁹ This phenomenon is defined as Exciton Coupled Circular Dichroism. A classical example illustrating the application of ECCD theory in absolute stereochemical determination is shown in Figure I-13 by examining the exciton coupling between two benzoate chromophores of steroidal bisbenzoate derived from cyclohexanediol moiety.^{39, 40}

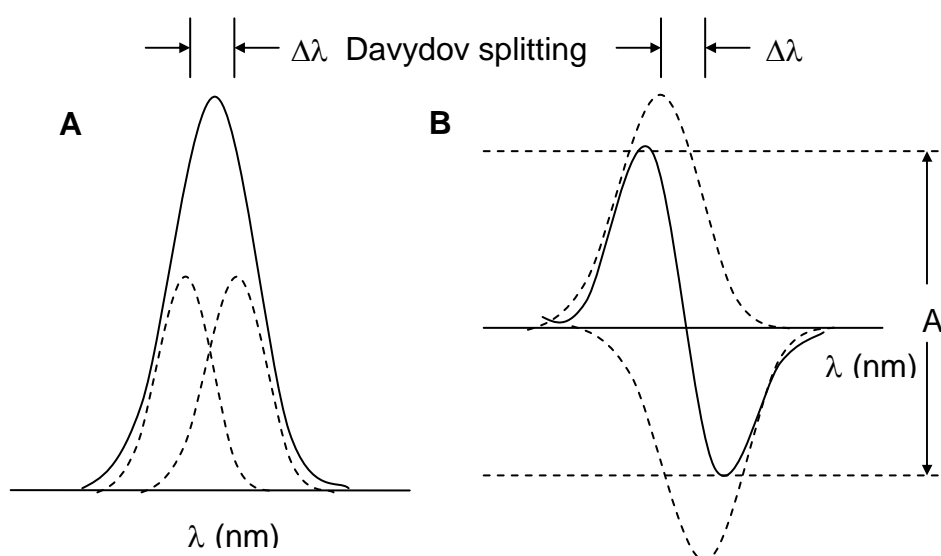


Figure I-12. The UV spectrum (A) and ECCD spectrum (B) upon through space interaction of two degenerate chromophores. The two observed Cotton effects are shown using dashed lines, while the summation curves are in solid lines.

The strong UV-Vis absorption band of benzoate esters at around 230 nm is attributed to $\pi \rightarrow \pi^*$ transition involving the benzene ring and the ester group. The

large electric dipole transition moment μ of each benzoate group oscillates along with the long axis of the molecule, almost parallel to the direction of the C-O bond (Figure I-13A). Determination of absolute configuration means determination of the absolute sense of chirality between the C(2)-O and C(3)-O bonds, by looking down the C-C bonds from front to back, the relative orientation of the two benzoate groups is clockwise corresponding to positive chirality. The absolute sense of twist is the same regardless of whether it is viewed from C(3) to C(2) or vice versa.

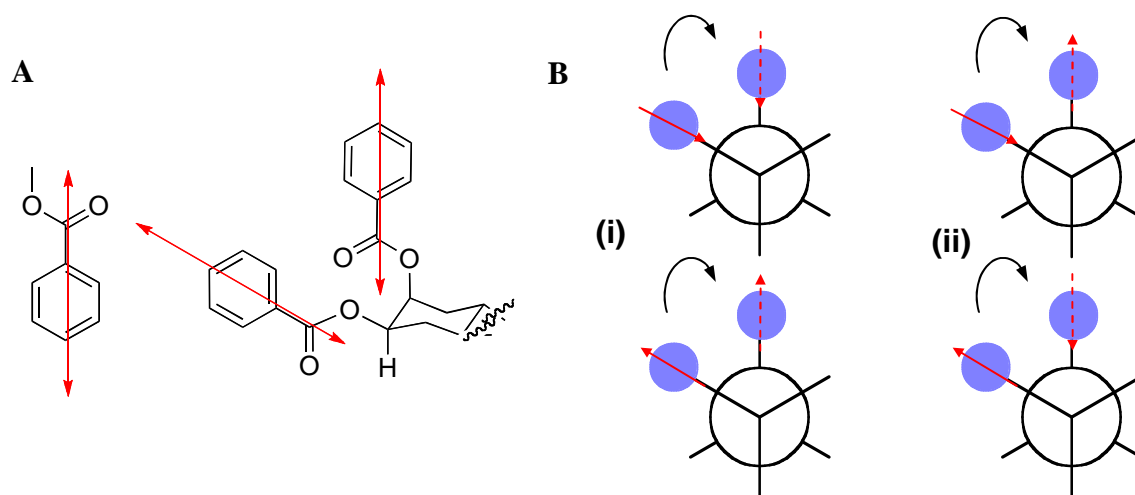


Figure I-13. A qualitative view of ECCD. **A.** Structures of steroidal dibenzoate. edtm's are shown in red; **B.** Possible in phase (i) and out of phase (ii) interactions of the edtm's of the degenerate chromophores (shown in blue).

The individual edtm μ of an electric transition, for each chromophore, couples to the other in phase (symmetric) or out of phase (asymmetric), Figure I-13 i and ii respectively. In the case i, where the two electric transition dipole moments couple in phase, the “total” electric transition dipole moments are oriented along the chromophoric C2 axis, and in case B, where they couple out of phase, the “total”

electric transition moments are oriented perpendicular to the chromophoric C2 axis. The helix associated with the charge rotation generated from the transition can be visualized by placing the partial edtm in a cylinder, aligned along the axis of the “total” edtm, μ . As shown, in Figure I-14-i, the symmetric coupling results in a counterclockwise helical movement and, therefore, according to the right hand rule, the magnetic transition dipole moment (m) is anti-parallel to μ . As expected, the out of phase interaction causes the opposite effect, leading to parallel m and μ vectors (Figure I-14-ii); and that leads to a negative Cotton effect (negative CD band), and positive Cotton effect (positive CD band) respectively.

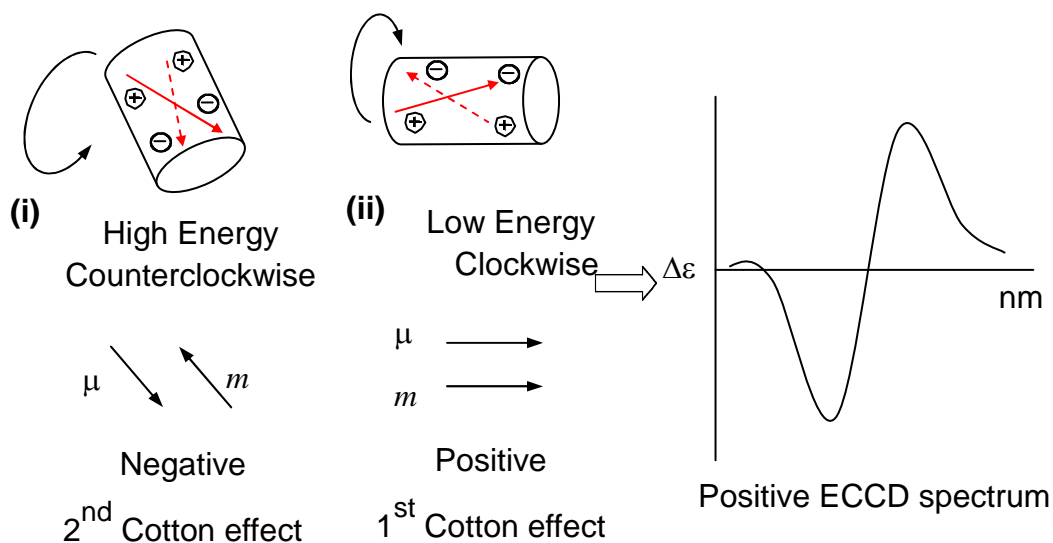


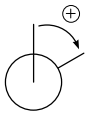
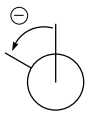
Figure I-14. The rationalization of ECCD spectrum for dibenzoate.

To gain a deeper understanding about the factors affecting the sign and strength of ECCD spectrum, one need to look into the rotational strength (R) which can be defined by Equation I-8 for a system containing two identical chromophores which couple through space interactions.³⁹ The positive and negative signs correspond to

α - and β - state respectively, R_{ij} is the distance vector between two chromophores, μ_{ioa} and μ_{joa} are the etdm of excitations, and σ_0 is the excitation number of transition from ground state to α state.

$$R_{\alpha,\beta} = \pm \frac{1}{2} \pi \sigma_0 \vec{R}_{ij} \bullet (\vec{\mu}_{ioa} \times \vec{\mu}_{joa}) \quad (\text{I-8})$$

Table I-1. Definition of exciton chirality for a binary system

	Qualitative Definition	Quantitative Definition	Cotton effects
Positive Chirality		$\vec{R}_{ij} \bullet (\vec{\mu}_{ioa} \times \vec{\mu}_{joa}) V_{ij} > 0$	positive first and negative second Cotton effects
Negative Chirality		$\vec{R}_{ij} \bullet (\vec{\mu}_{ioa} \times \vec{\mu}_{joa}) V_{ij} < 0$	negative first and positive second Cotton effects

From the equation above, the sign of the bisignate curve completely depends on the spatial orientation of the two chromophores.^{42, 43} As shown in Table I-1,⁴² if the electric transition dipole moments of the two chromophores from front to back constitutes a clockwise orientation, then according to Equation I-8 above, a positive bisignate spectrum will be observed, which refers to a positive 1st and negative 2nd Cotton effects, while an opposite but otherwise identical spectrum is produced by the counterclockwise orientation.^{44, 45} Therefore, the sign of the ECCD spectrum for a chiral molecule can be predicted as long as the spatial orientation of two chromophores is known. On the other hand, the sign of a bisignate ECCD spectrum

can directly reflect the relative orientation of two chromophores in space as well as the stereochemistry of substrates. In this way, the absolute stereochemistry of chiral molecules can be elucidated in a non-empirical manner.

The difference in $\Delta\epsilon$ between the 1st and 2nd Cotton effects is defined as the amplitude (A) of the ECCD couplet reflecting the signal strength. There are several factors that can affect the amplitude according to Equation I-8. The first factor is the molar absorption coefficient (ϵ) of the interacting chromophores since the amplitude is proportional to ϵ^2 . Therefore, in order to have increased sensitivity in the ECCD methods, chromophores with strong absorptions are preferred. Secondly, interchromophoric distance (R_{ij}) also has significant contribution to amplitude. The amplitude is inversely proportional to the distance R_{ij} .⁴⁶ This relation is self-evident since the exciton coupling occurs through space. To achieve enhanced interaction, the coupling chromophores should be oriented close to each other. This tendency is exemplified by a series of dibenzoates as shown by Nakanishi.³⁹ Projection angle between the interacting chromophores is another important factor affecting the amplitude. It is found that the amplitude usually maximizes at a chromophoric projection angle of around 70° . There is no exciton coupling when the chromophores are either parallel or perpendicular to each other. Lastly, the number of interacting chromophores (X, Y, Z) also plays a role in CD signal strength when more than two chromophores are involved in exciton coupling. The amplitude of the system is the summation of the amplitude of each pair of interacting chromophores, i.e. the principle of pair-wise additivity holds in systems containing of three or more

chromophores. This observation has been proven by experiments and theoretical calculations.⁴⁷⁻⁵⁰

Exciton coupling can also take place between different chromophores if their λ_{max} of UV-vis absorption are close enough for effective coupling because closer λ_{max} values correspond to the closer energy levels of excited states which have a higher probability to interact. The interacting chromophores do not have to be within the same molecule. They can interact as long as they are in close proximity in space and this feature is particularly interesting in supramolecular compounds.

I.3.2 The application of the ECCD method in stereochemical determination

Owing to the high sensitivity and nonempirical feature, the ECCD method has attracted great attention in the study of absolute stereochemical determination. By making use of the chromophores preexistent in molecules or introducing chromophores into molecules via covalent or non-covalent interaction, one may obtain bisignate ECCD spectra whose sign can be used for assigning the substrate chirality in a nonempirical fashion. This method has proved to be highly versatile used in a wide range of chromophore-containing molecules such as polyols,⁵¹⁻⁵³ carbohydrates,⁴⁷ and hydroxy acids.⁵⁴ It is also very sensitive requiring as low as submilligram of sample.

A classical example regarding the use of exciton chirality with preexistent chromophores within a molecule is stereochemical determination of (+)-abscisic acid.^{55, 56} The enone moiety and dienoid acid functionality are the two

chromophores in this molecule and they are close in space. The transition dipole moments of the two chromophores would exhibit exciton coupling through space and a positive ECCD couplet was observed indicating a clockwise twist between the two chromophoric units. Therefore, β -configuration of the hydroxyl group was revealed as shown in Figure I-15 for this plant hormone.

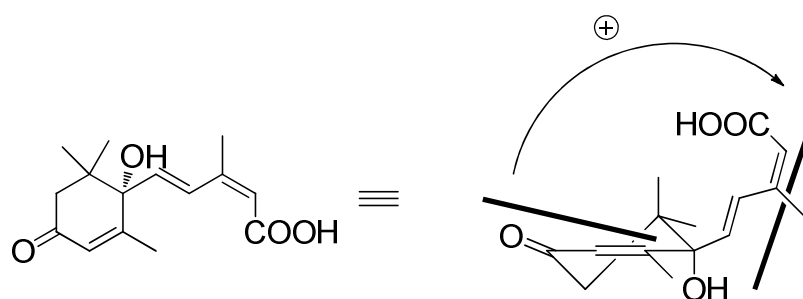


Figure I-15. Observed ECCD in (+)-Absciscic acid.

For those compounds containing only one chromophore or no chromophore, chemical derivatization was usually conducted to introduce chromophores for desired spatial interaction generating exciton chirality which can be detected in CD spectropolarimeter. Figure I-16 illustrates the introduction of second chromophore into periplanone B by reduction of ketone moiety and following esterification to enable the stereochemical determination using the ECCD method.⁵⁷ The counterclockwise twist of chromophoric units defines the stereochemistry shown in Figure I-16.

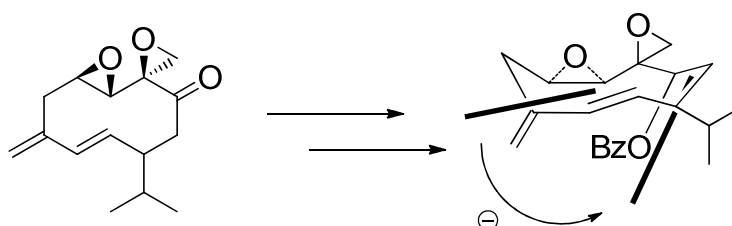


Figure I-16. ECCD was observed after derivatization of Periplanone B.

Canary and coworkers have devised a system to incorporate quinoline or porphyrin chromophores into amino acids or amino alcohols through covalent bond formation leading to chiral propellers.⁵⁸⁻⁶⁰ After complexation of Cu(II) or Zn(II) one of the two possible propeller conformations is preferentially formed rendering the corresponding characteristic ECCD couplet which reflected the chirality of the original molecule (Figure I-17).

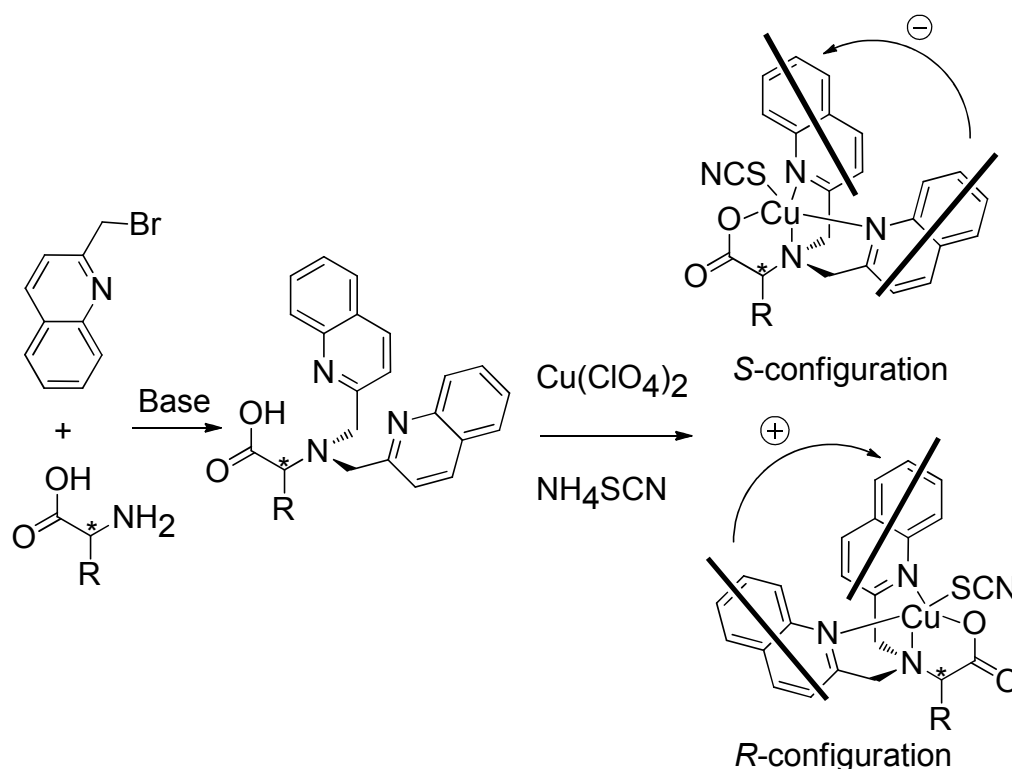


Figure I-17. Chromophoric derivatization of amino acids for stereochemical determination.

In a recent report,⁶¹ Gawronski elegantly employed the trityl ethers of chiral secondary alcohols as molecular bevel gears to transfer the chirality information of alcohol into the molecular propeller of trityl unit. The introduction of chirality efficiently broke the C_3 symmetry of the propeller as well as the equilibrium between enantiomeric pair, *P* and *M* due to sterics (Figure I-18). This equilibrium bias was

consistently reflected on CD spectrum of the trityl ethers and can be used for assigning the chirality of chiral alcohols. This conceptually simple system proved to be effective and was supported by X-ray analysis as well as computational study.

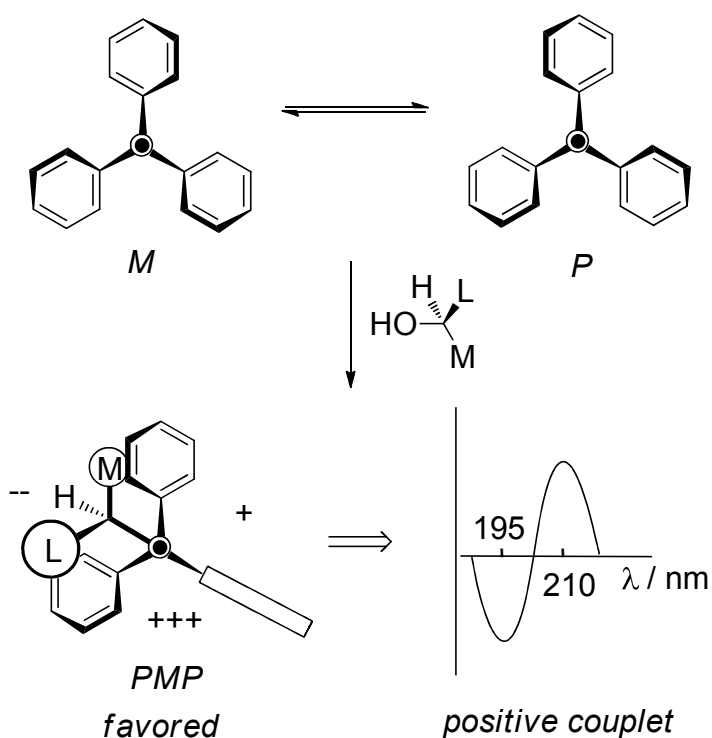


Figure I-18. Trityl ether as molecular bevel gears for assigning chirality of alcohols.

The requirement of chemical derivatization for molecules without chromophores limits the application of conventional ECCD method. In addition, the stability of analyte under derivatization condition is also an important concern. Intrigued by the nonempirical nature and high sensitivity of ECCD method, people have developed a number of chromophoric hosts to incorporate the chromophores into analyte through non-covalent interaction in a rapid and efficient manner. Upon complexation of host

with the chiral guest, a preferred chiral conformation of host chromophores will be induced, which can be detected as an ECCD couplet. To simplify the observed ECCD signal, the chromophoric hosts used for ECCD studies are either achiral or in the form of racemates and they should be able to efficiently transfer the chirality information of chiral guest. The idea of this chiral induction was first demonstrated on dyes bound to polypeptides in their helical conformations, which led to the helical orientation of the chromophoric molecules.⁶²

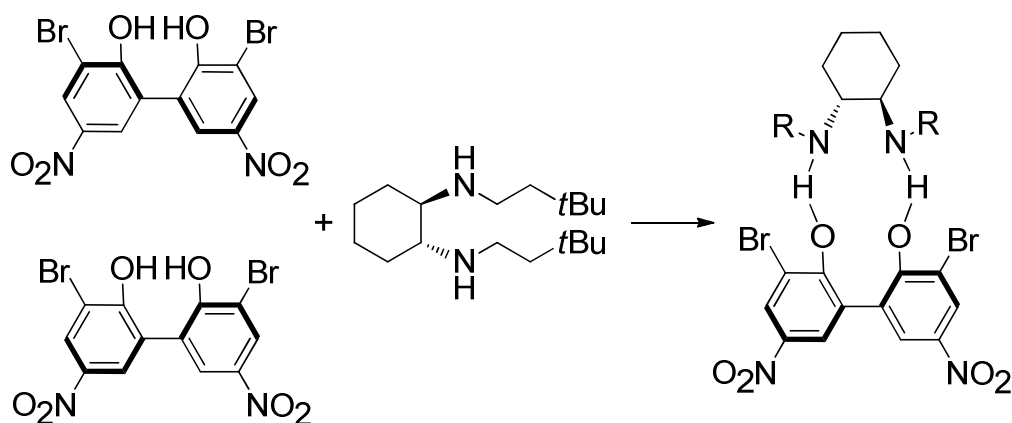


Figure I-19. Determination of chirality for chiral amine through H-bonding with biphenol host.

Figure I-19 revealed another simple example for chirality induction of chromophoric host upon binding with a chiral guest.⁶³⁻⁶⁵ The biphenol host is not planar and exists as a mixture of the two enantiomeric forms due to steric interactions between the two hydroxyl groups. After complexation with chiral *trans*-1,2-cyclohexane diamine through hydrogen bonding between the phenols and the amine groups, an energetically preferred complex is formed. The absolute stereochemistry of the chiral diamine was transferred into the complex and detected as

a bisignate ECD spectrum in which the sign directly reflected the chirality of the substrate.

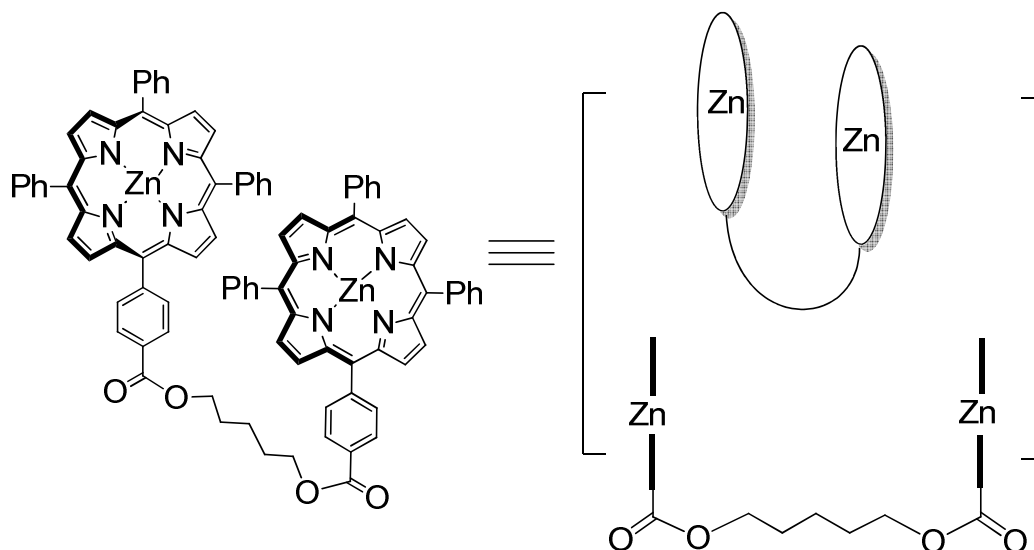


Figure I-20. Porphyrin tweezer and schematic representations.

Porphyrins and metalloporphyrins are extensively utilized as chromophoric hosts for chiral recognition⁶⁶⁻⁶⁹ and have demonstrated great potential as chirality sensors for a large number of organic molecules. Porphyrin tweezers with an alkyl chain linking two metalloporphyrins (usually zinc porphyrins) were developed by Nakanishi (Figure I-20)⁷⁰⁻⁷⁴ and Inoue.⁷⁵⁻⁸² It proved to be excellent chromophoric host system for stereochemical determination of a variety of chiral molecules especially for amines. The detailed discussion of chirality transfer process as well as the applications of the porphyrin tweezer system will be revealed in section II-1.

I.4 Research aim for our project using ECD

During our continuous effort employing porphyrin tweezers for absolute

stereochemical determination, we have acquired a good understanding of chiral recognition involved with porphyrin tweezers. We also realized that the current zinc porphyrin tweezer system has limitations. It works best for bifunctional molecules bearing strong binding affinity toward zinc porphyrins, and usually an amino or amide group must be present. For oxygen containing molecules, derivatization has to be performed to introduce a strong binding site, which restricts the application of this system for rapid assignment of molecular chirality. The absolute configuration of a wide variety of organic molecules (diols, epoxy alcohols, aziridines, hydroxyl ketones, hydroxyl THF rings, etc.) has yet to be successfully addressed using zinc porphyrin tweezer system or other methods for chirality recognition. Our goal of this research project is to design, synthesis and study a range of electronically tuned porphyrin tweezers to afford a couple of candidates with enhanced binding affinity as well as sensitivity. With the improved binding affinity, these porphyrin tweezers will be applied for ECCD study for several different classes of oxygen-containing chiral molecules. The outcome of this research will provide chemists a facile, reliable, and general method for nonempirical assignment of chirality for a series of important organic molecules in microscale devoid of any chemical derivation, which is a challenging task for conventional methods. This study will open a broad pathway for absolute stereochemical determination using porphyrin tweezer system. In the mean time, it will also better our understanding of chirality recognition while probing the stereodifferentiation processes and eventually offer critical insights and guidelines for further development of chromophore-based chirality sensors.

REFERENCES

References

1. Eliel, E. L.; Wilen, S. H., *Stereochemistry of Organic Compounds*. Wiley & Sons: New York, 1993.
2. Cahn, R. S.; Ingold, C.; Prelog, V., Specification of Molecular Chirality. *Angewandte Chemie-International Edition* **1966**, 5, (4), 385-415.
3. Rossi, R.; Diversi, P., SYNTHESIS, ABSOLUTE CONFIGURATION, AND OPTICAL PURITY OF CHIRAL ALLENES. *Synthesis-Stuttgart* **1973**, (1), 25-36.
4. Laarhoven, W. H.; Prinsen, W. J. C., CARBOHELICENES AND HETEROHELICENES. *Topics in Current Chemistry* **1984**, 125, 63-130.
5. Prinsen, W. J. C.; Laarhoven, W. H., DETERMINATION OF THE ENANTIOMERIC EXCESS OF HEXAHELICENE AND ITS METHYL-SUBSTITUTED DERIVATIVES BY HIGH-PERFORMANCE LIQUID-CHROMATOGRAPHY. *Journal of Chromatography* **1987**, 393, (3), 377-390.
6. Breslow, R.; Cheng, Z. L., On the origin of terrestrial homochirality for nucleosides and amino acids. *Proceedings of the National Academy of Sciences of the United States of America* **2009**, 106, (23), 9144-9146.
7. Mason, S. F., Extraterrestrial handedness. *Nature* **1997**, 389, (6653), 804-804.
8. Cohen, J., Biochemistry - Getting All Turned around over the Origins of Life on Earth. *Science* **1995**, 267, (5202), 1265-1266.
9. Kahr, B.; Freudenthal, J. H., Dendritic crystal growth, differential circular scattering, and the origin of biomolecular homochirality. *Chirality* **2008**, 20, (9), 973-977.
10. Stinson, S. C., Chiral drugs (vol 78, pg 55, 2000). *Chemical & Engineering News* **2000**, 78, (44), 4-4.
11. Stinson, S. C., Chiral chemistry. *Chemical & Engineering News* **2001**, 79, (20), 45-+.
12. Dale, J. A.; Mosher, H. S., Nuclear Magnetic Resonance Nonequivalence of Diastereomeric Esters of Alpha-Substituted Phenylacetic Acids for Determination of

Stereochemical Purity. *Journal of the American Chemical Society* **1968**, 90, (14), 3732-&.

13. Dale, J. A.; Dull, D. L.; Mosher, H. S., Alpha-Methoxy-Alpha-Trifluoromethylphenylacetic Acid, a Versatile Reagent for Determination of Enantiomeric Composition of Alcohols and Amines. *Journal of Organic Chemistry* **1969**, 34, (9), 2543-&.

14. Dale, J. A.; Mosher, H. S., Nuclear Magnetic-Resonance Enantiomer Reagents - Configurational Correlations Via Nuclear Magnetic-Resonance Chemical-Shifts of Diastereomeric Mandelate, O-Methylmandelate, and Alpha-Methoxy-Alpha-Trifluoromethylphenylacetate (Mtpa) Esters. *Journal of the American Chemical Society* **1973**, 95, (2), 512-519.

15. Parker, D., Nmr Determination of Enantiomeric Purity. *Chemical Reviews* **1991**, 91, (7), 1441-1457.

16. Seco, J. M.; Quinoa, E.; Riguera, R., The assignment of absolute configuration by NMR. *Chemical Reviews* **2004**, 104, (1), 17-117.

17. Hoye, T. R.; Jeffrey, C. S.; Shao, F., Mosher ester analysis for the determination of absolute configuration of stereogenic (chiral) carbinol carbons. *Nature Protocols* **2007**, 2, (10), 2451-2458.

18. Sullivan, G. R.; Dale, J. A.; Mosher, H. S., Correlation of Configuration and F-19 Chemical-Shifts of Alpha-Methoxy-Alpha-Trifluoromethylphenylacetate Derivatives. *Journal of Organic Chemistry* **1973**, 38, (12), 2143-2147.

19. Freire, F.; Seco, J. M.; Quinoa, E.; Riguera, R., The assignment of the absolute configuration of 1,2-diols by low-temperature NMR of a single MPA derivative. *Organic Letters* **2005**, 7, (22), 4855-4858.

20. Leiro, V.; Freire, F.; Quinoa, E.; Riguera, R., Absolute configuration of amino alcohols by H-1-NMR. *Chemical Communications* **2005**, (44), 5554-5556.

21. Freire, F.; Calderon, F.; Seco, J. M.; Fernandez-Mayoralas, A.; Quinoa, E.; Riguera, R., Relative and absolute stereochemistry of secondary/secondary diols: Low-temperature H-1 NMR of their bis-MPA esters. *Journal of Organic Chemistry* **2007**, 72, (7), 2297-2301.

22. Freire, F.; Seco, J. M.; Quinoa, E.; Riguera, R., Challenging the absence of observable hydrogens in the assignment of absolute configurations by NMR: application to chiral primary alcohols. *Chemical Communications* **2007**, (14), 1456-1458.

23. Leiro, V.; Seco, J. M.; Quinoa, E.; Riguera, R., Assigning the configuration of amino alcohols by NMR: A single derivatization method. *Organic Letters* **2008**, 10, (13), 2733-2736.
24. Kusumi, T.; Fujita, Y.; Ohtani, I.; Kakisawa, H., Anomaly in the Modified Mosher Method - Absolute-Configurations of Some Marine Cembranolides. *Tetrahedron Letters* **1991**, 32, (25), 2923-2926.
25. Ohtani, I.; Kusumi, T.; Kashman, Y.; Kakisawa, H., High-Field Ft Nmr Application of Mosher Method - the Absolute-Configurations of Marine Terpenoids. *Journal of the American Chemical Society* **1991**, 113, (11), 4092-4096.
26. Louzao, I.; Garcia, R.; Seco, J. M.; Quinoa, E.; Riguera, R., Absolute Configuration of Ketone Cyanohydrins by H-1 NMR: The Special Case of Polar Substituted Tertiary Alcohols. *Organic Letters* **2009**, 11, (1), 53-56.
27. Kabuto, K.; Sasaki, K.; Sasaki, Y., Absolute-Configuration of Aldonic Acids and Lanthanoid Induced Shift by the Chiral Shift-Reagent Propylenediaminetetraacetatoeuropium(III) in Aqueous-Solution. *Tetrahedron-Asymmetry* **1992**, 3, (11), 1357-1360.
28. Tsukube, H.; Shinoda, S., Lanthanide complexes in molecular recognition and chirality sensing of biological substrates. *Chemical Reviews* **2002**, 102, (6), 2389-2403.
29. Tsukube, H.; Shinoda, S.; Tamiaki, H., Recognition and sensing of chiral biological substrates via lanthanide coordination chemistry. *Coordination Chemistry Reviews* **2002**, 226, (1-2), 227-234.
30. Kuhn, W., The physical significance of optical rotatory power. *Transactions of the Faraday Society* **1930**, 26, 0293-0307.
31. Kirkwood, J. G., On the theory of optical rotatory power. *Journal of Chemical Physics* **1937**, 5, (6), 479-491.
32. Stephens, P. J.; Devlin, F. J.; Cheeseman, J. R.; Frisch, M. J., Calculation of optical rotation using density functional theory. *Journal of Physical Chemistry A* **2001**, 105, (22), 5356-5371.
33. Giorgio, E.; Roje, M.; Tanaka, K.; Hamersak, Z.; Sunjic, V.; Nakanishi, K.; Rosini, C.; Berova, N., Determination of the absolute configuration of flexible molecules by ab initio ORD calculations: A case study with cytoxazones and isocytoxazones. *Journal of Organic Chemistry* **2005**, 70, (17), 6557-6563.

34. Nafie, L. A.; Keiderling, T. A.; Stephens, P. J., Vibrational Circular-Dichroism. *Journal of the American Chemical Society* **1976**, 98, (10), 2715-2723.
35. Stephens, P. J.; Devlin, F. J.; Pan, J. J., The determination of the absolute configurations of chiral molecules using vibrational circular dichroism (VCD) spectroscopy. *Chirality* **2008**, 20, (5), 643-663.
36. Stephens, P. J.; Devlin, F. J., Determination of the structure of chiral molecules using ab initio vibrational circular dichroism spectroscopy. *Chirality* **2001**, 12, 172-179.
37. Solomons, T. W., *Organic chemistry*. John Wiley & Sons Inc.: New York, 1978.
38. Lambert, J. B. S.; Lightner, D. A.; Cooks, R. G., *Organic Structural Spectroscopy*. Prentice Hall: Upper Saddle River, 1998.
39. Harada, N.; Nakanishi, K., *Circular Dichroic Spectroscopy: Exciton Coupling in Organic Stereochemistry*. University Science Books: Mill Valley, CA, 1983.
40. Sneath, G., CIRCULAR-DICHOISM AND ABSOLUTE CONFORMATION - APPLICATION OF QUALITATIVE MO THEORY TO CHIROPTICAL PHENOMENA. *Angewandte Chemie-International Edition in English* **1979**, 18, (5), 363-377.
41. Sneath, G., SEMI-EMPIRICAL RULES IN CIRCULAR-DICHOISM OF NATURAL-PRODUCTS. *Pure and Applied Chemistry* **1979**, 51, (4), 769-785.
42. Harada, N.; Chen, S. L.; Nakanishi, K., QUANTITATIVE DEFINITION OF EXCITON CHIRALITY AND DISTANT EFFECT IN EXCITON CHIRALITY METHOD. *Journal of the American Chemical Society* **1975**, 97, (19), 5345-5352.
43. Harada, N.; Nakanishi, K., EXCITON CHIRALITY METHOD AND ITS APPLICATION TO CONFIGURATIONAL AND CONFORMATIONAL STUDIES OF NATURAL-PRODUCTS. *Accounts of Chemical Research* **1972**, 5, (8), 257-&.
44. Hug, W.; Wagniere, G., OPTICAL-ACTIVITY OF CHROMOPHORES OF SYMMETRY C₂. *Tetrahedron* **1972**, 28, (5), 1241-&.
45. Wagniere, G.; Hug, W., POLARIZATION AND SIGN OF LONG-WAVELENGTH COTTON-EFFECTS IN CHROMOPHORES OF SYMMETRY C₂. *Tetrahedron Letters* **1970**, (55), 4765-&.
46. Oancea, S.; Formaggio, F.; Campestri, S.; Broxterman, Q. B.; Kaptein, B.;

Toniolo, C., Distance dependency of exciton coupled circular dichroism using turn and helical peptide spacers. *Biopolymers* **2003**, 72, (2), 105-115.

47. Vazquez, J. T.; Wiesler, W. T.; Nakanishi, K., CIRCULAR-DICHROISM SPECTRA OF BICHROMOPHORICALLY DERIVATIZED METHYL-D-GALACTOPYRANOSIDES, CALCULABLE BY PAIRWISE ADDITIVITY, PROVIDE A BASIS FOR NOVEL MICROANALYSIS OF OLIGOSACCHARIDES. *Carbohydrate Research* **1988**, 176, (2), 175-194.

48. Dong, J. G.; Akritopoulou-Zanze, I.; Guo, J. S.; Berova, N.; Nakanishi, K.; Harada, N., Theoretical calculation of circular dichroic exciton-split spectra in presence of three interacting 2-naphthoate chromophores. *Enantiomer* **1997**, 2, (5), 397-409.

49. Liu, H. W.; Nakanishi, K., A MICROMETHOD FOR DETERMINING THE BRANCHING POINTS IN OLIGOSACCHARIDES BASED ON CIRCULAR-DICHROISM. *Journal of the American Chemical Society* **1981**, 103, (23), 7005-7006.

50. Wiesler, W. T.; Vazquez, J. T.; Nakanishi, K., PAIRWISE ADDITIVITY IN EXCITON-COUPLED CD CURVES OF MULTICHROMOPHORIC SYSTEMS. *Journal of the American Chemical Society* **1987**, 109, (19), 5586-5592.

51. Rele, D.; Zhao, N.; Nakanishi, K.; Berova, N., Acyclic 1,2-/1,3-mixed pentols. Synthesis and general trends in bichromophoric exciton coupled circular dichroic spectra. *Tetrahedron* **1996**, 52, (8), 2759-2776.

52. Zhao, N.; Berova, N.; Nakanishi, K.; Rohmer, M.; Mougnot, P.; Jurgens, U. J., Structures of two bacteriohopanoids with acyclic pentol side-chains from the cyanobacterium Nostoc PCC 6720. *Tetrahedron* **1996**, 52, (8), 2777-2788.

53. Wiesler, W. T.; Nakanishi, K., RELATIVE AND ABSOLUTE CONFIGURATIONAL ASSIGNMENTS OF ACYCLIC POLYOLS BY CIRCULAR-DICHROISM .1. RATIONALE FOR A SIMPLE PROCEDURE BASED ON THE EXCITON CHIRALITY METHOD. *Journal of the American Chemical Society* **1989**, 111, (26), 9205-9213.

54. Gimple, O.; Schreier, P.; Humpf, H. U., A new exciton-coupled circular dichroism method for assigning the absolute configuration in acyclic alpha- and beta-hydroxy carboxylic acids. *Tetrahedron-Asymmetry* **1997**, 8, (1), 11-14.

55. Harada, N., ABSOLUTE CONFIGURATION OF (+)-TRANS-ABSCISIC ACID AS DETERMINED BY A QUANTITATIVE APPLICATION OF EXCITON CHIRALITY METHOD. *Journal of the American Chemical Society* **1973**, 95, (1),

240-242.

56. Koreeda, M.; Weiss, G.; Nakanishi, K., ABSOLUTE CONFIGURATION OF NATURAL (+)-ABSCISIC ACID. *Journal of the American Chemical Society* **1973**, 95, (1), 239-240.

57. Adams, M. A.; Nakanishi, K.; Still, W. C.; Arnold, E. V.; Clardy, J.; Persoons, C. J., SEX-PHEROMONE OF THE AMERICAN COCKROACH - ABSOLUTE-CONFIGURATION OF PERIPLANONE-B. *Journal of the American Chemical Society* **1979**, 101, (9), 2495-2498.

58. Canary, J. W.; Allen, C. S.; Castagnetto, J. M.; Chiu, Y. H.; Toscano, P. J.; Wang, Y. H., Solid state and solution characterization of chiral, conformationally mobile tripodal ligands. *Inorganic Chemistry* **1998**, 37, (24), 6255-6262.

59. Canary, J. W.; Allen, C. S.; Castagnetto, J. M.; Wang, Y. H., CONFORMATIONALLY DRIVEN, PROPELLER-LIKE CHIRALITY IN LABILE COORDINATION-COMPLEXES. *Journal of the American Chemical Society* **1995**, 117, (32), 8484-8485.

60. Holmes, A. E.; Zahn, S.; Canary, J. W., Synthesis and circular dichroism studies of N,N-bis(2-quinolylmethyl)amino acid Cu(II) complexes: Determination of absolute configuration and enantiomeric excess by the exciton coupling method. *Chirality* **2002**, 14, (6), 471-477.

61. Sciebura, J.; Skowronek, P.; Gawronski, J., Trityl Ethers: Molecular Bevel Gears Reporting Chirality through Circular Dichroism Spectra. *Angewandte Chemie-International Edition* **2009**, 48, (38), 7069-7072.

62. Blout, E. R.; Stryer, L., ANOMALOUS OPTICAL ROTATORY DISPERSION OF DYE - POLYPEPTIDE COMPLEXES. *Proceedings of the National Academy of Sciences of the United States of America* **1959**, 45, (11), 1591-1593.

63. Hanessian, S.; Simard, M.; Roelens, S., MOLECULAR RECOGNITION AND SELF-ASSEMBLY BY NON-AMIDIC HYDROGEN-BONDING - AN EXCEPTIONAL ASSEMBLER OF NEUTRAL AND CHARGED SUPRAMOLECULAR STRUCTURES. *Journal of the American Chemical Society* **1995**, 117, (29), 7630-7645.

64. Mizutani, T.; Yagi, S.; Honmaru, A.; Ogoshi, H., Interconversion between point chirality and helical chirality driven by shape-sensitive interactions. *Journal of the American Chemical Society* **1996**, 118, (22), 5318-5319.

65. Mizutani, T.; Takagi, H.; Hara, O.; Horiguchi, T.; Ogoshi, H., Axial chirality

induction in flexible biphenols by hydrogen bonding and steric interactions. *Tetrahedron Letters* **1997**, 38, (11), 1991-1994.

66. Huang, X. F.; Nakanishi, K.; Berova, N., Porphyrins and metalloporphyrins: Versatile circular dichroic reporter groups for structural studies. *Chirality* **2000**, 12, (4), 237-255.

67. Matile, S.; Berova, N.; Nakanishi, K., Intramolecular porphyrin pi,pi-stacking: Absolute configurational assignment of acyclic compounds with single chiral centers by exciton coupled circular dichroism. *Enantiomer* **1996**, 1, (1), 1-12.

68. Matile, S.; Berova, N.; Nakanishi, K.; Fleischhauer, J.; Woody, R. W., Structural studies by exciton coupled circular dichroism over a large distance: Porphyrin derivatives of steroids, dimeric steroids, and brevetoxin B. *Journal of the American Chemical Society* **1996**, 118, (22), 5198-5206.

69. Matile, S.; Berova, N.; Nakanishi, K.; Novkova, S.; Philipova, I.; Blagoev, B., PORPHYRINS - POWERFUL CHROMOPHORES FOR STRUCTURAL STUDIES BY EXCITON-COUPLED CIRCULAR-DICHOISM. *Journal of the American Chemical Society* **1995**, 117, (26), 7021-7022.

70. Huang, X. F.; Borhan, B.; Rickman, B. H.; Nakanishi, K.; Berova, N., Zinc porphyrin tweezer in host-guest complexation: Determination of absolute configurations of primary monoamines by circular dichroism. *Chemistry-a European Journal* **2000**, 6, (2), 216-224.

71. Huang, X. F.; Fujioka, N.; Pescitelli, G.; Koehn, F. E.; Williamson, R. T.; Nakanishi, K.; Berova, N., Absolute configurational assignments of secondary amines by CD-sensitive dimeric zinc porphyrin host. *Journal of the American Chemical Society* **2002**, 124, (35), 10320-10335.

72. Huang, X. F.; Rickman, B. H.; Borhan, B.; Berova, N.; Nakanishi, K., Zinc porphyrin tweezer in host-guest complexation: Determination of absolute configurations of diamines, amino acids, and amino alcohols by circular dichroism. *Journal of the American Chemical Society* **1998**, 120, (24), 6185-6186.

73. Proni, G.; Pescitelli, G.; Huang, X. F.; Nakanishi, K.; Berova, N., Magnesium tetraarylporphyrin tweezer: A CD-sensitive host for absolute configurational assignments of alpha-chiral carboxylic acids. *Journal of the American Chemical Society* **2003**, 125, (42), 12914-12927.

74. Proni, G.; Pescitelli, G.; Huang, X. F.; Quraishi, N. Q.; Nakanishi, K.; Berova, N., Configurational assignment of alpha-chiral carboxylic acids by complexation to dimeric Zn-porphyrin: host-guest structure, chiral recognition and circular dichroism.

Chemical Communications **2002**, (15), 1590-1591.

75. Borovkov, V. V.; Lintuluoto, J. M.; Inoue, Y., Supramolecular chirogenesis in zinc porphyrins: Mechanism, role of guest structure, and application for the absolute configuration determination. *Journal of the American Chemical Society* **2001**, 123, (13), 2979-2989.

76. Borovkov, V. V.; Yamamoto, N.; Lintuluoto, J. M.; Tanaka, T.; Inoue, Y., Supramolecular chirality induction in bis(zinc porphyrin) by amino acid derivatives: Rationalization and applications of the ligand bulkiness effect. *Chirality* **2001**, 13, (6), 329-335.

77. Lintuluoto, J. M.; Borovkov, V. V.; Inoue, Y., Direct determination of absolute configuration of monoalcohols by bis(magnesium porphyrin). *Journal of the American Chemical Society* **2002**, 124, (46), 13676-13677.

78. Bhyrappa, P.; Borovkov, V. V.; Inoue, Y., Supramolecular chirogenesis in bis-porphyrins: Interaction with chiral acids and application for the absolute configuration assignment. *Organic Letters* **2007**, 9, (3), 433-435.

79. Borovkov, V.; Inoue, Y., A Versatile Bisporphyrinoid Motif for Supramolecular Chirogenesis. *European Journal of Organic Chemistry* **2009**, (2), 189-197.

80. Borovkov, V.; Yamamoto, T.; Higuchi, H.; Inoue, Y., Supramolecular chirogenesis in weakly interacting hosts: Role of the temperature, structural, and electronic factors in enhancement of chiroptical sensitivity. *Organic Letters* **2008**, 10, (6), 1283-1286.

81. Borovkov, V. V.; Hembury, G. A.; Inoue, Y., Origin, control, and application of supramolecular chirogenesis in bisporphyrin-based systems. *Accounts of Chemical Research* **2004**, 37, (7), 449-459.

82. Borovkov, V. V.; Hembury, G. A.; Yamamoto, N.; Inoue, Y., Supramolecular chirogenesis in zinc porphyrins: Investigation of zinc-freebase bis-porphyrin, new mechanistic insights, extension of sensing abilities, and solvent effect. *Journal of Physical Chemistry A* **2003**, 107, (41), 8677-8686.

Chapter II

Electronically Tuned Porphyrin Tweezers in ECCD Study – Development of Highly Sensitive Chirality Sensor

II.1 Design and Synthesis of Electronically Tuned Porphyrin Tweezers

II.1.1 Stereochemical determination using porphyrin tweezers

Porphyrins have received great attention as receptors for chiral recognition due to several unique features. First, porphyrins are good chromophores with absorption maximum around 416 nm (Soret band).¹ The absorption of the *tetra*-arylporphyrins is more red shifted than most other chromophores that may preexist in the system under investigation, thus will not complicate chiroptical measurement. Second, these powerful chromophores have effective electric transition dipole moments that can couple over a distance of ~ 50 Å.^{2, 3} Third, they have large extinction coefficient and the ϵ is ca. 440,000 for *tetra*-arylporphyrins.¹ Intensities of Cotton Effects depend on the extinction coefficient of the chromophores, and hence the intense absorption of the porphyrins greatly enhances the sensitivity of CD. Finally, elaboration of metalloporphyrins can provide well-defined binding pockets in which both steric and electronic properties can be easily tuned to afford optimal binding affinity as well as sensitivity facilitating chiral recognition process.

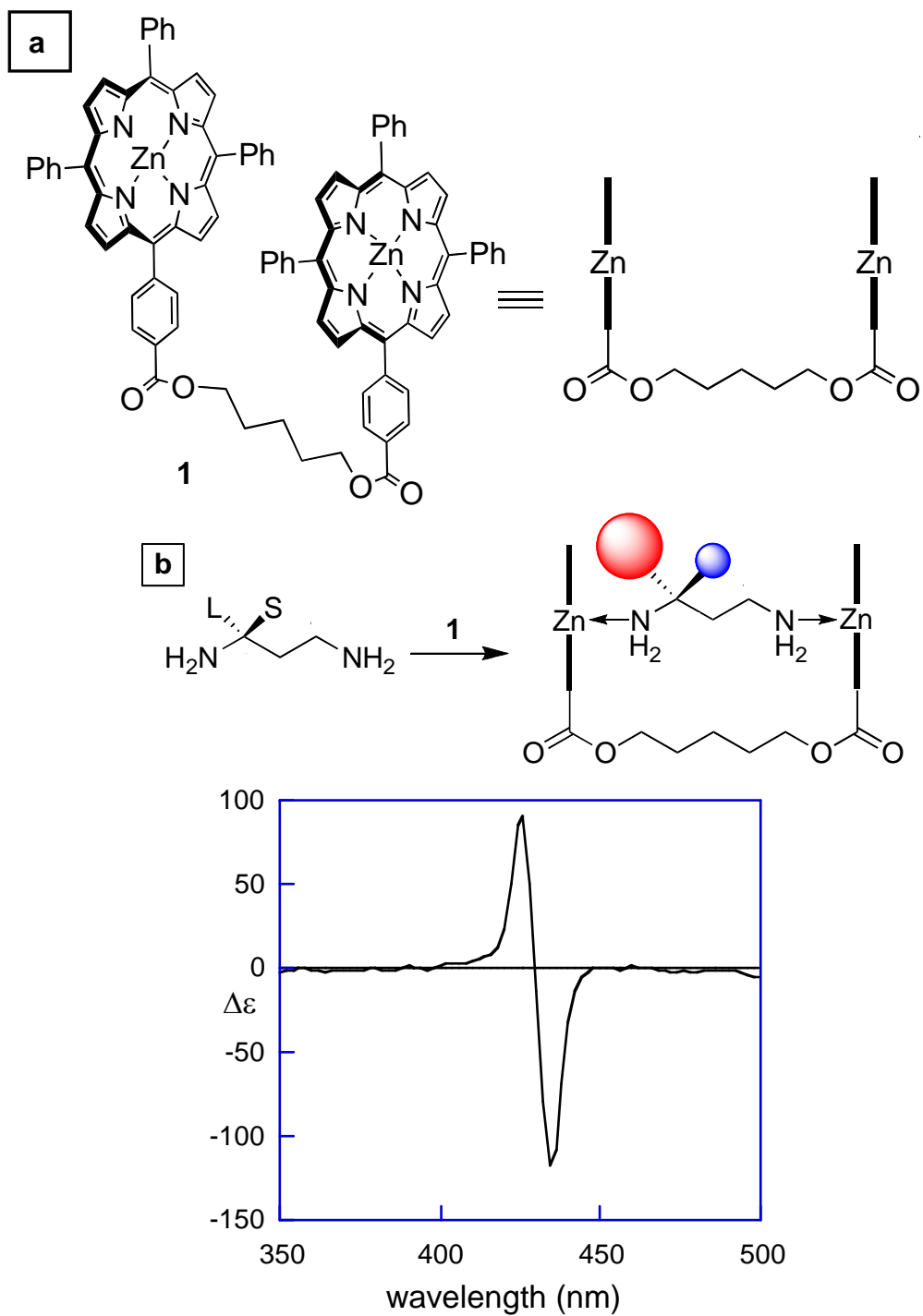


Figure II-1. Zn-Porphyrin tweezer for stereochemical determination of chiral diamines.

The alkyl-linked bisporphyrins have been used as host systems for binding with small guest molecules because of their ability to report the chirality of bound guests using ECCD. The tweezer system shown in Figure II-1a has been used for

stereo-determination of chiral diamines, amino acids and amino alcohols,⁴ carboxylic acids,^{5, 6} monoamines,^{7, 8} and chiral alcohols.^{9, 10} For example, in the case of diamines bearing a single chiral center, the zinc porphyrin tweezer serves as a host to form a complex with diamines by tight coordination between zinc and nitrogen. Although the zinc porphyrin tweezer itself is not chiral, after binding with the chiral substrate it adopts an induced chirally oriented conformation due to steric interaction between porphyrin and chiral centers.⁴ The sign of the resultant ECCD couplet reflects the helicity of the interacting porphyrin chromophores, and consequently the chirality of the derivatized system. There are two possible conformations the host-guest complex can adopt (Figure II-1b): one in which the porphyrin slides towards the small group at the chiral center and the other in which the porphyrin slides towards the large group. One would assume that the first conformation is more energetically favored because of decreased steric repulsion in the system compared to the second conformation. As Figure II-1b shows, the binding of (*R*)-1,3-diamine compound to the tweezer results in a negative ECCD spectrum. According to the size (A-value)¹¹ of the substituents at the chiral center, the hydrogen is assigned as the small group and the methyl group as the large group, thus the favored conformation of the tweezer/substrate complex is the one in which the porphyrin slides away from the bulky methyl (**L**) and towards the small hydrogen (**S**). This forms an angle (bite angle Ψ) between the electric dipole transition moments of the two chromophores. The direction of this rotation is determined by the chirality of the bound compound.

Among the two bound porphyrins, the one closer to the chiral center encounters the most steric interaction dictating the overall rotation and prefers to slide towards the smaller group (based on A-values)¹¹ in order to minimize the steric interaction with the larger group generating the optically active and sterically favorable conformation of the tweezer – a “chiral screw” which is detected by the CD spectrometer. Since the sign of the resultant ECCD spectrum depends on the chirality of the bound substrate, a direct and non-empirical relationship is established, which results in assigning the absolute stereochemistry of the bound guest based on the helicity of the host.

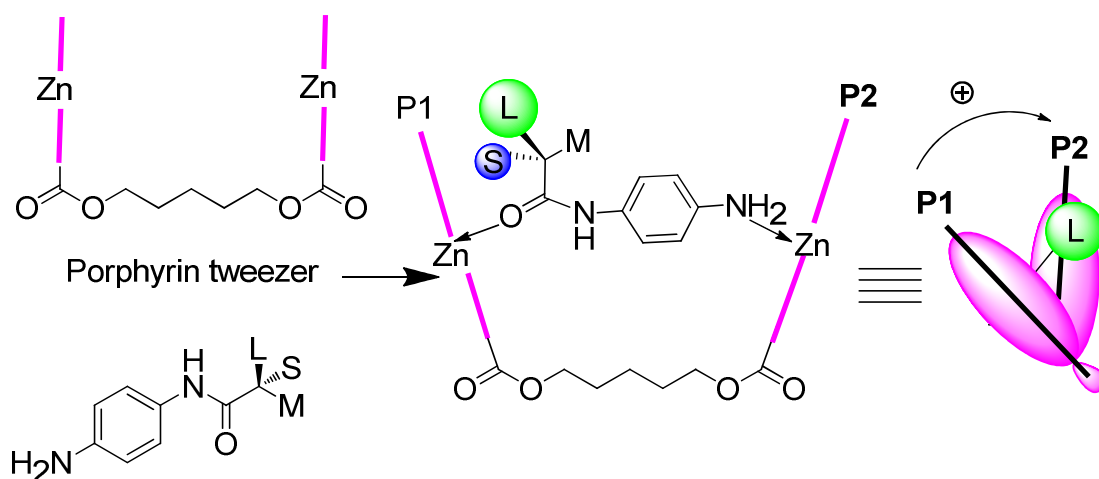


Figure II-2. Determination of chirality for derivatized α -carboxylic acids.

Chiral primary and secondary amines, alcohols, amino alcohols and carboxylic acids cannot be directly used in the stereo-determination with the porphyrin tweezer because they can not form strong ditopic binding with host molecule. The one site of attachment (coordination to only one metalloporphyrin) provided by one amino group does not lead to the formation of a sandwiched host-guest complex, in which a chiral substrate is locked inside the tweezer. Consequently, the relative orientation

of the two porphyrin chromophores as well as the electric transition dipole moments will be random due to the free rotation around the pentylene linker resulting in unpredictable or zero CD signal. In order to solve this problem, these molecules have been derivatized with “carriers” which offer the required extra binding sites (usually nitrogen-containing functionality) for ditopic complexation (Figure II-2).^{4-10, 12}

In the picture shown in Figure II-2, the large and small group are projected towards porphyrin **P1**, which leads to stereodifferentiation and an observable helicity.⁶ Apparently, porphyrin **P1** would rotate towards small group and away from large group to minimize steric repulsion leading to a clockwise twist of the two porphyrin chromophores which corresponds to a positive helicity and gives rise to positive CD couplet. One drawback of this approach is that each potential carrier required the development of its own mnemonic to relate the observed sign of the ECCD couplet to the absolute stereochemistry of the analyte.

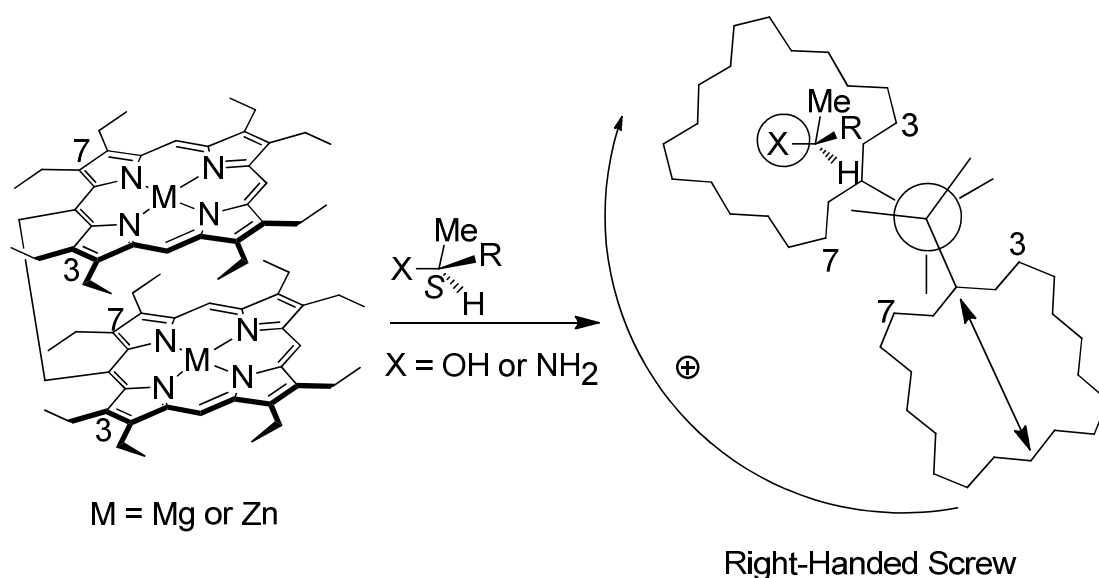


Figure II-3. Inoue's porphyrin tweezer for stereochemical determination.

Inoue and coworkers devised an octaethyl substituted porphyrin tweezer linked

by an ethylene group at porphyrin *meso* positions (Figure II-3) and directly employed monoalcohols and monoamines for ECCD measurement.¹³⁻¹⁵ Upon binding with one porphyrin of this tweezer, the steric interaction between the chiral center and the ethyl groups at 3,7 positions of the non-bound porphyrin drove the non-bound porphyrin to slide away generating right-handed screw for *S*-substrates and left-handed screw for *R*-substrates. The free tweezer also was used for chirality assignment of chiral acid through electrostatic binding and similar stereodifferentiation process. However, this method requires a large excess of chiral substrates (1000-10000 equiv.) and the signals for alcohols are also very weak.

The signal strength is often used as a criterion of sensitivity for the receptor molecule. Obviously, improving the sensitivity of the receptor is one of our primary goals to develop more efficient chirality sensors. The amplitude (**A**) of ECCD signal is affected by following factors:¹⁶

- (1) The interchromophoric distance. A smaller distance would lead to stronger interaction between transition dipole moments and consequently a higher amplitude;
- (2) The dihedral angle (bite angle) between the two electric dipole transition moments. Based on theoretical calculations, when the dihedral angle changes from 0° to 180° the amplitude increases and reaches a maximum at ~70° before decreasing;
- (3) The molar extinction absorption of the chromophore. Chromophores with high absorption will tend to yield high amplitude.

Based on the above principles, two approaches were adopted to develop more sensitive porphyrin tweezers for chirality sensing. One approach is based on the hypothesis that increasing the bulkiness of the porphyrin host could lead to a stronger steric interaction between the host porphyrin and the chiral guest molecule as well as a large bite angle. Consequently, stronger ECCD signal is expected. An extra benefit of this approach is that the bulky porphyrin host may sense the subtle size difference of substituents at the chiral center making it capable of effectively differentiating between substituents with similar sizes. A closer look at the porphyrin tweezer binding pocket revealed that the phenyl rings at the *meso* positions are perpendicular to the porphyrin plane and the *ortho* and *meta* hydrogens of the phenyl rings experienced the most steric interaction with guest causing the porphyrin to slide away from the large group to cover the small group. So, it is reasonable to propose that introduction of bulky groups into these positions will result in greater steric differentiation and a more pronounced bite angle, thus allowing for the enhancement of the ECCD amplitude.

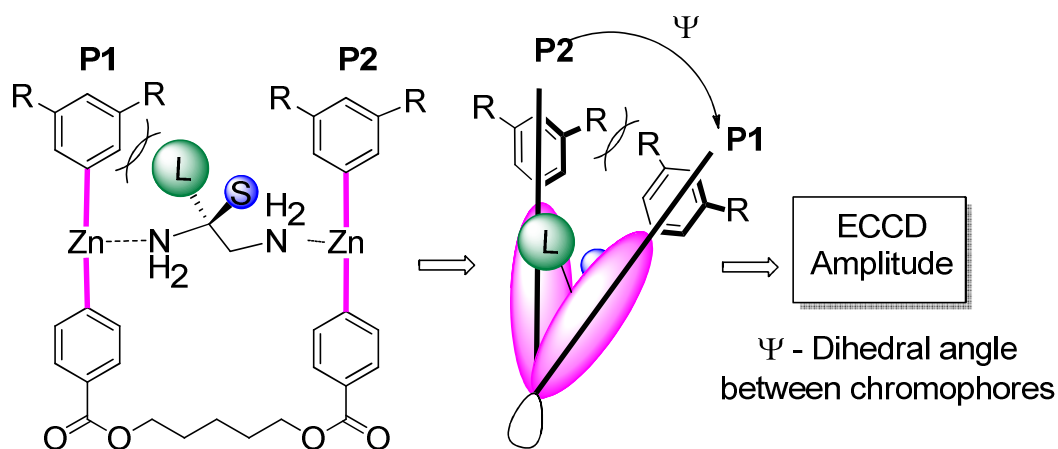


Figure II-4. Improving the sensitivity of porphyrin tweezer by tuning sterics.

Our group has already synthesized and tested a series of bulky porphyrin

tweezers (Figure II-5) with increased sterics at the *ortho* or *meta* position of *meso*-phenyl rings.¹⁷ Due to the enhanced steric repulsion with the chiral center of guest molecule, increased amplitudes were observed for derivatized chiral α -carboxylic acids compared to that of 5-(4-carboxyphenyl)-10,15,20-triphenyl porphyrin tweezer (**II-1**). The introduction of *tert*-butyl groups at two meta positions was found to be most beneficial for increasing the steric interaction between tweezer and chiral molecule, thus improving the sensitivity of porphyrin tweezer.

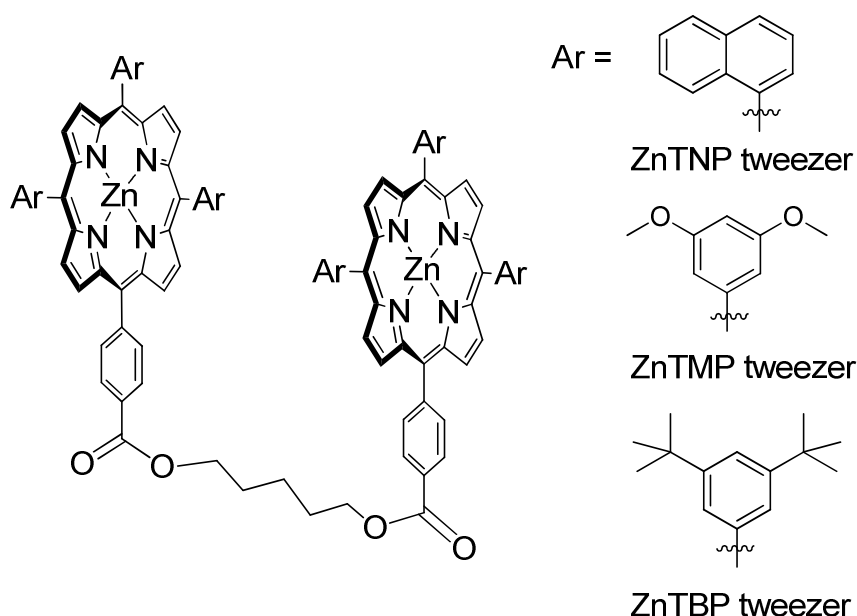


Figure II-5. Bulky porphyrin tweezers for ECCD study.

Another way to approach the goal of inventing a more sensitive porphyrin tweezer is to increase the binding affinity of the tweezer host by either introducing electron-withdrawing groups (Figure II-6) at the *para*-positions of the *meso*-phenyl rings within the porphyrin, or using other more Lewis acidic metal cations. The increased electrostatic interaction between the positively charged metal center of porphyrin and the electron-rich nucleophile should lead to a stronger binding

interaction. As a result, the complexation equilibrium between the Lewis acidic metallotweezer and the nucleophilic guest is greatly favored and enhanced ECCD amplitudes would be expected.

Most importantly, we anticipated that the enhanced binding affinity would enable the direct attachment of non-derivatized amino alcohols and diols bearing one or even two chiral functionalities which would tremendously expand the application of porphyrin tweezer methodology.

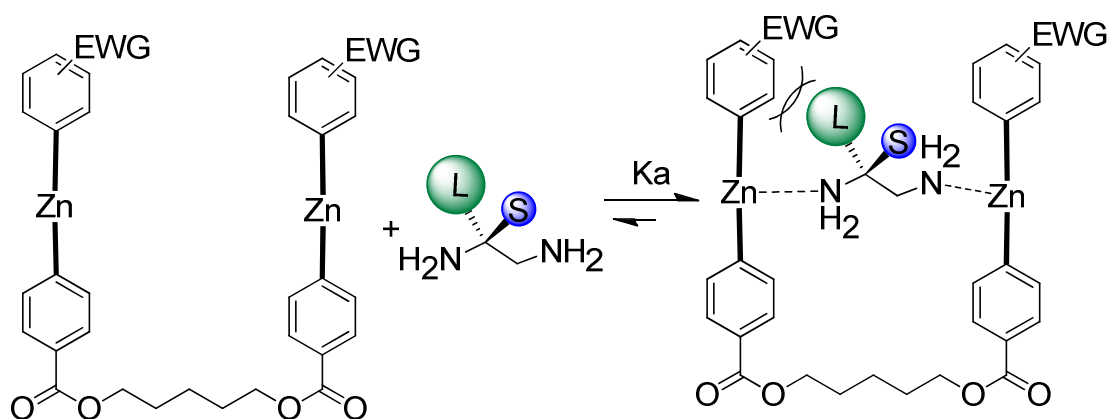
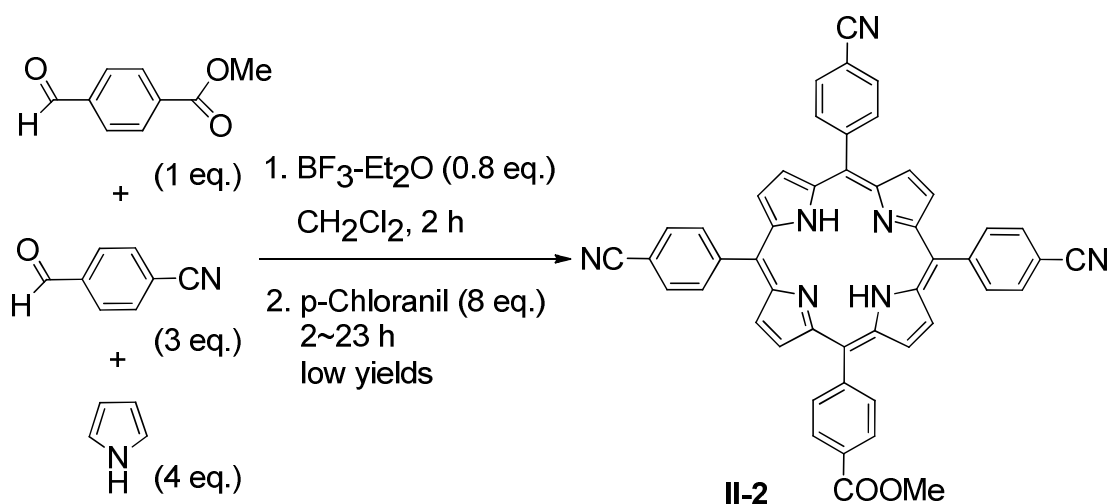


Figure II-6. Improving the sensitivity of porphyrin tweezer by tuning electronics.

Electron rich tweezers bearing electron-donating substituent at *para*-position of *meso*-phenyl rings were also synthesized and examined for comparison to complete the electronic effect study of tweezer systems.

II.1.2 Synthesis of electronically tuned porphyrin tweezers

The first electron-deficient porphyrin that was designed and synthesized was 5-(4-methylcarboxyphenyl)-10, 15, 20-tri(4-cyanophenyl)porphyrin (TCP monoester **II-2**). Standard procedures as shown in Scheme II-1 turned out to be not suitable for



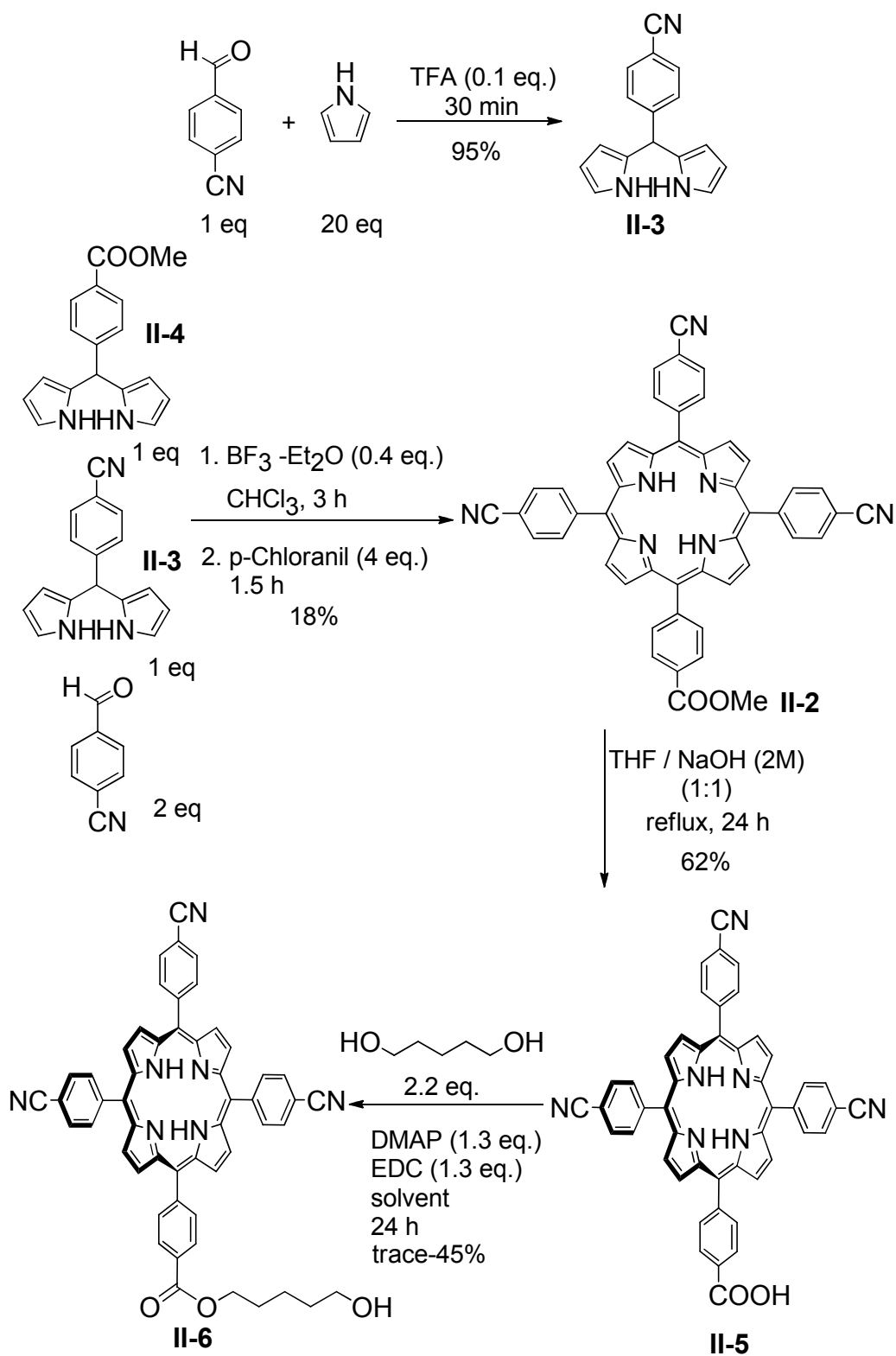
Scheme II-1. Synthesis of porphyrin ester **II-2**.

this substrate after a couple of trials in CH_2Cl_2 or CHCl_3 . The desired product was obtained in low and non-reproducible yields. The reaction was very slow; simply extending the reaction time to 23 h did not help. An alternative approach using dipyrromethane for porphyrin condensation was then employed as shown in Scheme II-2. This protocol is useful especially for improving the selectivity. Satisfactory yield (18%) was obtained and slow column chromatography was necessary to separate the pure desired porphyrin monoester **II-2** from the side product 5,10,15,20-tetra(4-cyanophenyl) porphyrin. Hydrolysis of **II-2** was carried

Table II-1. Effect of solvent in the synthesis of TCP monolinker **II-6**^a

Solvent	CH_2Cl_2	$\text{CH}_2\text{Cl}_2/\text{THF}$ (20:1)	$\text{CH}_2\text{Cl}_2/\text{Dioxane}$ (20:1)	Dioxane	DMF^b	CHCl_3
Time / h	24	36	36	24	24	24
Yield %	trace	15	16	trace	--	45

^a yield indicated as 'trace' was based on TLC; ^b DCC was used instead of EDC

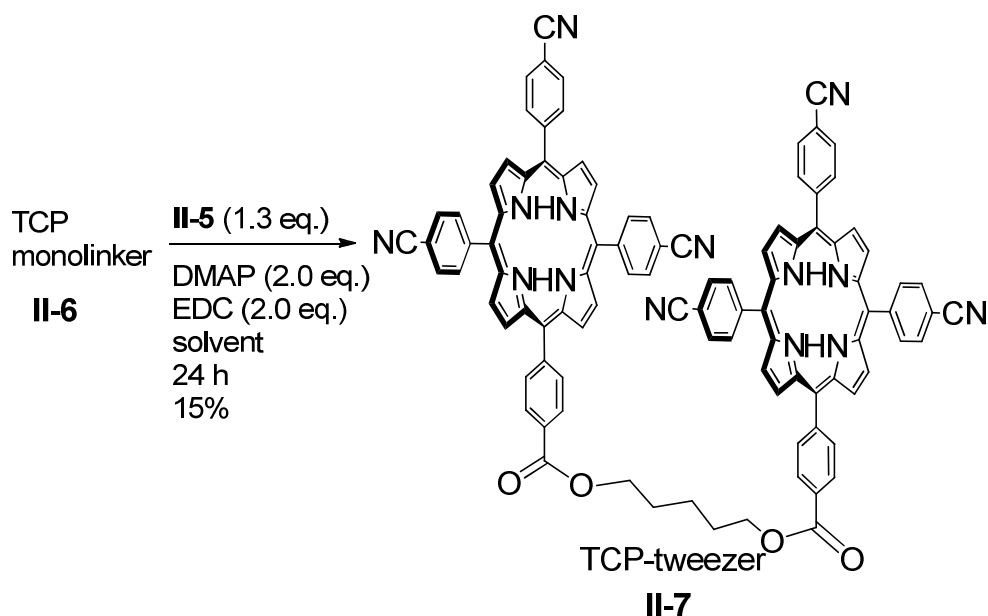


Scheme II-2. Synthesis of TCP porphyrin monolinker **II-6**.

out in refluxing THF / NaOH (2 M). After aqueous work-up, the porphyrin acid **II-5** was obtained as a purple solid which was pure enough for next step without the need

for column chromatography. Unfortunately, the next two steps of coupling reactions (Scheme II-2) turned out to be problematic due to poor solubility of acid **II-5**.

In CH_2Cl_2 which is typical solvent for porphyrin coupling with 1,5-pentanediol, the acid formed suspension and only trace amount of porphyrin monolinker **II-6** was detected by TLC. To solve the solubility issue, several solvents were screened to get better yield (Table II-1). DMF was the only solvent that completely dissolved the substrates yielding a clear purple solution. However, the DCC coupling in DMF only gave an unknown compound. THF and 1,4-dioxane can partially dissolve the porphyrin acid, but the esterification reaction did not proceed well. Slow conversion was also seen when mixed solvents were used.



Scheme II-3. Synthesis of TCP porphyrin tweezer **II-7**.

CHCl_3 dissolved the porphyrin acid better than CH_2Cl_2 and THF. But, the first trial with CHCl_3 afforded 48% of porphyrin ethyl ester in addition to 23% of monolinker. Formation of porphyrin ethyl ester is the result of the 1% ethyl alcohol present in reagent grade CHCl_3 . Purified CHCl_3 was employed for the coupling and

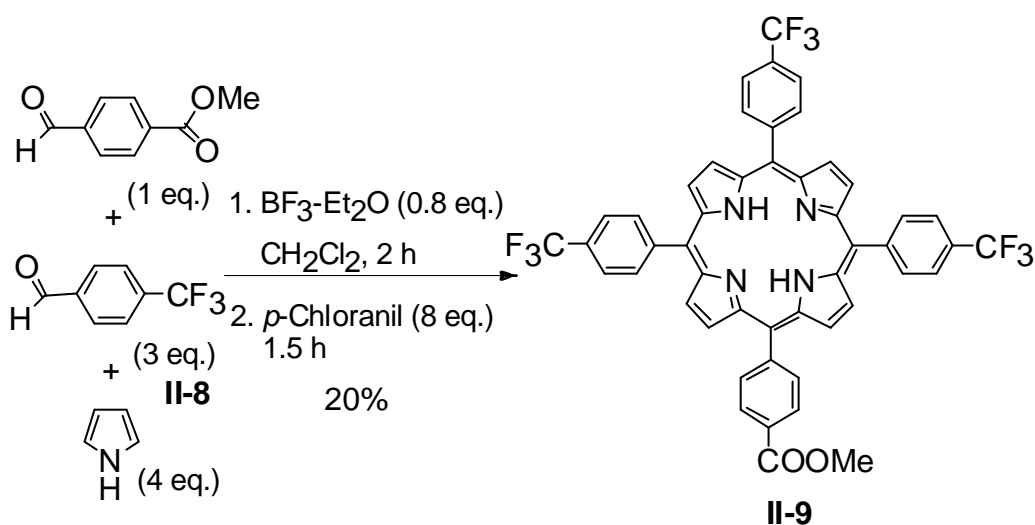
an improved yield of **II-6** was obtained. CHCl_3 was also used in following coupling reaction for making TCP tweezer **II-7**, but low yield was obtained. Other solvents were also tested and afforded similar or worse results. FAB-MS confirmed the presence of tweezer **II-7** in the isolated product. However, ^1H NMR revealed a lot of impurities which were difficult to remove.

Table II-2. Effect of solvent in synthesis of TCP tweezer **II-7**^a

Solvent	$\text{CH}_2\text{Cl}_2/\text{THF}$ (20:1)	$\text{CH}_2\text{Cl}_2/\text{DMSO}$ (20:1)	DMF	CHCl_3
Time / h	24	48	24	24
Yield %	trace to 26	trace	trace	15

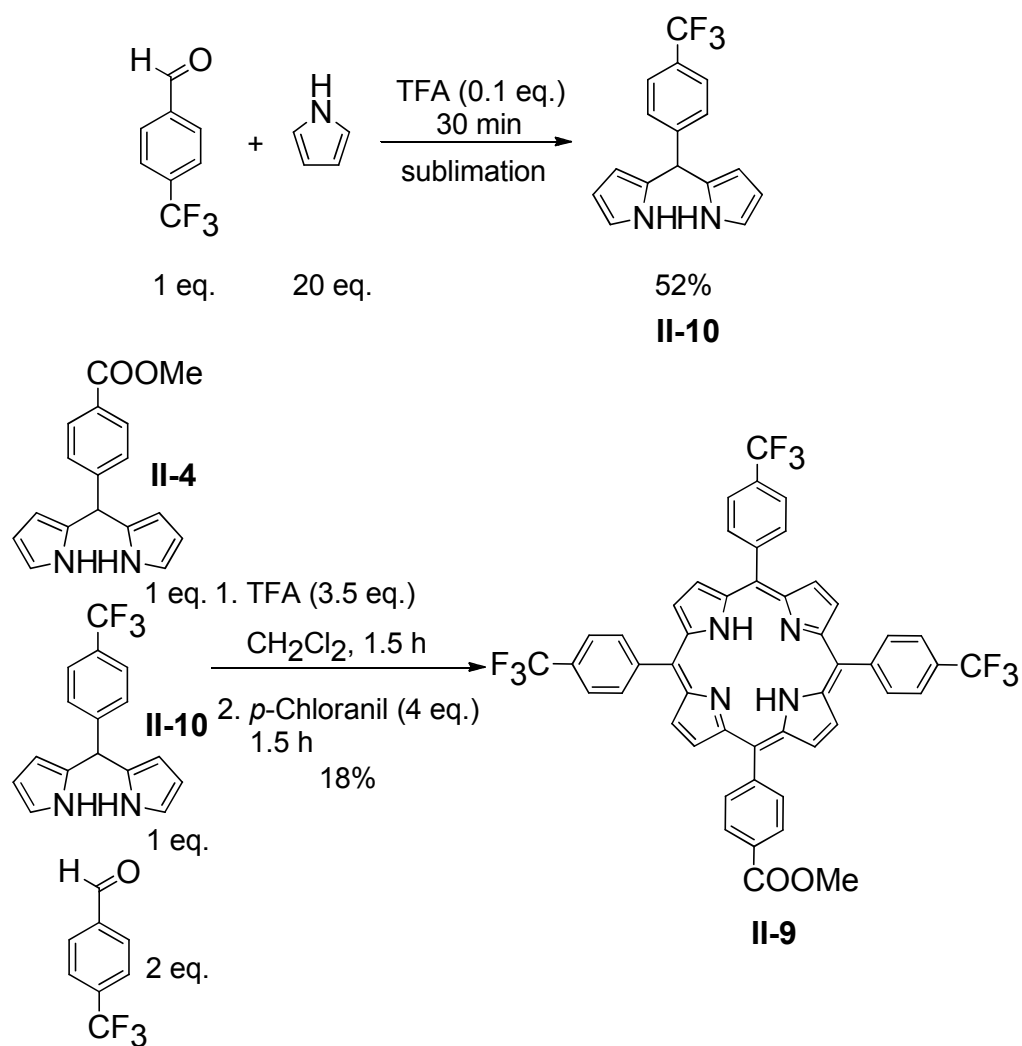
^a yield indicated as 'trace' was based on TLC

To overcome the solubility problem, the $-\text{CF}_3$ group was used as the electron-withdrawing group. The porphyrin synthesis using 4-trifluoromethyl benzaldehyde **II-8** proceeded uneventfully (Scheme II-4) under standard condition affording pure monoester in good yield (20%).

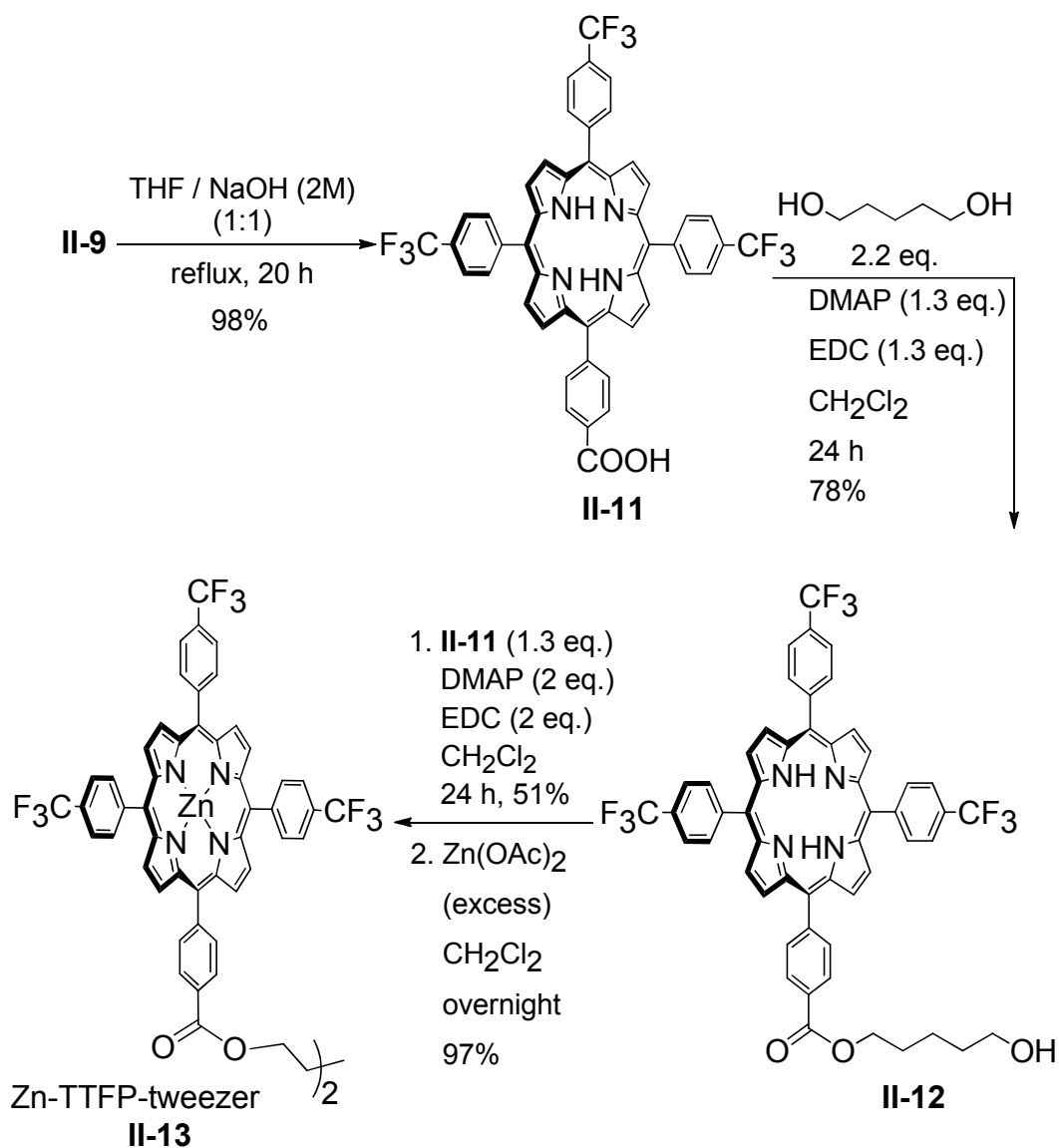


Scheme II-4. Synthesis of porphyrin monoester **II-9** via condensation of aldehydes.

The dipyrromethane protocol was also examined to evaluate its efficiency for porphyrin synthesis (Scheme II-5) and a comparable yield was obtained (18%). But isolation of 5-(4-trifluoromethylphenyl) dipyrromethane **II-10** from residue pyrrole and impurities was not easy since it was hard to recrystallize this compound. Sublimation was finally employed to get pure product but with low yield. Considering the use of large amount of pyrrole and the low yield in dipyrromethane synthesis, the standard procedure (Scheme II-4) was preferred for synthesis of other porphyrins.



Scheme II-5. Synthesis of porphyrin monoester **II-9** via condensation of dipyrromethanes.

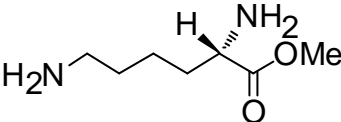
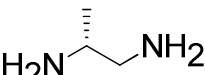
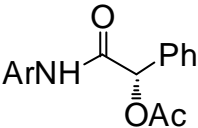
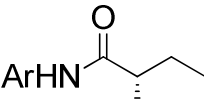
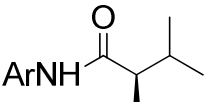
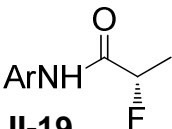


Scheme II-6. Synthesis of Zn-TTFP porphyrin tweezer **II-13**.

With ample amount of porphyrin monoester **II-9** in hand, the synthesis of tri(4-trifluoromethylphenyl) porphyrin (TTFP) tweezer was accomplished with satisfactory yields (Scheme II-6) owing to the good solubility and reactivity of 5-(4-hydroxycarbonylphenyl)-10, 15, 20-tri(4-trifluoromethyl phenyl)porphyrin (TTFP monoacid **II-11**). Incorporation of zinc was proved by FAB-MS and ¹H NMR which indicated the metallation via the disappearance of N-H protons of porphyrins. ECCD study using this new porphyrin tweezer was then carried out to examine its

efficiency for chirality sensing. ECCD studies were performed in hexanes for diamines and in methylcyclohexane for chiral carboxylic acids (Table II-3). The latter were derivatized via EDC coupling with 1,4-phenylenediamine as a carrier⁶ providing two binding sites for the porphyrin tweezer: one through the amino-group, and another through the carbonyl oxygen.

Table II-3 ECCD data for chiral diamines and derivatized α -chiral carboxylic acids bound with tweezer **II-1** and **II-13**

 II-14		 II-15		 II-16		
	λ nm, ($\Delta\epsilon$)	A^a	λ nm, ($\Delta\epsilon$)	A^a	λ nm, ($\Delta\epsilon$)	A^b
TPP-Zn	433 (-154)	-321	435 (-93)	-169	430 (-14)	-28
	423 (+167)		426 (+76)		418 (+14)	
TTFP-Zn	430 (-337)	-572	430 (-175)	-232	429 (+63)	+114
	420 (+235)		420 (+147)		421 (-51)	
 II-17		 II-18		 II-19		
	λ nm, ($\Delta\epsilon$)	A^b	λ nm, ($\Delta\epsilon$)	A^b	λ nm, ($\Delta\epsilon$)	A^b
TPP-Zn	423 (-23)	-41	428(-43)	-84	428 (+33)	+69
	413 (+18)		418 (+41)		420 (-36)	
TTFP-Zn	430 (+76)	+106	429 (-202)	-382	429 (+182)	+340
	421 (-30)		422 (+180)		420 (-158)	

^a Hexane was used as solvent, ^b Methylcyclohexane was used as solvent; Spectra were taken at 0 °C with tweezer (1 μ M) and 40 eq. of guest.

As shown in Table II-3, the Zn-TTFP tweezer (**II-13**) complex with chiral diamines and derivatized α -chiral carboxylic acids yielded ECCD of much stronger

amplitudes compared to those from the electron-neutral Zn-TPP tweezer **II-1** indicating greatly improved sensitivity as chirality sensor. This improvement was presumably attributed to the enhanced binding affinity, which is induced by the electron-withdrawing *p*-trifluoromethylphenyl groups.

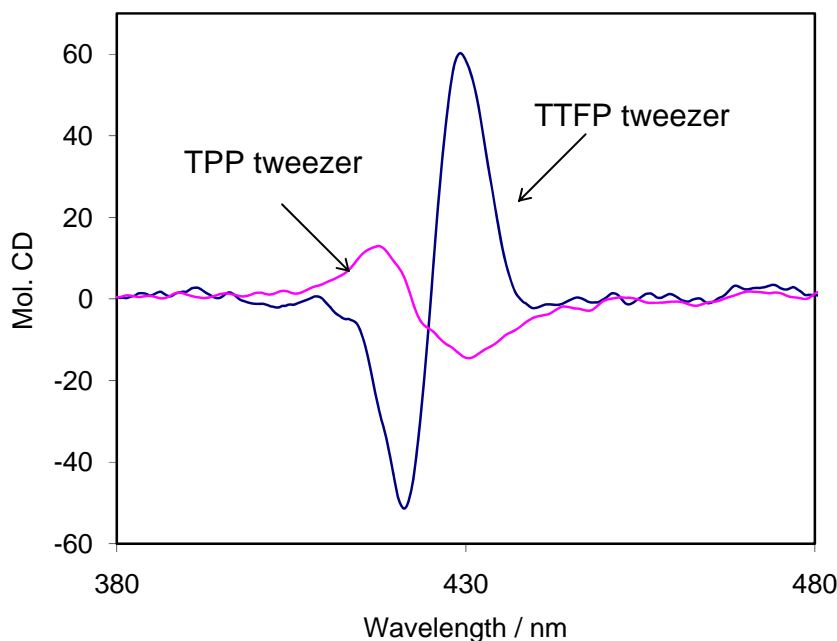


Figure II-7. The reversed ECCD spectra of **II-16** with different tweezers

However, an interesting trend was noticed for derivatized α -chiral acids; the new tweezer **II-13** rendered intense ECCD signals with signs opposite to the predicted ones implying a different stereodifferentiation process. For example, **II-16** exhibited a weak *negative* ECCD signal ($A = -28$) upon complexation with Zn-TPP tweezer **II-1**, but rendered a prominent *positive* ECCD couplet in the presence of Zn-TTFP tweezer **II-13** (Figure II-7). Interestingly, in the case of α -halogenated chiral acid (**II-19**), both tweezers seem to behave similarly by giving the same sign. These inconsistencies compromised the utility of TTFP tweezer **II-13** for chirality sensing of

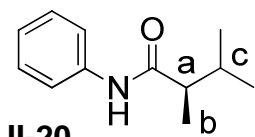
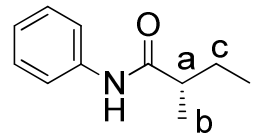
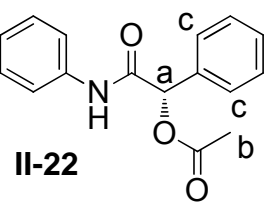
α -chiral acids and prompted us to conduct ^1H NMR binding experiments, which could offer important insights about the ECCD active conformations of the tweezer complexes. Zinc porphyrin monoesters have been used previously as simplified models of the zinc porphyrin tweezers for ^1H NMR binding studies and proved to be reliable.¹⁸ Therefore, zinc TTFP monoester (**II-9**) and zinc TPP monoester were chosen as tweezer models in our binding study. Some insights can be obtained through the comparison of proton chemical shift changes of substituents at α positions of chiral amides before and after complexation with zinc porphyrin monoesters. Obviously, all the protons should shift up-field upon complexation with zinc porphyrins due to the strong shielding effect of the huge porphyrin aromatic ring. For substituents that are closer to the porphyrin ring, more significant up-field shift should be observed compared to the one farther away from the porphyrin ring. Hence, the $\Delta\delta = \delta_{\text{complex}} - \delta_{\text{free}}$ of different substituents at the same α carbon can be used to probe the preferred conformations of the chiral center. Three α -chiral amides (**II-20~II-22**) were synthesized as guest models and subjected to NMR binding analysis.

As shown in Table II-4, all protons of interest shifted up-field upon complexation of amides with the metalloporphyrins. More significant up-field shifts were observed for the Zn-TTFP model system that is consistent with its stronger binding affinity. This explains the higher ECCD amplitude with the Zn-TTFP tweezer. In all cases, the small substituent (Ha) on the chiral carbon shifted most, followed by the large group (Hc) and then the middle group (Hb). This trend is also

observed in similar ^1H NMR analysis of Zn-porphyrin complex with chiral amides.¹⁸

Since both porphyrin model systems in Table II-4 exhibited the same trend indicating the similar conformation of porphyrin-amide complex in CDCl_3 at millimolar concentrations, the NMR binding experiment does not provide a clue for the reversed ECCD sign with the Zn-TTFP tweezer system in methylcyclohexane at micromolar concentrations. Due to solvent competition for coordination to the Lewis acidic Zn-TTFP tweezer, the derivatized α -chiral carboxylic acids were ECCD silent in CDCl_3 solution precluding further solvent studies with this new host.

Table II-4 NMR analysis of α -chiral amides in Zn-TPP and Zn-TTFP tweezer complex^a

Substrate	TPP-Zn			TTFP-Zn		
	$\Delta\delta = \Delta\delta_{\text{complex}} - \Delta\delta_{\text{free}}$			$\Delta\delta = \Delta\delta_{\text{complex}} - \Delta\delta_{\text{free}}$		
	$\Delta\delta$ (Ha)	$\Delta\delta$ (Hb)	$\Delta\delta$ (Hc)	$\Delta\delta$ (Ha)	$\Delta\delta$ (Hb)	$\Delta\delta$ (Hc)
 II-20	-0.201	-0.108	-0.157	-0.223	-0.146	-0.208
 II-21	-0.077	-0.046	-0.062	-0.143	-0.093	-0.125
 II-22	-0.058	-0.011	-0.028	-0.087	-0.018	-0.043

^a CDCl_3 was used as solvent, porphyrin : substrate = 1:1

The inconsistency of the Zn-TTFP tweezer did not stop our quest for a highly

sensitive chirality sensor using porphyrin tweezer methodology. We already saw the improved sensitivity for the new tweezer and the reversed ECCD signals. Clearly, more electron deficient porphyrin tweezers needed to be synthesized and evaluated along with the electron rich analogs to reveal a complete picture of the electronic factors in the stereochemical determination using porphyrin tweezers.

Table II-5. Synthetic yields for synthesis of new porphyrin tweezers

Aromatic substituent	Yield %				
	Monoester	Monoacid	Monolinker	Tweezer	Zn-Tweezer
<i>p</i> -CN-C ₆ H ₄ - (TCP)	18 ^{a,b}	91	45 ^{b,c}	15 ^{b,c,d}	--
<i>p</i> -MeO-C ₆ H ₄ - (TMOP)	-- ^c	6 ^e	53	31	83
<i>p</i> -CF ₃ -C ₆ H ₄ - (TTFP)	20 ^b	98 ^b	78 ^b	51	97
<i>p</i> -CF ₃ -C ₆ H ₄ - (TTFP)	13	96	87	21	95
C ₆ F ₅ - (TPFP)	19 ^b	98 ^b	88 ^b	80 ^b	88 ^b
<i>p</i> -CH ₃ -C ₆ H ₄ - (TMP)	12	96	69	42	92

^aDipyrromethanes were used instead of aldehydes; ^boptimized yields; ^cCHCl₃ was used as solvent; ^ddifficult to purify; ^eyield over two steps; all yields were not optimized unless otherwise indicated.

Several new porphyrin tweezers were prepared following standard procedures depicted in Scheme II-4 and Scheme II-6 without difficulty. The synthetic yields for each step are tabulated in Table II-5.

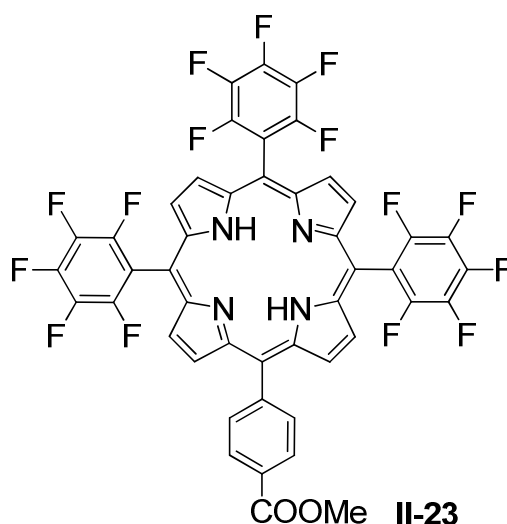
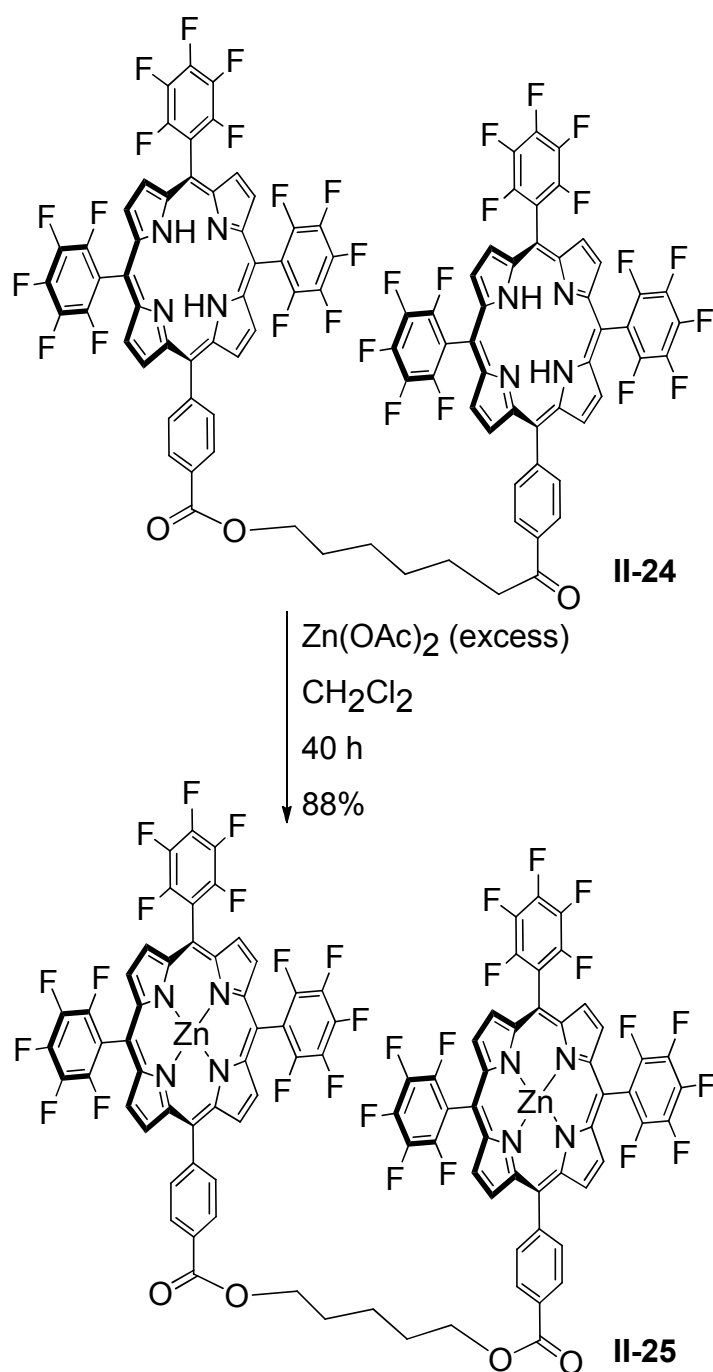


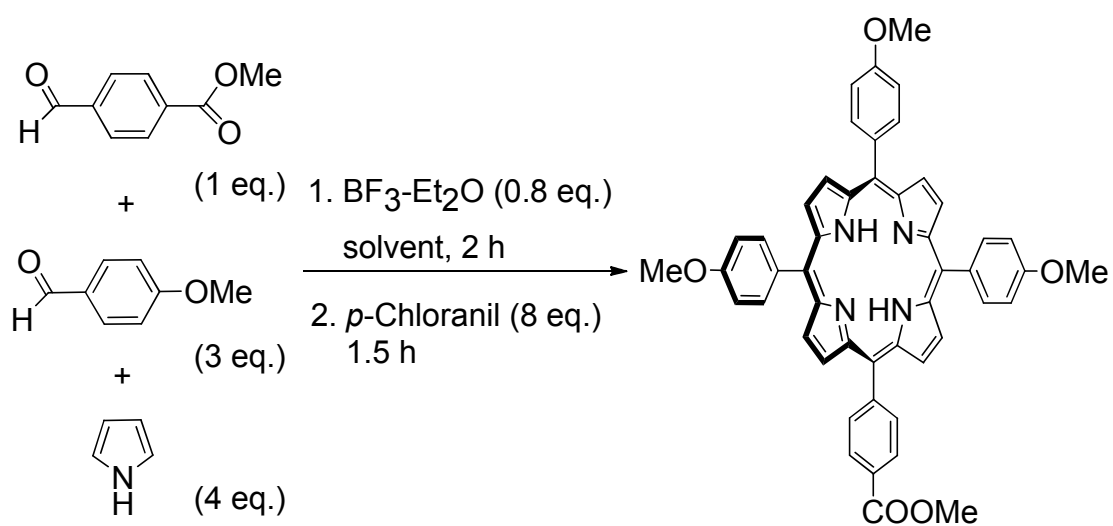
Figure II-8. The structure of TPFP monoester **II-23**.

5-(4-Methylcarboxyphenyl)-10,15,20-tri(pentafluorophenyl)porphyrin **II-23** (TPFP) was synthesized smoothly. This monoesters was washed with 0.5 M NaOH after first silica gel column to remove most of *p*-chloranil residue. This was found to be an efficient way to get rid of the *p*-chloranil residue facilitating the second silica gel column chromatography to get pure monoester products. Hydrolysis of monoester (**II-23**) in refluxing THF / NaOH (2 M) was completed within 12 h and pure monoacid were obtained in near quantitative yields without the need for further purification. Synthesis of free TPFP tweezer (**II-23**) required optimization of the reaction conditions (solvent, time) to reach a decent yield (80%). Initial trial of metalation of free TPFP tweezer (**II-23**) was surprisingly slow and significant amount of free tweezer remained after 24 h. After column separation, the recovered free tweezer was submitted to metalation again for 24 h giving a good overall conversion. Further optimization of solvent and reaction time can improve the yield of one-step metalation to 88% affording pure Zn-TPFP tweezer **II-25** (Scheme II-7).

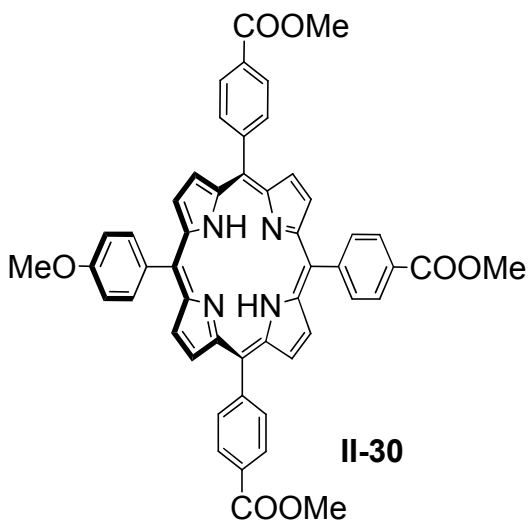
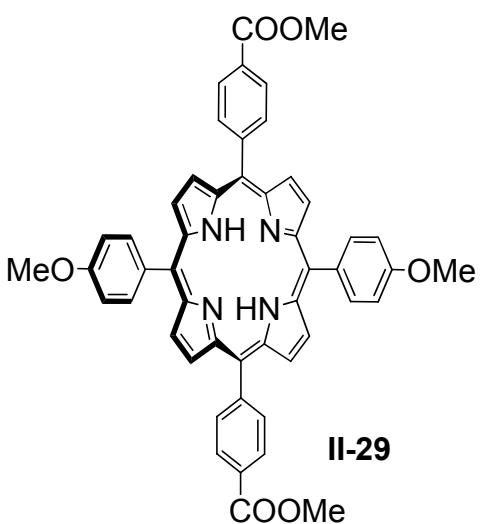
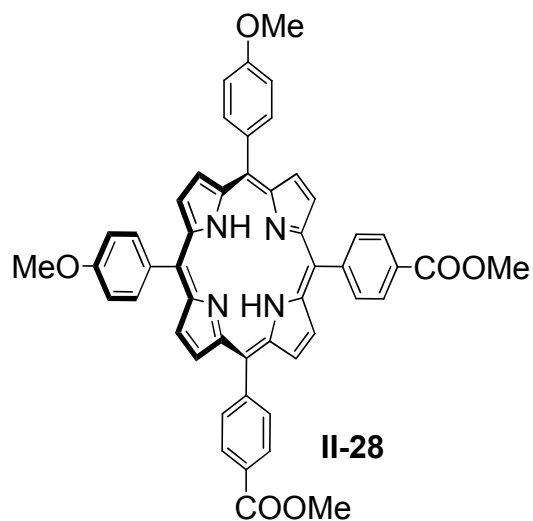
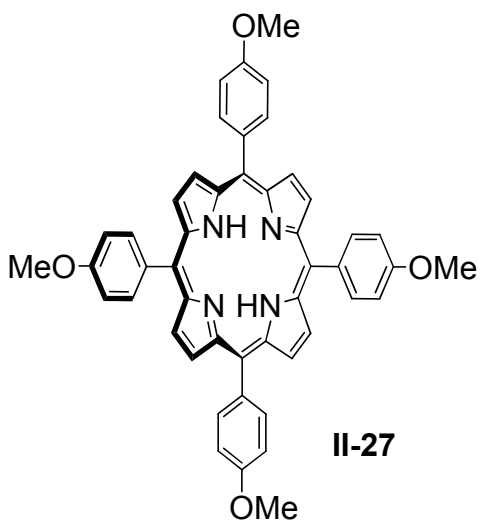


Scheme II-7. Metalation of freeTPFP porphyrin tweezer **II-24**.

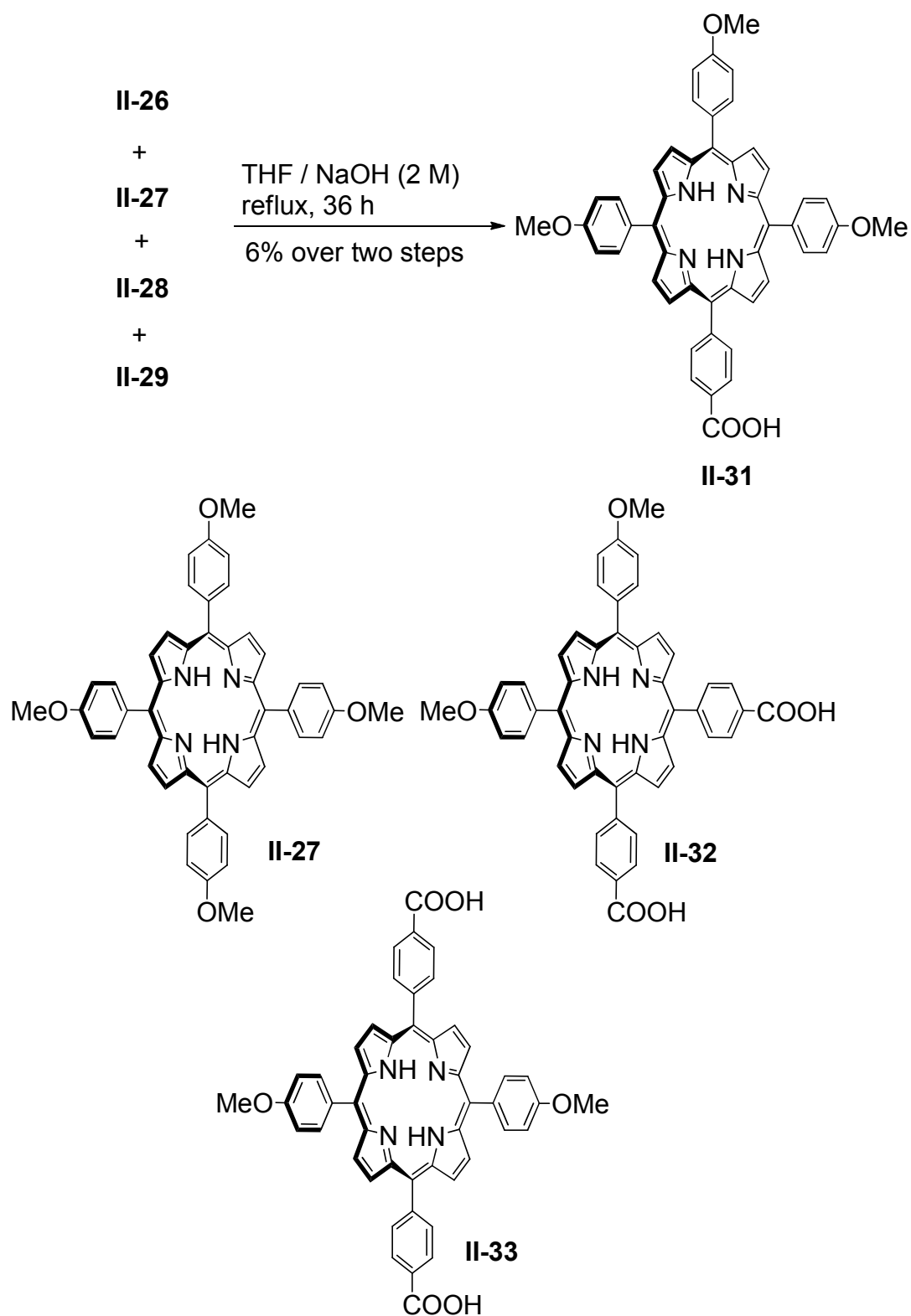
Though CH₂Cl₂ proved to be a good solvent for the synthesis of most porphyrin monoesters in Table II-5, the assembly of TMOP monoester required the use of CHCl₃. Best result (Table II-6) was in obtained CHCl₃ with apparent rate acceleration which can be easily observed through color change during the



II-26



Scheme II-8. Synthesis of TMOP monoester **II-26**.



Scheme II-9. Synthesis of TMOP monoacid **II-31**.

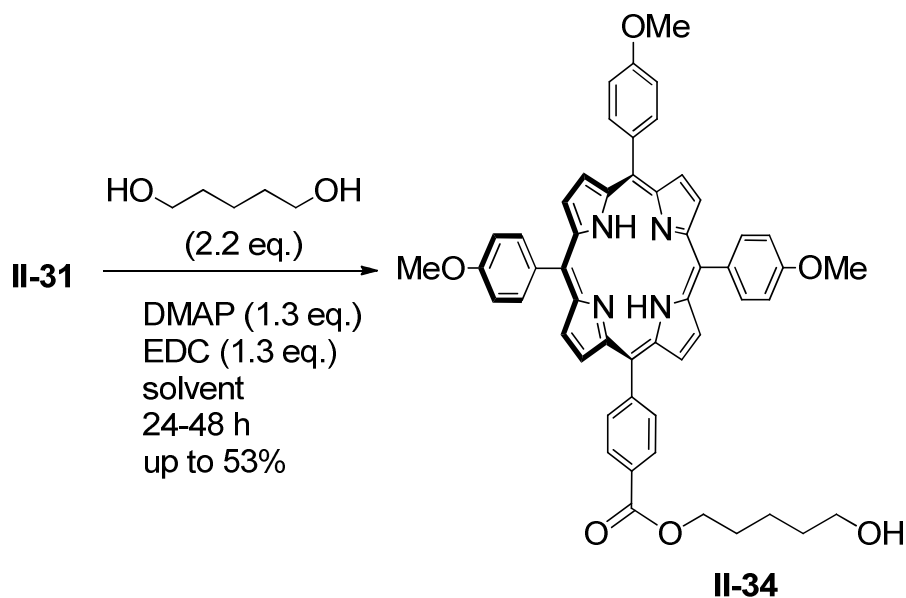
reaction. However, under optimal conditions, we still got the mixture of several side products (Scheme II-8). Isolation of pure monoester **II-26** from this mixture was difficult and required multiple column chromatography. Alternatively, after running through the first column to remove most of the non-porphyrin byproducts, the mixture can be directly subjected to hydrolysis affording a mixture of **II-27** and porphyrin acids (**II-31~II-33**) which could be separated by column chromatography giving the pure monoacid **II-31** in 6% yield after two steps (Scheme II-9).

Table II-6. Solvent & catalyst effect in the synthesis of TMOP monoester **II-26**

Solvent	Catalyst / Oxidant	Time / h	Product
CH ₂ Cl ₂	TFA (1.7 eq.) / <i>p</i> -Chloranil (2 eq.)	4	Mess
CH ₂ Cl ₂	BF ₃ ·Et ₂ O (0.2 eq.) / <i>p</i> -Chloranil (2 eq.)	4	II-27
CH ₂ Cl ₂	BF ₃ ·Et ₂ O (0.8 eq.) / <i>p</i> -Chloranil (8 eq.)	2	II-26~II-29
CHCl ₃	BF ₃ ·Et ₂ O (0.8 eq.) / <i>p</i> -Chloranil (8 eq.)	2	II-26~II-29

The esterification step in the synthesis of TMOP monolinker **II-34** did not provide good yields after several trials (Scheme II-10) in different solvents

(CHCl₃, CH₂Cl₂, THF) mainly due to the poor solubility of TMOP acid **II-31** (Table II-7).



Scheme II-10. Synthesis of TMOP monolinker **II-34**.

Table II-7. Effect of solvent effect in the synthesis of TMOP monolinker **II-34**^a

Solvent	Time / h	Yield %
CH ₂ Cl ₂	24	trace
CH ₂ Cl ₂ / THF 20 : 1	48	41
CH ₂ Cl ₂ / Dioxane 20 : 1	36	45
CHCl ₃	36	53

Overall, the synthesis of porphyrin tweezers bearing electron-withdrawing group at porphyrin *meso* positions proceeded well as long as the porphyrin monoacid has decent solubility in organic solvents used for esterification with diol. With

these new porphyrin tweezers in hand, a series of UV-vis and ECCD studies were conducted.

UV-vis profiles of these newly synthesized tweezers were first analyzed spectroscopy (Table II-8). The UV absorption data (λ_{max}) was obtained in different solvents and the molar extinction coefficient (ϵ) was calculated in methylcyclohexane (Table II-8). TPFP tweezer stood out with large molar extinction coefficient in methylcyclohexane. Coupled with the belief that TPFP tweezer will have greatly enhanced binding affinity owing to the introduction of highly electron-withdrawing penta-fluorophenyl groups at the porphyrin *meso* positions, we were optimistic that it would demonstrate enhanced sensitivity as a chirality sensor in ECCD-based stereochemical determination.

Table II-8. Absorptions and λ_{max} for different zinc porphyrin tweezers^a

		Methylcyclohexane		Hexane	CH ₂ Cl ₂
		λ , nm	ϵ	λ , nm	λ , nm
TPP	II-1	416.2	650,000	413.5	419.1
TMOP	II-35	418.6	850,000	418.4	422.7
TFP	II-36	414.5	580,000	411.7	418.9
TTFP	II-13	413.4	410,000	408.3	418.9
TPFP ^b	II-25	413.0	1100,000	412.0	416.4

^a concentration of tweezer is 1 μM unless otherwise indicated; ^b concentration of tweezer is 0.5 μM .

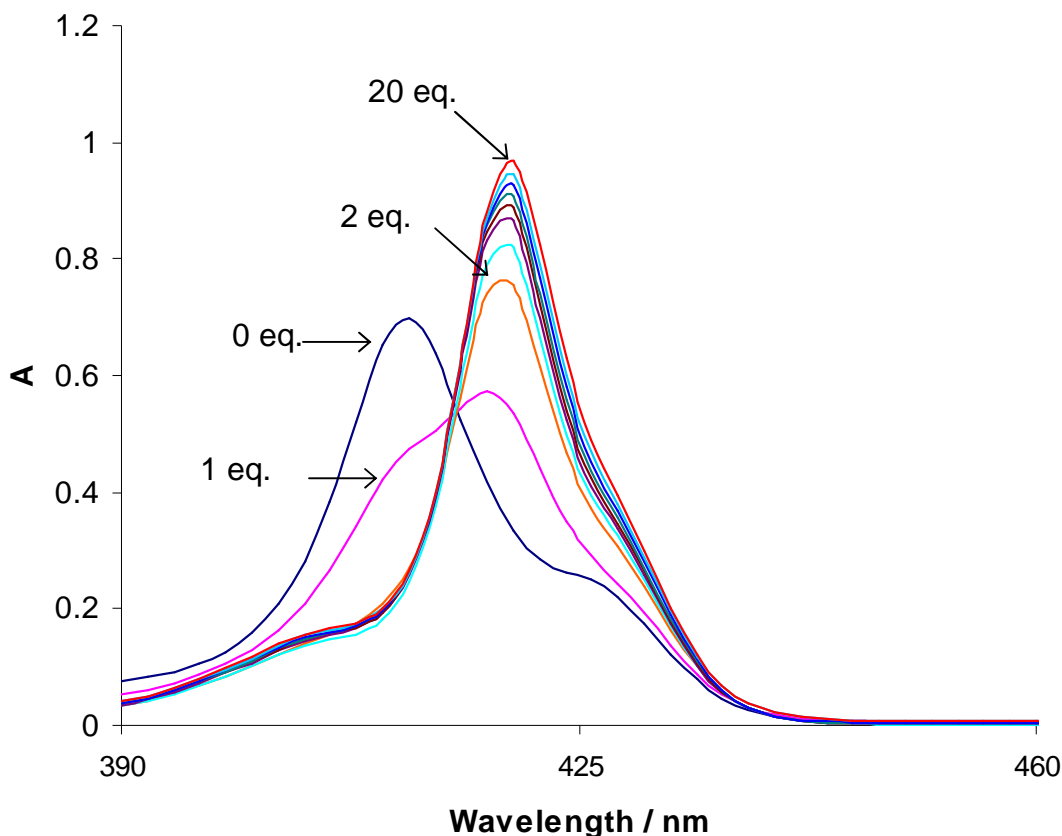


Figure II-9. UV-vis titration of Zn-TPFP tweezer (**II-25**) solution (0.5 μ M in MCH) with L-lysine methyl ester (1 mM in DCM).

The preliminary UV-vis binding study was carried out through titration of Zn-TPFP tweezer (**II-25**) solution (0.5 μ M in MCH) with L-lysine methyl ester (1 mM in DCM) from 1 eq. to 20 eq. and is shown in Figure II-9. Upon titration, the porphyrin Soret band (B band) underwent dramatic red-shifts from 413 nm to 424 nm in response to the binding with strong nucleophilic guest. This red-shift is accompanied with a clear isosbestic point indicating a smooth interconversion between two species, free tweezer and the tweezer-substrate complex. The Q band of the free tweezer at 544 nm also showed the same trend as revealed by the inset graph in Figure II-8. These results agree well with the common binding behavior of

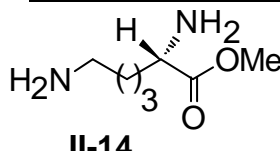
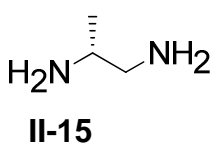
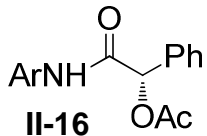
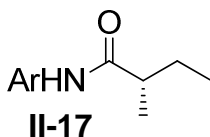
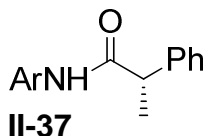
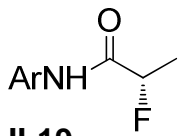
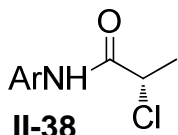
zinc porphyrins with nucleophilic small molecules.¹⁹

II.2 ECCD Study Using Electronically Tuned Porphyrin Tweezers

ECCD studies were then performed in hexanes for diamines and in methylcyclohexane for derivatized chiral carboxylic acids at 0 °C. Tweezers were titrated with chiral guests from 1 : 1 to 1 : 40 eq of guests and ECCD data at 1 : 20 eq. were reported (Table II-9).

As expected, the highly electron deficient Zn-TPFP tweezer demonstrated significantly improved sensitivity by yielding over two-fold increase in amplitudes for most substrates, as compared to the Zn-TPP tweezer. The observed ECCD signs are consistent with the ones obtained by using Zn-TPP tweezer suggesting a similar stereochemical differentiation mechanism in these two tweezer systems. It should be pointed out that, in the presence of Zn-TPFP tweezer the *S*-2-fluoropropyl acid gave the sign opposite to the predicted one. The origin of this sign inversion is not known. But we tentatively attribute it to the highly fluorinated nature of TPFP tweezer which might lead to certain secondary interaction since this phenomena is not found for other electronic deficient tweezers.

Table II-9 ECCD data of chiral diamines and derivatized carboxylic acids^a

Aromatic substituent	λ , nm ($\Delta\epsilon$)			A	
	TPP II-1	TPFP II-25	TTFP II-13	TFP II-24	TMOP II-23
 II-14	433(-154) 423(+167) -321	425 (-390) 417 (+200) -590	430 (-337) 420 (+235) -572	430(-315) 421(+228) -543	435(-155) 424 (+145) -300
 II-15	435 (-93) 426 (+76) -169	425 (-159) 417 (+126) -285	430 (-175) 420 (+147) -232	431(-143) 419(+122) -265	433 (-55) 423 (+65) -121
 II-16	430 (-14) 418 (+14) -28	426 (-126) 418 (+96) -222	429 (+63) 421 (-51) +114	428(+142) 421(-111) +253	No ECCD
 II-17	423 (-23) 413 (+18) -41	424 (-171) 417 (+134) -305	430 (+76) 421 (-30) +106	430(+57) 421 (-41) +98	No ECCD
 II-37	426 (120) 417 (-80) +200	424 (+539) 417 (-355) +894	431 (-21) 423 (+52) -73	426 (+84) 417 (-59) +143	431(+18) 423 (-22) +40
 II-19	428 (+33) 420 (-36) +69	425 (-67) 417 (+70) -137	429 (+182) 420 (-158) +340	428(+208) 419(-163) +371	ND
 II-38	429 (+64) 420 (-54) +118	425 (+259) 417 (-159) +418	428 (+253) 420 (-207) +461	428(+298) 419(-233) +531	ND

^a tweezer / substrate ratio - 1 : 20, ND = not determined

The electronic deficient Zn-TTFP (**II-13**) and Zn-TFP tweezer (**II-36**) also generally yielded more intense ECCD signals as compared Zn-TPP tweezer (**II-1**).

However, an interesting deviation was noticed as described previously for Zn-TTFP tweezer (**II-13**). For chiral carboxylic acids that do not have secondary interactions (halogen- π interaction in case of α -halogenated chiral amides¹⁸, see ref 18 for details about this interaction in ECCD study), Zn-TTFP (**II-13**) and Zn-TFP (**II-36**) tweezers reported signs opposite to the ones obtained using Zn-TPP tweezer. As discussed in the previous section, an interpretation of this sign switch is difficult especially in the tweezer system where multiple conformations may exist and compete.

Electron rich Zn-TMOP tweezer (**II-35**) exhibited much lower sensitivity and even failed to yield ECCD signal for some derivatized chiral carboxylic acids. This could be explained by the decreased binding affinity of this tweezer due to the reduced Lewis acidity of the zinc cation resulting from the strong electron-donating effect of MeO- group.

The electronic factors contributing to the determination of absolute configurations using the tweezer method has been demonstrated by the ECCD data in Table II-9. Though some deviations still remain, one can concluded that the influence of electronic factors can lead altered characteristics of porphyrin tweezers. To further investigate the change of binding affinity induced by tuning electronics at the porphyrin periphery, a computational study was conducted. The molecule mechanic (MM) methods and semi-empirical methods do not consider electronic correlation and, therefore, is not accurate enough for calculating the critical interactions between metal cations and ligands. Density Functional Theory (DFT) was chosen due to its accuracy and reliability in describing metal-ligand interactions.

In addition, DFT calculations only require moderate computation time and hence are less expensive compared to the classical *ab initio* Hartree Fock method. In our study, the most widely used B3LYP method was used in combination with Lanl2dz effective core potential (ECP) basis set to obtain critical charges and interaction energies. Considering the huge size of porphyrin tweezers, 5-(4-methylcarboxyphenyl)-10,15,20-triarylporphyrins were used as tweezer models.

Table II-10. Calculated charge and energetic information for porphyrin monoesters^a

	PM3			B3LYP/Lanl2dz // PM3	
	HOMO / ev	LUMO / ev	Dipole	HOMO / ev	LUMO / ev
TMOP-monoester	-7.710	-1.900	5.011	-5.265	-2.362
TPP-monoester	-7.748	-1.927	2.395	-5.286	-2.372
TFP-monoester	-7.948	-2.125	1.526	-5.626	-2.712
TTFP-monoester	-8.194	-2.353	2.377	-5.890	-2.954
TPFP-monoester	-8.353	-2.561	1.884	-6.224	-3.273

^a(S)-Lysin methylester: HOMO = -9.593 ev, LUMO = 0.983 ev, PM3; HOMO = -6.009 ev, LUMO = -0.209 ev, B3LYP/Lanl2dz // PM3

Geometry optimization was conducted using PM3 semi-empirical method which usually renders decent geometry description for rigid molecules. Single point energy calculations were performed using B3LYP/Lanl2dz method to provide more

accurate energetic information. As shown in Table II-10, with the increase of electron-withdrawing capability of the phenyl ring, the LUMO energy of the porphyrin decreases. This is important since the porphyrin host-guest complexation is a process in which the LUMO of the zinc porphyrin host interacts with the HOMO of the nucleophilic chiral guest. The decreased LUMO energy of the porphyrin would result in a smaller energy gap between the two interacting orbitals leading to a stronger orbital interaction as well as better binding. The TPFP model gave the lowest LUMO energy signifying the strongest orbital interaction with the guest molecule. The calculated dipoles at PM3 level are also shown in Table II-10.

In summary, a series of novel electron rich and electron deficient porphyrin tweezers were synthesized and employed in ECCD study. The electron deficient zinc porphyrin tweezers (TPFP, TTFP, TFP) have demonstrated greatly improved sensitivity in absolute stereochemical determination. Zn-TPFP tweezer stands out owing to its excellent sensitivity and consistency in ECCD measurements. We proposed that it could provide a direct and expedient approach towards the chirality sensing of normally weak binding or non-binding substrates such as diols and amino alcohols. Related ECCD study of these substrates will be discussed in next chapter.

II.3 Experimental Procedures

Anhydrous CH_2Cl_2 was dried and redistilled over CaH_2 . The solvents used for CD measurements were purchased from Aldrich and were spectra grade. All reactions were performed in dried glassware under nitrogen. Column chromatography was performed using SiliCycle silica gel (230-400 mesh). ^1H NMR and ^{13}C NMR spectra were obtained on a Varian Inova 300 MHz or 500 MHz instrument and are reported in parts per million (ppm) relative to the solvent resonances (δ), with coupling constants (J) in Hertz (Hz). IR studies were performed on a Nicolet FT-IR 42 instrument. UV/Vis spectra were recorded on a Perkin-Elmer Lambda 40 spectrophotometer, and are reported as λ_{max} [nm]. CD spectra were recorded on a JASCO J-810 spectropolarimeter, equipped with a temperature controller (Neslab 111) for low temperature studies, and were reported as $\lambda[\text{nm}]$ ($\Delta\epsilon_{\text{max}}$ [$\text{L mol}^{-1} \text{cm}^{-1}$]). HRMS analyses were performed on a Q-TOF Ultima system using electrospray ionization in positive mode.

Binding study of Zn TTFP monoester and Zn TPP monoester:

Guest molecules were synthesized according to following procedure: α -chiral carboxylic acid (50 mg), aniline (5 eq.), EDC (1.2 eq.), and DMAP (5 eq.) were dissolved by dry CH_2Cl_2 (15 mL) in a 50 mL round-bottom flask. The solution was stirred overnight under nitrogen and then concentrated under reduced pressure. Following purification by silica gel chromatography afforded α -chiral carboxylic benzamide in 70-80% yield. ^1H NMR of α -chiral carboxylic benzamide in CDCl_3

was first taken. Zinc porphyrin monoester was then added to the solution, shaken for 5 minutes and taken to ^1H NMR was measured (the integration showed that porphyrin : amide ratio is 1 : 1).

REFERENCES

REFERENCES

1. Huang, X. F.; Nakanishi, K.; Berova, N., Porphyrins and metalloporphyrins: Versatile circular dichroic reporter groups for structural studies. *Chirality* **2000**, 12, (4), 237-255.
2. Matile, S.; Berova, N.; Nakanishi, K.; Fleischhauer, J.; Woody, R. W., Structural studies by exciton coupled circular dichroism over a large distance: Porphyrin derivatives of steroids, dimeric steroids, and brevetoxin B. *Journal of the American Chemical Society* **1996**, 118, (22), 5198-5206.
3. Matile, S.; Berova, N.; Nakanishi, K.; Novkova, S.; Philipova, I.; Blagoev, B., Porphyrins - powerful chromophores for structural studies by exciton-coupled circular-dichroism. *Journal of the American Chemical Society* **1995**, 117, (26), 7021-7022.
4. Huang, X. F.; Rickman, B. H.; Borhan, B.; Berova, N.; Nakanishi, K., Zinc porphyrin tweezer in host-guest complexation: Determination of absolute configurations of diamines, amino acids, and amino alcohols by circular dichroism. *Journal of the American Chemical Society* **1998**, 120, (24), 6185-6186.
5. Proni, G.; Pescitelli, G.; Huang, X. F.; Quraishi, N. Q.; Nakanishi, K.; Berova, N., Configurational assignment of alpha-chiral carboxylic acids by complexation to dimeric Zn-porphyrin: host-guest structure, chiral recognition and circular dichroism. *Chemical Communications* **2002**, (15), 1590-1591.
6. Yang, Q.; Olmsted, C.; Borham, B., Absolute stereochemical determination of chiral carboxylic acids. *Organic Letters* **2002**, 4, (20), 3423-3426.
7. Huang, X. F.; Borhan, B.; Rickman, B. H.; Nakanishi, K.; Berova, N., Zinc porphyrin tweezer in host-guest complexation: Determination of absolute configurations of primary monoamines by circular dichroism. *Chemistry-a European Journal* **2000**, 6, (2), 216-224.
8. Huang, X. F.; Fujioka, N.; Pescitelli, G.; Koehn, F. E.; Williamson, R. T.; Nakanishi, K.; Berova, N., Absolute configurational assignments of secondary amines by CD-sensitive dimeric zinc porphyrin host. *Journal of the American Chemical Society* **2002**, 124, (35), 10320-10335.
9. Kurtan, T.; Nesnas, N.; Koehn, F. E.; Li, Y. Q.; Nakanishi, K.; Berova, N., Chiral

recognition by CD-sensitive dimeric zinc porphyrin host. 2. Structural studies of host-guest complexes with chiral alcohol and monoamine conjugates. *Journal of the American Chemical Society* **2001**, 123, (25), 5974-5982.

10. Kurtan, T.; Nesnas, N.; Li, Y. Q.; Huang, X. F.; Nakanishi, K.; Berova, N., Chiral recognition by CD-sensitive dimeric zinc porphyrin host. 1. Chiroptical protocol for absolute configurational assignments of monoalcohols and primary monoamines. *Journal of the American Chemical Society* **2001**, 123, (25), 5962-5973.

11. Eliel, E. L.; Wilen, S. H., *Stereochemistry of Organic Compounds*. Wiley & Sons: New York, 1993.

12. Proni, G.; Pescitelli, G.; Huang, X. F.; Nakanishi, K.; Berova, N., Magnesium tetraarylporphyrin tweezer: A CD-sensitive host for absolute configurational assignments of alpha-chiral carboxylic acids. *Journal of the American Chemical Society* **2003**, 125, (42), 12914-12927.

13. Borovkov, V. V.; Lintuluoto, J. M.; Inoue, Y., Supramolecular chirogenesis in zinc porphyrins: Mechanism, role of guest structure, and application for the absolute configuration determination. *Journal of the American Chemical Society* **2001**, 123, (13), 2979-2989.

14. Borovkov, V. V.; Lintuluoto, J. M.; Sugeta, H.; Fujiki, M.; Arakawa, R.; Inoue, Y., Supramolecular chirogenesis in zinc porphyrins: Equilibria, binding properties, and thermodynamics. *Journal of the American Chemical Society* **2002**, 124, (12), 2993-3006.

15. Lintuluoto, J. M.; Borovkov, V. V.; Inoue, Y., Direct determination of absolute configuration of monoalcohols by bis(magnesium porphyrin). *Journal of the American Chemical Society* **2002**, 124, (46), 13676-13677.

16. Harada, N.; Nakanishi, K., *Circular Dichroic Spectroscopy: Exciton Coupling in Organic Stereochemistry*. University Science Books: Mill Valley, CA, 1983.

17. Tanasova, M.; Vasileiou, C.; Olumolade, O. O.; Borhan, B., Enhancement of Exciton Coupled Circular Dichroism with Sterically Encumbered Bis-Porphyrin Tweezers. *Chirality* **2009**, 21, (3), 374-382.

18. Tanasova, M.; Yang, Q. F.; Olmsted, C. C.; Vasileiou, C.; Li, X. Y.; Anyika, M.; Borhan, B., An Unusual Conformation of alpha-Haloamides Due to Cooperative Binding with Zincated Porphyrins. *European Journal of Organic Chemistry* **2009**, (25), 4242-4253.

Chapter III

Determination of Absolute Configurations for *erythro* and *threo* Diols, Amino Alcohols, and Diamines using Zn-TPFP Tweezer

III.1 Background

III.1.1 The vicinal bisfunctionalized molecules

Vicinal substituted heterofunctionalized chiral molecules such as *erythro* and *threo* diols, amino alcohols, and diamines are widely present in biologically active natural and synthetic products such as alkaloids, polyketides and carbohydrates (Figure III-1). They also play a crucial role in asymmetric catalysis, functioning as fundamental building blocks or chiral auxiliaries and ligands (Figure III-1). The biological or catalytic activity of this class of compounds is often governed by their configurations. Consequently, development of methods to determine their absolute stereochemistry has been an active area of research.

III.1.2 Conventional methods for stereochemical determination of vicinal diols and amino alcohols

For the most part, the absolute stereochemical determination of *threo* substituted systems can be achieved with the implementation of the dibenzoate methodology.¹⁻³ This is accomplished via derivatization of the functional groups with benzoates (or other similar chromophores),⁴⁻¹⁴ which enable the absolute stereochemical determination of the chiral molecule based on the observed Exciton Coupled Circular

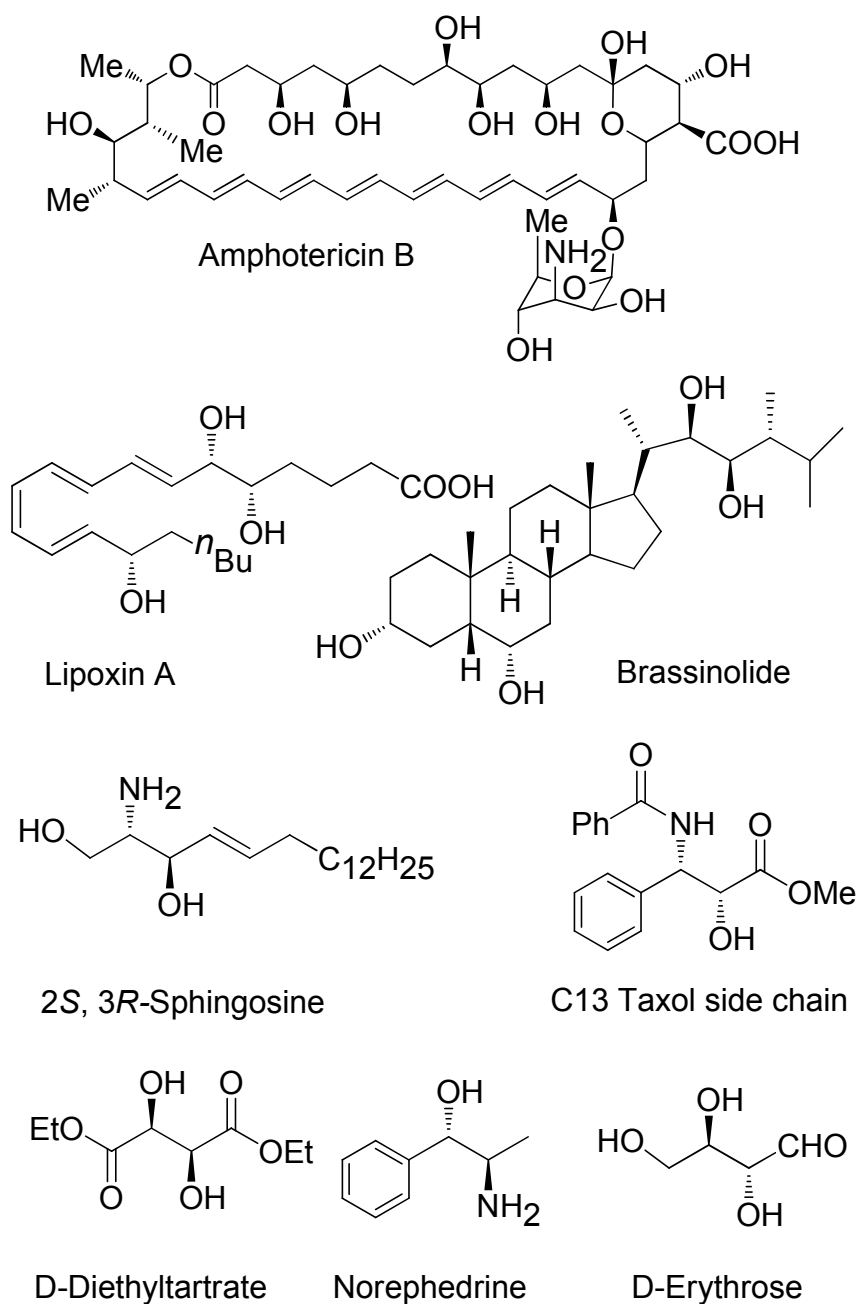


Figure III-1. Vicinal bisfunctionalized molecules in organic synthesis and catalysis.

Dichroism (ECCD).^{1, 2} Nonetheless, the need for derivatization is not ideal. The absolute stereochemistry of *erythro* systems, however, cannot be reliably assigned via existing strategies, and remains a challenging and largely unresolved issue.

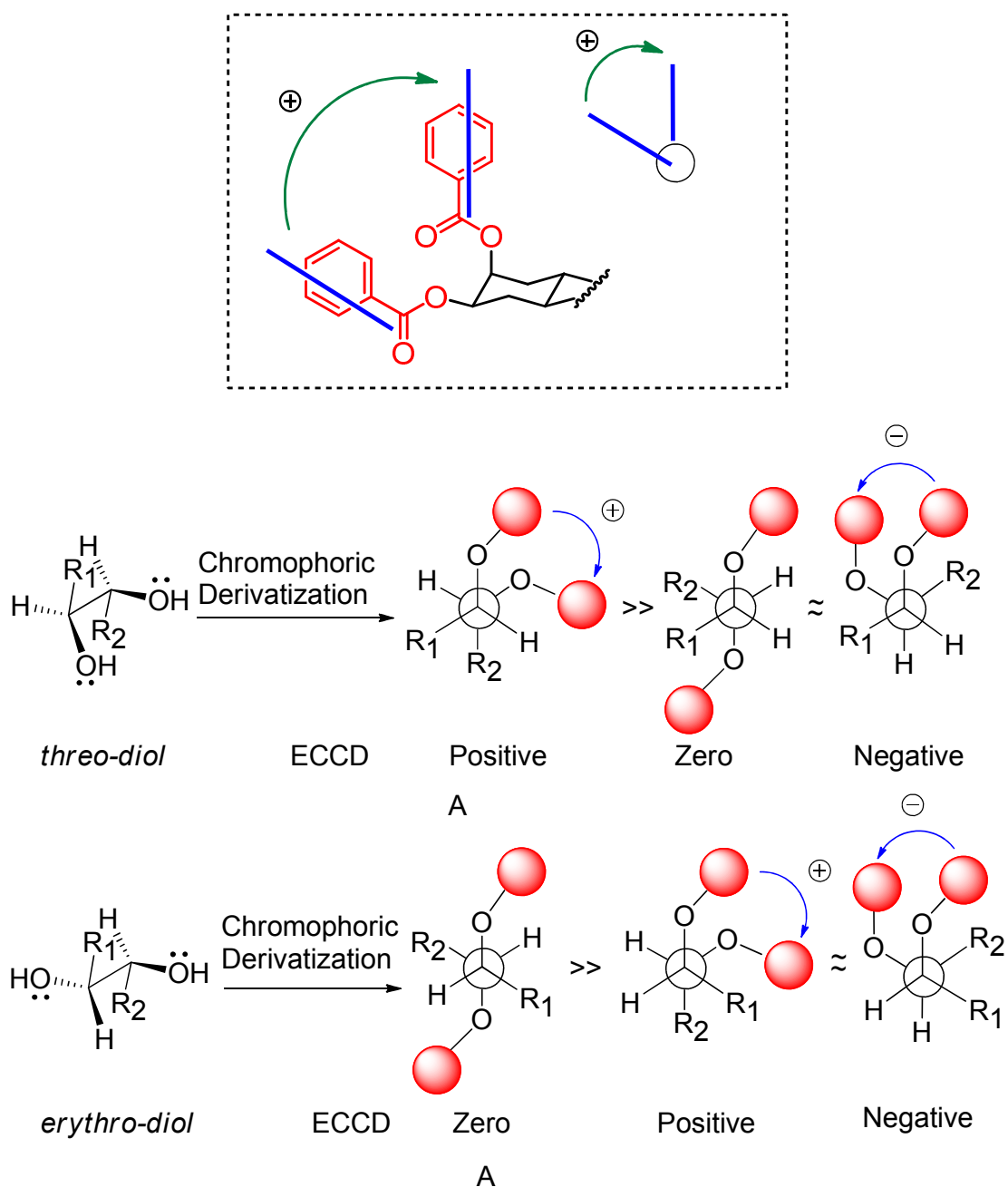


Figure III-2. Stereochemical determination of *threo* diols using dibenzoate method.

Briefly, the ECCD method relies on the coupling of the electric transition dipole moments of two or more chromophores held in space in a chiral fashion.² The sign of the resultant ECCD couplet reflects the helicity of the interacting chromophores, and consequently the chirality of the derivatized system (see Figure III-2, dashed box).

The challenge in utilizing ECCD for absolute stereochemical determinations is to not

only orient two or more chromophores in a chiral fashion dictated strictly by the chiral center, but also to arrive at a system robust enough that provides consistent results with structurally different compounds. Figure III-2 illustrates the dibenzoate method for *threo* and *erythro* diols. With *threo* diols, the expected high population (low energy) rotamer (A) leads to an observable and distinct ECCD spectrum. For the *threo* diol depicted in Figure III-2, the result is a positive ECCD irrespective of R_1 and R_2 . The expected high population rotamer (A) for derivatized *erythro* diols, however, is ECCD silent. The expected minor populations lead to opposing ECCD spectra, and thus cannot be used as a reliable indicator of absolute stereochemistry.

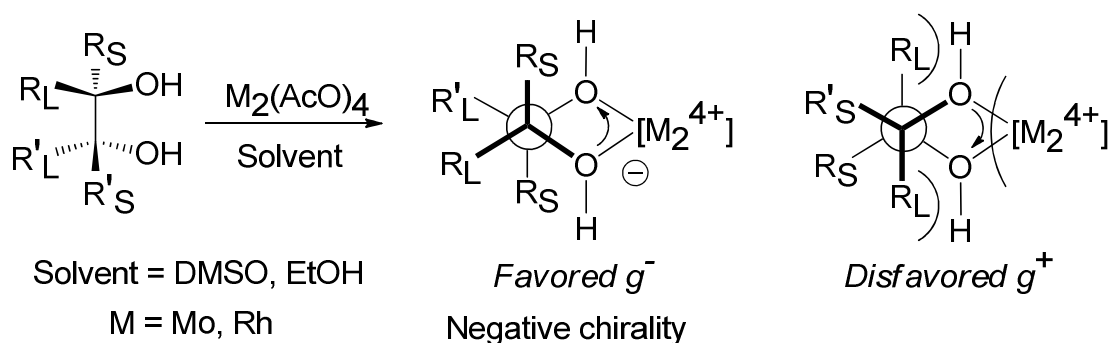


Figure III-3. Stereochemical determination of *threo* diols using $M_2(AcO)_4$.

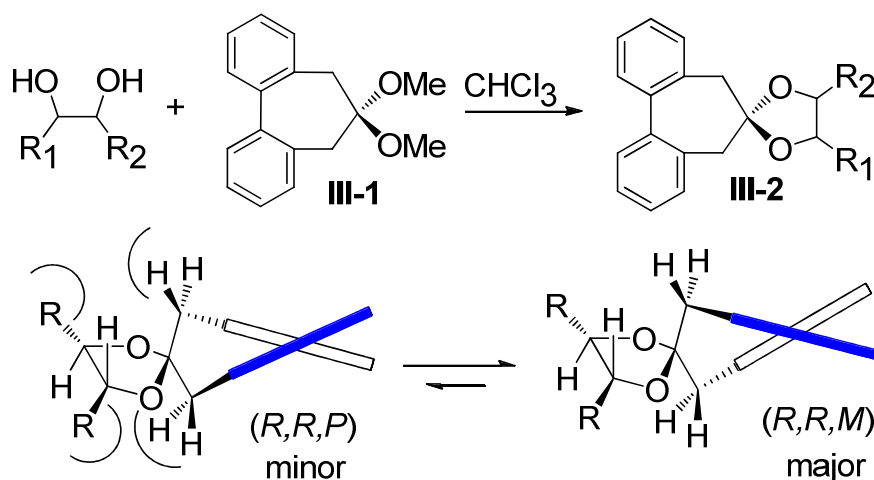


Figure III-4. Stereochemical determination of *threo* diols by forming dioxolanes.

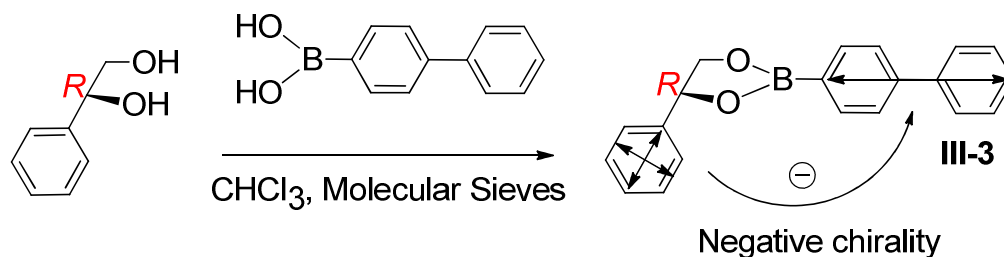


Figure III-5. Stereochemical determination of terminal diols by forming cyclicborate.

Other approaches have been developed to transform acyclic substrates into cyclic conformationally defined derivatives through generation of cottonogenic derivatives with metal complexes¹⁵⁻²³ (Figure III-3) or conversion into dioxolanes²⁴⁻²⁷ (Figure III-4) or 4-biphenylborates (Figure III-5).^{28, 29} These methods, however, suffer from fairly weak CD signals due to weak effective transition moments of the cottonogenic species, and few address the absolute stereochemical determination of *erythro* compounds. A practical and universally expedient method to unequivocally determine the chirality of *erythro* diols, amino alcohols, and diamines is a challenging task.

III.2 ECCD Study of Vicinal Bisfunctionalized Chiral Molecules Using Zn TFPF Tweezer

III.2.1 Binding affinity of zinc TFPF tweezer

Porphyrin tweezer systems (Figure III-6a) have been successfully used to determine the stereochemistry of chiral amines,³⁰⁻³⁴ alcohols,^{34, 35} and carboxylic acids.³⁶⁻³⁸ The principle advantage of the porphyrin tweezer system resides with the non-covalent binding of the chiral guest, which precludes the need for chemical derivatizations. Prior work, however, has focused on the absolute stereochemical

determination of single chiral centers. As depicted in Figure III-6b, the binding of the Zn-porphyrin tweezer to a diamine with a single chiral center leads to an induced helical arrangement of the bound porphyrins that yield a predictable ECCD spectrum.³² Since the tweezer strategy is based on the steric interaction between the substituents at the chiral center and one of the two porphyrins, it was envisaged that the second porphyrin could participate in steric differentiation with chiral guests that have two chiral centers such as 1,2-bisfunctionalized systems. In other words, we hypothesized that a system with two chiral centers could be considered as two independent systems with a single chiral center each (Figure III-6c). In this manner, *erythro* diols, amino alcohols, and diamines could yield reproducible ECCD spectra based on the steric differentiation at each chiral center. We predict that the porphyrin would bind the hydroxyl group *anti* to the largest substituent on the chiral center and stereodifferentiate between the two remaining groups attached to the same chiral carbon. Upon steric differentiation at each chiral center, the two porphyrins would adopt a specific helicity.

A problematic issue was the weak binding of alcoholic chiral guests with zinc porphyrin tweezers employed previously. For this approach to work, we required a strong binding tweezer such that a large population of the chiral guest (for example 1,2-diols) would bind, and thus increase the observed signal. Also, weak binding complexes could lead to small energetic differences between a number of complexed conformations. Inconsistent trends in observed ECCD are possible upon binding of different structures if different conformations could yield opposite ECCD. The latter

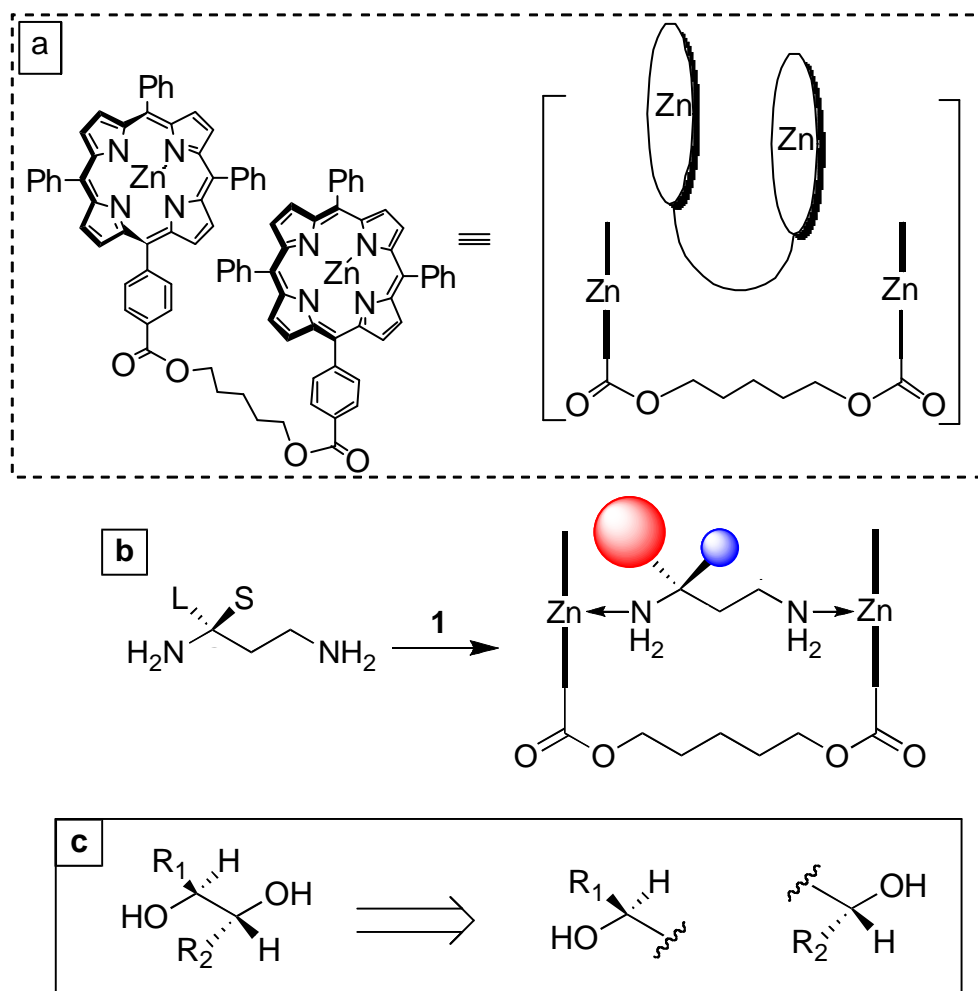


Figure III-6. a) Structure of Zn-TPP tweezer **II-1**. b) Binding of a chiral diamine to **II-1** leads to a helical disposition of the porphyrin rings dictated by the sterics at the chiral center. The resultant ECCD is used to assign the absolute stereochemistry of the chiral center. c) A 1,2-diol with two chiral centers can be envisioned as two independent chiral alcohols.

criteria led to the design and synthesis of a series of electron deficient porphyrin tweezers as described in Chapter 2 which eventually afforded 5-(4-methylcarboxyphenyl)-10,15,20-tri(pentafluorophenyl) porphyrin tweezer **II-25** ($\lambda_{\text{max}} = 416 \text{ nm}$, $\varepsilon = 1,120,000 \text{ cm}^{-1}\text{M}^{-1}$ in CH_2Cl_2 ; $\lambda_{\text{max}} = 412 \text{ nm}$, $\varepsilon = 890,000 \text{ cm}^{-1}\text{M}^{-1}$ in hexane) as our best candidate for strong binding with hydroxyl groups.

Calculations, ^1H NMR binding experiments, and UV-vis titrations corroborate the enhanced Lewis acidity and binding affinity of the new fluorinated porphyrin tweezer.

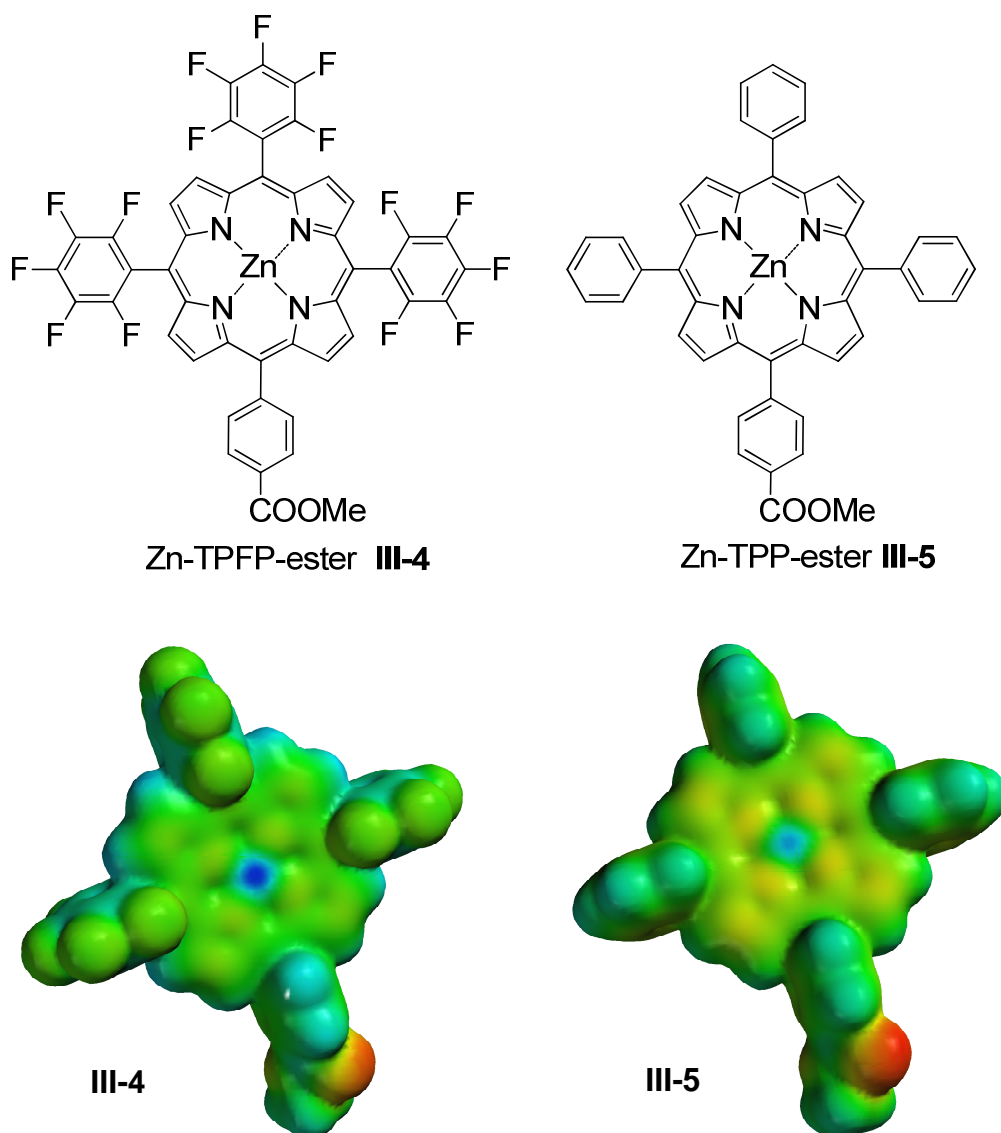


Figure III-7. Electrostatic potential surface of Zn-TPFP-monoester (**III-4**) and Zn-TPP-monoester (**III-5**) based on B3LYP/6-31G(d)//PM3 calculation. Property range was set from -45 (red color) to +45 (blue color).

Computational modeling was first utilized to investigate the change in Lewis acidity of the zinc atom in the fluorinated porphyrin as compared to its nonfluorinated counterpart. Zinc 5-(4-methylcarboxyphenyl)-10,15,20-tri(pentafluorophenyl)

porphyrin (Zn-TPFP-monoester, **III-4**) and zinc 5-(4-methylcarboxyphenyl)-10,15,20-triphenyl porphyrin (Zn-TPP-monoester, **III-5**) were used as model compounds. Geometry optimization was performed by the semiempirical method (PM3) followed by DFT single point energy calculation at B3LYP/6-31G(d) level.

Table III-1. Frontier orbital energy and charges of zinc porphyrins.

	E_{LUMO} eV	$E_{\text{LUMO}} - E_{\text{HOMO}}$ eV ^a	Mulliken Charge of Zn ²⁺	Electrostatic Charge of Zn ²⁺
Zn-TPFP-monoester	-2.818	3.284	0.961	1.387
Zn-TPP-monoester	-2.211	3.891	0.942	1.337

^aS-lysine methyl ester was chosen as a typical chiral guest. HOMO energy calculated using the same method was -6.102 eV.

As shown in fluorinated porphyrin has a lower LUMO energy. This indicates an increased Lewis acidity as well as binding affinity towards nucleophilic guest molecules since the decreased LUMO energy would lead to a smaller energy gap between the LUMO of the electrophilic host and the HOMO of the nucleophilic guest. The calculated charges also provide evidence that the zinc atom bound to the Zn-TPFP-monoester (**III-4**) is more electropositive, presumably due to the strong electron-withdrawing effect of the pentafluorophenyl groups as compared to Zn-TPP-monoester (**III-5**). Electrostatic potential surfaces (Figure III-7) provide a visual perspective of the charge difference between the two zinc porphyrins. The

Zn-TPFP-monoester is clearly more electron deficient than the Zn-TPP-monoester as represented by the ‘colder’ surface.

The enhanced binding could also be observed through $^1\text{H-NMR}$ analysis. Binding of ethanol to zincated porphyrin **III-4** (1:1 ratio) led to a 0.5 ppm upfield shielding of the methylene protons. Ethanol bound to zincated tetraphenyl porphyrin **III-5** upfield shifted the methylene protons by only 0.1 ppm; clearly indicating stronger binding affinity of fluorinated porphyrin **III-4** with hydroxyl group.

Table III-2. Binding affinity^a of ROH and RNH₂ with **III-4** and **III-5**

porphyrin	$K_{\text{assoc.}} (\text{iPrOH}) \text{ M}^{-1}$	$K_{\text{assoc.}} (\text{iPrNH}_2) \text{ M}^{-1}$
Zn-TPFP-monoester (III-4)	$2,170 \pm 140$	$473,000 \pm 8,700$
Zn-TPP-monoester (III-5)	49 ± 2	$11,400 \pm 950$

^a K_{assoc} for each ligand/porphyrin complex was obtained via fitting the data obtained from the change in the absorption upon titration of the porphyrin with ligand in hexane to a nonlinear least square analysis (see experimental section for details)

Finally, quantitative measures of amine and alcohol binding with both Zn-TPP and Zn-TPFP were obtained via titration of the ligands and analysis of the spectroscopic changes. The Zn-TPFP-ester **III-4** and Zn-TPP-ester **III-5** were used again as simplified models of each tweezer for initial measurements. Figure III-8 illustrates the changes observed in the UV-vis spectra upon titration of iso-propanol and iso-propylamine with Zn-TPFP-ester **III-4**. The change of absorption at 418 nm for *iso*-propanol and 412 nm for *iso*-propylamine as a function of concentration of

ligand added yields an exponential saturation curve. The binding constants can be derived from fitting the latter data via a non-linear least square method as has been previously reported.³⁹ Table III-2 lists the binding constants obtained for Zn-TPFP-ester **III-4** and Zn-TPP-ester **III-5**. As expected, iso-propylamine binds stronger to the Zn-porphyrins as compared to iso-propanol. Of note, however, is greater than 1 order of magnitude increase in binding affinity of the ligands (both amine and alcohol) for the fluorinated Zn-porphyrin **III-4** as compared to the non-fluorinated Zn-porphyrin **III-5**.

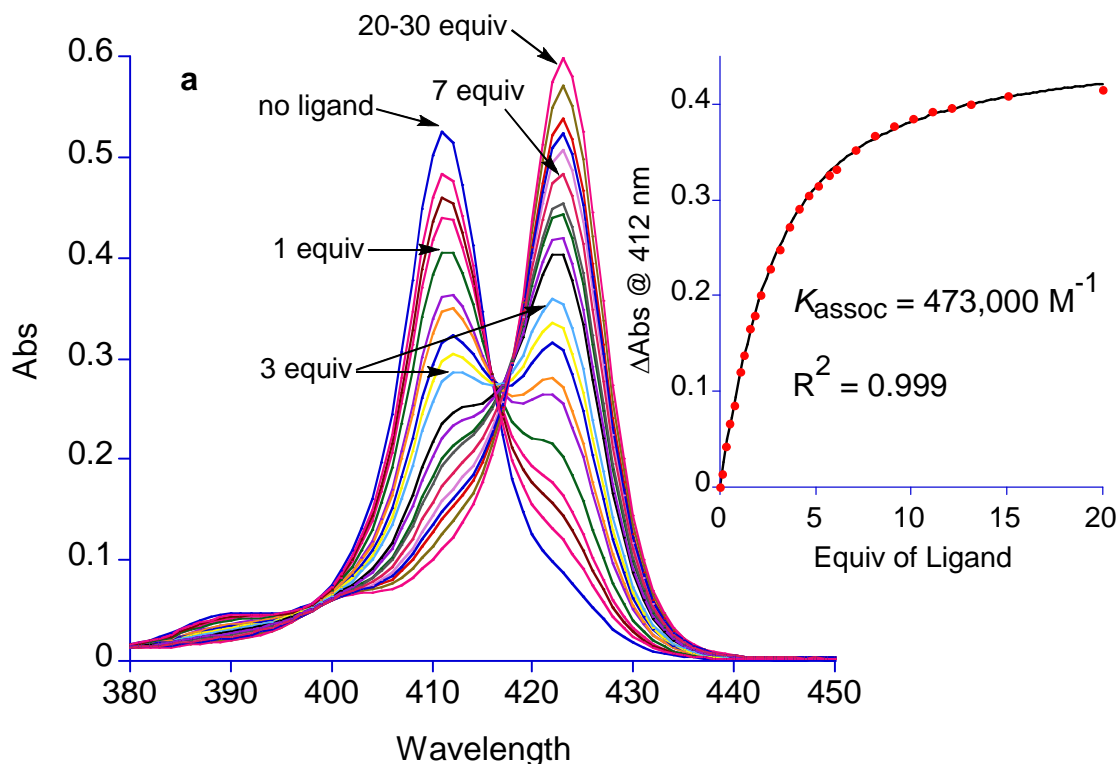


Figure III-8a. Titration of Zn-TPFP ester **III-4** with *i*PrNH₂ (0-30 equiv, bathochromic shift from 412 nm to 424 nm) in hexane. The inset graph is non-linear least square fit of the change in absorption vs. equiv of ligand.

We next turned our attention to the binding of bis-functionalized substrates with the Zn-porphyrin tweezers derived from TPP and TPFP. Figure III-9 illustrates the

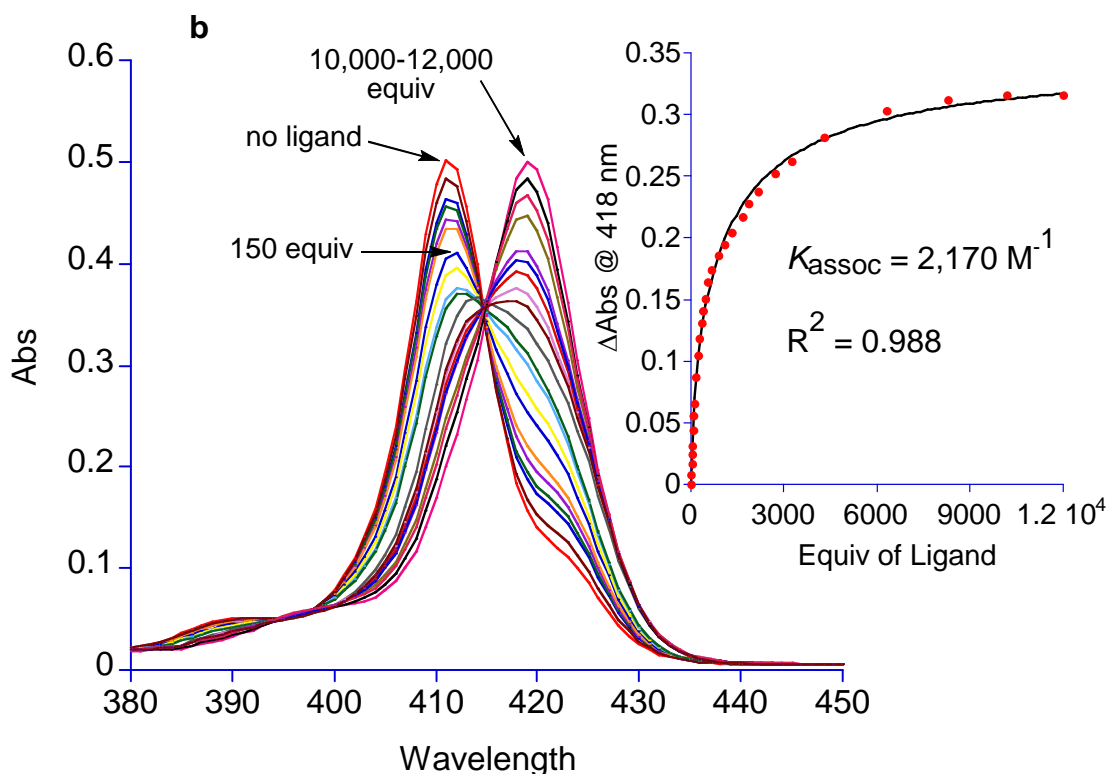


Figure III-8b. Titration of Zn-TPFP ester **III-4** with *i*PrOH (0-12,000 equiv, bathochromic shift from 412 nm to 418 nm) in hexane. The inset graph is non-linear least square fit of the change in absorption vs. equiv of ligand.

binding titration of amino alcohol **III-12** (see Table III-3) with fluorinated TPFP tweezer. Close inspection of the UV-vis spectra reveals the presence of two processes as the concentration of the ligand is increased. From prior work it is well recognized that a ~13 nm bathochromic shift is expected upon coordination of a strong nucleophile such as an amino group with the zinc porphyrin.⁴⁰

It has also been demonstrated previously that a hypsochromic shift occurs when the two porphyrin rings are brought close in space.⁴¹ Thus, there are two opposing effects that in combination lead to the observed λ_{max} . For example, upon complexation of 1,2-diaminoethane, a 4 nm bathochromic shift is observed (as opposed to the expected 12 nm); as the separation between the porphyrin rings is

increased the λ_{max} gradually redshifts such that binding of 1,10-diaminodecane results in a 9 nm bathochromic shift.⁴¹

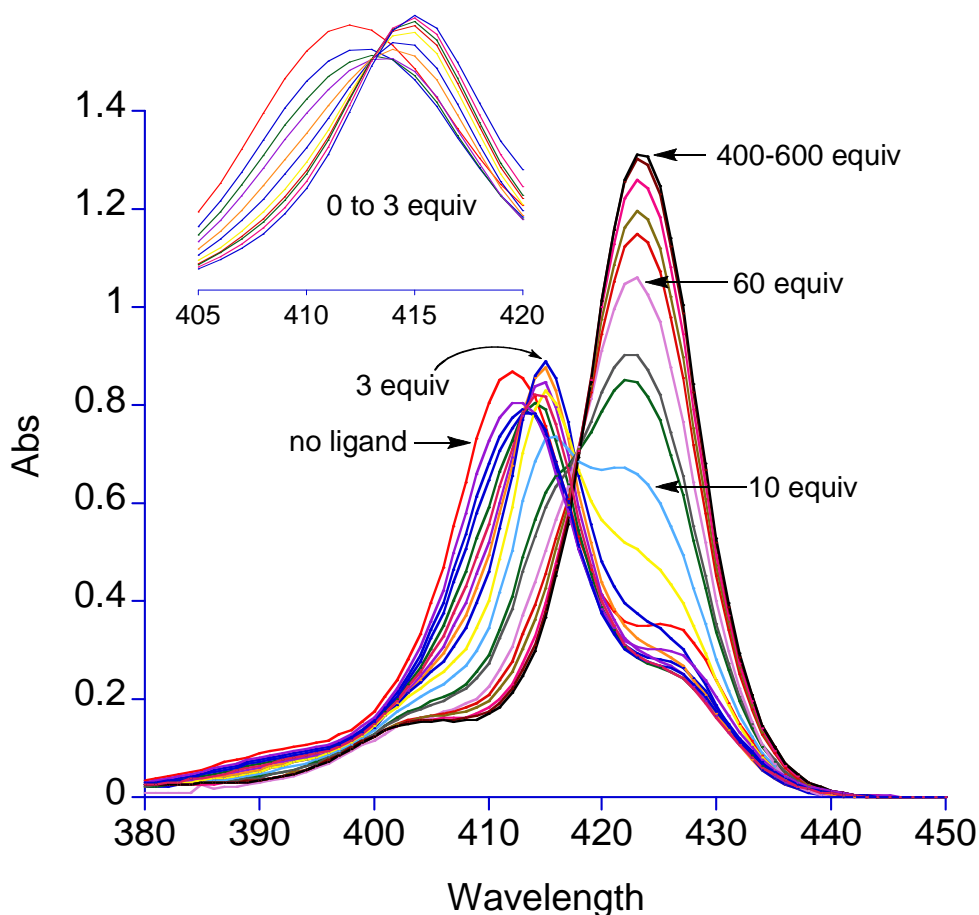


Figure III-9. Titration of Zn-TPFP-tweezer **II-25** with amino alcohol **III-12**. Two isosbestic points are apparent. The first at lower equiv of amino alcohol (leading to the absorption at 415 nm) signifies the 1:1 ligand:complex formation. The second (leading to the absorption at 423 nm) appearing at higher concentrations of amino alcohol indicates the formation of the 2:1 ligand:tweezer complex.

The titration curves depicted in Figure III-9 exhibit an initial bathochromic shift of the absorption maximum from 412 nm to 415 nm when the first 3 equiv of the 1,2-amino alcohol **12** are added to the tweezer in hexane. As the equivalence is increased, however, a second bathochromic shift to 423 nm is evident. This

behavior can be explained based on observations discussed above, i.e.; the initial 3 nm bathochromic shift is due to a 1:1 complexation of the 1,2-amino alcohol with TPFP tweezer, which brings the porphyrins close to each other. This results in the observed 3 nm redshifting that gives rise to the peak at 415 nm. Further increase in the concentration of the 1,2-amino alcohol leads to the breakup of the 1:1 complex (binding of an amine to the zincated porphyrin is much stronger than that of an alcohol, Figure III-10) such that each porphyrin is bound to an amino group (1:2 complex), effectively maximizing the distance between the porphyrin rings that leads to an 11 nm redshift. This is analogous to a mono amine binding to the porphyrin, which would result in the same level of redshifting. We would thus expect that excess addition of 1,2-amino alcohols to the tweezer would diminish the ECCD.

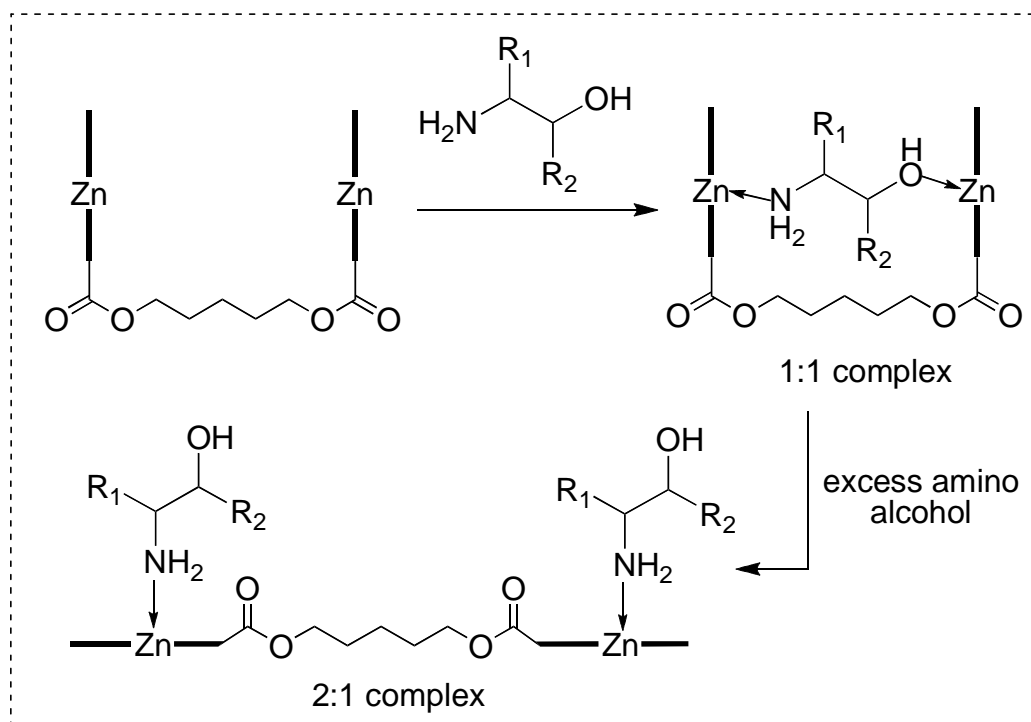


Figure III-10. Two step binding of amino alcohol with Zn-TPFP tweezer

Based on the above discussion, the binding constant for a 1:1 complexation of **III-12** with TPFP tweezer was measured based on the data obtained for up to 3 equiv of amino alcohol added. Nonlinear least square analysis of the change in absorption at 412 nm as a function of guest concentration provided a binding constant (K_{assoc}) of $1.31 \times 10^7 \text{ M}^{-1}$ for binding of **III-12** with the fluorinated tweezer in hexane. Similar UV titrations in methycyclohexane with guest **III-12** rendered a binding constant of $2.71 \times 10^6 \text{ M}^{-1}$. The better binding in hexane might lead to stronger ECCD amplitudes.

As anticipated, the binding of 1,2-diols with TPFP tweezer is weaker due to the tempered nucleophilicity of alcohols compared to amines. Figure III-11 depicts the UV-vis titration curves of diol **III-16** complexed with tweezer **II-25** ($K_{\text{assoc}} = 152,000 \text{ M}^{-1}$ in hexane, $36,100 \text{ M}^{-1}$ in MCH). Two observations are notable; first a large bathochromic shift is not present upon binding of the hydroxyl group with the zincated porphyrin. This is the result of two opposing effects, the anticipated 6 nm bathochromic shift as a result of alcohol binding with the zincated porphyrin (see Figure III-8b for alcohol-porphyrin binding) and the hypsochromic shift that results from bringing the two porphyrins close to each other. Second, since addition of excess 1,2-diol does not compete with the 1:1 complexation (previously, excess amine competed with the hydroxyl bound porphyrin), breakup of the 1:1 complex is not apparent. Addition of excess 1,2-diol to tweezer **II-25** mimics addition of excess diamines to porphyrin tweezers, which does not exhibit the breakup of the 1:1 complex until ~500 equiv added.

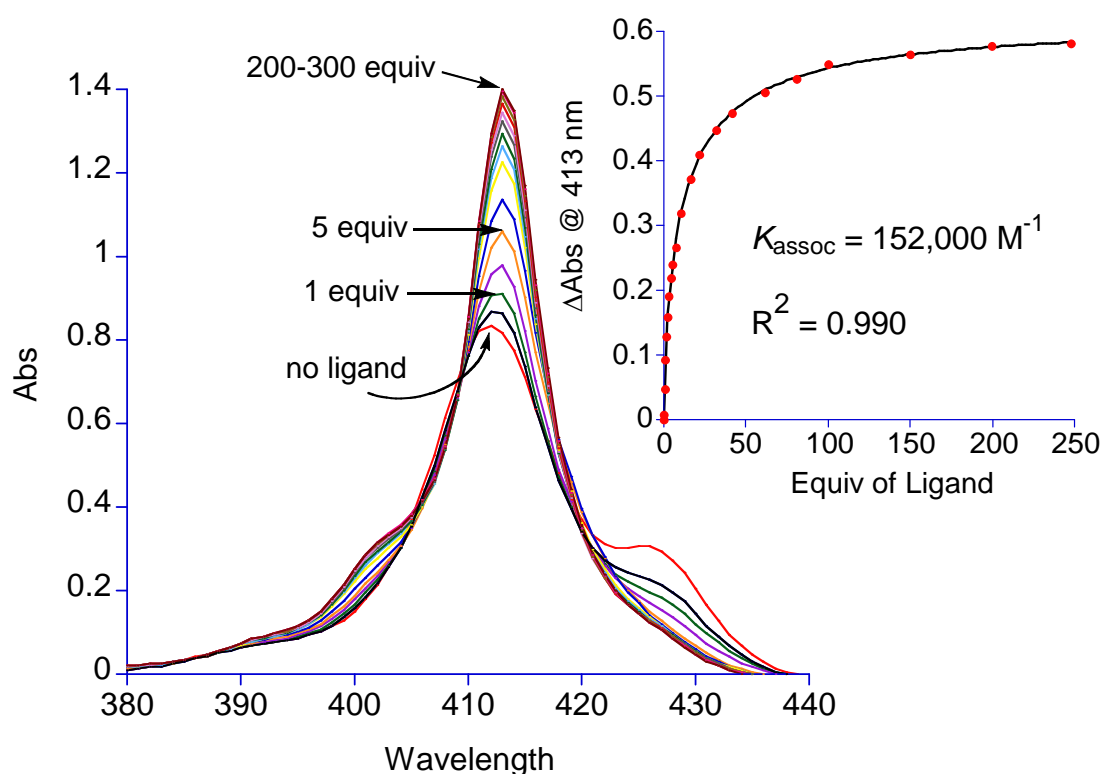


Figure III-11. Titration of Zn-TPFP tweezer **II-25** with diol **III-16** (0-300 equiv) in hexane. The non-linear least square fit of the change in absorption vs. equiv of ligand provides the binding constant.

III.2.2 Determination of chirality of *erythro* substrates

Our initial foray focused on the use of the Zn-TPFP tweezer with *erythro* diols and amino alcohols. Diol **III-6** and **III-8** were prepared through non-chelation controlled Grignard addition to α -chiral aldehydes.⁴² Diol **III-7** was synthesized via proline catalyzed asymmetric aldol reaction.⁴³ Diol **III-9** was obtained from 2-deoxy-D-ribose.⁴⁴ Diol **III-10** was made from Sharpless asymmetric dihydroxylations.⁴⁵ As can be seen from Figure III-12 and Table III-3, the binding

of the chiral *erythro* guests yielded a host-guest complex with observable ECCD couplets. A consistent and predictable trend is observed, where the *R,S erythro* compounds (the first stereochemical designation refers to the chiral site with the largest substituent as determined by A-values) gave rise to positive ECCD, while the *S,R erythro* compounds produced negative ECCD spectra. The Cahn, Ingold and Prelog stereochemical designation should be used with caution since priorities do not necessarily correlate with sterics as can be seen in **7**, an example of *R,R-erythro* diol.

Figure III-12 illustrates a conceptual model that suggests each chiral center orients the bound porphyrin independently through steric differentiation. This is illustrated with the binding of norephedrine **III-12** with TPFP tweezer. We propose that **P2** approaches the amino group of *R,S*-norephedrine opposite to the largest substituent, in this case the methyl group. In this manner, the methyl group is *anti* to the complexed porphyrin and does not participate in the steric differentiation. The two remaining groups attached to C1, namely H and the C2 dictate the disposition of the bound porphyrin ring; as such **P2** rotates clockwise towards the smaller hydrogen atom. Similarly, binding of **P1** with the OH group places **P1** *anti* to the phenyl group attached to C1. Steric differentiation of the remaining substituents (H and C2) leads to the rotation of **P1** in a counterclockwise manner to reduce repulsion with the bulky C2 substituent. As described, **P1** adopts a clockwise (positive) helicity relative to **P2**, which would predict a positive ECCD spectrum. Indeed, as illustrated in Figure III-12, the complexation of **III-12** with TPFP tweezer leads to the anticipated spectrum. This is a working model that fits the data and by no means is

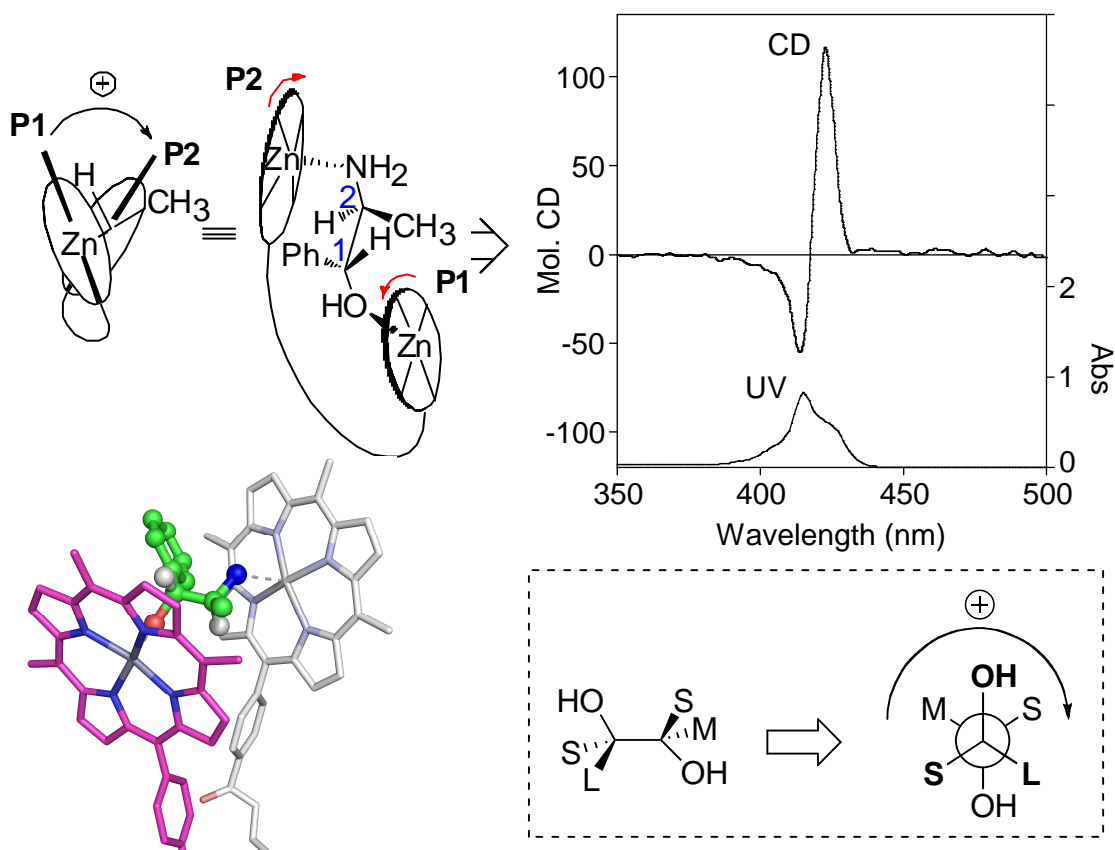


Figure III-12. Proposed binding conformation between tweezer **II-25** and *erythro* amino alcohol **III-12**, yielding a positive ECCD spectrum. It is assumed that **P1** and **P2** bind to their respective functional groups opposite the large group at each chiral center. The pentafluorophenyl groups in the modeled picture have been omitted for clarity. A simplified mnemonic is illustrated in the dashed box. The sign of the ECCD spectrum will depend only on the absolute stereochemistry of the chiral center that bears the largest group.

the only possible mode of binding.

Since the assumption is that each porphyrin undergoes independent steric differentiation, while keeping in mind that the observed ECCD is the result of the helical disposition of the two porphyrins, a more simplified mnemonic can be envisioned where the helicity of the tweezer can be determined by analyzing the

chirality of one carbon center. Based on the proposal above, in which the two porphyrins (**P1** and **P2**) rotate counter to each other, one can consider solely the arrangement of **P1**, the porphyrin bound to the chiral center with the largest substituent, as the stereochemical determinant group (assuming the other porphyrin **P2** does not rotate and is static). As depicted in Figure III-12 (dashed box) the stereochemistry of the chiral center with the largest substituent leads to the predicted ECCD; namely, looking at the Newman projection, a clockwise arrangement of S→OH→L leads to a positive ECCD and *vice versa*.

As can be seen from Table III-3, a number of alkyl and aryl systems produced the expected results upon binding with TPFP tweezer. In all cases the predicted sign was arrived at after considering the A-values of the substituents on the carbinol carbon (the structures in Table III-3 are drawn such that the larger group is on the left hand side). The system is tolerant of other potential coordinating groups such as ketones, esters, and ethers (Table III-3, compounds **III-7** and **III-9**). As expected, enantiomeric pairs yield opposite ECCD spectra (compounds **III-6** ~ **III-8**, and **III-12** along with their enantiomers). Of note are the higher ECCD amplitudes obtained for amine containing guests **III-11** and **III-12**, which is presumably due to their stronger binding with tweezer **II-25** as compared to diols.

ECCD amplitudes of tweezer/guest complexes in hexane were consistently larger than those measured in MCH. This is most probably attributed to the stronger observed binding of 1,2-diols and 1,2-amino alcohols with Zn-TPFP tweezer in hexane as compared to MCH (see section III. 2.2). It seems reasonable that binding

Table III-3. ECCD data of Zn-TPFP tweezer bound *erythro*-1,2- diols and amino alcohols.

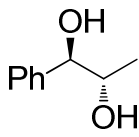
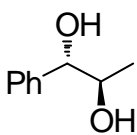
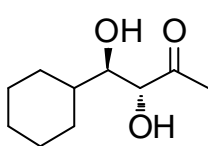
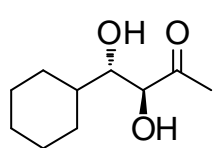
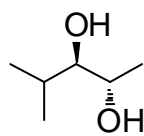
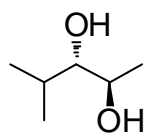
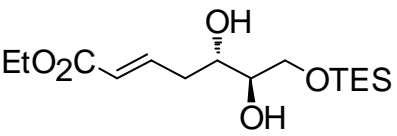
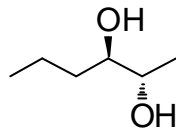
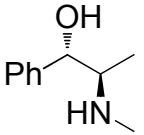
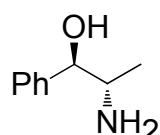
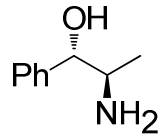
<i>Erythro</i> substrates ^[a]		Predicted sign	Solvent	λ nm, ($\Delta\epsilon$)	A
III-6 ^{[b],[c]} <i>R,S</i>		+	MCH	420 (+24) 415 (-5)	+29
			Hexane	421 (+43) 411 (-15)	+58
III-6-ent ^{[b],[c]} <i>S,R</i>		-	MCH	421 (-8) 414 (+20)	-28
			Hexane	421 (-18) 414 (+34)	-52
III-7 ^{[d],[e]} <i>R,R</i>		+	MCH	423 (+22) 414 (-9)	+31
			Hexane	420 (+90) 410 (-41)	+131
III-7-ent ^{[d],[e]} <i>S,S</i>		-	MCH	423 (-17) 413 (+18)	-35
			Hexane	423 (-72) 413 (+62)	-134
III-8 ^{[b],[c]} <i>R,S</i>		+	MCH	420 (+24) 413 (-5)	+29
			Hexane	419 (+56) 409 (-9)	+65
III-8-ent ^{[b],[c]} <i>S,R</i>		-	MCH	420 (-13) 413 (+15)	-28
			Hexane	419 (-39) 410 (+27)	-66

Table III-3-continued. TPFP tweezer bound *erythro*-1,2- diols and amino alcohols.

<i>Erythro</i> substrates ^[a]	Predicted sign	Solvent	λ nm, ($\Delta\epsilon$)	A
III-9 ^{[b],[d]} <i>S,R</i> 	-	MCH	422 (-23) 414 (+25)	-48
		Hexane	420 (-43) 413 (+36)	-79
III-10 ^{[d],[e]} <i>R,S</i> 	+	MCH	422 (+13) 415 (-6)	+19
		Hexane	423 (+48) 409 (-16)	+64
III-11 ^{[e],[f]} <i>S,R</i> 	-	MCH	425 (-181) 416 (+114)	-295
		Hexane	425 (-341) 414 (+167)	-508
III-12 ^{[e],[f]} <i>R,S</i> 	+	MCH	423 (+92) 416 (-53)	+145
		Hexane	423 (+118) 414 (-56)	+174
III-12-ent ^[e] ^[f] <i>S,R</i> 	-	MCH	423 (-93) 415 (+56)	-149
		Hexane	423 (-112) 414 (+65)	-177

^[a] All substrates were >98% *ee* except for **III-10** (25% *ee*), ^[b] 2 μ M tweezer concentration,

^[c] tweezer/substrate ratio - 1:100, ^[d] tweezer/substrate ratio - 1:40, ^[e] 1 μ M tweezer

concentration, ^[f] tweezer/substrate ratio - 1:5.

constants could be used as a guide for choosing the appropriate solvent in such cases. Other solvents such as dichloromethane or acetonitrile failed to yield observable ECCD for many substrates under the same conditions. Cooling of the solution to 0 °C produced strong observable ECCD spectra, however, further lowering of the temperature to –10 °C only led to limited increase in the amplitude.

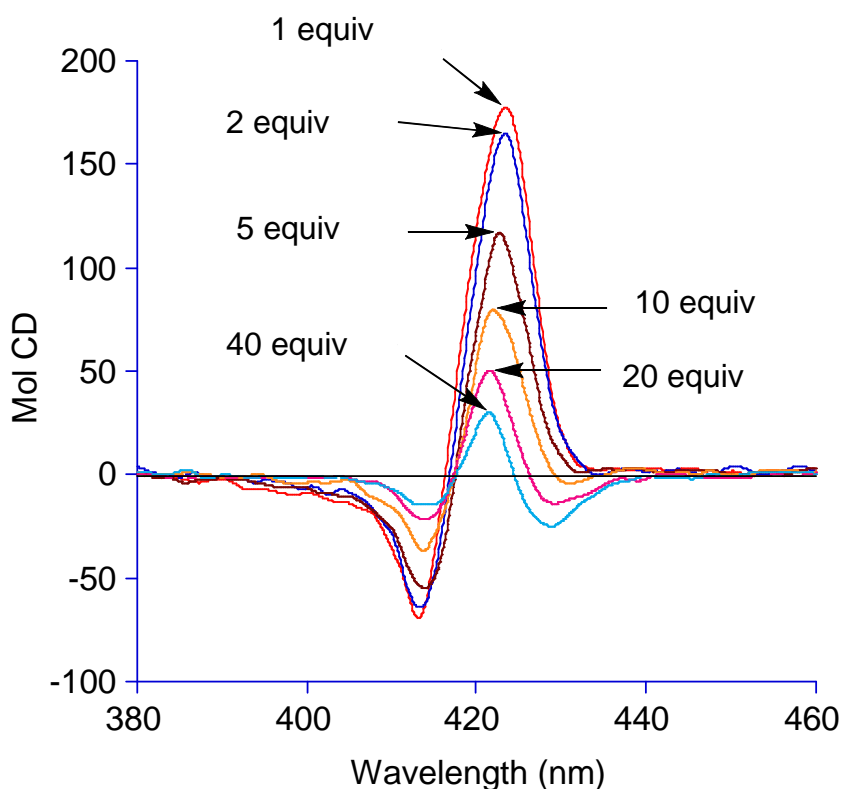


Figure III-13. Increasing concentration of amino alcohol **III-12** leads to diminished ECCD signals. This is presumably a result of breaking up the ECCD active 1:1 ligand:tweezer complex (see Figure III-10) due to the fact that amines have a much higher binding affinity for the zincated porphyrin. The resultant 2:1 complex is not ECCD active.

A note of caution is warranted with amino alcohols. As was eluted to above, the large difference in binding affinity of alcohols and amines with zincated porphyrins

does lead to the breakup of the 1:1 complex with increasing equivalence of amino alcohols added. The resultant 2:1 complex is not ECCD active. Thus, increasing the equivalence of amino alcohols is detrimental to obtaining a strong ECCD signal. Figure III-13 demonstrates the decrease in signal as a function of increasing concentration of amino alcohol **III-12**, clearly suggesting the breakup of the 1:1 complex at higher equivalences.

III.2.3 Determination of chirality for *threo* substrates

Next we investigated *threo* vicinal bis-functionalized systems. Most *threo* diols were made from standard Sharpless asymmetric dihydroxylation.⁴⁵ Both aliphatic and aromatic *R,R-threo* substrates yielded positive ECCD signals while the *S,S-threo* compounds produced negative ECCD spectra (Table III-4). Figure III-14 illustrates the ECCD spectrum obtained from the complexation of Zn-TPFP tweezer with the *threo* diol **III-13**. The expected positive couplet is again assumed to derive from the independent steric differentiation of bound porphyrins at each chiral site. As depicted in Figure III-14, each chiral center induces the same helical twist of the porphyrin tweezer (**P1** and **P2** twist counter to each other as indicated by the two arrows). As was described for *erythro* systems, we assume that the complexed porphyrins approach their ligands such that the largest group on the chiral center is *anti* with respect to the bound chromophores. The conformation illustrated for *threo* diol **III-13** in Figure III-14, where the large groups (Ph on C1 and CO₂Me on C2) are

Table III-4. ECCD data of Zn-TPFP tweezer^[a] bound *threo*- 1,2- diols,^[b] amino alcohols^[c] and diamines.^[c]

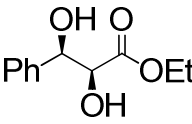
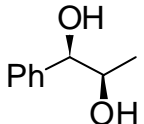
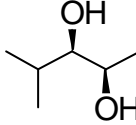
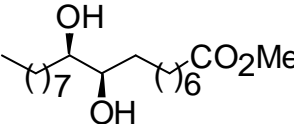
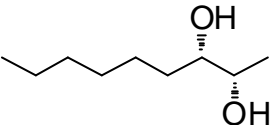
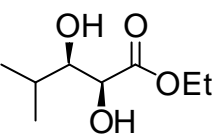
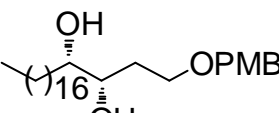
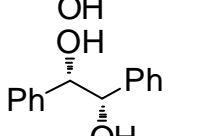
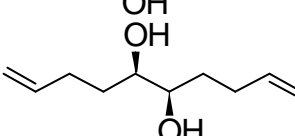
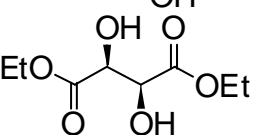
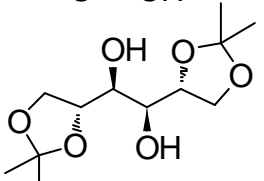
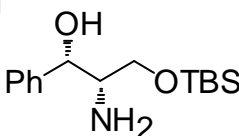
	<i>threo</i> substrates ^[d]	predicted sign	λ nm, ($\Delta\epsilon$)	A
III-13 ^[e] <i>R,S</i>		+	424 (+21) 415 (-16)	+37
III-14 ^[e] <i>R,R</i>		+	422 (+25) 412 (-8)	+33
III-15 ^[e] <i>R,R</i>		+	424 (+75) 413 (-30)	+105
III-16 ^[e] <i>R,R</i>		+	426 (+118) 413 (-33)	+151
III-17 <i>S,S</i>		-	426 (-25) 412 (+16)	-41
III-18 <i>S,S</i>		+	423 (+16) 412 (-4)	+20
III-19 <i>S,S</i>		-	427 (-29) 415 (+12)	-41
III-20 <i>S,S</i>		-	423 (-27) 417 (+23)	-50
III-21 <i>R,R</i>		+	425 (+37) 414 (-17)	+54
III-22 ^[f] <i>S,S</i>		+	423 (+37) 414 (-22)	+59
III-23 <i>R,R</i>		+	420 (+47) 412 (-21)	+68
III-24 <i>S,S</i>		-	426 (-54) 421 (+35)	-89

Table III-4-continued. TPFP tweezer^[a] bound *threo*- 1,2- diols,^[b] amino alcohols^[c] and diamines.^[c]

	<i>threo</i> substrates ^[d]	predicted sign	λ nm, ($\Delta\epsilon$)	A
III-25 ^[e]		-	428 (-41) 420 (+31)	-72
S,S				
III-26 ^[e]		+	430 (+222) 419 (-142)	+364
R,R				
III-27 ^[b]		+	420 (+39) 410 (-15)	+54
S,S				

^[a] 1 μ M tweezer concentration was used for all measurements except for **III-19** and **III-27** (2 μ M), ^[b] tweezer/substrate ratio - 1:40, ^[c] tweezer/substrate ratio - 1:5, ^[d] All substrates were >95% *ee* except for **III-15** and **III-27** (91% *ee*), ^[e] the enantiomer showed mirror image CD spectrum, ^[f] tweezer/substrate ratio - 1:200, methyl cyclohexane was used as solvent for all CD measurements.

placed *anti* to each other (similar to the conformation assumed for *erythro* systems), leads to the least sterically encumbered arrangement for the bound porphyrins. Steric differentiation at **P1** (H vs. C2) leads to a counterclockwise rotation of the porphyrin towards the smaller hydrogen atom, while a clockwise rotation of **P2** (steric differentiation of H vs. C1) is anticipated. This would lead to a positive helical arrangement of the porphyrins, which is verified by the positive ECCD spectrum observed for diol **III-13** bound to Zn-TPFP tweezer. Each stereocenter of a *threo* system would thus reinforce the same overall helicity of the bound tweezer. The latter statement would suggest that *C*₂ symmetric diols and diamines would lead to observable ECCD spectra. This is indeed observed (Table III-4, compounds **III-20** ~ **III-23** and **III-26** ~ **III-27**) making this methodology applicable to the absolute

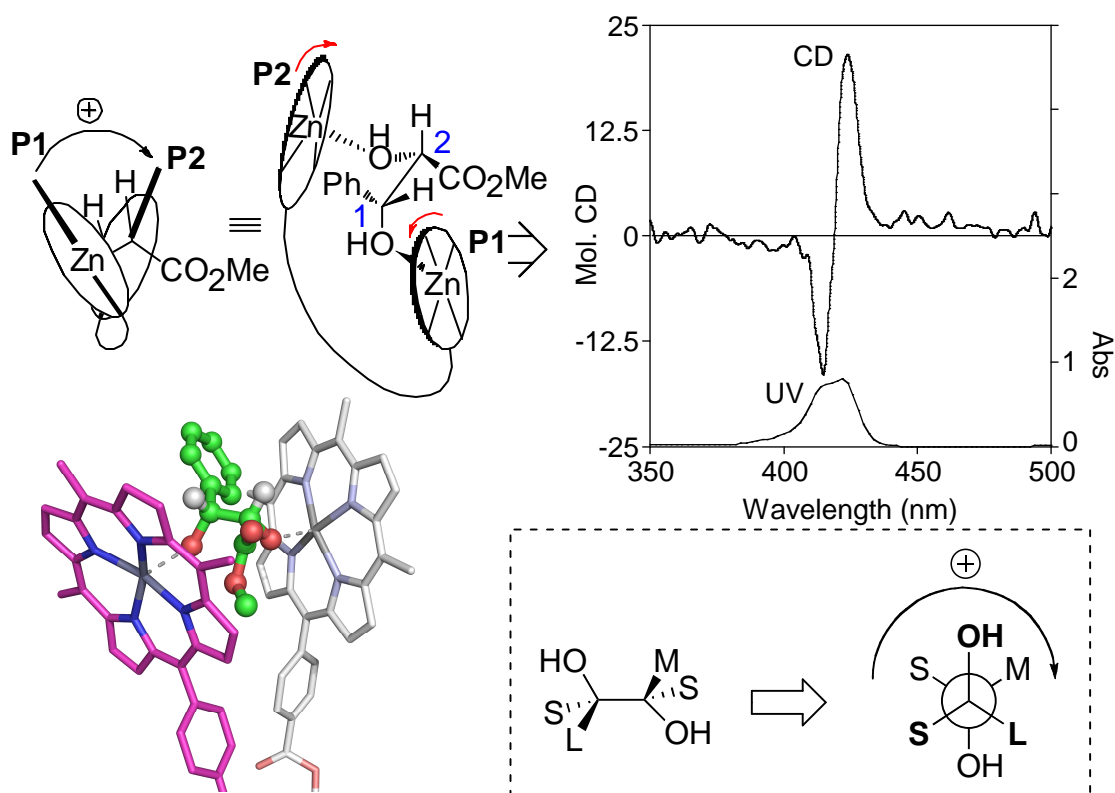
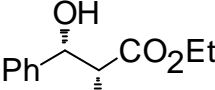
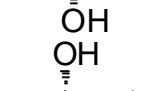
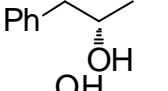
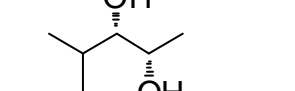
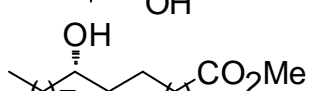
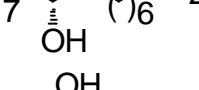
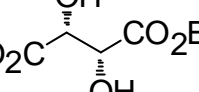


Figure III-14. Proposed conformation of the complex generated between the binding of tweezer **II-25** (two arrows indicate the directions which the porphyrins would rotate to minimize steric repulsion) and *threo* diol **III-13**, resulting in a positive ECD spectrum. The depicted arrangement is arrived at by placing **P1** and **P2** opposite the large group at each chiral center. The model illustrates the binding of diol **III-13** with tweezer **II-25** (the pentafluorophenyl groups have been omitted for clarity). The dashed box depicts a simplified mnemonic for the absolute stereochemical determination of *threo* systems.

stereochemical identification of C_2 symmetric compounds, which are an important subgroup of chiral molecules used in enantioselective processes. The same simplified mnemonic that was used for *erythro* systems is applicable for *threo* compounds as well. As illustrated in Figure III-13 (dashed box), the sign of the ECD couplet can be predicted by analyzing the substituent on the chiral center that bears the largest group.

As can be seen from Table III-4, a variety of substituents and functional groups produced the expected results. Also, the presence of other potential coordinating groups such as esters (Table III-4, compounds **III-13**, **III-16**, **III-18**, and **III-22**) or acetonide (**III-23**) did not interfere with the complexation of the substrates with TPFP tweezer.

Table III-5. ECCD Data for enantiomers of chiral *threo* substrates in Table III-4

	<i>threo</i> chiral substrates ^[d]	predicted sign	λ nm, ($\Delta\epsilon$)	A
III-13-ent^a S, R		-	424 (-13) 415 (+20)	-33
III-14-ent^a S, S		-	425 (-15) 415 (+18)	-33
III-15-ent^a S, S		+	425 (-46) 413 (+56)	+102
III-16-ent^a S, S		-	426 (-103) 413 (+42)	-145
III-22-ent^b R, R		-	424 (-27) 414 (+31)	-58
III-25-ent^c R, R		+	428 (+45) 419 (-27)	+72
III-26-ent^c S, S		-	430 (-217) 419 (+153)	-370

^[a]tweezer / substrate ratio - 1:40, ^[b]tweezer / substrate ratio - 1:200, ^[c]tweezer / substrate ratio - 1:5, All CD spectra were measured in in methyl cyclohexane with 1 μ M tweezer.

Seven pairs of *threo* enantiomers all exhibited mirror image CD couplets (Table III-5). As expected, *threo* diamines produced much higher ECCD amplitudes than diols due to their stronger binding with Zn TPFPP tweezer. Interestingly, this tweezer was capable of binding diepoxide **III-27** and produced the expected ECCD spectrum based on the binding mode explained above. The absolute stereochemical determination of epoxy alcohols via binding of the epoxide will be discussed in next chapter.

As described above, the proposed binding of Zn-TPFP tweezer with *erythro* and *threo* systems is similar, in which each porphyrin binds the coordinating functional group opposite the largest substituent on the chiral center. In all examples discussed thus far the nature of the acyclic system can lead to a number of rotomers upon complexation (Figures III-12 and III-14 only depict the rotomer believed to lead to the observed ECCD spectra for *erythro* and *threo* systems, respectively). It is difficult to predict whether or not the conformation of the complexed guest molecules retains the lowest energy conformation of unbound molecules (such as those depicted in Figure III-2) since complexation with the large porphyrin tweezer can lead to compensating interactions with an overall effect of the guest system adopting a higher energy conformation. NMR experiments have not been helpful in assigning the conformation of the bound guest molecules since aggregation of the Zn-TPFP porphyrin tweezer is observed at concentrations necessary for observing NMR signals (see section III-2-4 for details).

A single rotomer can be investigated, however, if cyclic 1,2-bisfunctional

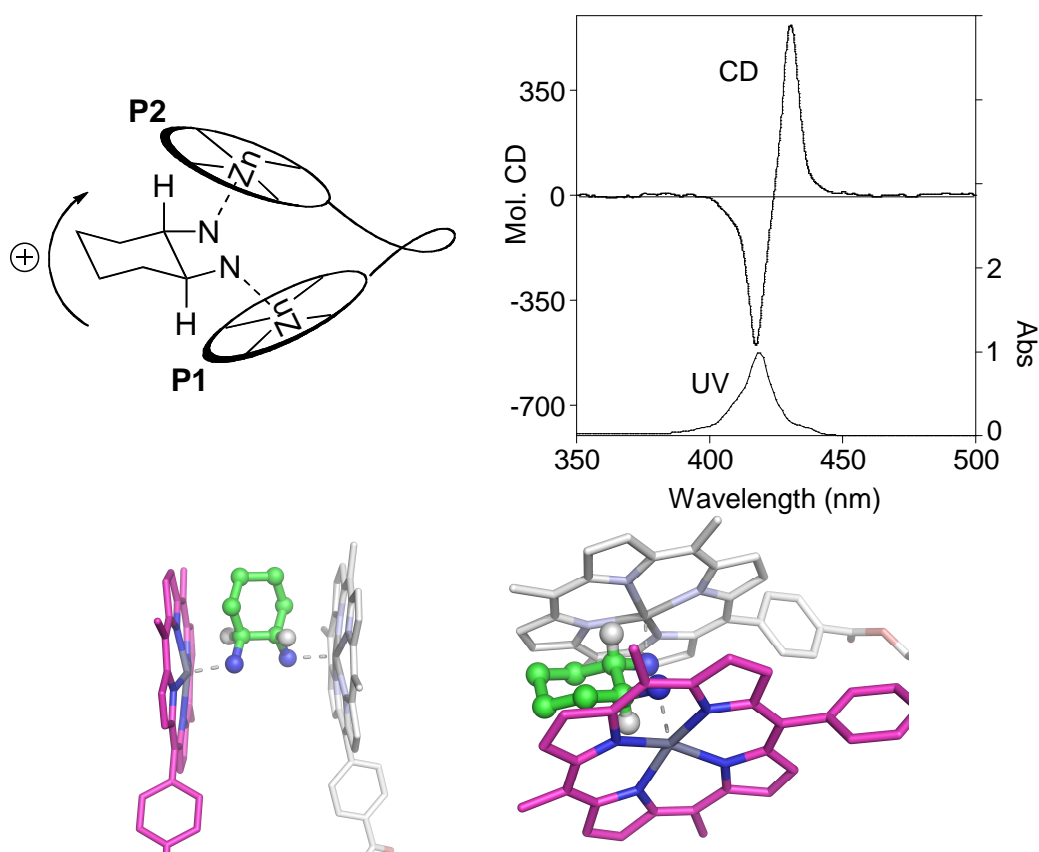


Figure III-15. Proposed conformation of the complex generated between Zn-TPFP tweezer and *S,S*-1,2-diamino cyclohexane (**III-28**), resulting in a positive ECCD spectrum (430 nm, +582; 417 nm, -513; $A = +1095$). Each porphyrin rotate toward the small hydrogen away from the bulky carbon C1 and C2.

compounds are investigated. As such we analyzed the ECCD of *S,S*-1,2-diamino cyclohexane **III-28** (model of a *threo* diamine; clearly the *erythro* example is a *meso* compound and would not lead to an observable ECCD), the results of which are depicted in Figure III-14. Since there is no free rotation about the bond attaching the two chiral centers, the relative disposition of the amine groups is fixed. Porphyrins **P1** and **P2** must approach the diamine from the opposite direction to avoid steric clash, which translates to an arrangement where the two porphyrins are bound *anti* to the bond connecting the two chiral centers (C1-C2 bond, see Figure III-15). Steric

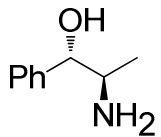
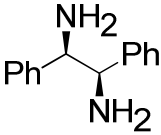
differentiation for each bound porphyrin leads to the rotation of each chromophore towards the smaller group on the chiral center, in both cases the hydrogen atom attached to the chiral centers (**P1** rotates counterclockwise, **P2** rotates clockwise) leading to a positive helicity. The observed ECCD of **III-28** bound to TPFP tweezer **II-25** results in a strong positive signal ($A = +1095$) in accordance with the proposed.

III.2.4 NMR for binding studies of Zn-TPFP tweezer system

Zn-TPFP porphyrin tweezer has a high tendency to aggregate even at low concentrations which is a major hurdle for probing the tweezer binding process as well as active conformations of bound substrates using NMR spectroscopy. To examine the influence of aggregation upon our ECCD study, the CD experiments were conducted with *S,R*-norephedrine (**III-12-ent**) and *R,R*-1,2-diphenylethylene diamine (**III-26**) in hexane by varying the Zn-TPFP tweezer concentration from 10^{-6} M to 10^{-3} M (Table III-6). These two substrates were chosen because they gave strong CD signals under standard conditions.

ECCD study of Zn-TPFP tweezer is normally performed at 10^{-6} M concentration using 1 cm CD cell as described before. When concentration of tweezer is increased above 5 μ M, the background noise is too strong due to the very high absorption and smaller CD cell has to be used. At 10^{-5} M concentration, a much weaker negative ECCD signal was observed using 1 mm CD cell for **III-12-ent**, while **III-26** could still yield a strong positive ECCD signal due to strong binding. No ECCD was observed at 10^{-4} M $\sim 2 \times 10^{-3}$ M concentrations for **III-12-ent**. Compound **III-26**

Table III-6 Effect of concentration on ECCD using TPFP tweezer

	10^{-6} M	10^{-5} M	10^{-4} M	10^{-3} M
	-177 In hexane 1 cm cell	-57 In hexane 1 mm cell	No ECCD In hexane 0.5 mm cell	No ECCD In hexane 0.5 mm cell
	+364 In MCH 1 cm cell	+280 In hexane 1 mm cell	+7 In hexane 0.5 mm cell	No ECCD In hexane 0.5 mm cell

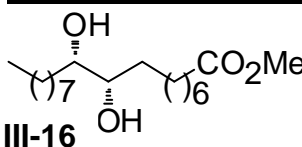
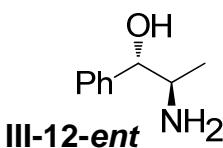
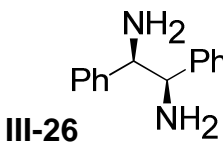
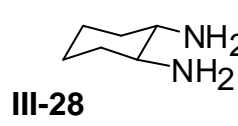
^[a] 1 μ M tweezer concentration at 0 °C was used for all measurements, ^[b] tweezer / substrate ratio – 1 : 5.

yielded observable ECCD ($A = +7$, 5 eq.) at 1×10^{-4} M, but lost the signal after further increasing the concentration. When those 10^{-5} M and 10^{-4} M stock solutions were diluted to 10^{-6} M, prominent ECCD signals returned as observed before. Clearly, significant aggregation of porphyrin tweezer occurred in non-polar solvent hexane at concentrations above 10^{-4} M interfering with the CD measurement. This aggregation phenomenon is actually visible. Based on these results, we believe that at concentrations above 10^{-4} M in hexane, the dominant conformation of tweezer complex is not ECCD active.

Another important issue concerning the NMR binding study is the competitive binding from the NMR solvent due to the high Lewis acidity of Zn-TPFP tweezer. Diol **III-16** and amino alcohol **III-12-ent** did not yield ECCD at 1-100 equivalents in chloroform when the tweezer concentration was gradually increased from 1 μ M to 1 mM (Table III-7) presumably attributed to the solvent competition for complexation

towards the Lewis acidic tweezer. Diamine **III-26** is ECCD silent in chloroform when concentration of tweezer is below 10^{-4} M. At 1 mM tweezer concentrations, diamine **III-26** exhibited a positive signal ($A = +6$). The fairly weak CD signal in such high concentration implies that the population of ECCD active species is low and hard to be discerned by NMR. Consequently, NMR study of the 1 : 1 complex in coordinating solvents like CDCl_3 , ACN, acetone or DMSO is not suitable to reveal the true conformation of the ECCD active complex.

Table III-7 Effect of concentration on ECCD in CHCl_3

	10^{-6} M	10^{-5} M	10^{-4} M	10^{-3} M
 III-16	No ECCD 1 cm cell	No ECCD 1 mm cell	No ECCD In hexane 0.5 mm cell	No ECCD In hexane 0.5 mm cell
 III-12-ent	No ECCD 1 cm cell	No ECCD 1 mm cell	No ECCD 0.5 mm cell	No ECCD 0.5 mm cell
 III-26	No ECCD 1 cm cell	No ECCD 1 mm cell	No ECCD 0.5 mm cell	+ 6 0.5 mm cell
 III-28	No ECCD 1 cm cell	No ECCD 1 mm cell	No ECCD 0.5 mm cell	+8 0.5 mm cell

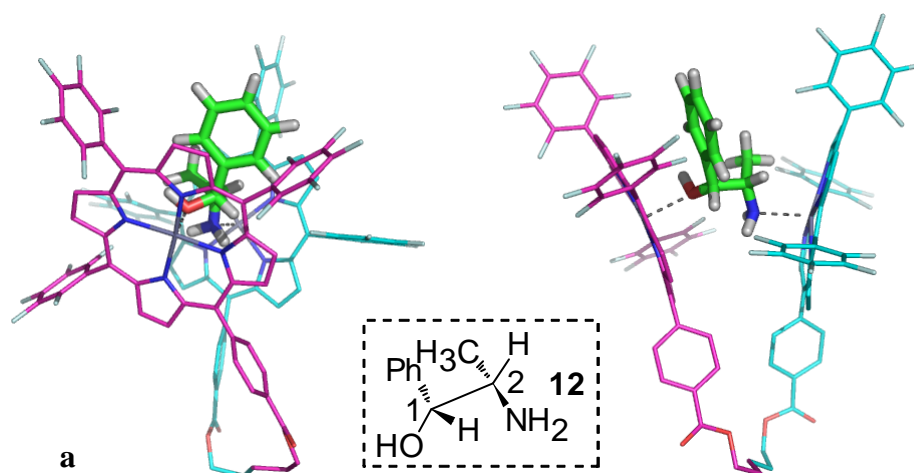
^[a] 1 μM tweezer concentration was used for all measurements, ^[b] tweezer/substrate ratio – 1 : 5.

III.2.5 Conformational Study of Zn-TPFP Tweezer Complex

The inability to employ NMR spectroscopy to investigate the conformations of the

bound substrates prompted us to conduct systematic conformational study using computational method to unveil the preferred conformation of the bound substrate within the tweezer-guest complex since it will help us understand the operational binding mechanism. Monte Carlo conformational study on the Zn-TPFP tweezer complex with chiral substrates was performed using Spartan V 5.1.3 with SYBYL as the force field. The porphyrin ring dihedral angles and the 10,15,20 phenyl torsions were constrained to prevent deformation of porphyrin skeleton during calculation. The O-Zn and N-Zn distance were constrained as 2.3 Å and 2.2 Å respectively to avoid the dissociation of complex. After 1200-1500 fully optimized steps, conformers within 2 kcal / mol energy window were collected for analysis.

Conformation search of *R,S*-erythro compound **III-12**



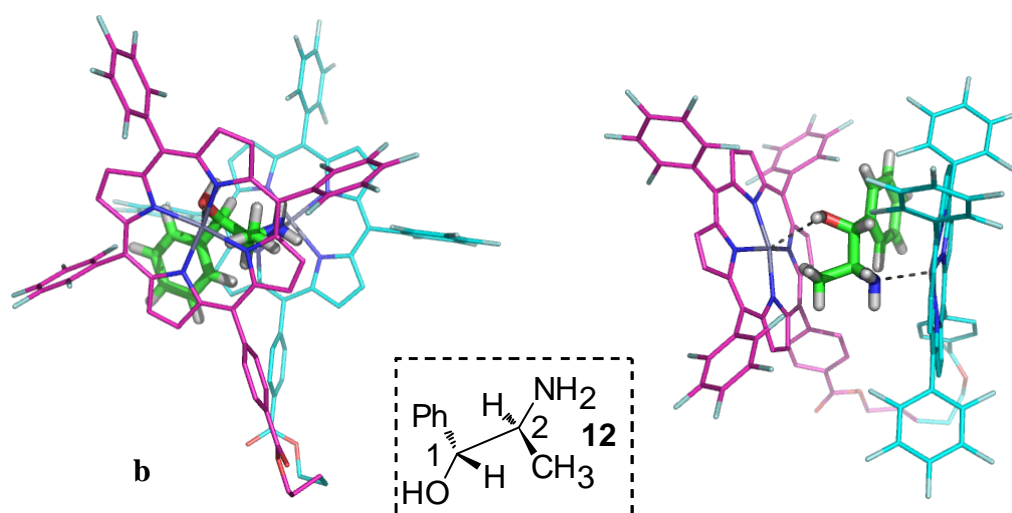


Figure III-16 Front view (left) and side view (right) of the **III-12**-tweezer complex (hydrogen atoms in the tweezer were omitted for clarity).

Within 2 kcal / mol energy window, 28 conformers were generated. Twenty five of these conformers rendered positive projection angles of the two porphyrins indicating clockwise helicity while the remaining 3 conformers showed negative projection angles as well as counterclockwise helicity. Clearly, the **III-12**-tweezer complex has high preference for clockwise helicity as revealed by ECCD measurement. Analysis of the 25 conformers revealed that beside the *anti* conformation (Figure III-16, graph **b**), the chiral molecule could also take a conformation in which the OH and NH₂ groups are *gauch* to each other (Figure III-16, graph **a**).

Conformation search of *R,R*-threo compound **III-15**

Four conformers were collected and all indicated clockwise helicity as proposed. The predominant conformation was found to be similar as the one proposed for compound **III-15** in Figure III-14. The calculated model shown below indicated that the two OH groups are *gauch* to each other and the two substituents (*i*Pr. and Me) are

at *anti*.

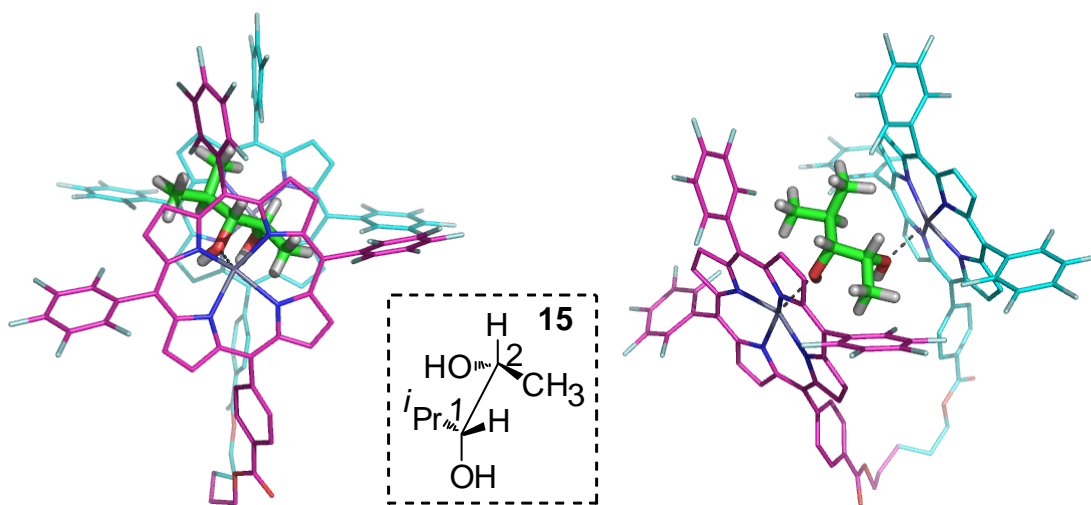


Figure III-17 Front view (left) and side view (right) of the preferred conformation for **III-15**-tweezer complex (hydrogen atoms in the tweezer were omitted for clarity).

Conformation search of *S,S*-threo diepoxide **III-27**

Five conformers were collected within 2 kcal / mol energy window and all indicated clockwise helicity which matched well with the observed positive ECCD signal. All five conformers revealed the same preferred conformation of complexed diepoxide as depicted in Figure III-18.

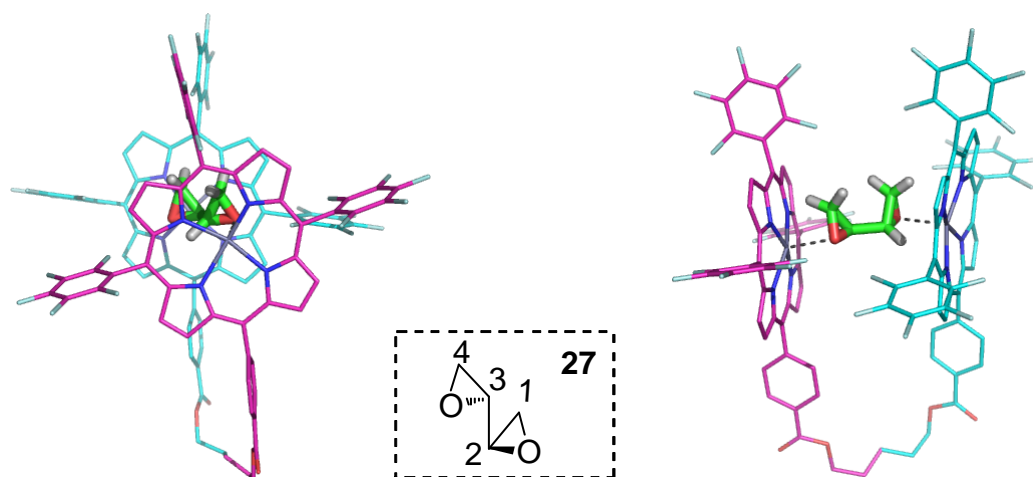


Figure III-18 Front view (left) and side view (right) of the preferred conformation for **III-27**-tweezer complex (hydrogen atoms in the tweezer were omitted for clarity); The C1-C2-C3-C4 dihedral angle is around -55° .

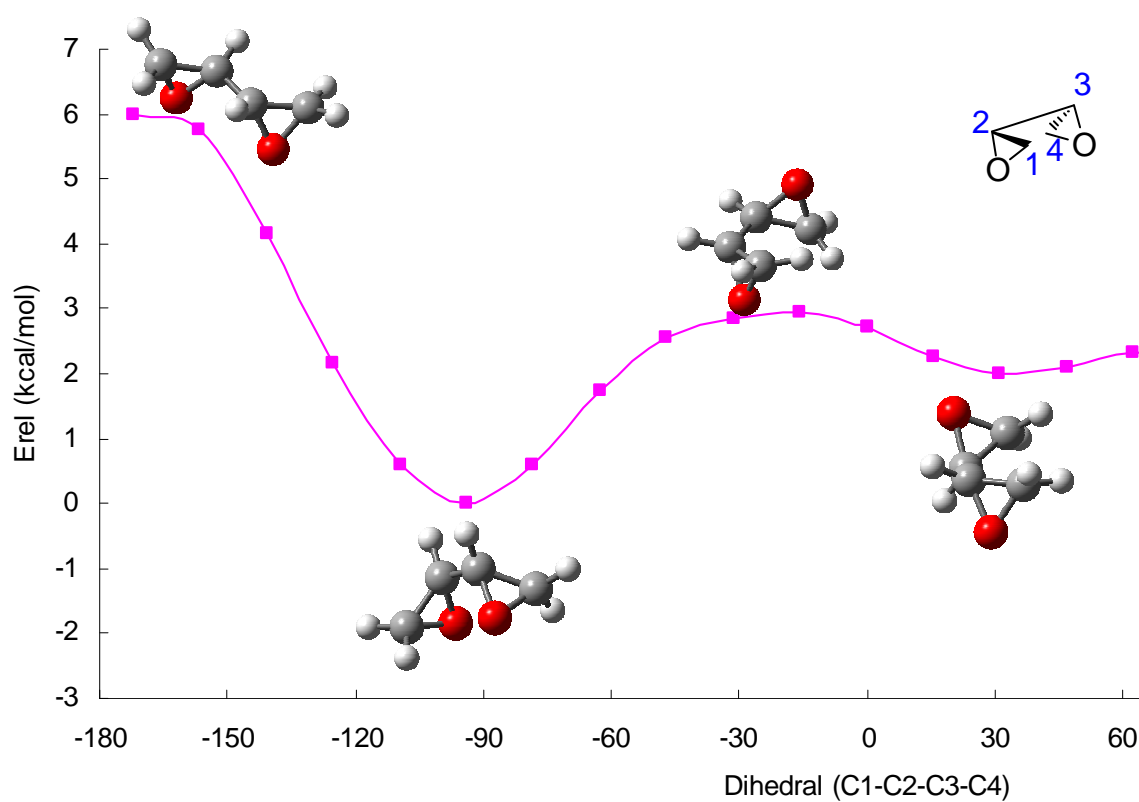


Figure III-19. Energy profile of diepoxide **III-27** at HF/6-31G(d) level.

Coordinative driving for diepoxide **III-27** was performed at HF/6-31G(d) level as shown in Figure III-19 revealing that the preferred conformation of complexed diepoxide is a local minimal (**I**) in the energy profile. To minimize steric interaction, the two porphyrins slide away from two methylene (C1 and C4) groups (Figure III-20) leading to a positive ECCD signal expected for the (*S,S*)-diepoxide.

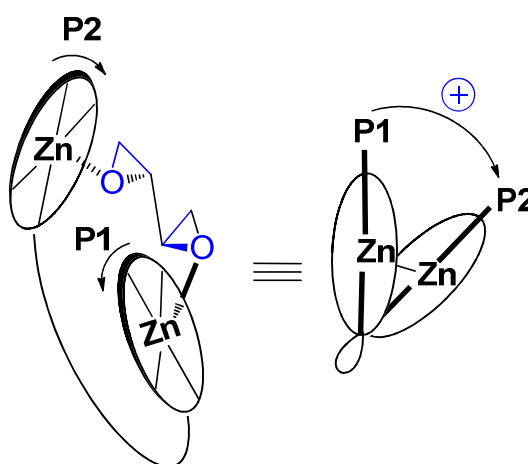


Figure III-20. Proposed complexation pattern between Zn-TPFP tweezer and diepoxide **III-27**.

III.2.6 Comparison between Zn-TPFP tweezer and Zn-TPP tweezer

Initially, this project was pursued based on the supposition that independent steric differentiation of each chiral site bound to the porphyrin tweezer will result in an induced helicity that is observable as an ECCD signal. Although, as described above, this has come to fruition, the initial attempts were discouraging due to the fact that different structures with the same chirality produced differing ECCD signs or none at all. It should be noted that initially the Zn-TPP tweezer was utilized, and it became

apparent that weak binding of substrates potentially contributes to a number of different, energetically close conformations of the complex. As we have documented above, the solution to this problem was to increase the binding of the guest molecules with the host porphyrin tweezer by increasing the Lewis acidity of the zincated porphyrins. Functional comparison of the porphyrin tweezers (Zn-TPP **II-1** vs. Zn-TPFP **II-25**) in deducing the absolute stereochemistry of a number of *threo* and *erythro* diols is provided in Table III-8. The measurements were taken in hexane to assure maximum binding. As was described above and shown in Table III-5, the predicted sign for ECCD matched the observed spectra for all substrates tested with Zn-TPFP tweezer. However, among *erythro* diols only **III-8** and **III-9** yielded observable ECCD signals with Zn-TPP tweezer, albeit with lower amplitudes as compared to those obtained with Zn-TPFP tweezer. Moreover, diol **III-8** did not yield the expected ECCD. All other *erythro* diols tested did not exhibit an ECCD signal. As shown in Table III-7, many *threo* diols were also ECCD silent in the presence of Zn-TPP tweezer. From those that did provide a signal, compounds **III-15** and **III-16**, which led to the highest amplitudes among the diols with Zn-TPFP tweezer, showed much weaker signals when bound with Zn-TPP tweezer. Other *threo* diols such as **III-19** generated signals with signs that are opposite to the predicted model.

Table III-8. ECCD data of Zn-TPP tweezer ^[a] bound *erythro* and *threo* 1,2-diols. ^[b]

	chiral substrates ^[d]	predicted sign	λ nm, ($\Delta\epsilon$)	A
III-8 <i>R,S</i>		+	430 (-9) 414 (+11)	-20
III-9 <i>S,R</i>		-	426 (-6) 416 (+10)	-16
III-14 <i>R,R</i>		+	No ECCD	-
III-15 <i>R,R</i>		+	429 (+17) 414 (-8)	+25
III-16 <i>R,R</i>		+	429 (+34) 416 (-18)	+52
III-17 <i>S,S</i>		-	No ECCD	-
III-18 <i>S,S</i>		+	No ECCD	-
III-19 ^[c] <i>S,S</i>		-	426 (+42) 414 (-24)	+66
III-20 <i>S,S</i>		-	No ECCD	-

^[a] 1 μ M Zn-TPP tweezer concentration was used for all measurements except for **III-8** and **III-9** (2 μ M), ^[b] tweezer/substrate ratio - 1:40, ^[c] tweezer/substrate ratio - 1:100, hexane was used as solvent for all CD measurements.

It seems reasonable to conclude that binding affinity of host-guest complexes used in absolute stereochemical determinations must be considered, especially if weak CD signals and/or inconsistent signs are obtained. In this case, with the use of the electron deficient Zn-TPFP tweezer, diols bound sufficiently strong to produce consistent ECCD spectra leading to a general approach for absolute stereochemical determination of 1,2-systems.

To conclude, we demonstrate the prompt microscale determination of absolute configurations for *threo* and most importantly the often difficult to determine *erythro* diols, amino alcohols, and diamines utilizing the porphyrin tweezer methodology. To the best of our knowledge this is the first routine method that addresses the absolute stereochemical determination of *erythro* compounds. This methodology also requires no derivatizations, which is often used for the absolute stereochemical determination of *threo* compounds. Most importantly, the study demonstrated the possibility of stereochemical determination of two chiral centers simultaneously via porphyrin tweezer method and represents a new concept for chirality sensing. The unique binding mechanism disclosed would be very instructive for further development of chirality sensors as well as the application of this newly developed porphyrin tweezer for other chiral molecules. The enhanced binding affinity opened a broad pathway for determining absolute configurations of a wide range of organic molecules with oxygen-containing functionalities like epoxy alcohols, tetrahydrofurans, hydroxyl ketones, and aziridinols all of which are important building blocks in organic synthesis. The methodology thus developed will attract

chemists in both academic labs and companies who are interested in rapid and facile determination of molecular chirality.

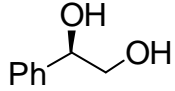
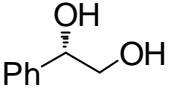
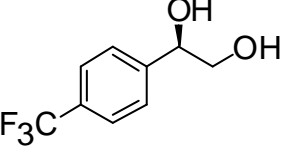
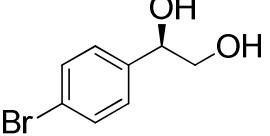
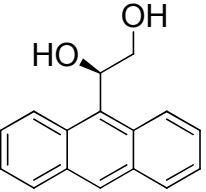
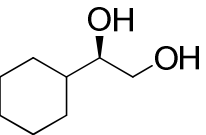
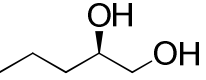
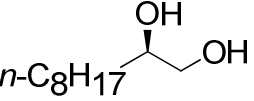
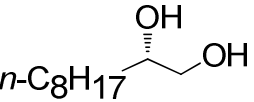
III.3 ECCD Study of 1,2-Terminal Diols and Amino Alcohols Using Zn TFPF Tweezer

Chiral 1,2-terminal diols and amino alcohols are also important building blocks in organic chemistry and frequently encountered in organic synthesis and catalysis. Stereochemical determination of these compounds using conventional NMR analysis is difficult and time consuming. A few CD-based methods were reported for the chirality assignment of terminal diol and amino alcohols. However, the requirement of chemical derivatization and weak CD signals limited their practical applications. A general, facile, and sensitive method addressing the absolute stereochemical determination of this type of substrates is still highly desired.

In the preceding section, Zn-TFPF tweezer **II-25** successfully demonstrated its efficiency in chirality sensing of *erythro* and *threo* diols. Those highly encouraging results made us believe that **II-25** should also be suitable for determining the stereochemistry of terminal diols which are close analogs to *erythro* and *threo* diols. The presence of only one chiral center should make this case even easier since only one stereodifferentiation process would occur. A series of chiral 1,2-terminal diols were then synthesized through Sharpless asymmetric dihydroxylation of terminal olefins. The optical purity of the prepared chiral terminal diols ranged from 78% *e.e.* to 99% *e.e.* and were good enough for ECCD measurements. All the diols exhibited steady bisignate CD curves upon complexation with tweezer **II-25** in

methylcyclohexane at 0 °C. The ECCD data were summarized in Table III-9.

Table III-9. ECCD data of Zn-TPFP tweezer bound terminal 1,2- diols.

	chiral substrates ^[d]	λ nm, ($\Delta\epsilon$)	A
III-29^a <i>R</i>		424 (+32) 415 (-15)	+47
III-29-ent^a <i>S</i>		425 (-23) 414 (+25)	-48
III-30^a <i>R</i>		423 (+16) 415 (-12)	+28
III-31^a <i>R</i>		424 (+24) 413 (-7)	+31
III-32^b <i>R</i>		425 (+22) 400 (-16)	+38
III-33^a <i>R</i>		422 (+33) 413 (-8)	+41
III-34^c <i>R</i>		424 (-26) 413 (+19)	-45
III-35^c <i>R</i>		425 (-42) 412 (+39)	-81
III-35-ent^c <i>S</i>		424 (+49) 411 (-24)	+73

^a 1 μ M tweezer, tweezer/substrate ratio - 1:200; ^b 2 μ M tweezer, tweezer/substrate ratio - 1:200; ^c 1 μ M tweezer, tweezer/substrate ratio - 1:40, methylcyclohexane was used as solvent for all CD measurements.

For aromatic terminal diols (**III-29~III-32**) bearing *R* configuration, *positive* CD couplet was observed when 200 eq. of guests were added to tweezer **II-25** solution (1 μ M in MCH). The binding interaction of the aromatic terminal diols with zinc tweezer seemed weaker than that of *erythro* and *threo* diols since in the latter case only 40 eq. of guest was required to obtain a steady ECCD spectrum. Compound **III-32** was a challenging substrate for other CD based chirality sensing protocol since the molecule itself has a strong circular dichroism across a broad range (250-380 nm) which often interfered with the ECCD measurement by other methods.²⁹ However, prominent ECCD signal at increased tweezer concentration (2 μ M) was acquired and it was well separated from the CD band of **III-32** (Figure III-21). This should thank the much red shifted solet band of porphyrin chromophores.

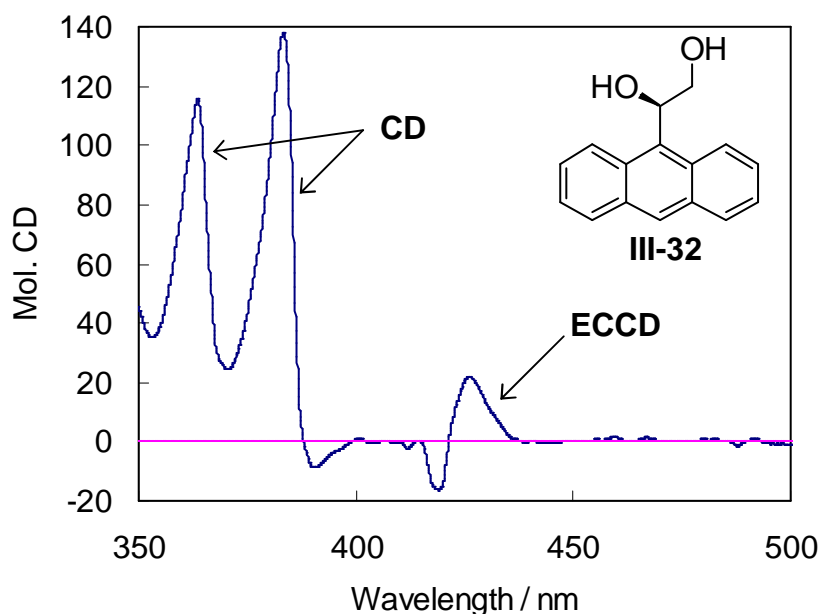


Figure III-21. ECCD spectrum of diol **III-32** (200 eq.) bound with Zn-TPFP tweezer **II-25** (2 μ M) in MCH.

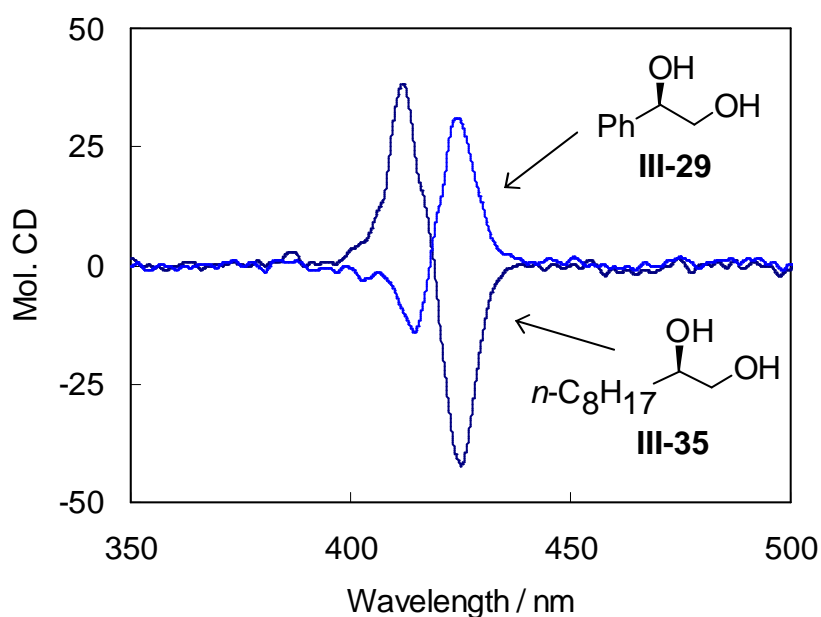


Figure III-22. ECCD spectra of diol **III-29** (200 eq.) and **III-35** (40 eq.) bound with Zn-TPFP tweezer **II-25** (1 μ M) in MCH.

Interestingly, straight chain aliphatic terminal diols (**III-34~III-35**) bearing the same configuration exhibited *negative* CD couplet upon mixing with porphyrin tweezer. The aliphatic diols demonstrated better binding interaction than aryl substrates by yielding stronger ECCD signals in the presence of only 40 eq. of substrate. Aliphatic compound **III-33** bearing *R* stereochemistry rendered positive CD couplet, thus behaved the same as aryl substrates. It also showed weak binding by giving weak CD signal when 200 eq. of guest were introduced. Those observations led to a speculation that two different binding mechanisms may operate for 1,2-terminal diols according to the binding strength of substrates. Changing the solvent to hexane seems to enhance the binding interaction between diols and zinc tweezer because increased ECCD amplitudes were observed. For instance, **III-34** in

hexane with tweezer (1 μ M) rendered much stronger CD signal ($A = -111$ at 40 eq. of guest). However, the change of solvent did not affect the sign of ECCD.

Terminal diols containing tertiary chiral center were also synthesized and subjected to ECCD study. In MCH, the aryl substrate **III-36** bound zinc tweezer slowly and returned stable negative CD signal when over 100 eq. of guest were added. The aliphatic substrate **III-37** bound tweezer strongly and rendered steady positive CD couplet in the presence of 40 eq. of guest.

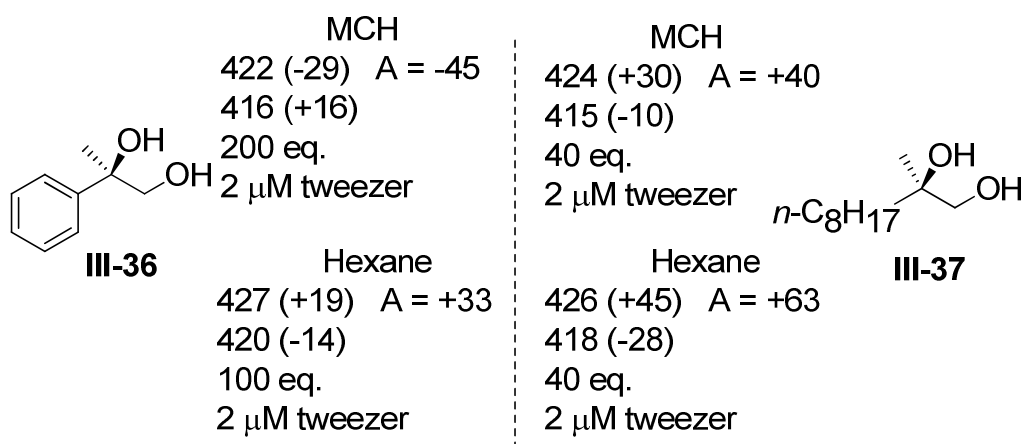
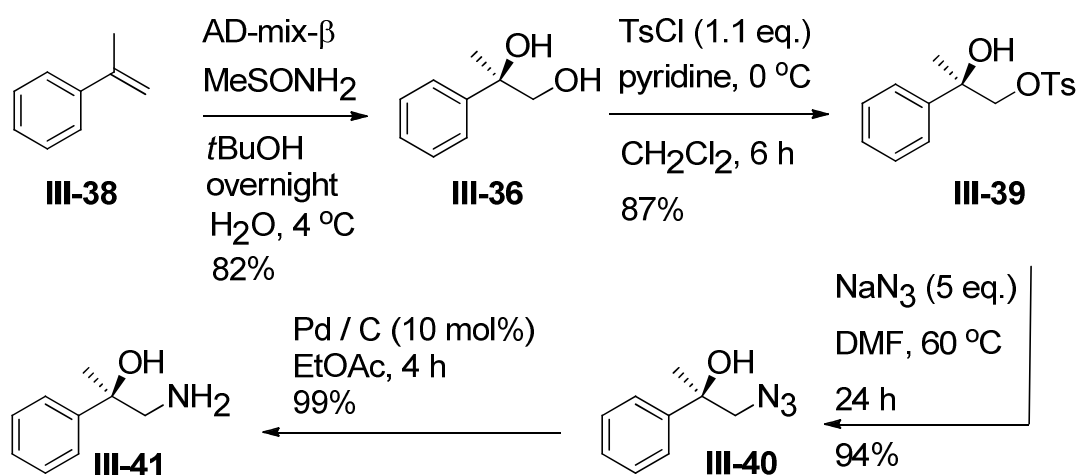


Figure III-23. ECCD data of diol **III-36** and **III-37** bound with Zn-TPFP tweezer **II-25** (2 μ M).

In section III.2.1, we discussed that diol substrates could bind Zn-TPFP tweezer **II-25** several times stronger in hexane than in MCH. As such, we believe that in hexane the tertiary diols could bind zinc tweezer well to form stable ECCD active complex providing reliable assignment of substrates chirality. Therefore, the discrepancy of ECCD signs in MCH between **III-36** and **III-37**, which bear the same

absolute stereochemistry, was tentatively attributed to the weak binding interaction of **III-36** in MCH since it yielded steady *positive* ECCD spectrum in hexane. For substrate **III-37** that binds well with tweezer in either solvent, the sign of the ECCD signal stayed the same.



Scheme III-1. Synthesis of amino alcohol **III-41**.

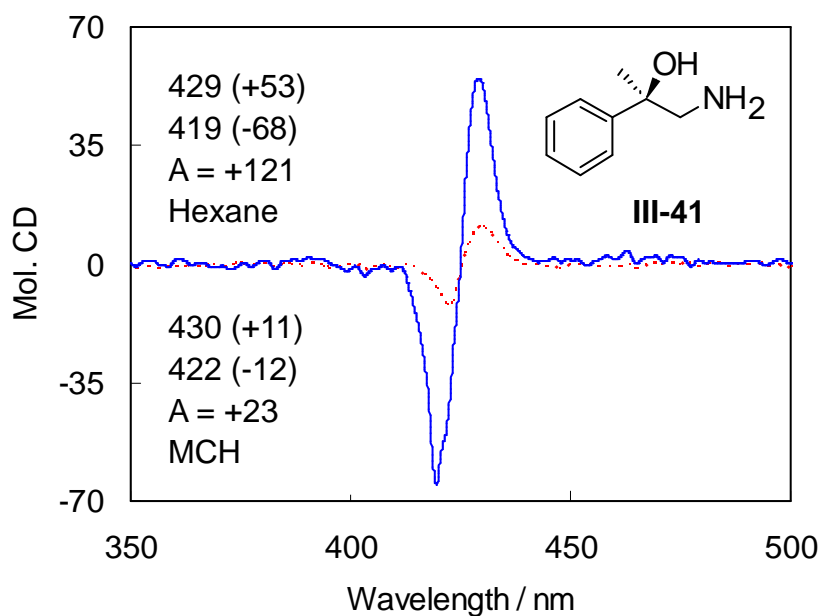


Figure III-24. ECCD spectra of amino alcohol **III-41** (20 eq.) bound with Zn-TPFP tweezer **II-25** in MCH (1 μ M, dashed line) and in hexane (2 μ M, solid line).

To further probe the influence of binding affinity, amino alcohol **III-41** was synthesized from **III-36** (Scheme III-1). This compound has the same absolute configuration as **III-36** at the tertiary chiral center, but has much stronger binding affinity due to the more nucleophilic terminal amino group. The synthesis of **III-41** was completed uneventfully. Subsequent ECCD experiments with tweezer **II-25** clearly revealed intense positive CD couplet in both MCH and hexane (Figure III-24). This result proved that binding affinity did affect the stereodifferentiation process of terminal tertiary diols. When substrates bind strongly with zinc porphyrin tweezer, both aromatic and aliphatic diols behave the same and a consistent trend can be derived, namely the terminal diols bearing *R* configuration at tertiary chiral center would yield positive ECCD signal.

Amino alcohol **III-42** was also prepared from **III-29-ent** using similar procedures described in Scheme III-1. Negative CD couplet was detected for this compound in the ECCD experiment with tweezer **II-25**. This

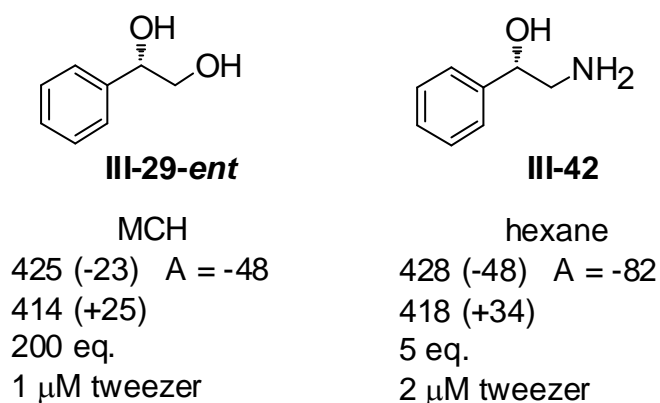


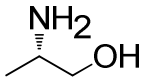
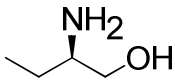
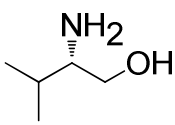
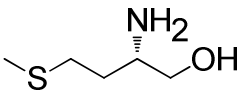
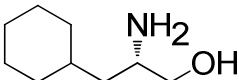
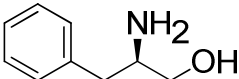
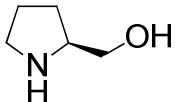
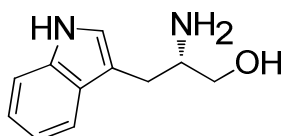
Figure III-25. ECCD data of **III-29-ent** and **III-42** with tweezer **II-25**

behavior is the same as the diol analog the **III-29-ent** suggesting that the opposite trends of ECCD signs between aromatic secondary terminal diols and aliphatic ones

are not induced by the weak binding interaction of the former with the tweezer.

Further investigation is needed to probe the origin of this discrepancy.

Table III-10. ECCD data of Zn-TPFP tweezer bound terminal amino alcohols.

	chiral substrates	λ nm, ($\Delta\epsilon$)	A
III-43 ^a S		427 (+286) 414 (-152)	+438
III-44 ^a R		427 (-344) 414 (+231)	-575
III-45 ^b S		428 (+269) 415 (-200)	+469
III-46 ^a S		428 (+486) 418 (-242)	+728
III-47 ^b S		428 (+290) 414 (-177)	+467
III-48 ^c R		431 (-98) 422 (+98)	-196
III-49 ^b S		426 (+28) 419 (-31)	+59
III-50 ^b S		428 (+71) 421 (-72)	+143

^a 1 μ M tweezer, tweezer/substrate ratio - 1:5; ^b tweezer/substrate ratio - 1:10;

^c tweezer/substrate ratio - 1:20, MCH was used as solvent for all CD measurements.

Eight terminal amino alcohols (III-43~III-50) were obtained from commercial

sources or LAH reduction of amino acids. All the amino alcohols demonstrated excellent binding affinity toward Zn-TPFP tweezer **II-25** and exhibited prominent ECCD signals as tabulated in Table III-10.

A consist trend was disclosed from Table III-10. Positive ECCD signals reflected *S* stereochemistry of NH₂ group within amino alcohols (**III-43**, **III-45~III-47**, **III-49**, **III-50**), while negative CD couplet corresponded to the *R* configuration of substrates (**III-44**, **III-48**). This trend is in well agreement with the observation for aliphatic secondary terminal diols (Table III-9, **III-34**, **III-35**). The aromatic secondary terminal diols (Table III-9, **III-29~III-33**) seemed to follow a different binding mechanism which is still not clear. The unusually high ECCD amplitudes of **III-43~III-47** were attributed to the strong binding affinity of these substrates. This finding revealed great potential of Zn-TPFP tweezer for chirality sensing of amino alcohols.

III.4 Future Work of Developing Novel Zinc Porphyrin Tweezers for ECCD Study

The successful application of Zn-TPFP tweezer **II-25** in chirality sensing of diol system provided important guidelines for future development of novel chirality sensors. Figure III-21 illustrated new zincated porphyrin esters designed for future work, which will lead to more sensitive porphyrin tweezers with enhanced binding affinities. Introduction of eight fluorine atoms into β positions of porphyrin ring (**III-51**, **III-52**) by using 3,4-difluoropyrrole in the synthesis of porphyrin monoester

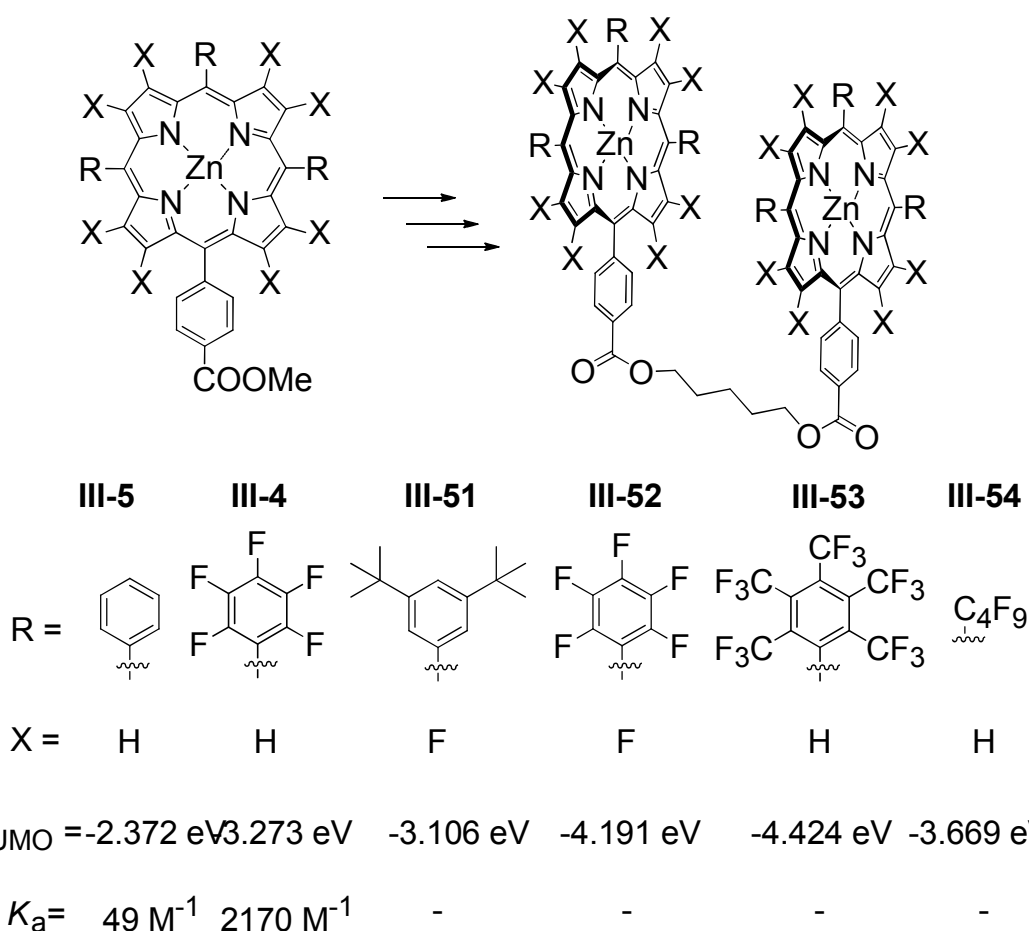


Figure III-26. Proposed zincated porphyrin esters and tweezers for future work (E_{LUMO} are the calculated LUMO energies of zinc porphyrin esters, K_a is the binding constant of zinc porphyrin ester with *i*PrOH determined via UV-vis titration).

should greatly lower the electron density of zincated porphyrin. Consequently the corresponding zinc porphyrin tweezers synthesized should demonstrate much increased binding affinity, thus facilitate the formation of stable tweezer complex with weak nucleophilic guest molecules. This feature is particularly desirable when chiral substrates exhibited weak ECCD signals or complicated cotton effects due to weak binding interactions under standard ECCD experiment conditions. The introduction of highly electron-withdrawing pertrifluoromethyl phenyl groups into porphyrin *meso*

positions (**III-53**) should also gain the same benefit from the increased binding affinity of the resultant zinc porphyrin tweezer.

As we discussed in section III.2.1, the binding affinities can be efficiently evaluated using DFT computational study. The LUMO energy of zinc porphyrin (E_{LUMO}) provides a good measure for the overall Lewis acidity of the metalloporphyrin. The lower the E_{LUMO} , the closer it is to the E_{HOMO} of the chiral guest; the higher its binding affinity. The E_{LUMO} of the proposed porphyrin systems were then calculated (Figure III-21) using DFT method at B3LYP/Lanl2dz // PM3 level and was compared to that of Zn-TPP ester (**III-5**), and Zn-TPFP ester (**III-4**). According to the calculations, metalloporphyrin esters (**III-5**, **III-5**) have much reduced E_{LUMO} , thus suggesting that their porphyrin rings would have higher binding affinities compared to Zn-TPFP ester (**III-4**). As a result, the porphyrin tweezers based on **III-52** and **III-53** are expected to exhibit stronger binding affinities than **II-25**. The *t*-butyl substituted porphyrin ester (**III-51**) has a similar E_{LUMO} as Zn-TPFP ester **III-4**, thus it should bind chiral substrates with enhanced affinity as observed with Zn-TPFP tweezer **II-25**. In addition, the *t*-butyl groups should result in increased steric differentiation and enhanced CD amplitudes in the CD experiment with the tweezer derived from **III-51**. This virtue is useful for analysis of molecules with stereochemistry remote from the functionality binding to the porphyrin. **III-54** is another porphyrin analog of interest. Unlike other candidates, it bears highly electron-withdrawing alkyl groups instead of aryl groups at the *meso* positions of porphyrin. It should also bind chiral guests with high affinity considering its low

E_{LUMO} value. However, we are more interested in looking into the stereodifferentiation behavior of the porphyrin tweezer derived from **III-54**. We speculate that the resultant new tweezer may behave differently from the aryl substituted ones since it does not have the *ortho* and *meta* substituents of aryl rings, which are important to the stereodifferentiation in ECCD study (Figure II-4). The related investigation would better our understanding of porphyrin tweezer system in chirality sensing.

Experimental Procedures

Materials and general instrumentations:

Anhydrous CH_2Cl_2 was dried and redistilled over CaH_2 . The solvents used for CD measurements were purchased from Aldrich and were spectra grade. All reactions were performed in dried glassware under nitrogen. Column chromatography was performed using SiliCycle silica gel (230-400 mesh). ^1H NMR and ^{13}C NMR spectra were obtained on Varian Inova 300 MHz or 500Hz instrument and are reported in parts per million (ppm) relative to the solvent resonances (δ), with coupling constants (J) in Hertz (Hz). IR studies were performed on a Nicolet FT-IR 42 instrument. UV/Vis spectra were recorded on a Perkin-Elmer Lambda 40 spectrophotometer, and were reported as λ_{max} [nm]. CD spectra were recorded on a JASCO J-810 spectropolarimeter, equipped with a temperature controller (Neslab 111) for low temperature studies, and were reported as λ [nm] ($\Delta\epsilon_{\text{max}}$ [$\text{L mol}^{-1} \text{cm}^{-1}$]). Optical rotations were recorded on a Perkin Elemer 341 Polarimeter ($\lambda = 589 \text{ nm}$, 1 dm cell). Chiral GC analyses were performed on a Hewlett Packard 6890 gas chromatograph equipped with a Supel Beta Dex 325 column. GC/MS analyses were performed on a Hewlett Packard 5890 gas chromatograph and a Trio-1 mass detector. RMS analyses were performed on a Q-TOF Ultima system using electrospray ionization in positive mode.

General procedure for CD measurement:

Zinc porphyrin tweezer **II-25** (1 μL of a 1 mM solution in anhydrous CH_2Cl_2) was

added to methylcyclohexane (1 mL) in a 1.0 cm cell to obtain a 1 μ M tweezer **II-25** solution. The background spectrum was then taken from 350 nm to 550 nm with a scan rate of 100 nm/min at 0 °C. Chiral substrate solution (5 to 200 μ L of a 1 mM solution in anhydrous CH₂Cl₂) was added into the prepared tweezer solution to afford the host/guest complex. The CD spectra were measured immediately (minimum of 4 accumulations). The resultant ECCD spectra recorded in millidegrees were normalized based on the tweezer concentration.

Determination of binding constant

The solution of Zn-porphyrin tweezer (1 mM in hexane) was titrated with guest molecule (10 mM in DCM) at different equivalents and the UV-vis spectra were recorded. The addition of the chiral substrate continued until no visible change in the spectra was observed. Upon formation of the chiral complex the Soret band of the porphyrin tweezers underwent red-shifts through an isosbestic point. The change of absorption at certain wavelength as a function of the substrate concentration yields an exponential saturation curve which can be fitted through the following non-linear least square equation previously reported by Shoji³⁹ to derive the binding constant.

$$f = L \{ (1 + kx + ka) - [L^2(1 + kx + ka)^2 - 4axk^2L^2]^{1/2} \} / 2ka$$

where: L - Δ abs at the point of saturation; x - chiral substrate equivalents; k - calculated K_a ; a - concentration of porphyrin tweezer

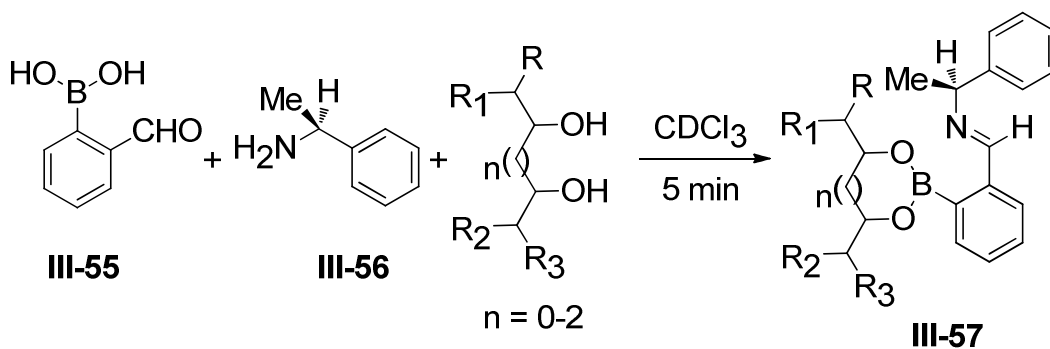
Synthesis of chiral diols

Chiral substrates **III-11**, **III-12**, **III-20**, **III-22**, **III-25**, **III-26**, **III-28** and their enantiomers were commercially available from Aldrich. Other substrates were synthesized using procedures described below.

Typical procedure for synthesis of chiral diols using sharpless asymmetric dihydroxylation (SAE):⁴⁵

AD-mix (1.4 g), MeSO₂NH₂ (95 mg, 1 mmol), *t*-BuOH (4.7 mL) and H₂O (4.7 mL) were mixed in a 50 mL round bottom flask and cooled to 4 °C. The orange suspension was stirred for 30 min followed by addition of olefin (1 mmol) via syringe. The resultant solution was stirred at 4 °C for 24 h, after which Na₂SO₃ (1.5 g) was added. After being stirred for further 45 min at room temperature, the clear solution was diluted by EtOAc (10 mL) and H₂O (2 mL). The aqueous layer was extracted with EtOAc (3 × 10 mL). Combined EtOAc extracts were dried over Na₂SO₄, concentrated under reduced pressure, and purified by flash column chromatography (30% EtOAc / Hexane) to afford pure diol.

Determination of enantiomeric excess of diols by forming iminoboronic ester



Scheme III-2. Formation of iminoboronic ester.

The determination of enantiomeric excess of chiral diols could be conducted using literature procedure.⁴⁶ Chiral diol (1.0 eq.), 2-formylphenylboronic acid **III-55** (1 eq.), and (S)- α -methylbenzylamine **III-56** (1.0 eq.) were dissolved in CDCl₃ in the presence of 4 Å molecular sieves and the solution was shaken briefly leading to the complete conversion into chiral iminoboronic ester **III-57**. An aliquot of the solution was then taken for ¹H NMR analysis. By analyzing the diastereomeric ratio of the imine protons, the enantiomeric excess of chiral diol could be derived. In certain cases, the chiral proton of chiral amine and the chiral protons of diol can also be used to elucidate diastereomeric ratio as well as the enantiomeric purity.

REFERENCES

References

1. Berova, N.; Nakanishi, K.; Woody, R. W., *Circular Dichroism: Principles and Applications*. 2nd ed.; Wiley-VCH: New York, 2000.
2. Harada, N.; Nakanishi, K., *Circular Dichroic Spectroscopy: Exciton Coupling in Organic Stereochemistry*. University Science Books: Mill Valley, CA, 1983.
3. Kawamura, A.; Berova, N.; Nakanishi, K.; Voigt, B.; Adam, G., Configurational assignment of brassinosteroid sidechain by exciton coupled circular dichroic spectroscopy. *Tetrahedron* **1997**, 53, (35), 11961-11970.
4. Cai, G. L.; Bozhkova, N.; Odingo, J.; Berova, N.; Nakanishi, K., CD Exciton Chirality Method - New Red-Shifted Chromophores for Hydroxyl-Groups. *Journal of the American Chemical Society* **1993**, 115, (16), 7192-7198.
5. Harada, N.; Saito, A.; Ono, H.; Gawronski, J.; Gawronska, K.; Sugioka, T.; Uda, H.; Kuriki, T., A CD Method for Determination of the Absolute Stereochemistry of Acyclic Glycols .1. Application of the CD Exciton Chirality Method to Acyclic 1,3-Dibenzoate Systems. *Journal of the American Chemical Society* **1991**, 113, (10), 3842-3850.
6. Jiang, H.; Huang, X. F.; Nakanishi, K.; Berova, N., Nanogram scale absolute configurational assignment of ceramides by circular dichroism. *Tetrahedron Letters* **1999**, 40, (43), 7645-7649.
7. Matile, S.; Berova, N.; Nakanishi, K.; Fleischhauer, J.; Woody, R. W., Structural studies by exciton coupled circular dichroism over a large distance: Porphyrin derivatives of steroids, dimeric steroids, and brevetoxin B. *Journal of the American Chemical Society* **1996**, 118, (22), 5198-5206.
8. Matile, S.; Berova, N.; Nakanishi, K.; Novkova, S.; Philipova, I.; Blagoev, B., Porphyrins - Powerful Chromophores for Structural Studies by Exciton-Coupled Circular-Dichroism. *Journal of the American Chemical Society* **1995**, 117, (26), 7021-7022.
9. Rele, D.; Zhao, N.; Nakanishi, K.; Berova, N., Acyclic 1,2-/1,3-mixed pentols. Synthesis and general trends in bichromophoric exciton coupled circular dichroic spectra. *Tetrahedron* **1996**, 52, (8), 2759-2776.
10. Uzawa, H.; Nishida, Y.; Ohru, H.; Meguro, H., Application of the Dibenzoate

Chirality Method to Determine the Absolute-Configuration of Glycerols and Related Acyclic Alcohols. *Journal of Organic Chemistry* **1990**, 55, (1), 116-122.

11. Weckerle, B.; Schreier, P.; Humpf, H. U., A new one-step strategy for the stereochemical assignment of acyclic 2-and 3-sulfanyl-1-alkanols using the CD exciton chirality method. *Journal of Organic Chemistry* **2001**, 66, (24), 8160-8164.

12. Wiesler, W. T.; Nakanishi, K., Relative and Absolute Configurational Assignments of Acyclic Polyols by Circular-Dichroism .1. Rationale for a Simple Procedure Based on the Exciton Chirality Method. *Journal of the American Chemical Society* **1989**, 111, (26), 9205-9213.

13. Zhao, N.; Berova, N.; Nakanishi, K.; Rohmer, M.; Mougnot, P.; Jurgens, U. J., Structures of two bacteriohopanoids with acyclic pentol side-chains from the cyanobacterium Nostoc PCC 6720. *Tetrahedron* **1996**, 52, (8), 2777-2788.

14. Zhou, P.; Berova, N.; Wiesler, W. T.; Nakanishi, K., Assignment of Relative and Absolute-Configuration of Acyclic Polyols and Aminopolyols by Circular-Dichroism - Trends Follow Fischer Sugar Family Tree. *Tetrahedron* **1993**, 49, (41), 9343-9352.

15. Di Bari, L.; Lelli, M.; Pintacuda, G.; Salvadori, P., Yb(fod)(3) in the spectroscopic determination of the configuration of chiral diols: A survey of the lanthanide diketonate method. *Chirality* **2002**, 14, (4), 265-273.

16. Di Bari, L.; Pescitelli, G.; Pratelli, C.; Pini, D.; Salvadori, P., Determination of absolute configuration of acyclic 1,2-diols with Mo-2(OAc)(4). 1. Snatzke's method revisited. *Journal of Organic Chemistry* **2001**, 66, (14), 4819-4825.

17. Dillon, J.; Nakanishi, K., Absolute Configurational Studies of Vicinal Glycols and Amino Alcohols .1. With Ni(Acac)₂. *Journal of the American Chemical Society* **1975**, 97, (19), 5409-5417.

18. Dillon, J.; Nakanishi, K., Absolute Configurational Studies of Vicinal Glycols and Amino Alcohols .2. With Pr(Dpm)₃. *Journal of the American Chemical Society* **1975**, 97, (19), 5417-5422.

19. Frelek, J.; Geiger, M.; Voelter, W., Transition metal complexes as auxiliary chromophores in chiroptical studies on carbohydrates. *Current Organic Chemistry* **1999**, 3, (2), 117-146.

20. Frelek, J.; Ikekawa, N.; Takatsuto, S.; Snatzke, G., Application of [Mo-2(OAc)(4)] for determination of absolute configuration of brassinosteroid vic-diols by circular dichroism. *Chirality* **1997**, 9, (5-6), 578-582.

21. Frelek, J.; Snatzke, G., Circular-Dichroism .80. Determination of the Absolute-Configuration of 1-Substituted Glycerol Derivatives and Other Aliphatic Vic-Glycols on Micro Scale. *Fresenius Zeitschrift Fur Analytische Chemie* **1983**, 316, (2), 261-264.
22. Scott, A. I.; Wrixon, A. D., Chirality of Olefin Complexes. *Journal of the Chemical Society D-Chemical Communications* **1969**, (20), 1184-1186.
23. Snatzke, G.; Wagner, U.; Wolff, H. P., Circular-Dichroism .75. Cottonogenic Derivatives of Chiral Bidentate Ligands with the Complex $[\text{Mo}_2(\text{O}_2\text{cch}_3)_4]$. *Tetrahedron* **1981**, 37, (2), 349-361.
24. Donnoli, M. I.; Scafato, P.; Superchi, S.; Rosini, C., Synthesis and stereochemical characterization of optically active 1,2-diarylethane-1,2-diols: Useful chiral controllers in the Ti-mediated enantioselective sulfoxidation. *Chirality* **2001**, 13, (5), 258-265.
25. Rosini, C.; Scamuzzi, S.; Pisani-Facati, M.; Salvadori, P., A General, Multitechnique Approach to the Stereochemical Characterization of 1,2-Diarylethane-1,2-diol. *Journal of Organic Chemistry* **1995**, 60, 8289.
26. Rosini, C.; Scamuzzi, S.; Uccellobarretta, G.; Salvadori, P., Synthesis and Stereochemical Characterization of Some Optically-Active 1,2-Dinaphthylethane-1,2-Diols. *Journal of Organic Chemistry* **1994**, 59, (24), 7395-7400.
27. Superchi, S.; Casarini, D.; Laurita, A.; Bavoso, A.; Rosini, C., Induction of a preferred twist in a biphenyl core by stereogenic centers: A novel approach to the absolute configuration of 1,2-and 1,3-diols. *Angewandte Chemie-International Edition* **2001**, 40, (2), 451-454.
28. Superchi, S.; Casarini, D.; Summa, C.; Rosini, C., A general and nonempirical approach to the determination of the absolute configuration of 1-aryl-1,2-diols. *Journal of Organic Chemistry* **2004**, 69, (5), 1685-1694.
29. Superchi, S.; Donnoli, M. I.; Rosini, C., Determination of the Absolute Configuration of 1-Arylethane-1,2-diols by a Nonempirical Analysis of the CD Spectra of Their 4-Biphenylboronates. *Org. Lett.* **1999**, 1, 2093-2096.
30. Huang, X. F.; Borhan, B.; Rickman, B. H.; Nakanishi, K.; Berova, N., Zinc porphyrin tweezer in host-guest complexation: Determination of absolute configurations of primary monoamines by circular dichroism. *Chemistry-a European Journal* **2000**, 6, (2), 216-224.

31. Huang, X. F.; Fujioka, N.; Pescitelli, G.; Koehn, F. E.; Williamson, R. T.; Nakanishi, K.; Berova, N., Absolute configurational assignments of secondary amines by CD-sensitive dimeric zinc porphyrin host. *Journal of the American Chemical Society* **2002**, 124, (35), 10320-10335.
32. Huang, X. F.; Rickman, B. H.; Borhan, B.; Berova, N.; Nakanishi, K., Zinc porphyrin tweezer in host-guest complexation: Determination of absolute configurations of diamines, amino acids, and amino alcohols by circular dichroism. *Journal of the American Chemical Society* **1998**, 120, (24), 6185-6186.
33. Kurtan, T.; Nesnas, N.; Koehn, F. E.; Li, Y. Q.; Nakanishi, K.; Berova, N., Chiral recognition by CD-sensitive dimeric zinc porphyrin host. 2. Structural studies of host-guest complexes with chiral alcohol and monoamine conjugates. *Journal of the American Chemical Society* **2001**, 123, (25), 5974-5982.
34. Kurtan, T.; Nesnas, N.; Li, Y. Q.; Huang, X. F.; Nakanishi, K.; Berova, N., Chiral recognition by CD-sensitive dimeric zinc porphyrin host. 1. Chiroptical protocol for absolute configurational assignments of monoalcohols and primary monoamines. *Journal of the American Chemical Society* **2001**, 123, (25), 5962-5973.
35. Lintuluoto, J. M.; Borovkov, V. V.; Inoue, Y., Direct determination of absolute configuration of monoalcohols by bis(magnesium porphyrin). *Journal of the American Chemical Society* **2002**, 124, (46), 13676-13677.
36. Proni, G.; Pescitelli, G.; Huang, X. F.; Nakanishi, K.; Berova, N., Magnesium tetraarylporphyrin tweezer: A CD-sensitive host for absolute configurational assignments of alpha-chiral carboxylic acids. *Journal of the American Chemical Society* **2003**, 125, (42), 12914-12927.
37. Proni, G.; Pescitelli, G.; Huang, X. F.; Quraishi, N. Q.; Nakanishi, K.; Berova, N., Configurational assignment of alpha-chiral carboxylic acids by complexation to dimeric Zn-porphyrin: host-guest structure, chiral recognition and circular dichroism. *Chemical Communications* **2002**, (15), 1590-1591.
38. Yang, Q. F.; Olmsted, C.; Borhan, B., Use of porphyrin tweezers in absolute stereochemical determination of chiral acids. *Organic. Lett.* **2002**, 4, 3423.
39. Shoji, Y.; Tashiro, K.; Aida, T., Sensing of chiral fullerenes by a cyclic host with an asymmetrically distorted pi-electronic component. *Journal of the American Chemical Society* **2006**, 128, 10690-10691.
40. Hunter, C. A.; Meah, M. N.; Sanders, J. K. M., Dabco Metalloporphyrin Binding - Ternary Complexes, Host Guest Chemistry, and the Measurement of Pi-Pi-Interactions. *Journal of the American Chemical Society* **1990**, 112, 5773-5780.

41. Huang, X.; Borhan, B.; Berova, N.; Nakanishi, K., UV-Vis Spectral Changes in the Binding of Acyclic Diamines with a Zinc Porphyrin Tweezer. *J. Indian Chem. Soc.* **1998**, 75, 725-728.
42. Kim, M. J.; Choi, G. B.; Kim, J. Y.; Kim, H. J., Lipase-Catalyzed Transesterification as a Practical Route to Homochiral Acyclic Anti-1,2-Diols - a New Synthesis of (+)-Endo-Brevicomin and (-)-Endo-Brevicomin. *Tetrahedron Letters* **1995**, 36, (35), 6253-6256.
43. Notz, W.; List, B., Catalytic asymmetric synthesis of anti-1,2-diols. *Journal of the American Chemical Society* **2000**, 122, (30), 7386-7387.
44. Narayan, R. S.; Sivakumar, M.; Bouhlel, E.; Borhan, B., Regiochemical control in intramolecular cyclization of methylene-interrupted epoxydiols. *Organic Letters* **2001**, 3, (16), 2489-2492.
45. Kolb, H. C.; Vannieuwenhze, M. S.; Sharpless, K. B., Catalytic Asymmetric Dihydroxylation. *Chemical Reviews* **1994**, 94, (8), 2483-2547.
46. Kelly, A. M.; Perez-Fuertes, Y.; Arimori, S.; Bull, S. D.; James, T. D., Simple protocol for NMR analysis of the enantiomeric purity of diols. *Organic Letters* **2006**, 8, (10), 1971-1974.

Chapter IV

Determination of Absolute Configurations for Chiral Epoxy Alcohols using Zn-TPFP Tweezer

IV.1 Background

IV.1.1 Conventional methods for stereochemical determination of epoxy alcohols

Chiral epoxy alcohols are invaluable building blocks in organic synthesis and are encountered in many biologically active natural products (Figure IV-1). In the pursuit for total synthesis of natural products, the absolute stereochemistry of certain epoxy alcohol moiety cannot be unambiguously assigned until several diastereomers are synthesized.¹⁻³

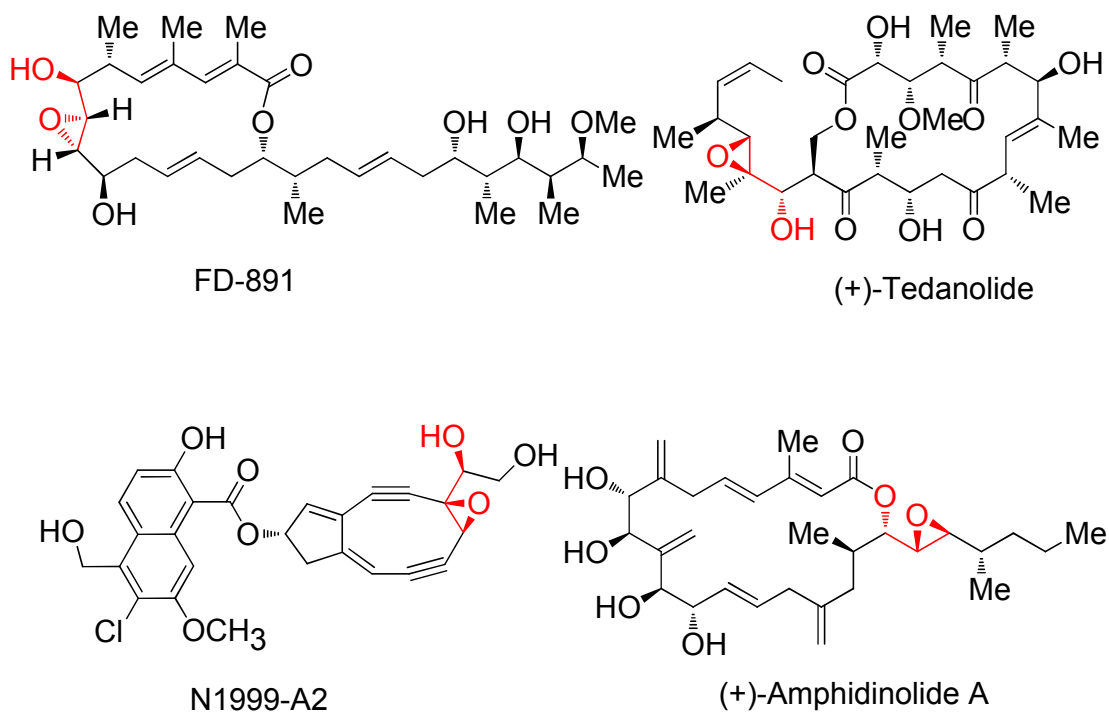


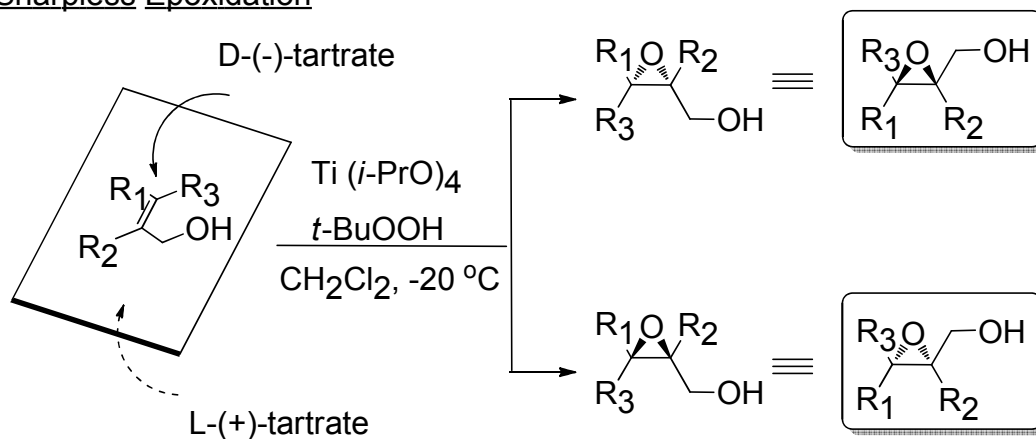
Figure IV-1. Epoxy alcohols in natural products.

For instance, after the isolation and structure elucidation of Amphidinolide A by Kobayashi,^{4, 5} Maleczka,⁶ Pattenden,⁷ and Trost^{2, 3} independently completed the total synthesis of proposed structure in order to figure out the absolute stereochemistry of this natural product. However, the proposed structures proved to be synthetic isomers of natural product since they gave identical ¹H NMR spectra which were different from the data of natural product reported by Kobayashi.⁵ The stereochemistry of epoxy alcohol moiety underwent several revisions and was finally conformed by Trost² through synthesis of all four diastereomers of epoxy alcohol moiety in Amphidinolide A and careful examination of the NMR data.

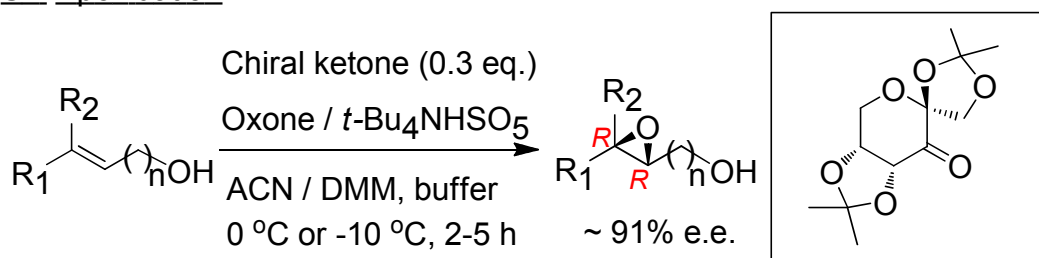
Conventionally, assignment of absolute configuration of chiral epoxy alcohols relies heavily on Mosher ester analysis^{8, 9} of the corresponding ring opened diol or established empirical mnemonics¹⁰⁻¹⁴ developed for different asymmetric epoxidation strategies (Figure IV-2). The former approach requires derivatization, which is inconvenient especially when only limited amount of substrate is available. The empirical nature of the latter approach may lead to unreliable assignment of chirality especially when the substrate contains chiral centers which may perturb the asymmetric induction process.

As important as chiral epoxy alcohols are in synthetic organic chemistry, there is no direct method for the assignment of their absolute stereochemistry. As such, we pursued the development of a microscale, nonempirical, expedient protocol to determine the absolute configuration of chiral epoxy alcohols without the need for any derivatization.

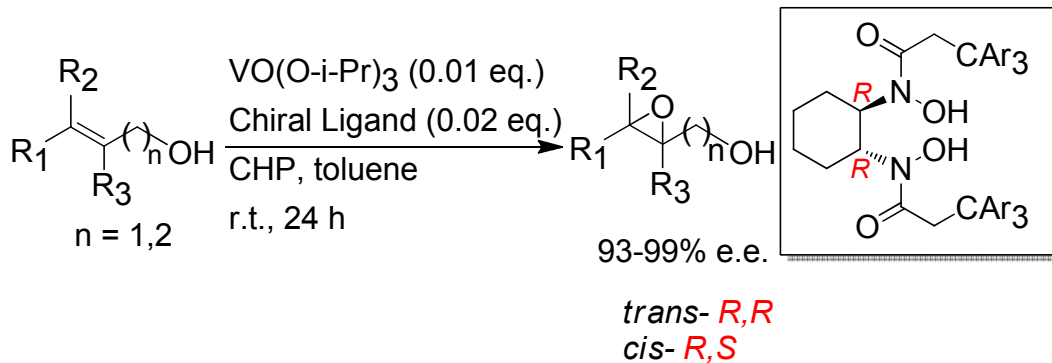
Sharpless Epoxidation



Shi Epoxidation



Yamamoto Epoxidation



Jacobsen Epoxidation

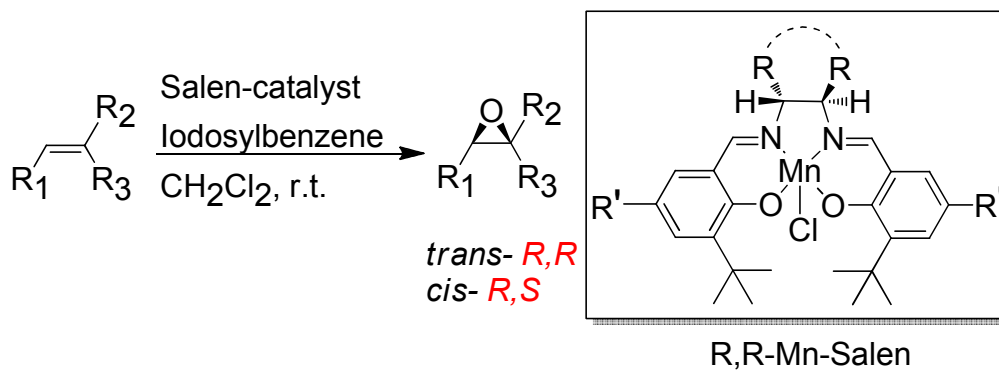


Figure IV-2. Mnemonics for asymmetric epoxidation.

IV.2 ECCD Study of Chiral Epoxy Alcohols Using TPFP Tweezer

IV.2.1 Binding affinity of Zn-TPFP tweezer

It was envisaged that the use of the porphyrin tweezer, utilized previously to assign the absolute stereochemistry of families of different chiral organic molecules such as diamines and amino alcohols could also lead to a successful strategy for assignment of chirality for epoxy alcohols.^{15, 16} Central to the success of this route would be the use of a porphyrin tweezer capable of efficient binding with the epoxy alcohol. In chapter 3, we have introduced the use of the highly Lewis acidic porphyrin tweezer **II-25** featuring a strong binding affinity for hydroxyl groups,¹⁶ and demonstrated its ability to bind 1,2,3,4-diepoxycyclobutane (see Figure III-18) and yield the ECCD signal. Indication of strong binding can be further demonstrated from the binding affinity of the epoxy alcohols with Zinc TPFP tweezer **II-25** which was determined through titration of porphyrin tweezer **II-25** with corresponding guest. The UV spectra of the titration of (2*S*,3*S*)-3-phenyloxiranemethanol **IV-1** shown below (Figure IV-3) demonstrates the change in the Soret band absorption upon binding of the guest to the host. Plot of the equivalents of the epoxy alcohol added as a function of the change in absorption (426 nm) leads to a saturation curve, which provides the binding constant of complex formed upon non-linear least square analysis using SigmaPlot 2001 program. Calculations of binding constants follows protocols in Chapter 3.¹⁷ The derived binding constant (K_{assoc} of **IV-1** with **II-25** is $2.88 \times 10^4 \text{ M}^{-1}$ in hexane) is comparable to that of vicinal diols (K_{assoc} of diol **III-16** with **II-25** is $1.52 \times 10^5 \text{ M}^{-1}$ in hexane) suggesting a good binding affinity of Zn tweezer with epoxy alcohols.

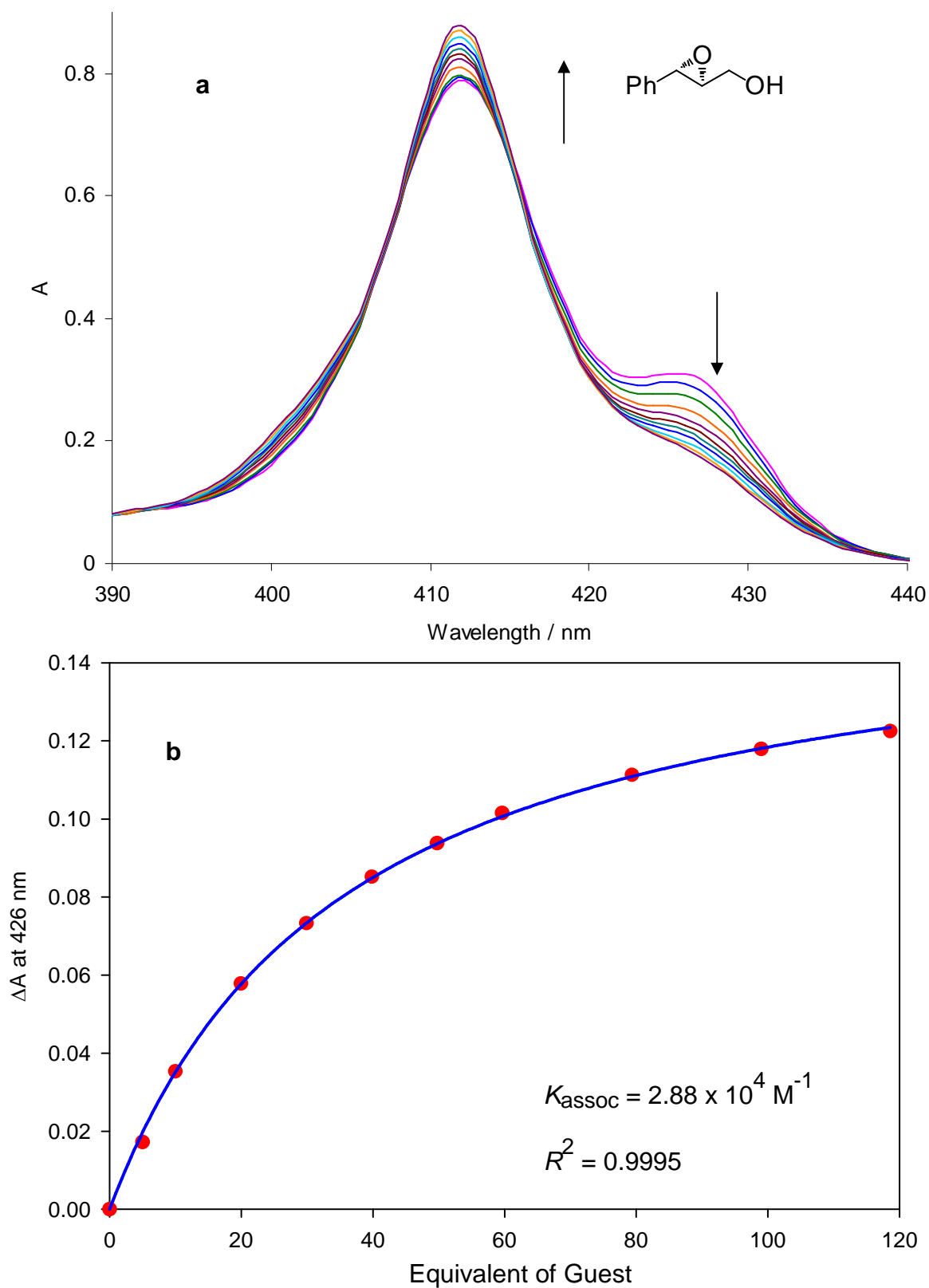


Figure IV-3. (a) UV-Vis spectra change upon titration of TFPF tweezer with **IV-1** at different equivalents. (b) Non-linear least square fit of the change in absorption.

The strong Lewis acidity of zinc porphyrin tweezer raised a concern about the possibility of ring opening of the reactive epoxide ring. We believe the ring opening of epoxide does not happen since the CD measurement was conducted in anhydrous solvent free of nucleophile like H₂O and most substrates gave consistent bisignate ECCD which did not deteriorate with time. If ring opening occurred, we would expect complicated or gradually diminished ECCD signals during measurement. We also mixed the Zn TPFP tweezer and **IV-1** with 1:2 ratio and let it stand for two hours. ¹H NMR indicated that the complex remained stable during this period and no ring opening product was detected. Subsequent silica gel column chromatography recovered both tweezer and epoxy alcohol in quantitative yields. We thus concluded that the epoxy alcohols are stable during ECCD measurements.

IV.2.2 Determination of chirality for epoxy alcohols

In light of the above observations, Zn-TPFP tweezer **II-25** was examined for configurational assignment of a variety of epoxy alcohols (synthetic details will be discussed in section IV.2.3) via the Exciton Coupled Circular Dichorism protocol. To our delight, prominent bisignate CD signals at the Soret region were observed upon complexation of Zn-TPFP tweezer with micromolar concentrations of a large number of chiral epoxy alcohols (Table IV-1).

As shown in Table IV-1, the (2*S*,3*S*) *trans*-disubstituted epoxy alcohols (**IV-1~IV-4**, **IV-6**, and **IV-7**) resulted in negative ECCD spectra while positive signals were observed for (2*R*,3*R*) substrates (**IV-8** and **IV-9**). The correlation between substrate

Table IV-1. ECCD data of 2,3- epoxy alcohols bound to Zn-TPFP tweezer in hexane^a

	Epoxy Alcohol	Predicted Sign	λ nm, ($\Delta\epsilon$)	A
IV-1^a 2S,3S		<i>neg</i>	423 (-55) 410 (+62)	-117
IV-2 2S,3S		<i>neg</i>	423 (-60) 412 (+45)	-105
IV-3 2S,3S		<i>neg</i>	Complex CD	
IV-4 2S,3S		<i>neg</i>	423 (-117) 412 (+89)	-206
IV-5^b 2R,3R		<i>pos</i>	Complex CD	
IV-6^c 2S,3S		<i>neg</i>	422 (-27) 413 (+31)	-58
IV-7 2S,3S		<i>neg</i>	423 (-65) 411 (+56)	-121
IV-8^d 2R,3R		<i>pos</i>	424 (+29) 412 (-17)	+46
IV-9 2R,3R		<i>pos</i>	420 (+45) 411 (-49)	+94
IV-10 2S,3R		<i>pos</i>	423 (+34) 411 (-31)	+65
IV-11 2S,3R		<i>pos</i>	423 (+40) 411 (-27)	+67
IV-12 2R,3S		<i>neg</i>	426 (-46) 411 (+24)	-70
IV-13 2R,3S		<i>neg</i>	423 (-66) 411 (+46)	-112

Table IV-1-continued. ECCD data of 2,3- epoxy alcohols bound to Zn-TPFP tweezer in hexane^a

	Epoxy Alcohol	Predicted Sign	λ nm, ($\Delta\epsilon$)	A
IV-14 2S,3S		<i>neg</i>	424 (-152) 411(+111)	-263
IV-15 2R,3R		<i>pos</i>	426 (+41) 418 (-20)	+61
IV-16 2R		<i>pos</i>	424 (+105) 412 (-63)	+168
IV-17^c 2S,3S		<i>neg</i>	425 (-10) 413 (+12)	-22
IV-18 2R,3R		<i>pos</i>	422 (+71) 413 (-72)	+143
IV-19 2S		<i>pos</i>	423 (+101) 410 (-73)	+174
IV-20 2S		<i>pos</i>	424 (+90) 411 (-65)	+155
IV-21^c 2R			No ECCD	

^a tweezer:substrate ratio - 1:40 unless otherwise indicated, ^b the enantiomer showed mirror image CD spectrum, ^c tweezer :substrate ratio - 1:200, ^d tweezer:substrate ratio - 1:100, 2 μ M tweezer concentration at 0 °C was used for all measurements.

chirality and the sign of ECCD is illustrated in Figure IV-4 and Figure IV-5a in which two binding interactions occur between the OH group and the epoxide oxygen with the zincated porphyrins. It is assumed that the binding of **P1**, the porphyrin bound to the epoxidic oxygen, occurs opposite the largest substituent on the epoxide. Since

P2 is bound to the alcohol, invariably this will be the largest group such that **P1** and **P2** avoid steric clash with each other. Since the lone pairs on the epoxidic oxygen are geometrically fixed due to the rigid nature of the epoxide ring, steric relief of **P1** is through rotation / sliding of the porphyrin ring to avoid the largest substituent on the epoxide that faces **P1**.

In case of *trans*-disubstituted epoxy alcohols ($R_2 = R_3 = H$) depicted in Figure IV-5a, **P1** slides away from R_1 in preference for the smaller hydrogen atom, thus generating the energetically favored complex in which the two chromophores are twisted in a counterclockwise fashion.

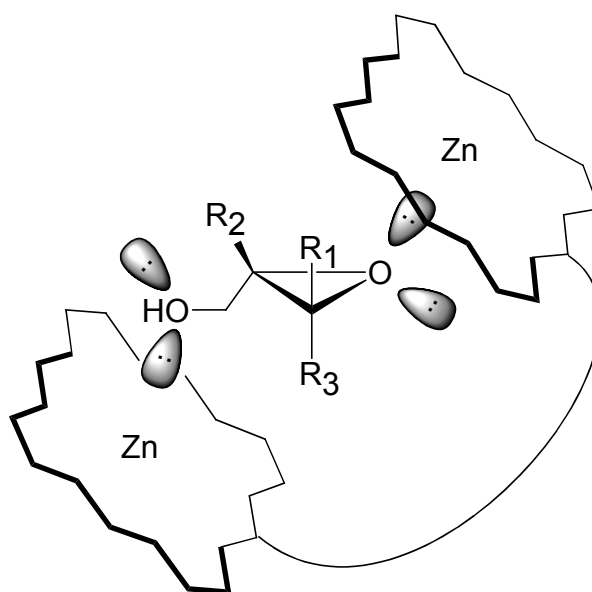


Figure IV-4. Complexation pattern of epoxy alcohol with porphyrin tweezer.

Consequently, a negative ECCD

spectrum is observed for (2*S*,3*S*) *trans*-disubstituted substrates. Though multiple factors could affect the amplitudes of CD signals, we see a general trend that the ECCD signal became stronger with the increase of steric size (defined by *A* values, the conformational energy¹⁸) of R_1 group. For example, compounds **IV-2**, **IV-1**, **IV-4** bear *n*-Pr (*A* value = 1.8), phenyl (*A* value = 3.0) and *ter*-butyl (*A* value = 4.5) group respectively and they demonstrated increasing ECCD amplitudes reflecting the influence of steric size at chiral center. Interestingly, compounds **IV-3** and **IV-5**

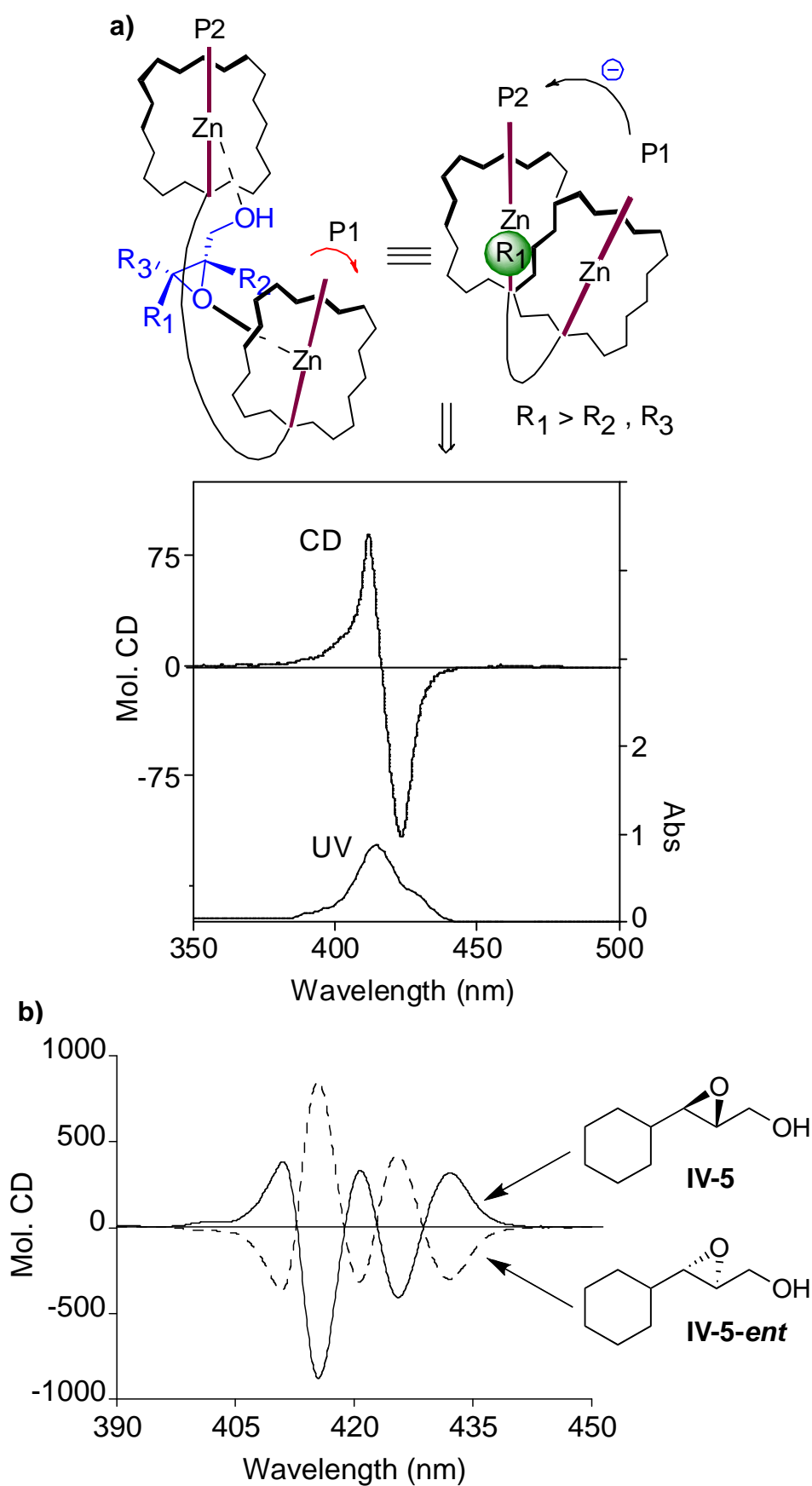


Figure IV-5. a) Proposed complexation pattern between tweezer and epoxy alcohol. Negative ECCD spectrum was obtained for compound **IV-4**; b) enantiomeric ECCD of **IV-5** and **IV-5-ent** (40 eq.) in hexane exhibiting complex CD.

exhibited complex CD patterns with fairly high amplitude when 1-100 equiv of guests were added (Figure IV-5b). This unique behavior was observed only in chiral epoxides with α -branched aliphatic substituents. Although the following statement is based on observation as has no theoretical basis, we have noticed that the sign of the 1st CE for the complex CD spectra is the same as the sign of anticipated ECCD.

The multiple Cotton effects (CE) were also observed for both enantiomers of **IV-5** in MCH (Figure IV-6a) and iso-octane. The significant decrease in CD amplitude in MCH as compared to hexane is observed for most epoxy alcohols. We speculate that the multiple CEs indicate multiple ECCD active conformations present in the complex, which could be affected by changes in solvent polarity and/or temperature.

Indeed, at room temperature (25 °C), a spectrum approaching a normal bisignate CD in MCH (Figure IV-6b) was observed, albeit with several fold decrease in amplitude. Interestingly, the change in spectral characteristics was not observed in hexane at rt. Further increasing the temperature (50 °C) resulted in complete loss of CD signals presumably due to the increased competition from ECCD silent conformations or weakening of the complex. Recooling the system (-10 °C) returned the same multiple CEs with increased CD amplitude.

Utilization of polar solvents such as CH₃CN and CH₂Cl₂ did not result in observable CD signals most probably due to competitive binding of solvent. The UV-Vis spectrum of **IV-5** bound to tweezer **II-25** share the same feature as the UV-Vis spectra obtained for other substrates, and thus was not instructive in

determining the origins of the observed complicated CD spectrum.

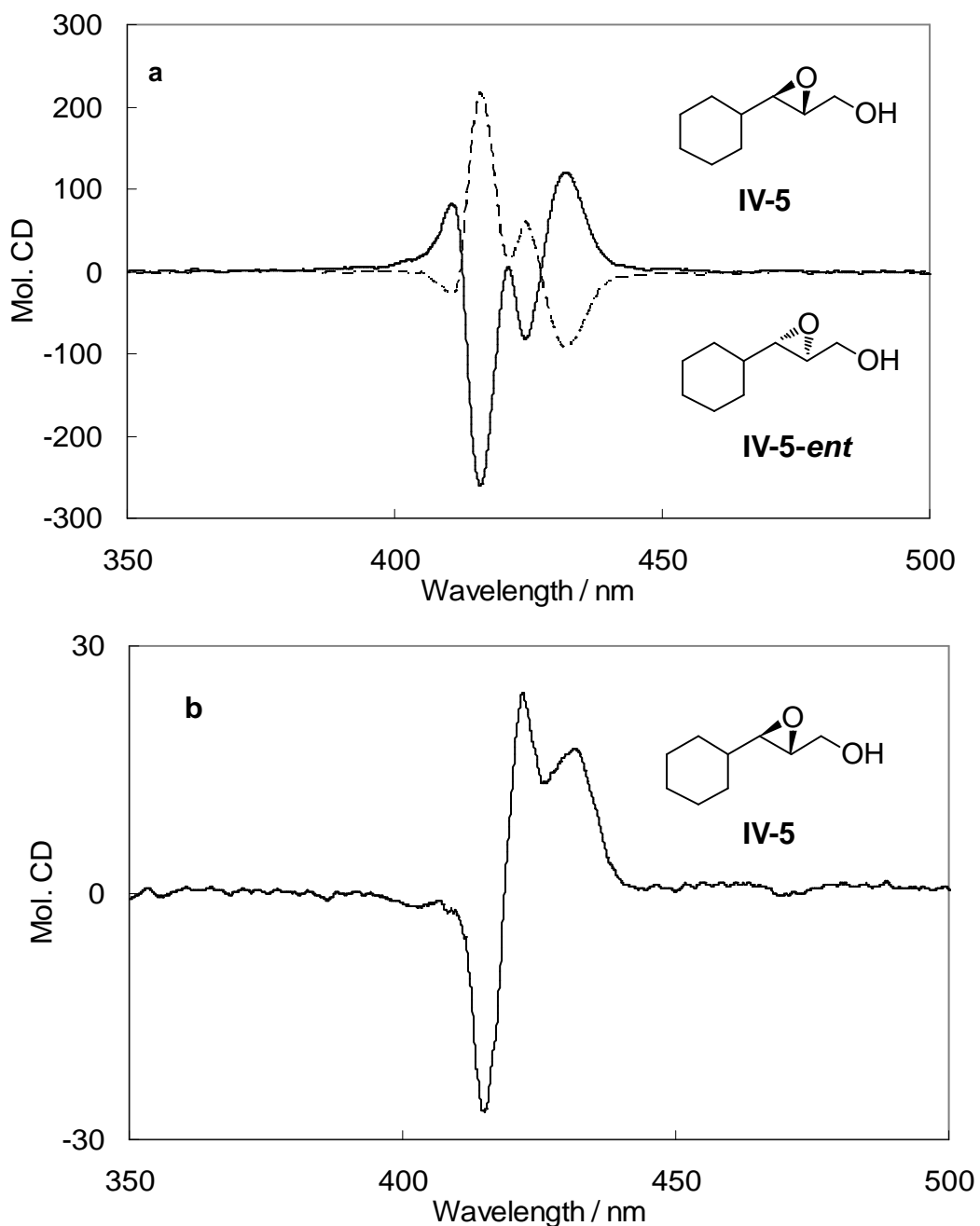


Figure IV-6. (a) ECCD of **IV-5** (solid) and **IV-5-ent** (dashed) with 2 μ M tweezer **II-25** in MCH at 0 °C; (b) ECCD spectrum of **IV-5** in MCH at rt.

The ‘ α -branching’ next to the epoxide seems to lead to the observed complex CD spectra in a small select group of compounds, which we presume is due to multiple

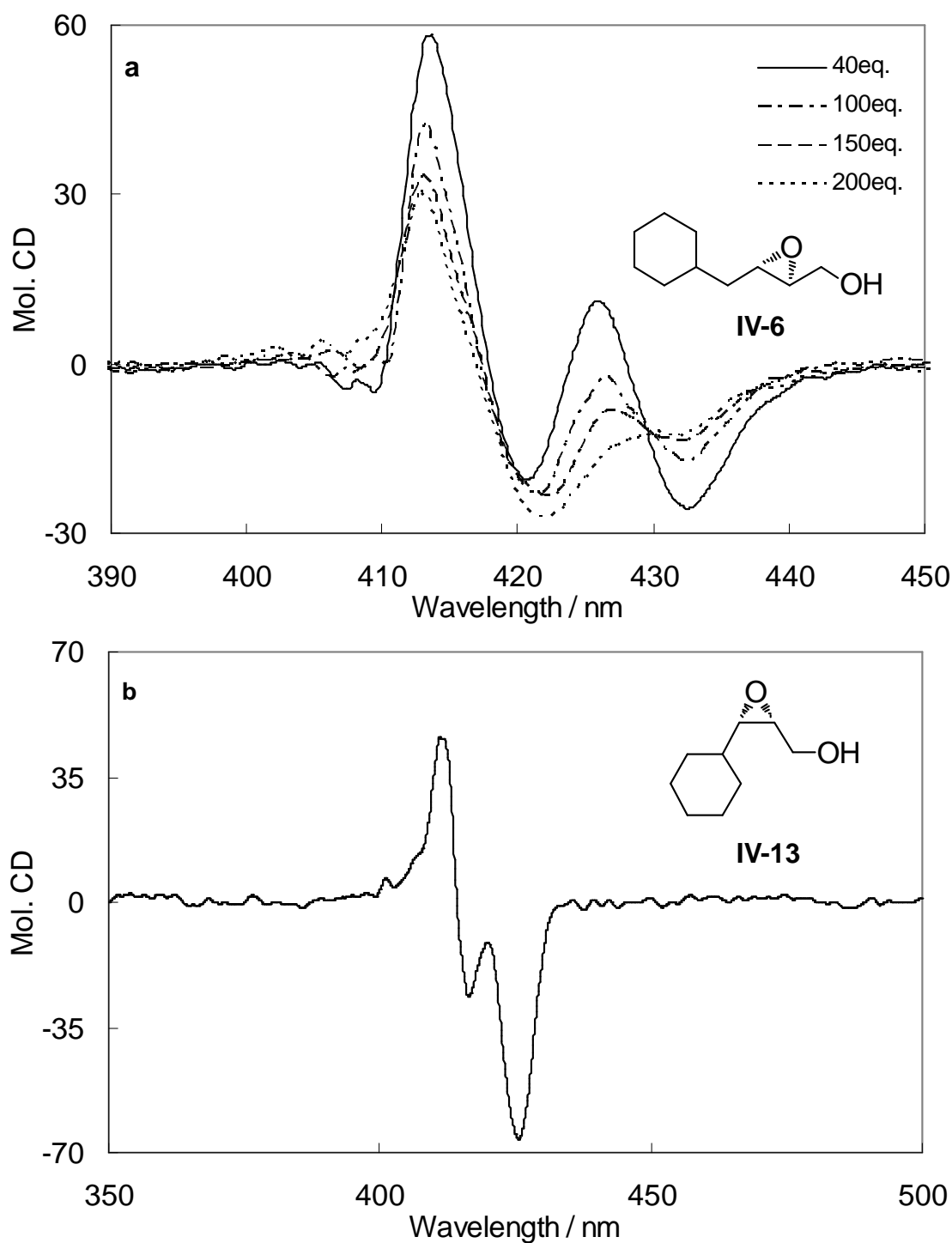


Figure IV-7. (a) ECCD signal change at increasing concentration of **IV-6** in hexane; (b) ECCD of **IV-13** in hexane.

conformations of the complexed tweezer/substrate system. Reduction of the complexed CD spectra to an interpretable ECCD is often achieved as stated above with changes in temperature and at times solvent. We observed a complicated CD

spectrum for substrate **IV-6** as well (Figure IV-7a), although this was the only substrate that was not α -branched that also exhibited similar chiroptical characteristics. The case of complicated CD spectra seems much weaker in *cis*-epoxy alcohol systems as can be observed from the comparison between compounds **IV-5** and **IV-13** (Figures IV-5b and IV-7b).

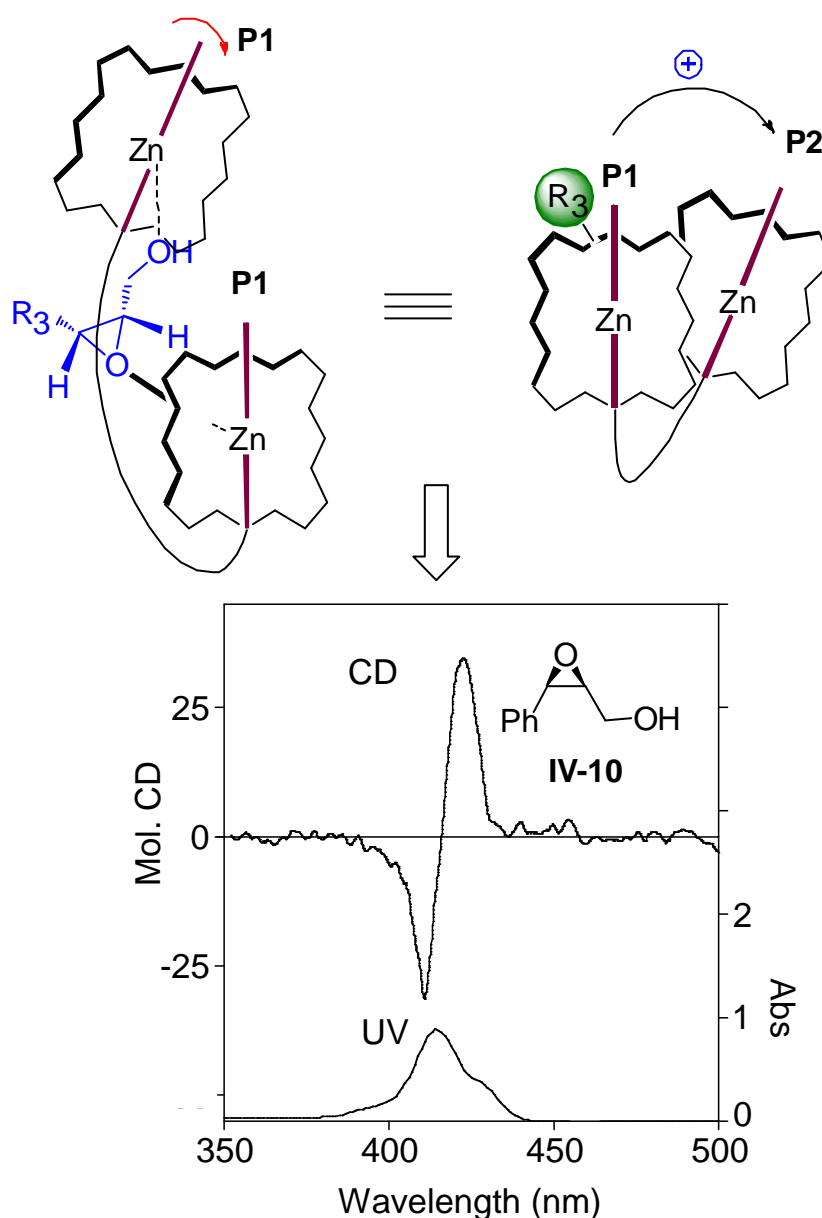


Figure IV-8. Proposed complexation pattern between tweezer **II-25** and *cis*-epoxy alcohol. Positive ECCD spectrum was obtained for **IV-10**

With *cis*-disubstituted epoxy alcohols complexed with tweezer, **P1** (assuming it also coordinates with the lone pair *anti* to the hydroxyl bound **P2**) faces no steric bias since both R₁ and R₂ are hydrogen atoms. The steric interaction between **P2** and R₃ would drive **P2** away from R₃, leading to a clockwise twist of **IV-6** the two porphyrins relative to each other (Figure IV-8), and hence a positive ECCD signal is expected for (2*S*,3*R*) *cis*-disubstituted substrates. This was indeed observed experimentally (compounds **IV-10** ~ **IV-13**). It is instructive to note that compound **IV-13** yields a strong ECCD signal despite its fairly low optical purity (22% *ee*).

Next, we turned our attention to trisubstituted epoxy alcohols (**IV-14** ~ **IV-18**), which upon complexation with tweezer **II-25** resulted in CD spectra that could be rationalized by the binding model depicted in Figure IV-5a. For both 2,3,3 (R₂ = H) and 2,2,3 (R₃ = H) trisubstituted substrates, **P1** slides away from the bulky R₁ group in a similar manner as was described for *trans*-disubstituted substrates to minimize steric clash. The resultant counterclockwise helicity results in a negative ECCD spectrum for 2*S*,3*S* substrates (**IV-14**, **IV-17**). Accordingly, positive signals would reflect 2*R*,3*R* configuration (**IV-15**, **IV-18**). It should be noted that with 2,3,3-trisubstituted olefins, the nature of R₃ is inconsequential, since **P1** is bound away from R₃ and undergoes steric differentiation between R₁ and the hydrogen atom (positioned at R₂ in Figure IV-5a). Conversely, with 2,2,3-trisubstituted olefins, both R₁ and R₂ face **P1**, and thus steric differentiation is governed by their relative sizes. In examples listed in Table IV-1 (**IV-17** and **IV-18**) R₁ is larger than R₂, thus leading to the observed ECCD spectra.

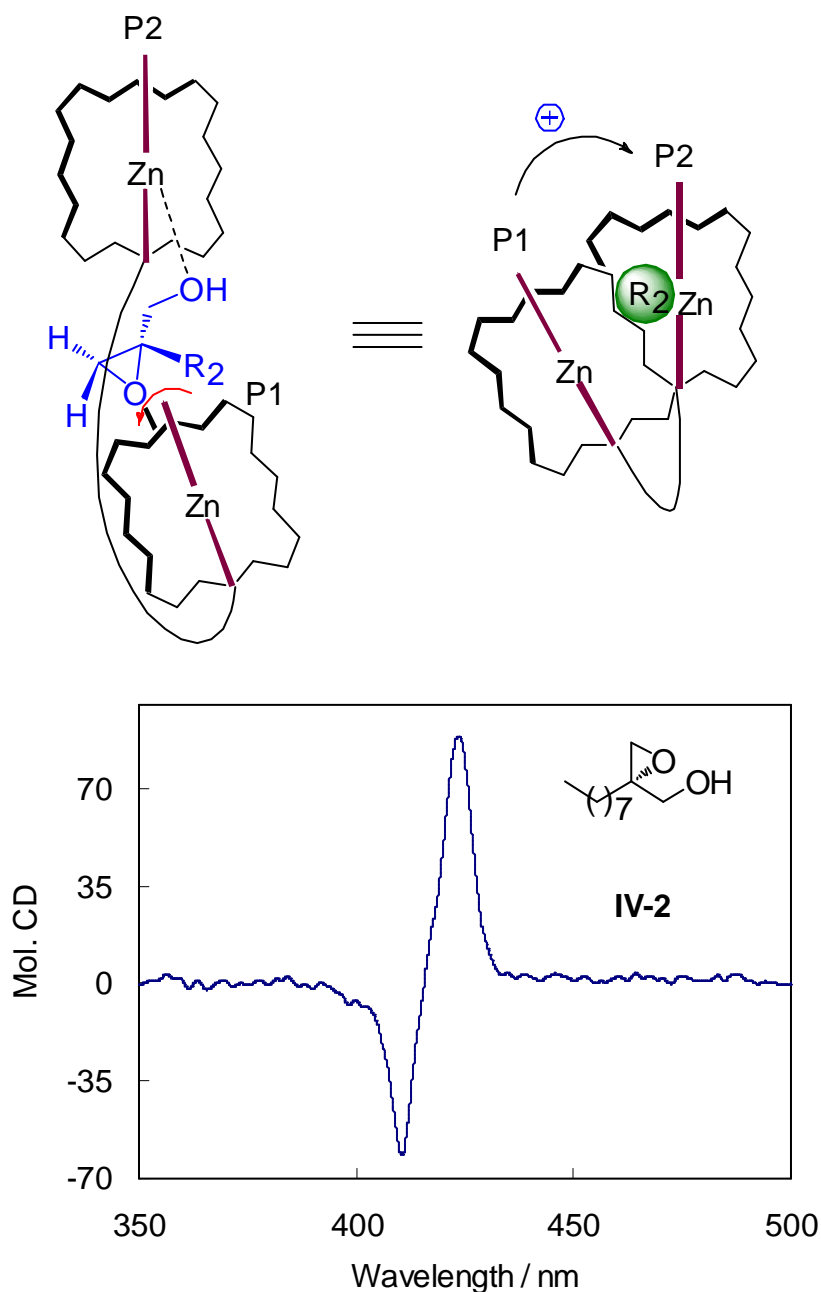


Figure IV-9. Proposed complexation pattern between tweezer **II-25** and 2,2-epoxy alcohol. Positive ECCD spectrum was obtained for **IV-20**

2,2-Disubstituted epoxy alcohols ($R_1 = R_3 = H$), with R_2 facing **P1** should also lead to predictable ECCD spectra based on the fact that **P1** would slide away from R_2 towards the hydrogen atom (R_1) (Figure IV-9). This is indeed observed, as the

anticipated sign of the ECCD for compounds **IV-19** and **IV-20** match the experimentally observed data (compound **IV-19** and **IV-20** bearing 2*S* configuration yield positive ECCD, resulting from steric discrimination between R₂ (*n*-octyl group or PhCH₂CH₂-) and R₁ (hydrogen)). In contrast, epoxy alcohol **IV-21** did not yield an observable ECCD. This is not surprising since there are no steric determinants that orient **P1** and **P2** relative to each other.

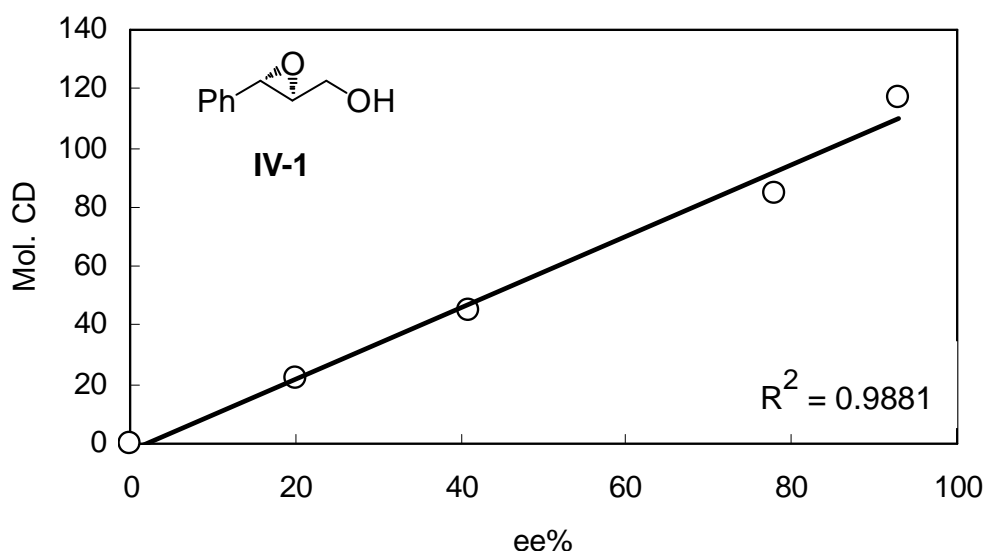


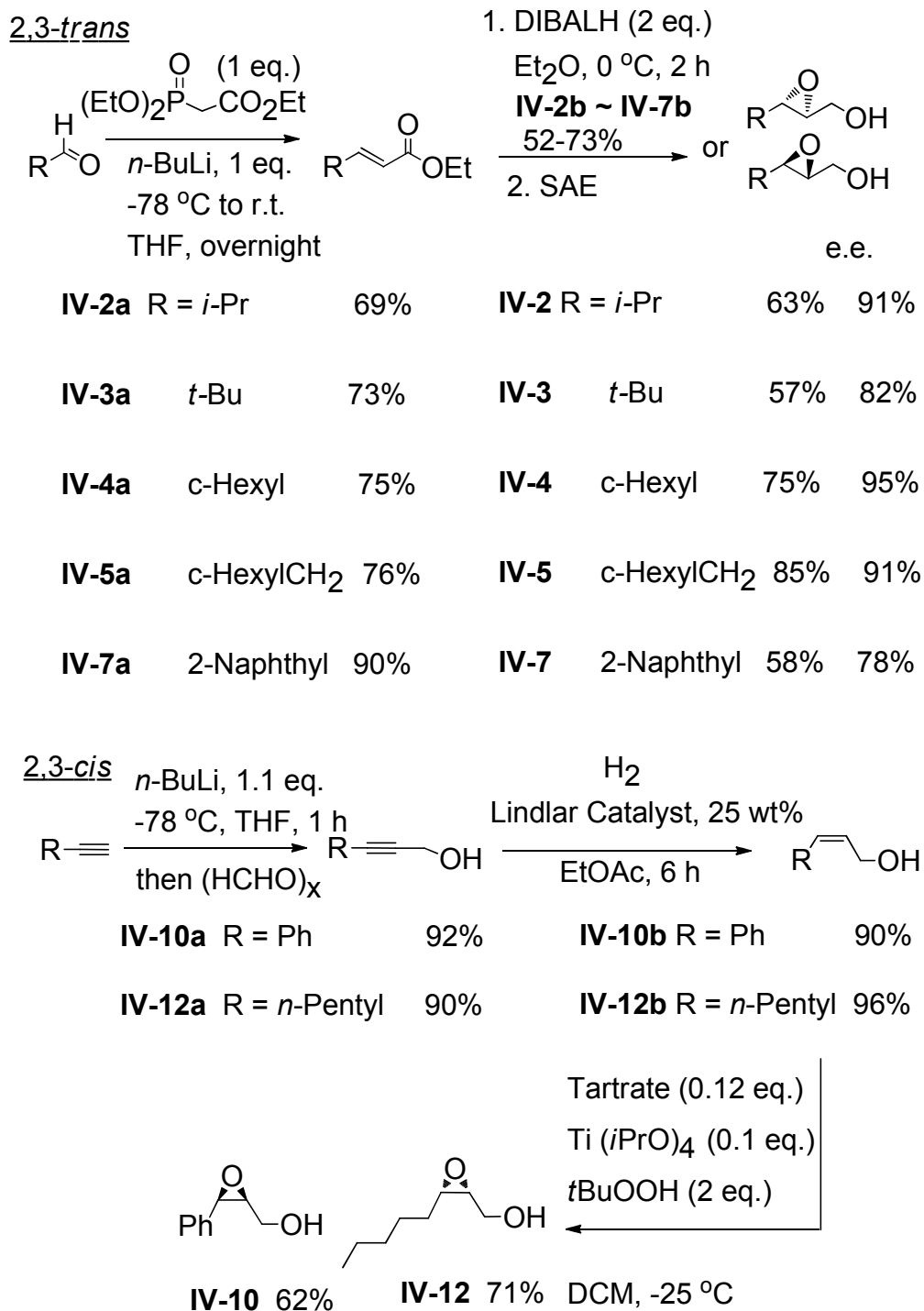
Figure IV-10. The plot of %ee of **IV-1** versus ECCD amplitudes of **IV-1** / Zn-TPFP tweezer complex (all ECCD amplitudes were reported at 40 eq. in hexane at 0 °C).

To reveal the relationship, between ECCD amplitude and optical purity of substrate, epoxy alcohol **IV-1** with varying %ee (20%, 41%, 78%, 93%) was prepared by mixing with **ent-IV-1** at different ratio. Subsequent ECCD measurements revealed a good linear relationship between the sample optical purity and ECCD amplitude. As shown in Figure IV-10, the ECCD amplitude increased

linearly with the increased %ee. In addition, the measurements also proved that the sign and shape of ECCD signal were not affected by the optical purity. Namely, there is no observed complex behavior caused by low optical purity as can also be manifested by substrates **IV-10** ~ **IV-13** and **IV-20** which exhibited prominent bisignate ECCD with low %ee. This demonstrates the excellent sensitivity of the Zn-TPFP tweezer host.

IV.2.3 Synthesis of chiral epoxy alcohols

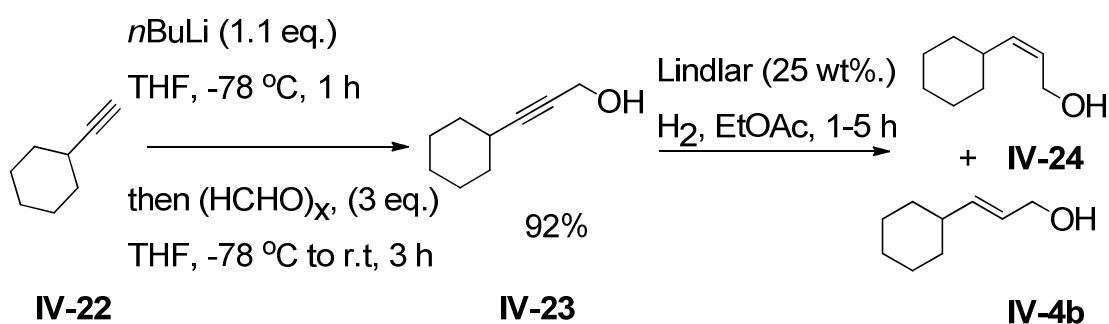
Synthesis of chiral epoxy alcohols was achieved through Sharpless asymmetric epoxidation of primary allylic alcohols. These allylic alcohols were mainly prepared from DIBALH reduction of corresponding allylic esters which were obtained from Wittig reaction or Horner-Wadsworth-Emmons reaction of aldehydes or ketones. Typical procedures for the synthesis of 2,3-*trans*, 2,3-*cis*, 2,2,3-trisubstituted, and 2,3,3-trisubstituted epoxy alcohols are depicted in Scheme IV-1 and Scheme IV-7.



Scheme IV-1. Synthesis of *trans* and *cis* disubstituted chiral epoxy alcohols.

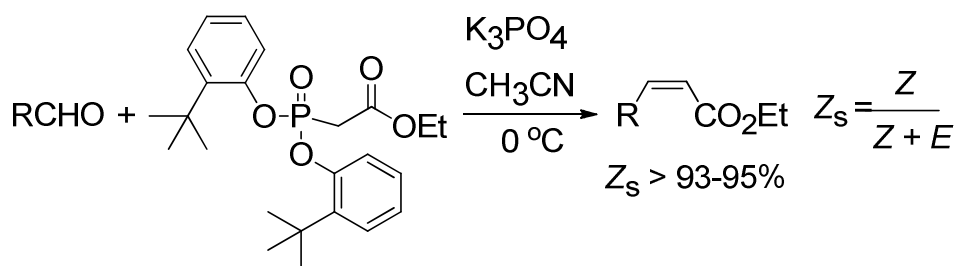
All the reactions are not optimized and the low yields of *i*-Pr and *t*-Bu substituted *trans*-epoxy alcohols are due to the volatility of product. Synthesis of cyclohexyl substituted *cis* epoxy alcohol (**IV-13**) following standard procedures (Scheme IV-2)

faced some challenges. The hydrogenation of alkynyl alcohol turned out to be problematic particularly for this substrate since an inseparable mixture of *cis*- and *trans*- isomers was obtained after a couple of trials under different conditions. Monitoring the reaction by GC-MS revealed that the hydrogenation was completed after 1 h but the *cis* product underwent rapid isomerization in the crude leading to mixture of both isomers. To solve this issue, a modified HWE reaction was utilized to make *cis* allylic ester followed by DIBALH reduction.

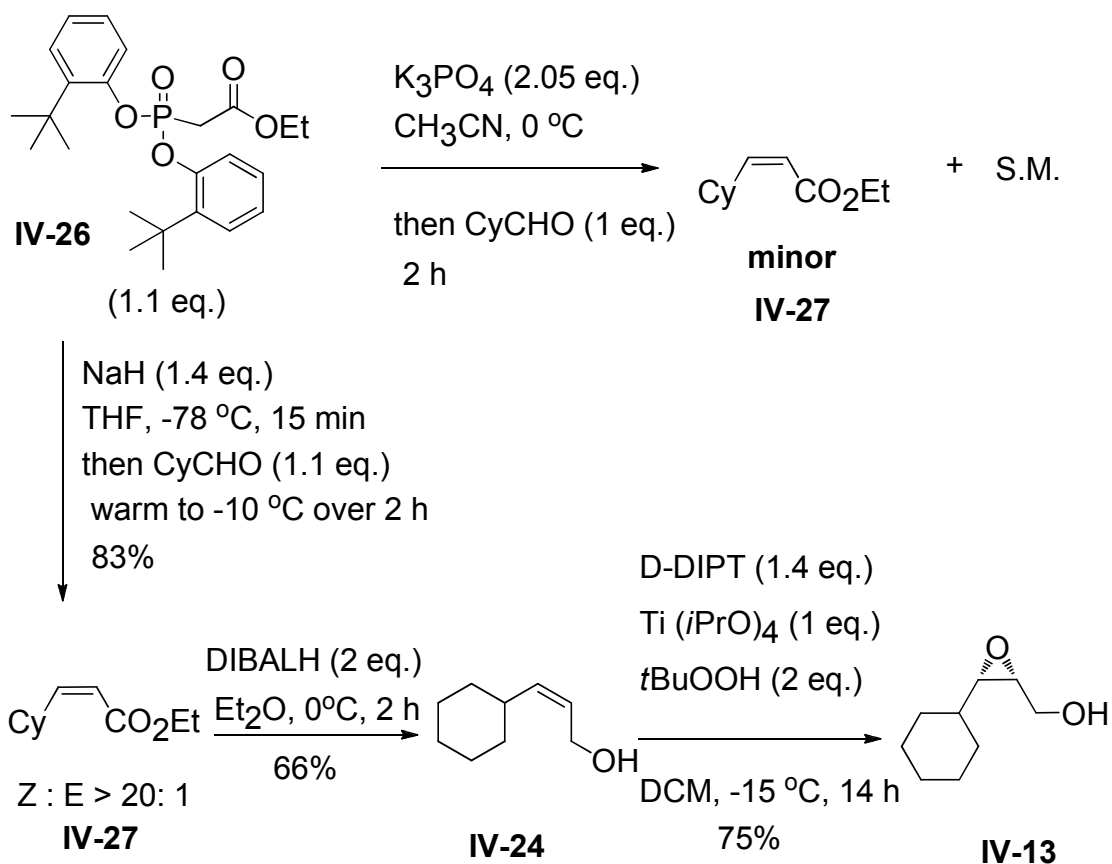
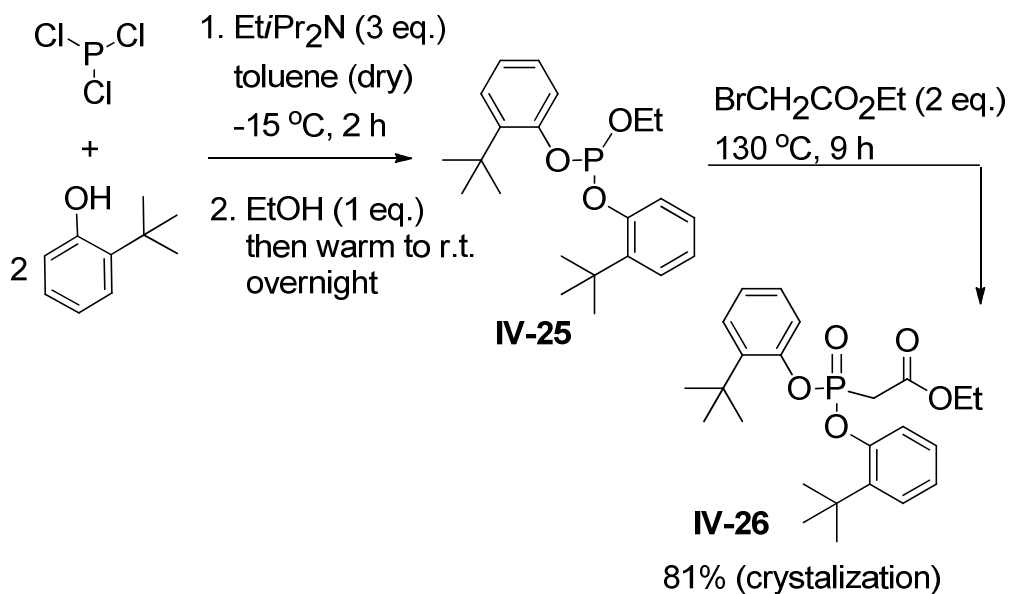


Scheme IV-2. Synthesis of *cis* allylic alcohol **IV-24** from propargylic alcohol.

Ando¹⁹ and Touchard^{20, 21} reported the use of electron-withdrawing bulky phenolic group instead of ethoxy group in stabilized phosphorus ylide could reverse the selectivity and afford *Z*-allylic ester (Scheme IV-3).^{20, 21}

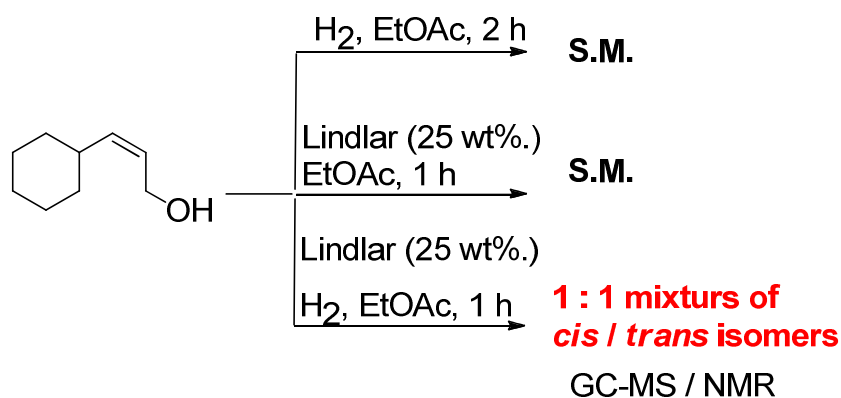


Scheme IV-3. Modified HWE condition for synthesis of *Z*-allylic ester.



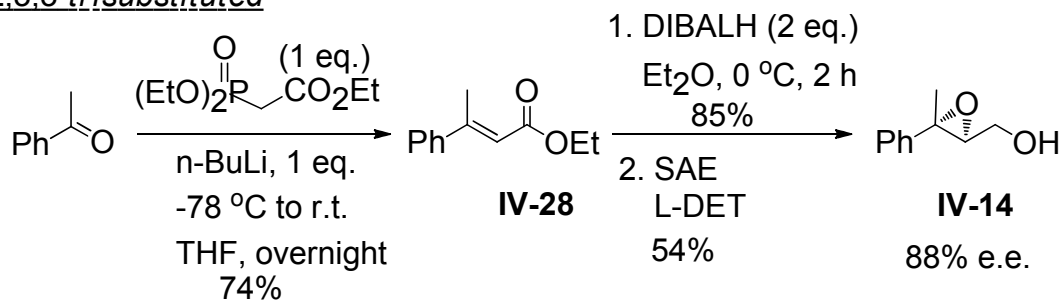
The modified phosphorus ylide was prepared as crystalline compound in 81% yield over three steps (Scheme IV-4).^{20, 21} The olefination was first conducted in CH₃CN with cyclohexanecarboxaldehyde using K₃PO₄ as base.²⁰ Unfortunately, only small amount of desired product was detected by ¹H NMR along with starting material. The low conversion is probably due to the fact that the mechanical stirrer did not provide good protection of reaction mixture from moisture. The reported procedure was conducted in large scale (> 100 g) and hence is less sensitive to the moisture in air. Ando's procedure was then followed using NaH as base in THF at -78 °C (Scheme IV-5).¹⁹ The *Z*-ester was obtained with good yield and excellent selectivity. DIBALH reduction of ester and following SAE reaction of resultant allylic alcohol afforded pure epoxy alcohol yielding negative ECCD signal as expected upon complexation with Zn-TPFP tweezer in hexane.

The pure *cis*-allylic alcohol was subjected to isomerization test. As shown in Scheme IV-6, the *cis*-allylic alcohol readily isomerizes under typical hydrogenation condition using Lindlar catalyst. The similar isomerization behavior for *cis* allylic alcohols or allylic amines is also documented in literature.²⁰

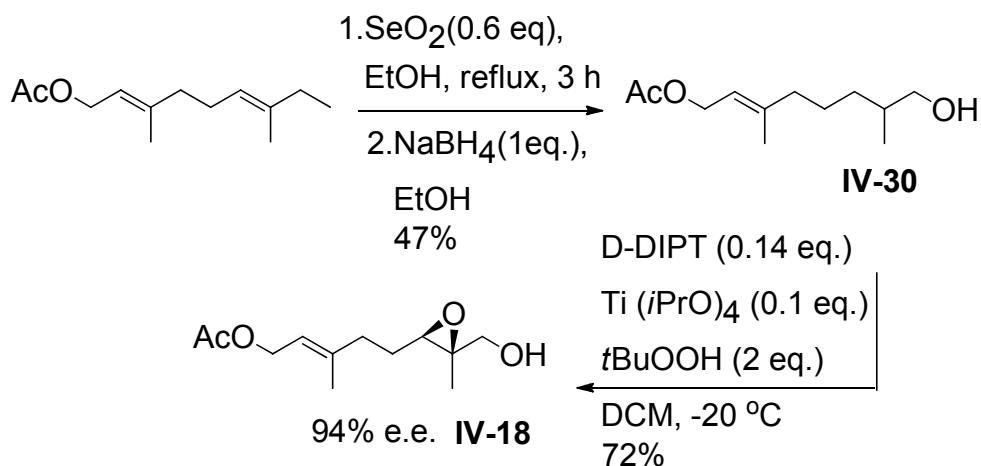
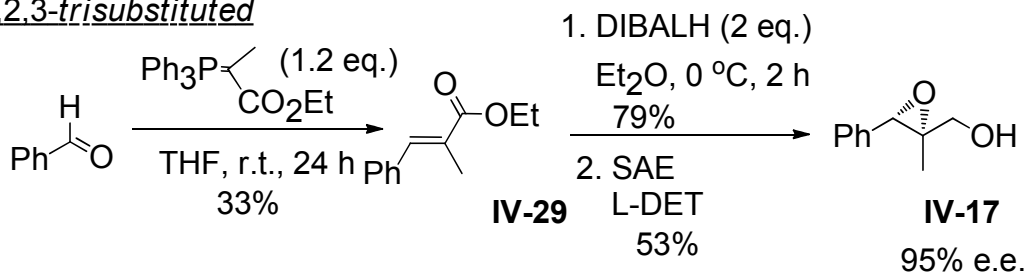


Scheme IV-6. Isomerization test of *cis* allylic alcohol **IV-24**.

2,3,3-trisubstituted



2,2,3-trisubstituted

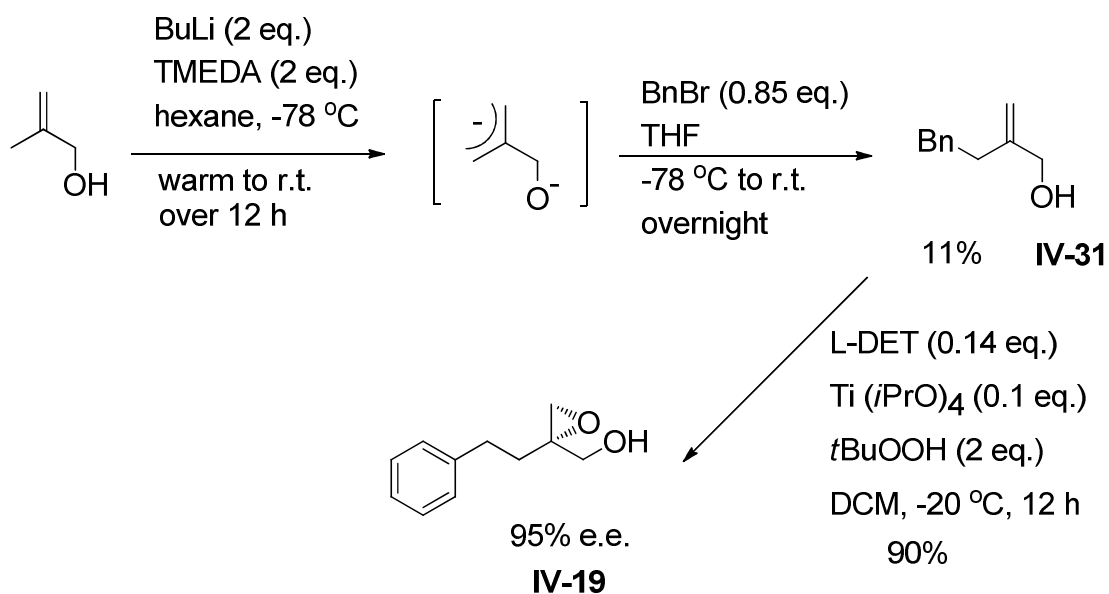


Scheme IV-7. Synthesis of trisubstituted epoxy alcohols

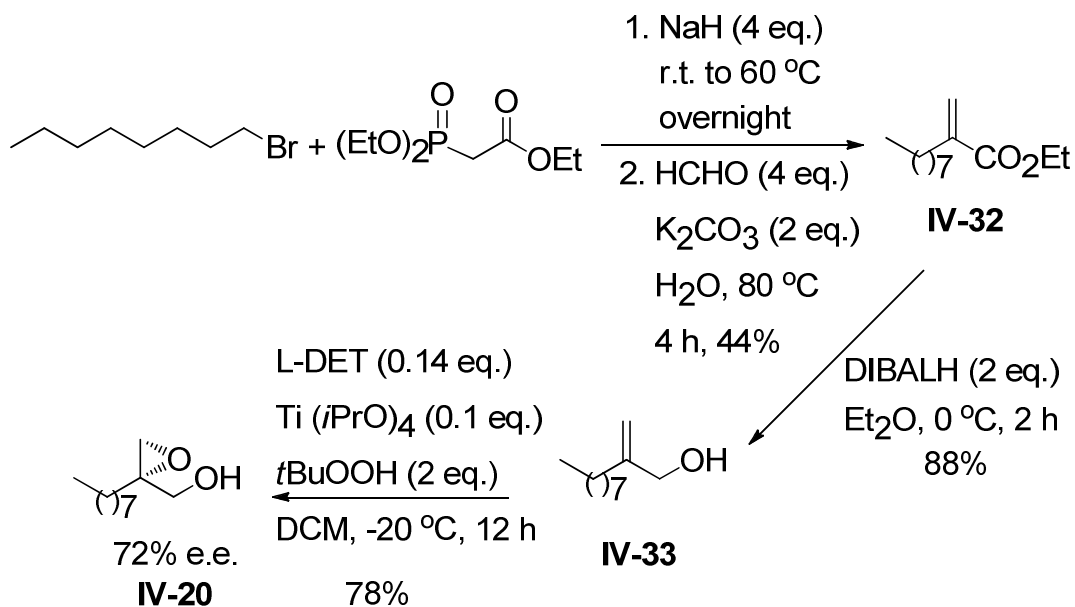
The trisubstituted epoxy alcohols were synthesized as shown in Scheme IV-7 uneventfully. Different ylides were needed to make the precursors for 2,3,3-trisubstituted²² and 2,2,3-trisubstituted allylic alcohols. To prepare the substrates for synthesizing 2,2-disubstituted epoxy alcohols, 2-methylpropenol was first deprotonated in hexane and following $\text{S}_{\text{N}}2$ displacement of alkyl halide afforded the desired allylic alcohol (Scheme IV-8).²³ Initial trial of this route only got

desired product in 11% yield. A different route was then followed as shown in

Scheme IV-9.^{24, 25}



Scheme IV-8. Synthesis of 2,2-disubstituted epoxy alcohol **IV-19**.



Scheme IV-9. Synthesis of 2,2-disubstituted epoxy alcohol **IV-20**.

IV.2.4 ECCD study of chiral secondary epoxy alcohols

The prevalence of secondary epoxy alcohols bearing chiral OH group in natural products (Figure IV-1) and organic synthesis intrigued us to further investigate the configurational assignment for this class of epoxy alcohols. A common approach to obtain these epoxy alcohols is Sharpless kinetic resolution of secondary allylic alcohols as illustrated in Figure IV-11.^{14, 26}

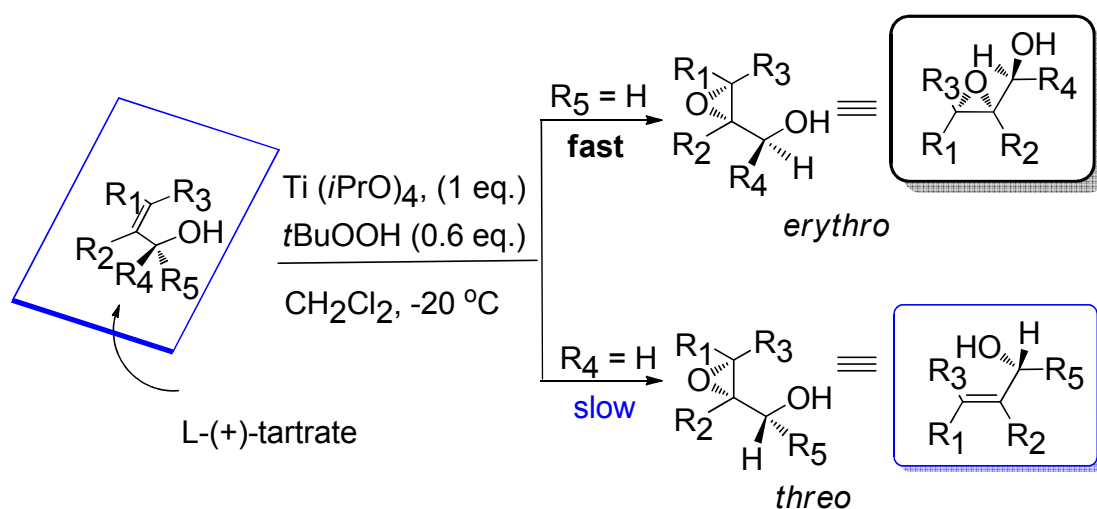
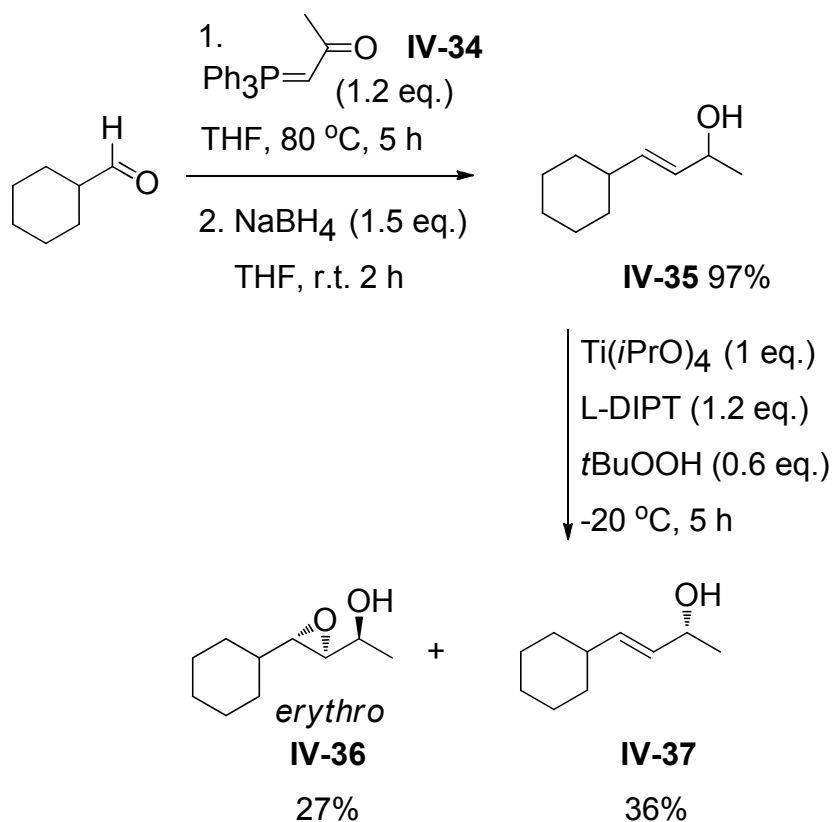


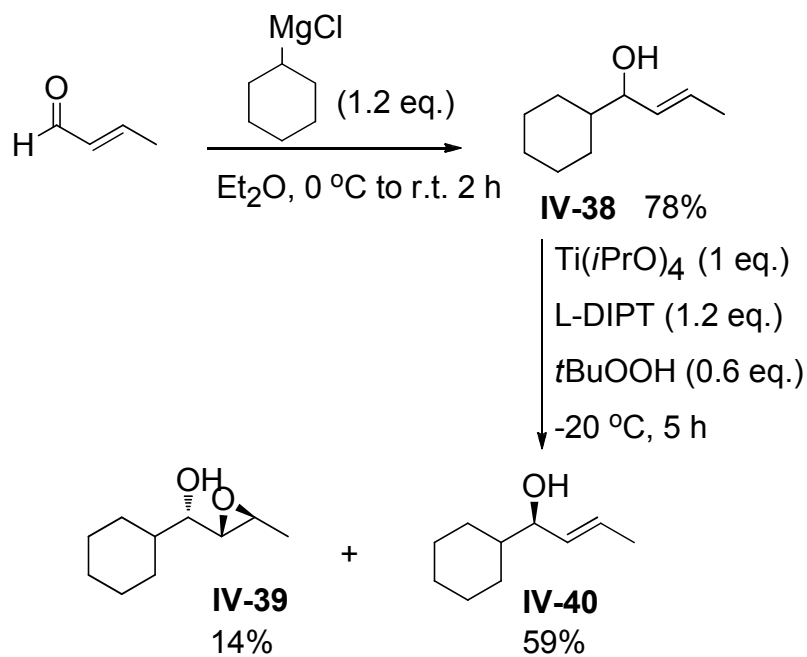
Figure IV-11. Sharpless kinetic resolution of allylic alcohols.

The secondary allylic alcohols were synthesized²⁷ as shown below and kinetically resolved to afford chiral allylic alcohols and epoxy alcohols with the *erythro* isomer as major product (Scheme IV-10).^{26, 27} In all the cases, the chiral epoxy alcohols were obtained with high *e.e.* (> 95%). The major *erythro* product and minor *threo* diastereomer (will show up if conversion is over 60%) could be separated on the column in some cases. Three secondary epoxy alcohols obtained were then submitted for ECCD study. Gratifyingly, all the substrates were ECCD active and a general trend was revealed though only a few examples were examined. The *erythro* substrates with *S,S,S* chirality exhibited positive ECCD signal and the *R,R,R* substrate rendered negative spectra (Figure IV-12). More substrates are necessary for further

study to probe the binding mechanism for this epoxy alcohol system.



Scheme IV-10. Synthesis of epoxy alcohol **IV-36** via Sharpless kinetic resolution.



Scheme IV-11. Synthesis of epoxy alcohol **IV-39** via Sharpless kinetic resolution.

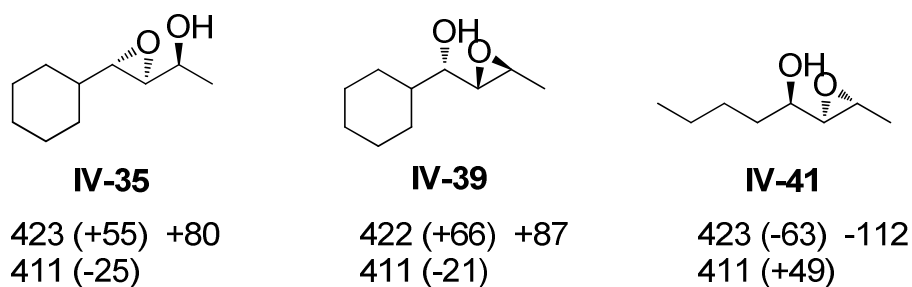


Figure IV-12. ECCD data of *trans* secondary epoxy alcohols (40 eq.) with tweezer **II-25** (2 μ M) in hexane at 0 °C.

In the collaboration with Professor Patrick Walsh at University of Pennsylvania who has developed reaction methodology^{28, 29} for preparing chiral secondary epoxy alcohols, we obtained six secondary epoxy alcohols from his lab with unknown (to us) stereochemistry (Figure IV-13).

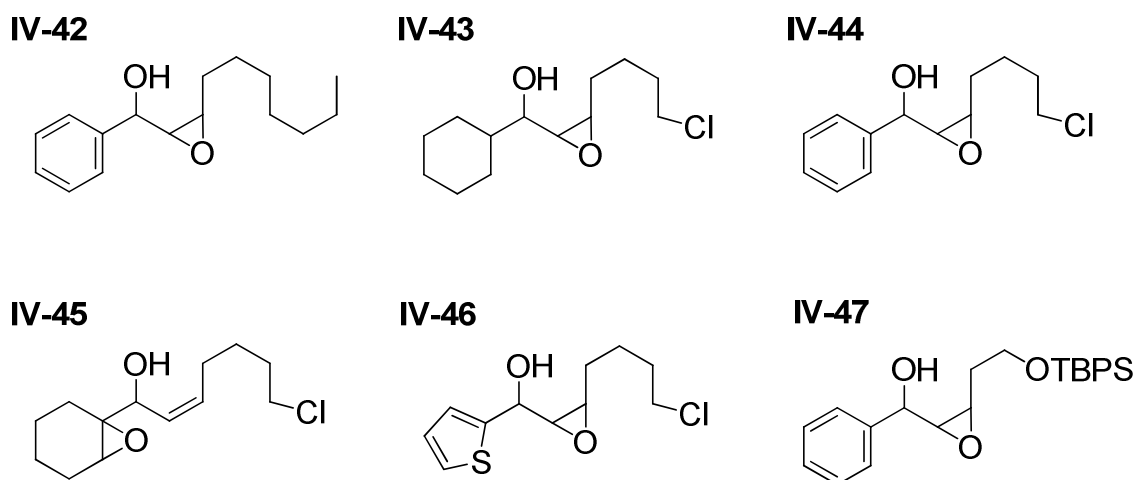
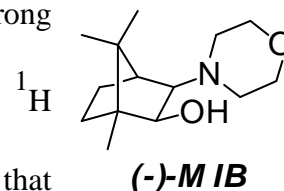


Figure IV-13. Samples obtained from Professor Walsh's lab.

All six epoxy alcohols were examined with zinc TFPF tweezer in hexane at 0 °C. Compounds **IV-42** and **IV-43** were first examined and yielded very strong ECCD signals ($A = + 538$ for **IV-42** and $A = + 320$ for **IV-43**). However, these values were suspicious since they were too high compared to those of *trans* secondary epoxy

alcohols we had prepared via the Sharpless kinetic resolution (Figure IV-12). We suspected that the samples might contain chiral impurity coming from chiral ligand MIB used during preparation of epoxide.²⁹ The ECCD method is extremely sensitive and trace amount of chiral ligand bearing amino alcohol groups in the rigid skeleton could bind Zn-TPFP tweezer well and exhibit strong ECCD signal interfering with the ECCD measurement.



¹H NMR spectra of these two compounds indicated tiny peaks that may be attributed to methyl groups of MIB residue. We then purified the substrates by column chromatography, and run the experiments again. Both samples gave cleaner ¹H NMR and decreased CD amplitudes (A = + 124 for **IV-42** and A = + 103 for **IV-43**). **IV-44** and **IV-45** also yielded positive signals. Two samples (**IV-46** and **IV-47**) did not give observable CD signals. We think the second lone pair of the sulfur in **IV-46** probably has competitive binding with porphyrin tweezer. Further UV-vis binding experiments of thiophene with monomeric Zn-TPFP porphyrin revealed strong binding affinity. The bulky TBDPS in **IV-47** might hinder the binding interaction with the porphyrin; this could be further tested by changing the OTBDPS to other smaller protecting group. We attempted to remove TBDPS under mild conditions such as HF / Py, but only small amount of desired product was obtained along with a large amount of side product coming from epoxide ring opening. Since no additional material of **IV-47** was available, further studies were not possible.

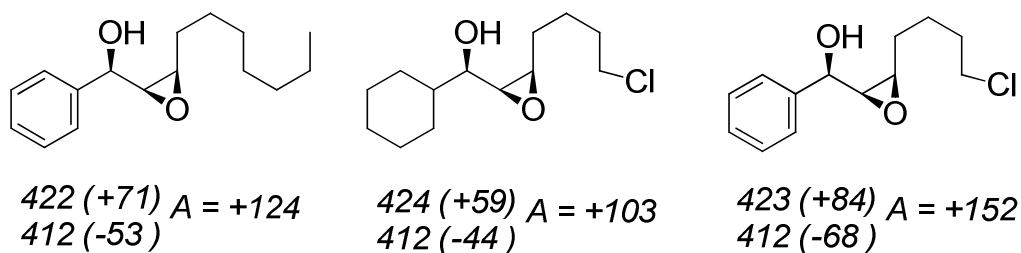


Figure IV-14. ECCD data of *cis* secondary epoxy alcohols **IV-41~IV-44** (40 eq.) with tweezer **II-25** (2 μ M) in hexane at 0 $^{\circ}$ C.

The binding model we proposed is similar to that of *cis* epoxy primary alcohol. As shown in Figure IV-15, after complexation of epoxy alcohol with tweezer, **P1** (assuming it also coordinates with the lone pair *anti* to the hydroxyl bound **P2**) faces no steric bias since both groups are hydrogen atoms. The steric interaction between **P2** and R₃ would drive **P2** away from R₃, leading to a clockwise twist of the two porphyrins relative to each other and hence a positive ECCD signal is expected.

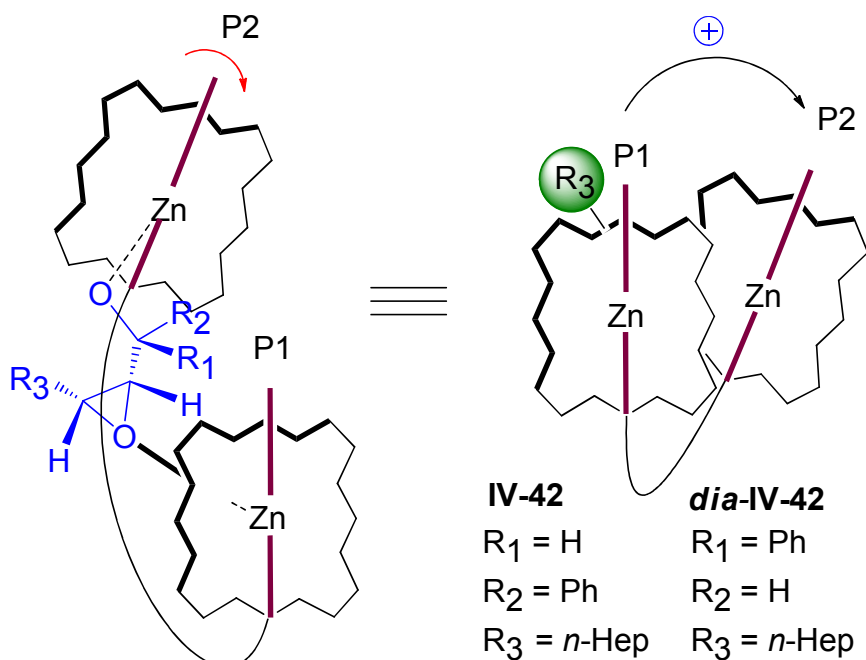


Figure IV-15. Proposed binding model for *cis* secondary epoxy alcohols with tweezer **II-25**.

In this case, the stereochemistry of hydroxyl group does not affect the outcome of helicity since in both diastereomers **P2** could approach OH groups *anti* to the large substituent at the chiral center as manifested in Figure IV-16. Consequently, the major sterics driving **P2** away still originates from the bulky R₃ group.

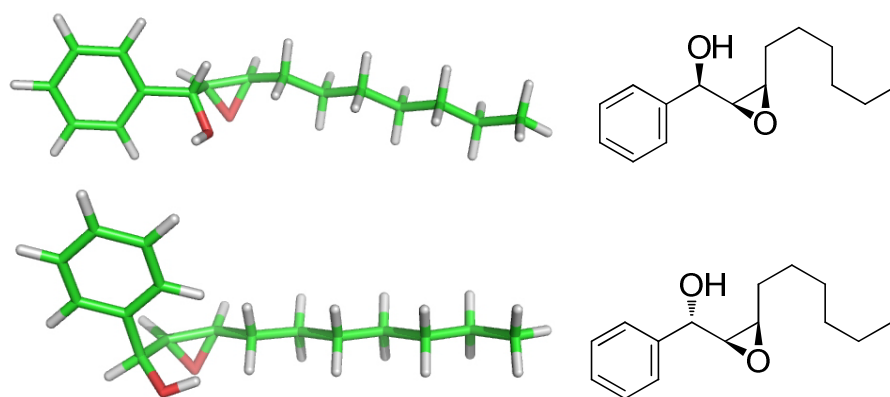
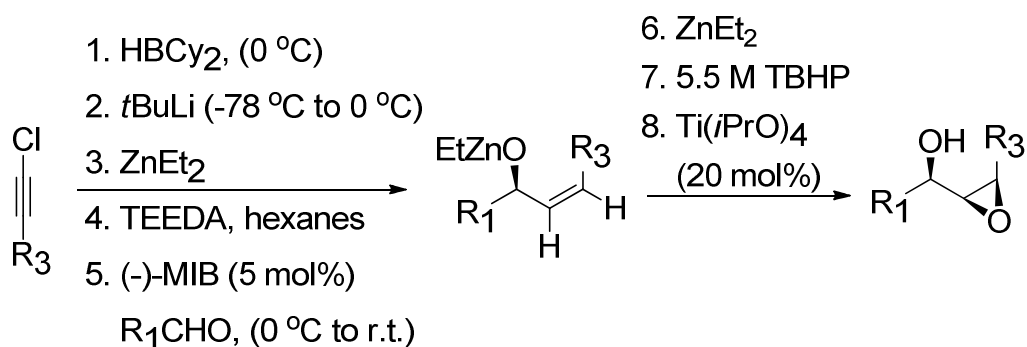


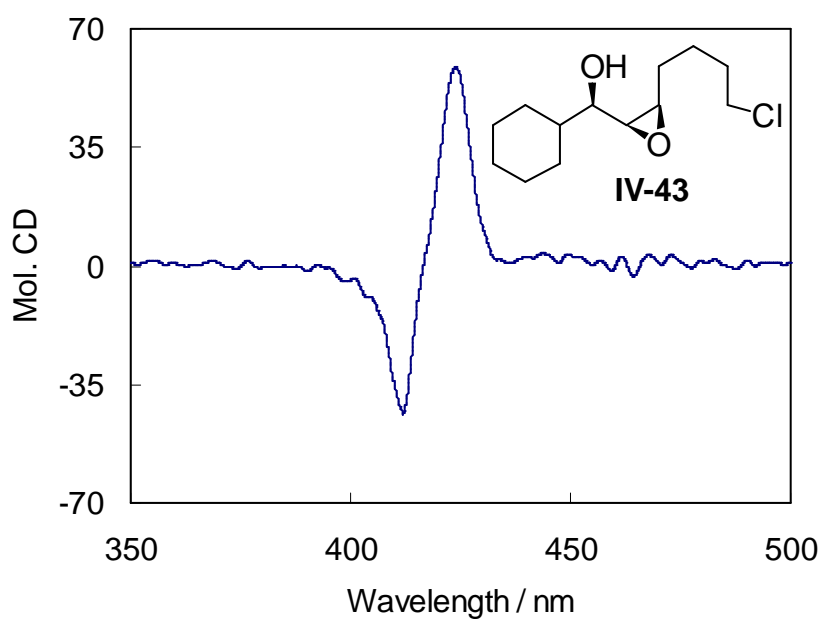
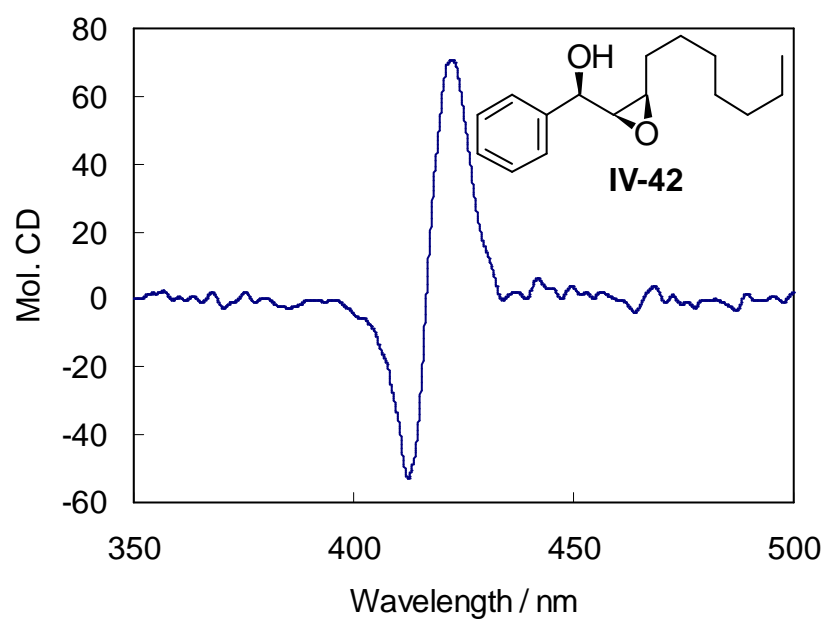
Figure IV-16. 3D models for diastereomers of epoxy alcohol **IV-42**.

Based on this binding mechanism, the positive ECCD signals observed reflected two possible configurations, namely 1*R*,2*S*,3*R* (for *threo* or *syn* epoxy alcohol) or 1*S*,2*S*,3*R* (for *erythro* or *anti* epoxy alcohol). Though Zn-TPFP tweezer does read out the chirality of epoxide ring, it cannot tell the stereochemistry of chiral OH group. This is not surprising since the porphyrin tweezer method was designed for differentiating enantiomers, not diastereomers.



Scheme IV-12. Walsh's route for synthesis of *cis* secondary epoxy alcohols.

According to Walsh's study, the relative stereochemistry of these epoxy alcohols is *threo* (Scheme IV-12).^{28, 29} So, we conclude that **IV-42** ~ **IV-44** should have 1*R*, 2*S*, 3*R* configuration according to the CD results. This conclusion was confirmed by Prof. Walsh. The binding mechanism for cyclic substrates (**IV-45**) is different from acyclic ones and deserves further investigation.



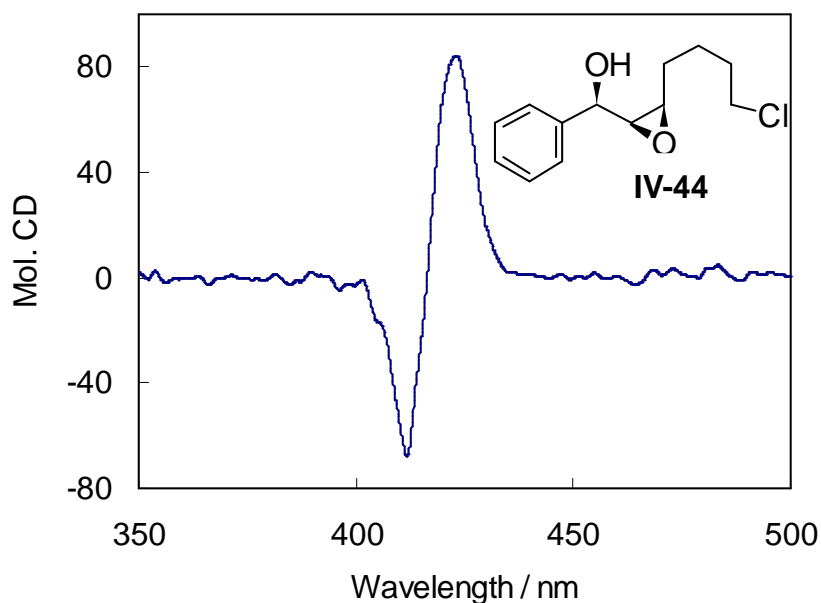


Figure IV-17. ECCD spectra of *cis* secondary epoxy alcohols (40 eq.) with Zn-TPFP tweezer **II-25** (2 μ M) in hexane at 0 °C.

IV.2.5 ECCD study of long chain epoxy alcohols - The Odd-Even effect

The odd-even effect of the number of methylene groups in straight chain organic molecules has been extensively studied in liquid crystals,³⁰ self-assembled monolayers,³¹⁻³⁶ gels,^{37, 38} chiral aggregates,^{32, 39} and polymers containing mesogenic substituents.⁴⁰ In most cases, the effect was observed in solid state and was interpreted as packing difference in crystal structure leading to the different orientation of molecular skeleton in their all-staggered conformations.⁴¹⁻⁴³ However, in solution state where multiple conformations usually exist, only a few recent reports demonstrated this interesting effect captured by vibrational circular dichroism⁴⁴ and fluorescence anisotropy study.⁴³

In the effort to further extend the application of Zn-TPFP tweezer for absolute stereochemical determinations, we discovered a novel odd-even effect (Figure IV-18) as described in this section. This remarkable effect was evidenced by ECCD of the supramolecular complex between zinc porphyrin tweezer and chiral epoxy alcohols with varying length of alkyl chains. Meanwhile, a facile and non-empirical determination of the absolute stereochemistry of these epoxy alcohols is also illustrated.

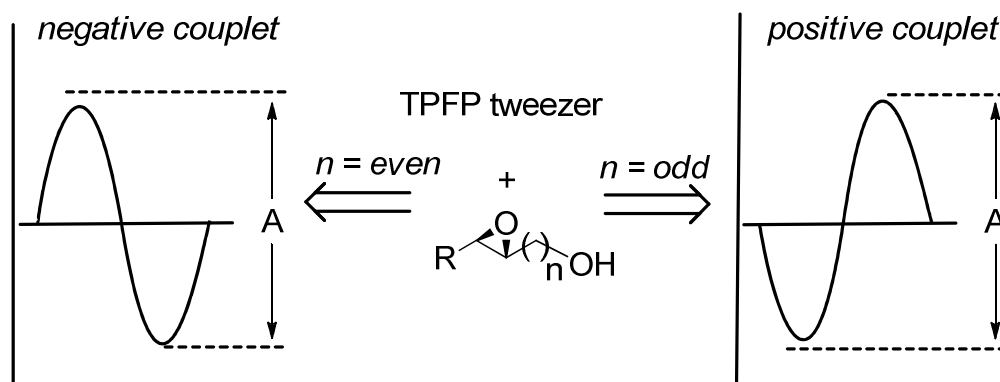
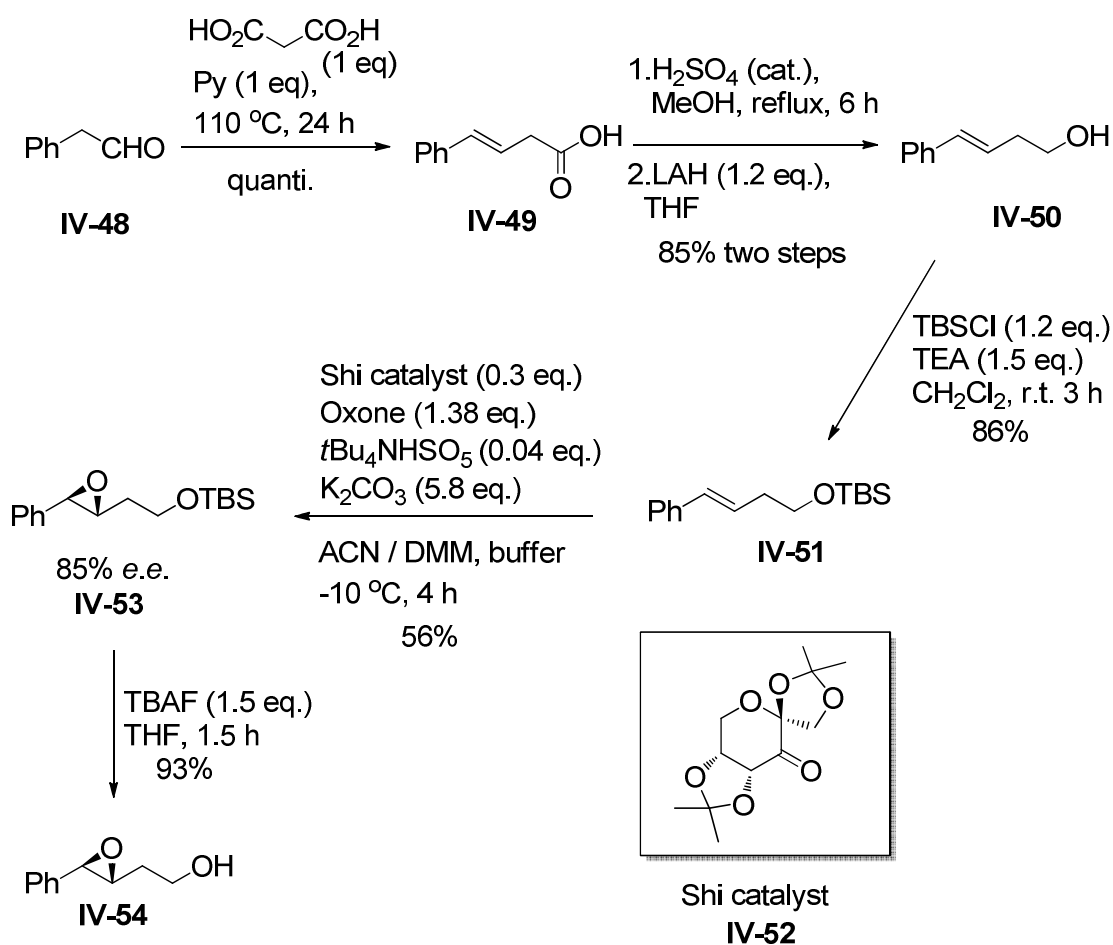


Figure IV-18. The odd-even effect of ECCD spectra of long chain epoxy alcohol-tweezer (**II-25**) complex.

IV.2.5.1 Synthesis of long chain epoxy alcohols

The synthesis of chiral epoxy alcohols with varying chain lengths was accomplished through Shi asymmetric epoxidation^{12, 45-47} of corresponding alkenyl alcohols which were prepared via Scheme IV-13 ~ IV-16. The homoallylic alcohol **IV-50** was prepared from commercially available phenylacetaldehyde which underwent one-pot condensation and decarboxylation with malonic acid in the

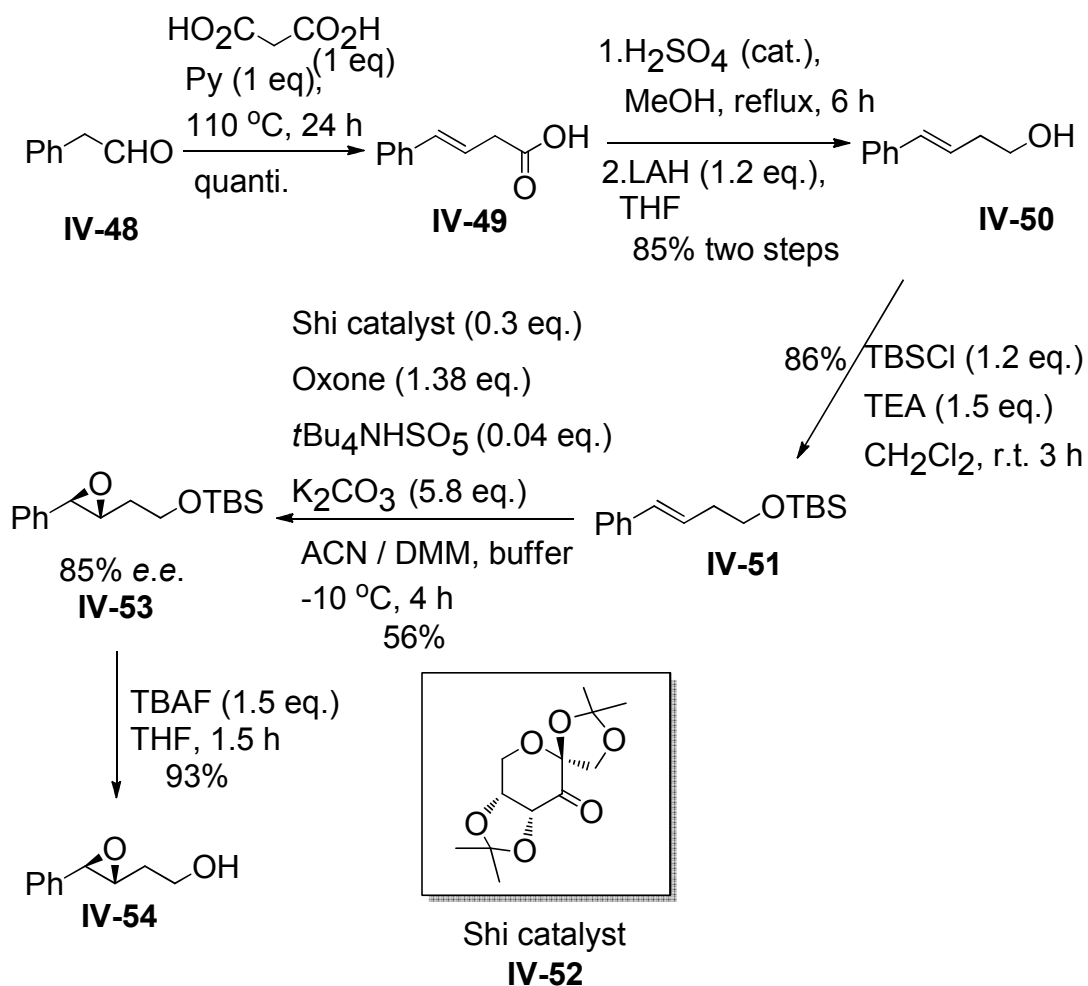
presence of pyridine (Scheme IV-13)^{48, 49} affording **IV-49**. Esterification of **IV-49** and subsequent LAH reduction led to alcohol **IV-50**. TBS protection of primary alcohol followed by Shi epoxidation gave the chiral epoxide **IV-53** which upon desilylation furnished *trans*-3*R*,4*R*-disubstituted epoxy alcohol **IV-54**.



Scheme IV-13. Synthesis of aryl substituted *trans* 3*R*,4*R*-epoxy alcohol.

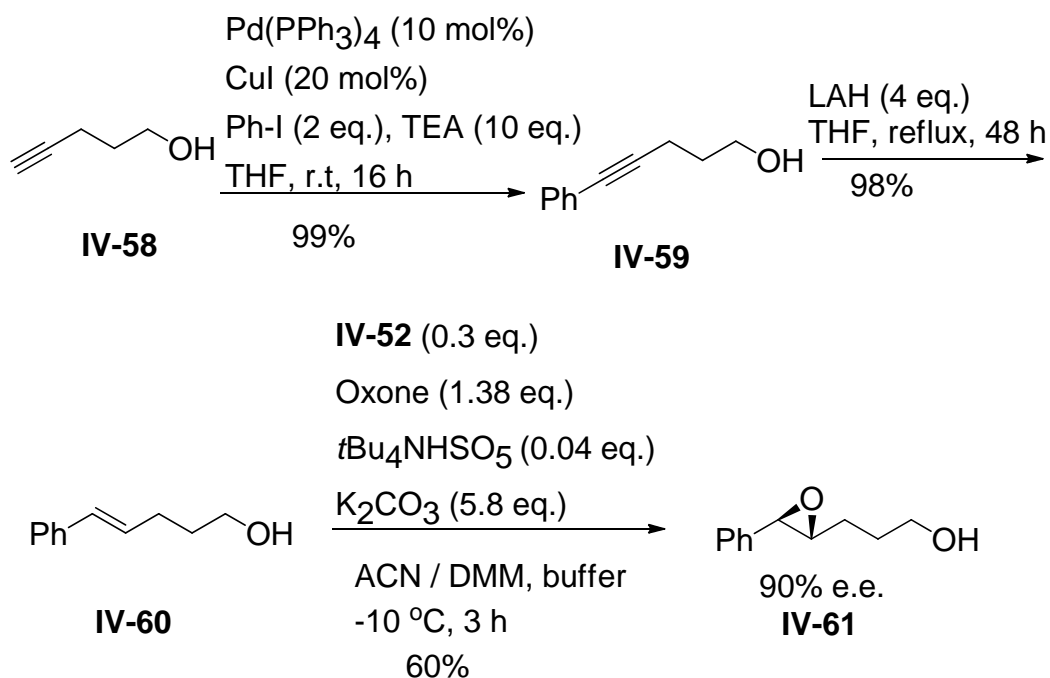
The bishomoallylic alcohols were obtained by Johnson-Claisen orthoester rearrangement of neat allylic alcohols⁵⁰ or alcohol solution in toluene⁵¹ and followed by LAH reduction (Scheme IV-14). Sonogashira coupling of iodobenzene with terminal alkynyl alcohols and subsequent LAH mediated *trans*-selective reduction afforded most other *trans*-aryl substituted alkenyl alcohols⁵² (Scheme IV-15 and

IV-16). The following Shi asymmetric epoxidations yielded the desired *trans*-epoxy alcohols bearing *R,R* configurations with good optical purity (80-92% ee).



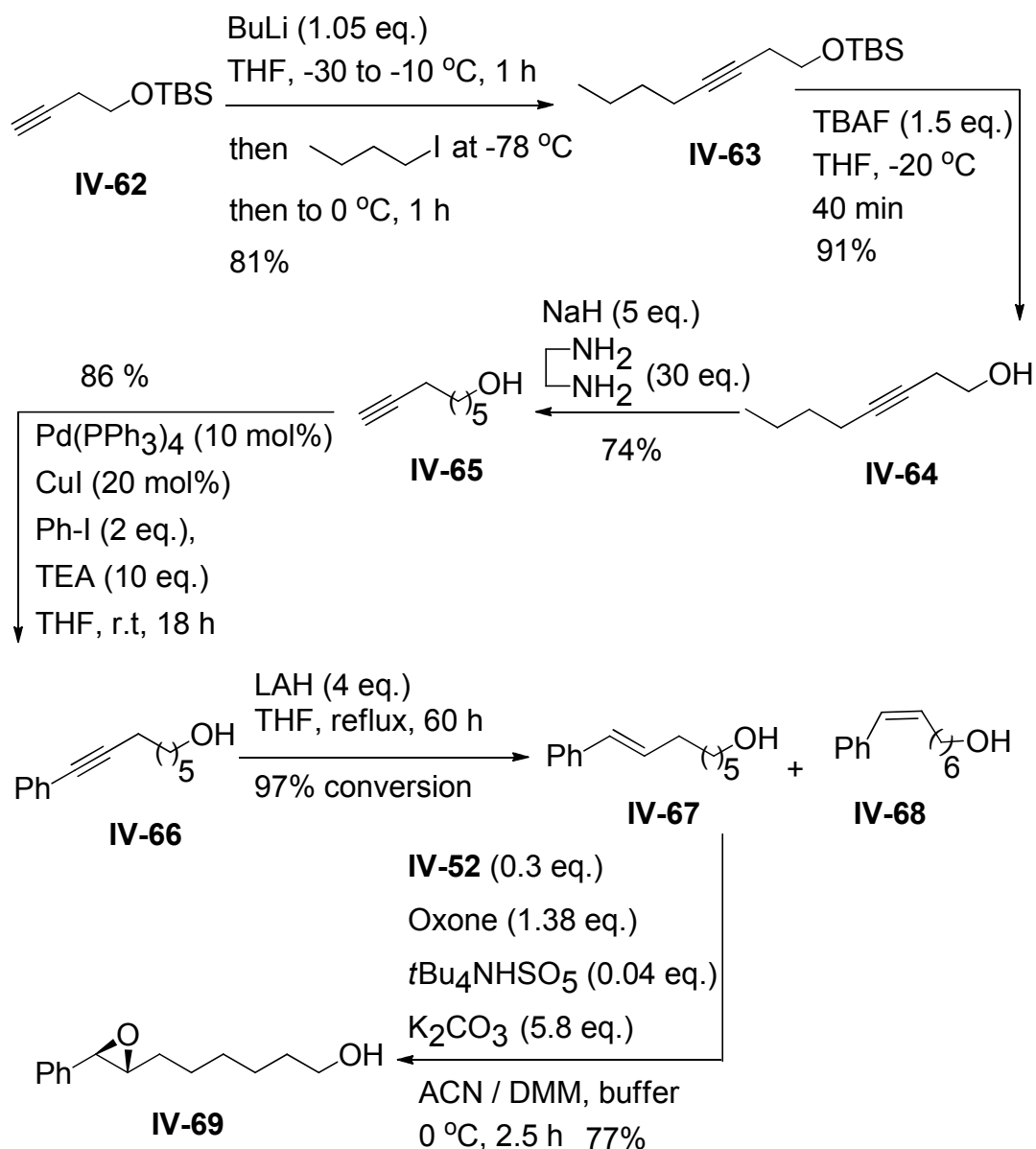
Scheme IV-14. Synthesis of alkyl substituted *trans* 4*R*,5*R*-epoxy alcohol.

The terminal alkynyl alcohols were either commercially available or were made from internal alkynyl alcohols via the alkyne zipper reaction in the presence of NaH in neat ethylenediamine (Scheme IV-16).⁵³ The selectivity of LAH reduction of **IV-65** was not good and considerable amount of *cis*-isomer was observed by ¹H NMR. These two isomers are very close in normal silica gel chromatography and hard to separate.



Scheme IV-15. Synthesis of aryl substituted *trans* 4*R*,5*R*-epoxy alcohol.

To solve this problem, 20 g of silica gel was pre-treated with AgNO₃ (5% in ACN, 100 mL) for 10 min and the ACN was evaporated under heat. The resultant Ag-impregnated silica gel would have a stronger interaction with *cis*-olefin than *trans*-olefin thus providing a better separation of the *cis* / *trans* mixture. The silica gel was suspended in hexane in the dark room and packed into a column. A mixture of **IV-67** and **IV-68** (200 mg) was loaded onto the column and eluted with 0-20 % EtOAc / hexane (*R_f* < 0.2). Gratifyingly, pure *trans*-isomer **IV-67** (68 mg) could be obtained. The AgNO₃ treated silica gel demonstrated much stronger interaction with *cis*-isomer since **IV-68** eluted slightly faster than **IV-67** in normal silica gel column while it eluted slower than **IV-67** in the treated silica gel column. With pure **IV-67** in hand, Shi epoxidation was conducted smoothly to afford the *trans*-7*R*,8*R* epoxy alcohol (**IV-69**).

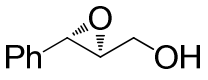
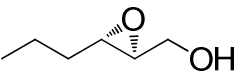
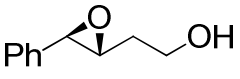
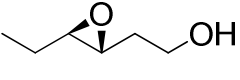
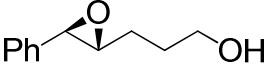
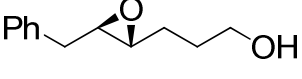
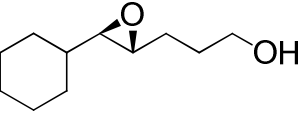
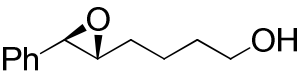
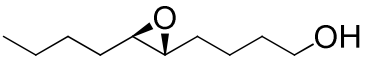
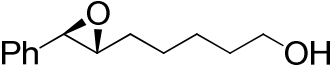
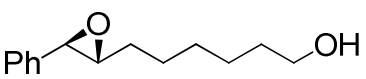


Scheme IV-16. Synthesis of *trans* 7*R*,8*R*-epoxy alcohol.

IV.2.5.2 Investigation of ECCD for long chain epoxy alcohols

As anticipated, prominent bisignate ECCD spectra were observed for all the epoxy alcohols right after being added to the Zn-TPFP tweezer **II-25** solution (2 μM) in hexane at 0 $^\circ\text{C}$ (Table IV-2). This suggested that the binding affinity was not compromised by the increased distance between two functionalities (epoxide ring and

Table IV-2. ECCD data of *trans*- epoxy alcohols bound to Zn-TPFP tweezer in hexane^a

	Epoxy Alcohol	ECCD Sign	λ nm, ($\Delta\epsilon$)	A
IV-1^b 2S,3S		<i>neg</i>	423 (-55) 410 (+62)	-117
IV-3 2S,3S		<i>neg</i>	423 (-60) 412 (+45)	-105
IV-54 3R,4R		<i>neg</i>	423 (-120) 411 (+80)	-200
IV-70 3R,4R		<i>neg</i>	423 (-104) 411 (+91)	-195
IV-61 4R,5R		<i>pos</i>	422 (+142) 413 (-109)	-251
IV-57 4R,3R		<i>pos</i>	422 (+78) 415 (-71)	+149
IV-71 4R,5R		<i>pos</i>	422 (+60) 412 (-49)	+109
IV-72^d 5R,6R		<i>neg</i>	422 (-78) 413 (+69)	-147
IV-73 5R,6R		<i>neg</i>	423 (-40) 413 (+42)	-82
IV-74 6R,7R		<i>pos</i>	424 (+79) 414 (-60)	+65
IV-69^d 7R,8R		<i>neg</i>	421 (-13) 413 (+15)	-28

^a tweezer:substrate ratio - 1:40, ^b the enantiomer showed mirror image CD spectrum, 2 μ M tweezer concentration at 0 °C was used for all measurements.

hydroxyl group) binding with the tweezer. The ECCD spectra consistently exhibited bisignate feature during the addition of 5-100 eq. of chiral guests, indicating the formation of stable ECCD active complex. These observations told us that the Zn-TPFP tweezer **II-25** could serve as a good chirality sensor for long chain epoxy alcohols. Surprisingly, a remarkable odd-even trend was revealed while comparing the ECCD data in listed in Table IV-2.

The *2R,3R*, *4R,5R*, and *6R,7R* epoxy alcohols with odd number of $-\text{CH}_2-$ groups separating epoxide ring and OH group gave a positive couplet (Figure IV-19), while *3R,4R*, *5R,6R*, and *7R,8R* epoxy alcohols rendered negative couplet (Figure IV-19). Both aliphatic and aromatic substrates behaved in the same fashion. The plot of Cotton effects versus methylene spacer length (Figure IV-20) also straightforwardly illustrates this intriguing effect.

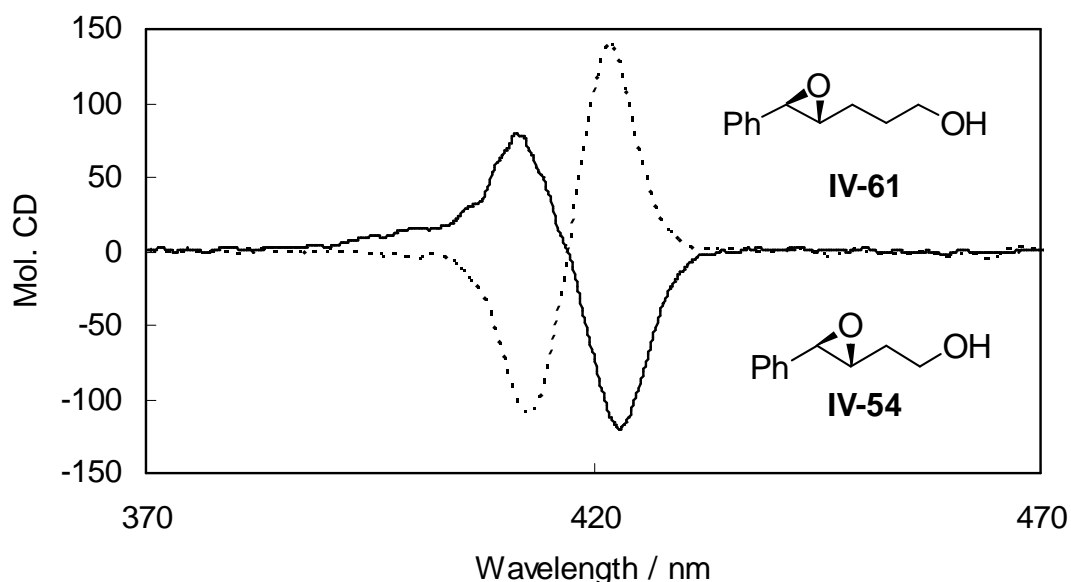


Figure IV-19. ECCD spectra of **IV-54** (solid line) and **IV-61** (dashed line) with Zn-TPFP tweezer **II-25**.

In terms of determining the absolute configurations, the above-mentioned observation does not compromise our initial goal. Though the ECCD results indicated that these homologues do not behave as we initially thought, we could still employ the Zn-TPFP tweezer to read out the chirality for epoxy alcohols bearing the same number of methylene groups. The observed odd-even effect just divided these homologues into two categories.

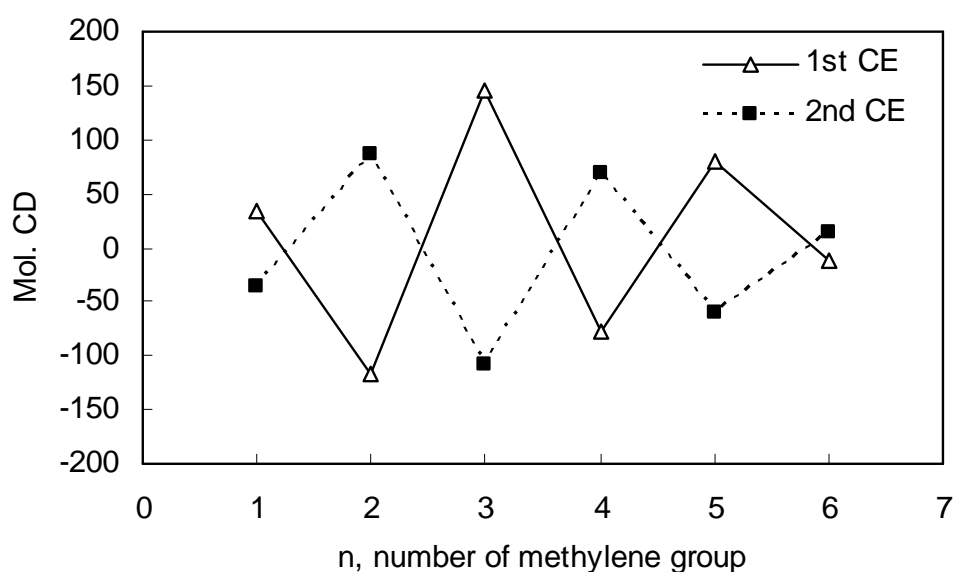


Figure IV-20. Plot of 1st Cotton effects (solid line) and 2nd Cotton effects (dashed

Probing the origin of this unique parity effect is of particular importance since it will better our understanding of the binding mechanism for porphyrin tweezer host with epoxy alcohols. In addition, it will also provide significant insights for odd-even phenomenon especially in solution state, revealing how it affects chemical properties as well as physical properties of compounds of interest.

Test of solvent indicated that it is not the cause of parity effect since similar odd-even observation was found in MCH with decreased amplitudes, while in polar solvent such as CH_2Cl_2 no ECCD signals were attained for most substrates presumably due to competitive binding of solvent with the highly Lewis acidic host. UV-vis profiles of these epoxy alcohols bound with Zn-TPFP tweezer in hexane are essentially the same (see Figure IV-21 and Figure IV-22). One feature disclosed from UV-vis studies is that the λ_{max} of the Soret band of porphyrin tweezer gradually red-shifted upon binding with chiral epoxy alcohols. A horizontal comparison of homologues **IV-1**, **IV-54**, **IV-61**, **IV-72**, **IV-74**, **IV-69** which contain same substituents (Ph) on the epoxide ring showed that longer alkyl chain guests generally led to larger red-shift of λ_{max} .

As discussed before, the shift of λ_{max} for porphyrin tweezer complex is the outcome of two opposing effects;^{16, 54} the bathochromic shift resulting from donor-acceptor interaction and hypsochromic shift when the two chromophores are brought close by guest molecules upon coordination. These homologues have very similar nucleophilicity owing to the same substituents, thus the donor-acceptor interactions are expected to be the same. Consequently, the red-shifts of λ_{max} would reflect the distance between two porphyrin chromophores. As revealed by Figure IV-21 and Figure IV-22, with the increase of chain length larger red-shift was observed (0 nm for **IV-1**, 0.6 nm for **IV-54**, 2.1 nm for **IV-61**, 2.2 nm for **IV-72**, 3.3 nm for **IV-69** in hexane). However, the UV-vis profiles are not instructive for the explaining the parity effect.

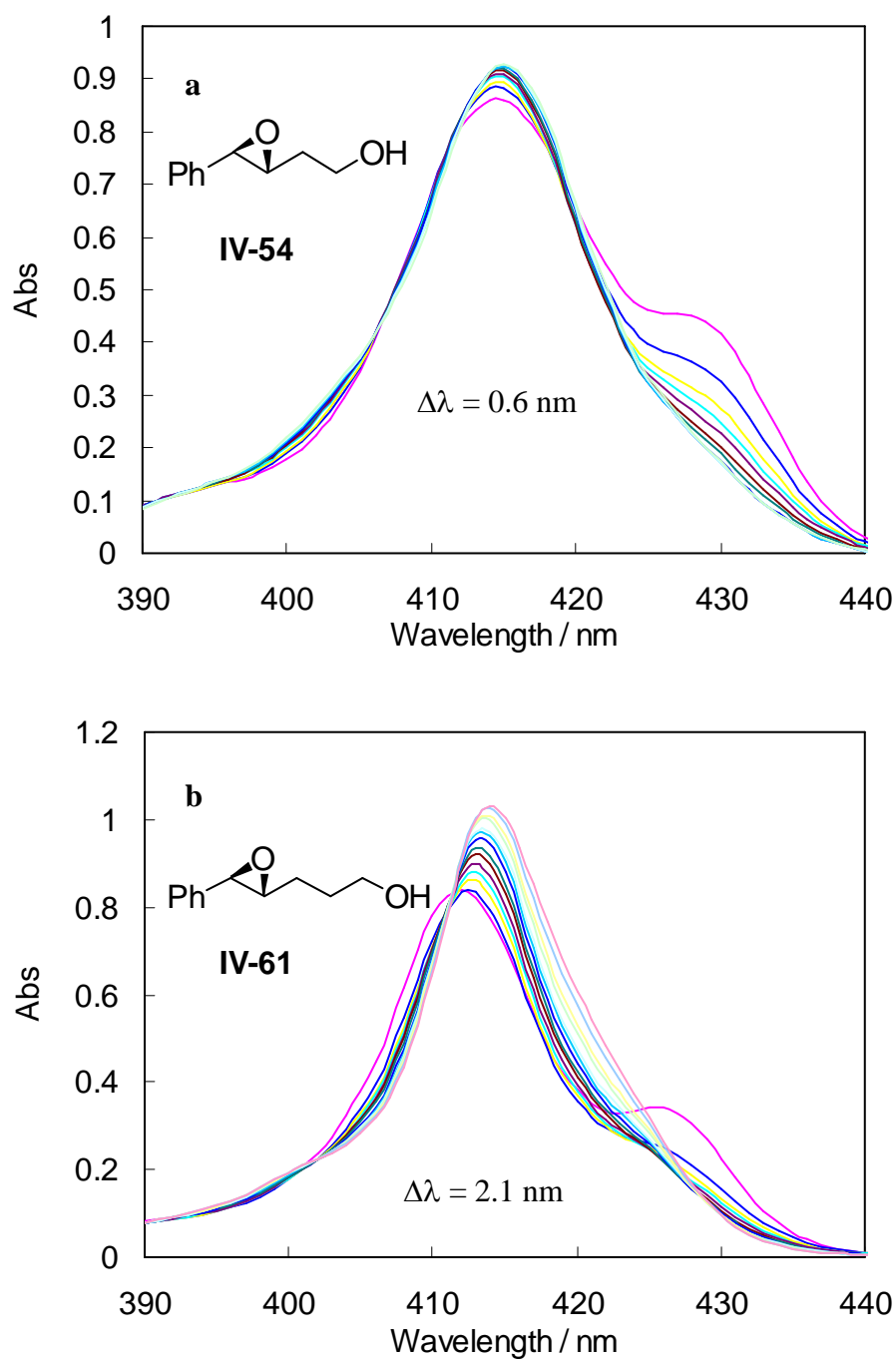


Figure IV-21. UV-Vis spectra change upon titration of TFPF tweezer (1 μ M in hexane) with **IV-54** (graph a) and **IV-61** (graph b) (10 mM in DCM) at different equivalents.

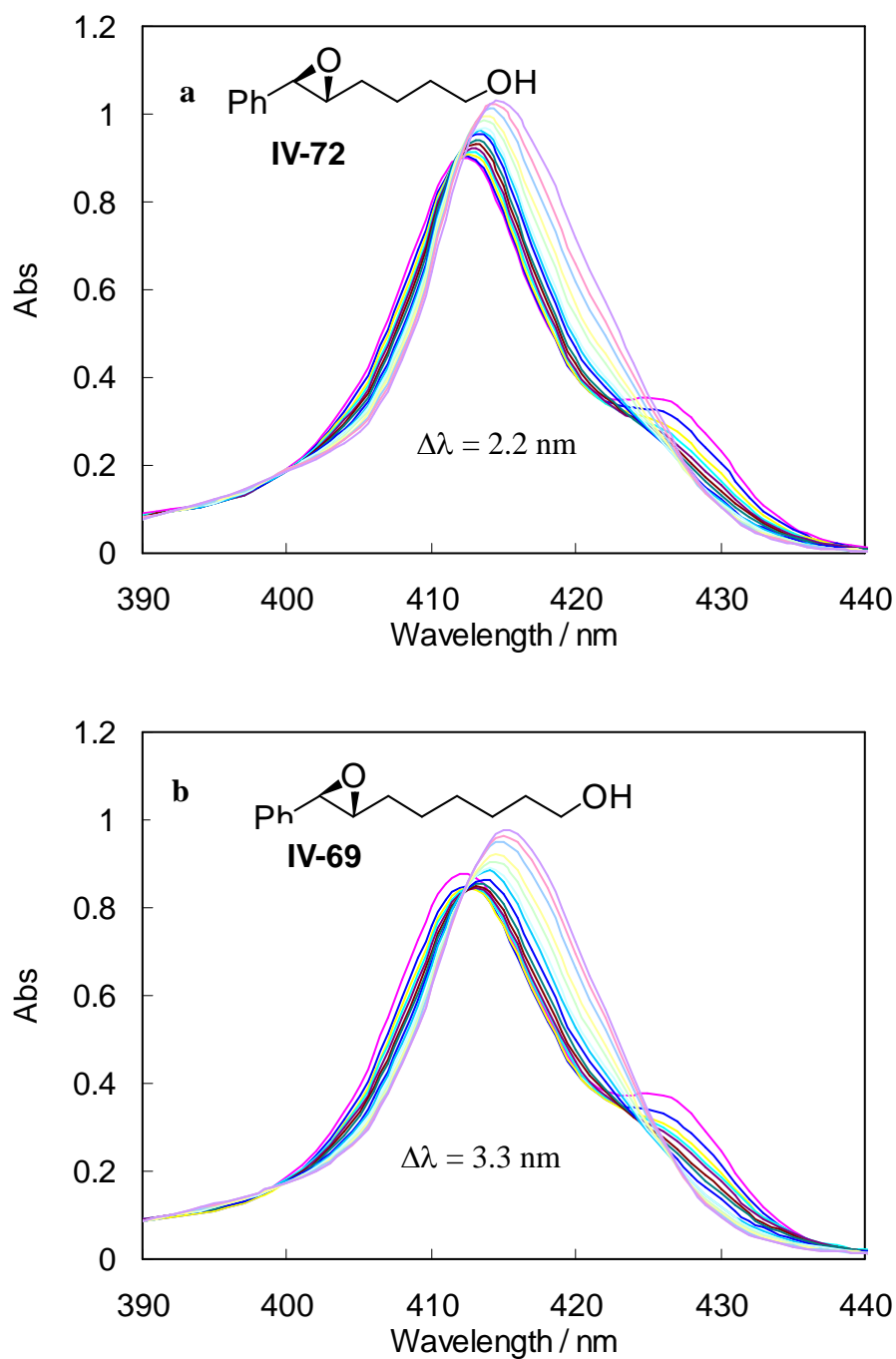


Figure IV-22. UV-Vis spectra change upon titration of Zn-TPFP tweezer (1 μM in hexane) with **IV-72** (graph a) and **IV-69** (graph b) (10 mM in DCM) at different equivalents.

Intuitively, the different orientations or motions of terminal OH group relative to the epoxide ring should account for the odd-even effect since that is the only variable directly induced by changing the methylene spacer length. Izumi and coworkers' study of odd-even effect for chiral alkyl monoalcohols offered some hints supported by DFT calculations suggesting that the orientation of terminal methyl groups of these monoalcohols are in zig-zag order, so are their dipole moments.⁴⁴ In the *trans*-all staggered conformation of these epoxy alcohols, we also see the zig-zag orientation of terminal OH groups (Figure IV-23) implying different binding patterns which need to be addressed in further study.

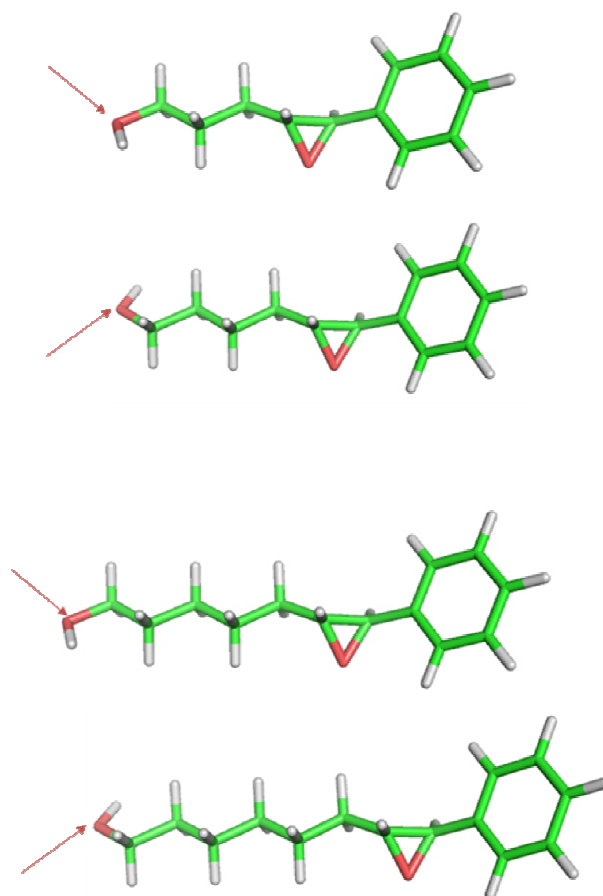


Figure IV-23. The zig-zag orientation of terminal OH groups in long-chain epoxy alcohols.

Cyclic substrates containing epoxy alcohol moiety were also examined and preliminary results proved that rigidified molecule skeleton was actually beneficial to fix conformation of epoxy alcohol leading to increased amplitude. Epoxy steroids complexed with Zn-TPFP tweezer rendered strong ECCD signals (A value is up to 1000) due to rigid skeleton despite the huge size. The details of this study will be discussed in Chapter VII.

Considering the great importance of epoxy alcohols in organic chemistry, the current protocol developed is particularly useful for organic chemists who are seeking expedient method to determine absolute configurations of epoxy alcohols. More importantly, the success of the epoxy alcohol case prompted us to look into the ECCD study of other oxygen-containing chiral heterocycles such as tetrahydrofurans and tetrahydropyrans which are widely present in drug candidates. Therefore, further development of this method will be important in a practical sense.

Experimental Procedures

Materials and general instrumentations:

Anhydrous CH_2Cl_2 was dried and redistilled over CaH_2 . The solvents used for CD measurements were purchased from Aldrich and were spectra grade. All reactions were performed in dried glassware under nitrogen. Column chromatography was performed using SiliCycle silica gel (230-400 mesh). ^1H NMR and ^{13}C NMR spectra were obtained on a Varian Inova 300 MHz or 500 MHz instrument and are reported in parts per million (ppm) relative to the solvent resonances (δ), with coupling constants (J) in Hertz (Hz). IR studies were performed on a Nicolet FT-IR 42 instrument. UV/Vis spectra were recorded on a Perkin-Elmer Lambda 40 spectrophotometer, and are reported as λ_{max} [nm]. CD spectra were recorded on a JASCO J-810 spectropolarimeter, equipped with a temperature controller (Neslab 111) for low temperature studies, and were reported as $\lambda[\text{nm}]$ ($\Delta\epsilon_{\text{max}}$ [$\text{L mol}^{-1} \text{cm}^{-1}$]). Optical rotations were recorded at 20 °C on a Perkin Elemer 341 Polarimeter ($\lambda = 589$ nm, 1 dm cell). Chiral GC analyses were performed on a Hewlett Packard 6890 gas chromatograph equipped with a Supelco Gamma Dex 225 column (0.25 mm \times 30 m) using helium as carrier gas. HRMS analyses were performed on a Q-TOF Ultima system using electrospray ionization in positive mode.

General procedure for CD measurement:

Zinc porphyrin tweezer **II-25** (2 μL of a 1 mM solution in anhydrous CH_2Cl_2) was added to hexane (1 mL) in a 1.0 cm cell to obtain a 2 μM tweezer **II-25** solution.

The background spectrum was recorded from 350 nm to 550 nm with a scan rate of 100 nm/min at 0 °C. Chiral epoxy alcohol (1 to 20 µL of a 10 mM solution in anhydrous CH₂Cl₂) was added into the prepared tweezer solution to afford the host/guest complex. The CD spectra were measured immediately (minimum of 4 accumulations). The resultant ECCD spectra recorded in millidegrees were normalized based on the tweezer concentration to obtain the molecular CD (Mol CD).

Determination of binding constant

The solution of Zn-porphyrin tweezer (1 mM in hexane) was titrated with guest molecule (10 mM in DCM) at different equivalents and the UV-vis spectra were recorded. The addition of the chiral substrate continued until no visible change in the spectra was observed. Upon formation of the chiral complex the Soret band of the porphyrin tweezers underwent red-shifts through an isosbestic point. The change of absorption at certain wavelength as a function of the substrate concentration yields an exponential saturation curve which can be fitted through the following non-linear least square equation previously reported by Shoji¹⁷ to derive the binding constant.

$$f = L \{ (1 + kx + ka) - [L^2(1 + kx + ka)^2 - 4axk^2L^2]^{1/2} \} / 2ka$$

where: L - Δ abs at the point of saturation; x - chiral substrate equivalents; k - calculated K_a ; a - concentration of porphyrin tweezer.

Typical procedure for synthesis of chiral epoxy alcohols using Sharpless asymmetric epoxidation (SAE)¹⁴ as described for the synthesis of IV-15:

To a flame dried 50 mL round bottom flask filled with 4 Å powered molecular sieves (200 mg, activated under high vacuum at 180 °C overnight), was added anhydrous CH₂Cl₂ (20 mL). The flask was cooled to -20 °C. D-(-)-Diethyl tartrate (83 µL, 0.49 mmol, 0.075 equiv) and Ti(O-*i*-Pr)₄ (95 µL, 0.33 mmol, 0.05 equiv) were added sequentially via syringe. The mixture was stirred for 20 min before TBHP (5.42 mL, 12.96 mmol, 2.39 M in anhydrous toluene) was introduced dropwise. The resulting mixture was stirred at -20 °C for 20 min. Geraniol alcohol (1.0 g, 6.48 mmol, dried over molecular sieve for 2 h) was dissolved in anhydrous CH₂Cl₂ (5 mL) and added dropwise via syringe pump over 40 min. The mixture was further stirred at -20 °C for 3 to 20 h monitored by TLC until completion. The reaction was quenched by adding saturated Na₂SO₃ solution (5 mL) at 0 °C and stirred for 3 h at room temperature. The cloudy suspension was filtered through Celite and washed with CH₂Cl₂. Hydrolysis of the tartrate complex in the filtrate was then effected by adding 30% aqueous NaOH (4.5 mL) solution saturated with NaCl and stirring vigorously for 30 min (longer time is needed when DIPT was used) at 0 °C. The aqueous layer was separated and washed with CH₂Cl₂ (4 × 20 mL). Combined organic layers were dried with anhydrous Na₂SO₄ and concentrated under reduced pressure. The light yellow residue was purified by flash chromatography (20-30% EtOAc / hexane) to afford the chiral epoxy alcohol (1.02 g, 93%) as a colorless oil.

REFERENCES

References

1. Kobayashi, S.; Ashizawa, S.; Takahashi, Y.; Sugiura, Y.; Nagaoka, M.; Lear, M. J.; Hirama, M., The first total synthesis of N1999-A2: Absolute stereochemistry and stereochemical implications into DNA cleavage. *Journal of the American Chemical Society* **2001**, 123, (45), 11294-11295.
2. Trost, B. M.; Harrington, P. E.; Chisholm, J. D.; Wroblewski, S. T., Total synthesis of (+)-amphidinolide A. Structure elucidation and completion of the synthesis. *Journal of the American Chemical Society* **2005**, 127, (39), 13598-13610.
3. Trost, B. M.; Wroblewski, S. T.; Chisholm, J. D.; Harrington, P. E.; Jung, M., Total synthesis of (+)-amphidinolide A. Assembly of the fragments. *Journal of the American Chemical Society* **2005**, 127, (39), 13589-13597.
4. Kobayashi, J.; Ishibashi, M.; Nakamura, H.; Ohizumi, Y.; Yamasu, T.; Sasaki, T.; Hirata, Y., Amphidinolide-a, a Novel Antineoplastic Macrolide from the Marine Dinoflagellate Amphidinium Sp. *Tetrahedron Letters* **1986**, 27, (47), 5755-5758.
5. Kobayashi, J.; Ishibashi, M.; Hirota, H., H-1-Nmr and C-13-Nmr Spectral Investigation on Amphidinolide-a, an Antileukemic Marine Macrolide. *Journal of Natural Products* **1991**, 54, (5), 1435-1439.
6. Maleczka, R. E.; Terrell, L. R.; Geng, F.; Ward, J. S., Total synthesis of proposed amphidinolide A via a highly selective ring-closing metathesis. *Organic Letters* **2002**, 4, (17), 2841-2844.
7. Lam, H. W.; Pattenden, G., Total synthesis of the presumed amphidinolide A. *Angewandte Chemie-International Edition* **2002**, 41, (3), 508-511.
8. Torres-Valencia, J. M.; Leon, G. I.; Villagomez-Ibarra, J. R.; Suarez-Castillo, O. R.; Cerda-Garcia-Rojas, C. M.; Joseph-Nathan, P., Stereochemical assignment of naturally occurring 2,3-epoxy-2-methylbutanoate esters. *Phytochemical Analysis* **2002**, 13, (6), 329-332.
9. Torres-Valencia, J. M.; Cerda-Garcia-Rojas, C. M.; Joseph-Nathan, P., Stereochemical assignment of 2,3-epoxy-2-methylbutanoate esters in natural products. *Phytochemical Analysis* **1999**, 10, (5), 221-237.
10. Johnson, R. A.; Sharpless, K. B., Catalytic Asymmetric Epoxidation of Allylic

Alcohols. In *Catalytic Asymmetric Synthesis*, Ojima, I., Ed. Wiley-VCH: New York, 1993; pp 103-158.

11. Jacobsen, E. N., Asymmetric Catalytic Epoxidation of Unfunctionalized Olefins. In *Catalytic Asymmetric Synthesis*, Ojima, I., Ed. Wiley-VCH: New York, 1993; pp 159-202.

12. Wang, Z. X.; Tu, Y.; Frohn, M.; Zhang, J. R.; Shi, Y., An efficient catalytic asymmetric epoxidation method. *Journal of the American Chemical Society* **1997**, 119, (46), 11224-11235.

13. Zhang, W.; Basak, A.; Kosugi, Y.; Hoshino, Y.; Yamamoto, H., Enantioselective epoxidation of allylic alcohols by a chiral complex of vanadium: An effective controller system and a rational mechanistic model. *Angewandte Chemie-International Edition* **2005**, 44, (28), 4389-4391.

14. Gao, Y.; Hanson, R. M.; Klunder, J. M.; Ko, S. Y.; Masamune, H.; Sharpless, K. B., Catalytic Asymmetric Epoxidation and Kinetic Resolution - Modified Procedures Including Insitu Derivatization. *Journal of the American Chemical Society* **1987**, 109, (19), 5765-5780.

15. Huang, X. F.; Rickman, B. H.; Borhan, B.; Berova, N.; Nakanishi, K., Zinc porphyrin tweezer in host-guest complexation: Determination of absolute configurations of diamines, amino acids, and amino alcohols by circular dichroism. *Journal of the American Chemical Society* **1998**, 120, (24), 6185-6186.

16. Li, X. Y.; Tanasova, M.; Vasileiou, C.; Borhan, B., Fluorinated porphyrin tweezer: A powerful reporter of absolute configuration for erythro and threo diols, amino alcohols, and diamines. *Journal of the American Chemical Society* **2008**, 130, (6), 1885-1893.

17. Shoji, Y.; Tashiro, K.; Aida, T., Sensing of chiral fullerenes by a cyclic host with an asymmetrically distorted pi-electronic component. *Journal of the American Chemical Society* **2006**, 128, (33), 10690-10691.

18. Eliel, E. L.; Wilen, S. H., *Stereochemistry of Organic Compounds*. Wiley & Sons: New York, 1993.

19. Ando, K., Highly selective synthesis of Z-unsaturated esters by using new Horner-Emmons reagents, ethyl (diarylphosphono)acetates. *Journal of Organic Chemistry* **1997**, 62, (7), 1934-1939.

20. Touchard, F. P.; Capelle, N.; Mercier, M., Efficient and scalable protocol for the Z-selective synthesis of unsaturated esters by Horner-Wadsworth-Emmons olefination.

Advanced Synthesis & Catalysis **2005**, 347, (5), 707-711.

21. Touchard, F. P., Phosphonate modification for a highly (Z)-selective synthesis of unsaturated esters by Horner-Wadsworth-Emmons olefination. *European Journal of Organic Chemistry* **2005**, (9), 1790-1794.

22. Martin, R.; Islas, G.; Moyano, A.; Pericas, M. A.; Riera, A., A new method for the enantioselective synthesis of N-Boc-alpha,alpha-disubstituted alpha-amino acids. *Tetrahedron* **2001**, 57, (30), 6367-6374.

23. Lipshutz, B. H.; Sharma, S.; Dimock, S. H.; Behling, J. R., Preparation of C-4 Alkylated Dideoxyribosides - Potential Precursors to a Novel Series of Nucleosides. *Synthesis-Stuttgart* **1992**, (1-2), 191-195.

24. Petter, R. C.; Banerjee, S.; England, S., Inhibition of Gamma-Butyrobetaine Hydroxylase by Cyclopropyl-Substituted Gamma-Butyrobetaines. *Journal of Organic Chemistry* **1990**, 55, (10), 3088-3097.

25. Kirschleger, B.; Queignec, R., Heterogeneous Mediated Alkylation of Ethyl Diethylphosphonoacetate - a One Pot Access to Alpha-Alkylated Acrylic Esters. *Synthesis-Stuttgart* **1986**, (11), 926-928.

26. Martin, V. S.; Woodard, S. S.; Katsuki, T.; Yamada, Y.; Ikeda, M.; Sharpless, K. B., Kinetic Resolution of Racemic Allylic Alcohols by Enantioselective Epoxidation - a Route to Substances of Absolute Enantiomeric Purity. *Journal of the American Chemical Society* **1981**, 103, (20), 6237-6240.

27. Belelie, J. L.; Chong, J. M., Stereoselective reactions of acyclic allylic phosphates with organocopper reagents. *Journal of Organic Chemistry* **2001**, 66, (16), 5552-5555.

28. Hussain, M. M.; Walsh, P. J., Tandem reactions for streamlining synthesis: Enantio- and diastereoselective one-pot generation of functionalized epoxy alcohols. *Accounts of Chemical Research* **2008**, 41, (8), 883-893.

29. Salvi, L.; Jeon, S. J.; Fisher, E. L.; Carroll, P. J.; Walsh, P. J., Catalytic asymmetric generation of (Z)-disubstituted allylic alcohols. *Journal of the American Chemical Society* **2007**, 129, (51), 16119-16125.

30. Mizuno, M.; Hirai, A.; Matsuzawa, H.; Endo, K.; Suhara, M.; Kenmotsu, M.; Han, C. D., Study of odd-even effect of flexible spacer length on the chain dynamics of main-chain thermotropic liquid-crystalline polymers using high-resolution solid-state C-13 nuclear magnetic resonance spectroscopy. *Macromolecules* **2002**, 35, (7), 2595-2601.

31. Wolf, K. V.; Cole, D. A.; Bernasek, S. L., Low-energy collisions of pyrazine and d(6)-benzene molecular ions with self-assembled monolayer surfaces: The odd-even chain length effect. *Langmuir* **2001**, 17, (26), 8254-8259.
32. Schneider, J.; Messerschmidt, C.; Schulz, A.; Gnade, M.; Schade, B.; Luger, P.; Bombicz, P.; Hubert, V.; Fuhrhop, J. H., Odd-even effects in supramolecular assemblies of diamide bolaamphiphiles. *Langmuir* **2000**, 16, (23), 8575-8584.
33. Hibino, M.; Sumi, A.; Tsuchiya, H.; Hatta, I., Microscopic origin of the odd-even effect in monolayer of fatty acids formed on a graphite surface by scanning tunneling microscopy. *Journal of Physical Chemistry B* **1998**, 102, (23), 4544-4547.
34. Tao, F.; Goswami, J.; Bernasek, S. L., Self-assembly and odd-even effects of cis-unsaturated carboxylic acids on highly oriented pyrolytic graphite. *Journal of Physical Chemistry B* **2006**, 110, (9), 4199-4206.
35. Heimel, G.; Romaner, L.; Bredas, J. L.; Zojer, E., Odd-even effects in self-assembled monolayers of omega-(biphenyl-4-yl)alkanethiols: A first-principles study. *Langmuir* **2008**, 24, (2), 474-482.
36. Auer, F.; Nelles, G.; Sellergren, B., Odd-even chain length-dependent order in pH-switchable self-assembled layers. *Chemistry-a European Journal* **2004**, 10, (13), 3232-3240.
37. Aoki, K.; Kudo, M.; Tamaoki, N., Novel odd/even effect of alkylene chain length on the photopolymerizability of organogelators. *Organic Letters* **2004**, 6, (22), 4009-4012.
38. Fujita, N.; Sakamoto, Y.; Shirakawa, M.; Ojima, M.; Fujii, A.; Ozaki, M.; Shinkai, S., Polydiacetylene nanofibers created in low-molecular-weight gels by post modification: Control of blue and red phases by the odd-even effect in alkyl chains. *Journal of the American Chemical Society* **2007**, 129, (14), 4134-+.
39. Henze, O.; Feast, W. J.; Gardebien, F.; Jonkheijm, P.; Lazzaroni, R.; Leclere, P.; Meijer, E. W.; Schenning, A., Chiral amphiphilic self-assembled alpha,alpha'-linked quinque-, sexi-, and septithiophenes: Synthesis, stability and odd-even effects. *Journal of the American Chemical Society* **2006**, 128, (17), 5923-5929.
40. Lee, S. K.; Heo, S.; Lee, J. G.; Kang, K. T.; Kumazawa, K.; Nishida, K.; Shimbo, Y.; Takanishi, Y.; Watanabe, J.; Doi, T.; Takahashi, T.; Takezoe, H., Odd-even behavior of ferroelectricity and antiferroelectricity in two homologous series of bent-core mesogens. *Journal of the American Chemical Society* **2005**, 127, (31), 11085-11091.

41. Berardi, R.; Muccioli, L.; Zannoni, C., Can nematic transitions be predicted by atomistic simulations? A computational study of the odd even effect. *Chemphyschem* **2004**, 5, (1), 104-111.
42. Duer, M. J.; Roper, C., A solid-state NMR investigation of the odd-even effect in a series of liquid-crystal dimers. *Physical Chemistry Chemical Physics* **2003**, 5, (14), 3034-3041.
43. Pistolis, G.; Andreopoulou, A. K.; Malliaris, A.; Kallitsis, J. K., Direct observation of odd-even effect in dilute polymeric solutions: A time-resolved fluorescence anisotropy study. *Journal of Physical Chemistry B* **2005**, 109, (23), 11538-11543.
44. Izumi, H.; Yamagami, S.; Futamura, S.; Nafie, L. A.; Dukor, R. K., Direct observation of odd-even effect for chiral alkyl alcohols in solution using vibrational circular dichroism spectroscopy. *Journal of the American Chemical Society* **2004**, 126, (1), 194-198.
45. Tian, H. Q.; She, X. G.; Shu, L. H.; Yu, H. W.; Shi, Y., Highly enantioselective epoxidation of cis-olefins by chiral dioxirane. *Journal of the American Chemical Society* **2000**, 122, (46), 11551-11552.
46. Wang, Z. X.; Shi, Y., A pH study on the chiral ketone catalyzed asymmetric epoxidation of hydroxyalkenes. *Journal of Organic Chemistry* **1998**, 63, (9), 3099-3104.
47. Tu, Y.; Wang, Z. X.; Shi, Y., An efficient asymmetric epoxidation method for trans-olefins mediated by a fructose-derived ketone. *Journal of the American Chemical Society* **1996**, 118, (40), 9806-9807.
48. Denmark, S. E.; Edwards, M. G., On the mechanism of the selenolactonization reaction with selenenyl halides. *Journal of Organic Chemistry* **2006**, 71, (19), 7293-7306.
49. Hoye, T. R.; Richardson, W. S., A Short, Oxetane-Based Synthesis of (+/-)-Sarracenin. *Journal of Organic Chemistry* **1989**, 54, (3), 688-693.
50. Pippel, D. J.; Curtis, M. D.; Du, H.; Beak, P., Complex-induced proximity effects: Stereoselective carbon-carbon bond formation in chiral auxiliary mediated beta-lithiation-substitution sequences of beta-substituted secondary carboxamides. *Journal of Organic Chemistry* **1998**, 63, (1), 2-3.
51. Va, P.; Roush, W. R., Total synthesis of amphidinolide E. *Journal of the American*

Chemical Society **2006**, 128, (50), 15960-15961.

52. Zheng, T.; Narayan, R. S.; Schomaker, J. M.; Borhan, B., One-pot regio- and stereoselective cyclization of 1,2,n-triols. *Journal of the American Chemical Society* **2005**, 127, (19), 6946-6947.

53. Denmark, S. E.; Yang, S. M., Sequential ring-closing metathesis/Pd-catalyzed, Si-assisted cross-coupling reactions: general synthesis of highly substituted unsaturated alcohols and medium-sized rings containing a 1,3-cis-cis diene unit. *Tetrahedron* **2004**, 60, (43), 9695-9708.

54. Kurtan, T.; Nesnas, N.; Koehn, F. E.; Li, Y. Q.; Nakanishi, K.; Berova, N., Chiral recognition by CD-sensitive dimeric zinc porphyrin host. 2. Structural studies of host-guest complexes with chiral alcohol and monoamine conjugates. *Journal of the American Chemical Society* **2001**, 123, (25), 5974-5982.

55. Jorgensen, M.; Leung, T., Cyclopropyl Conjugation in Olefinic Esters . Conformational Effects on Ultraviolet Absorption. *Journal of the American Chemical Society* **1968**, 90, (14), 3769-&.

56. Wardrop, D. J.; Bowen, E. G., A formal synthesis of (+)-lactacystin. *Chemical Communications* **2005**, (40), 5106-5108.

57. Jimeno, C.; Pasto, M.; Riera, A.; Pericas, M. A., Modular amino alcohol ligands containing bulky alkyl groups as chiral controllers for Et₂Zn addition to aldehydes: Illustration of a design principle. *Journal of Organic Chemistry* **2003**, 68, (8), 3130-3138.

58. Roush, W. R.; Ando, K.; Powers, D. B.; Palkowitz, A. D.; Halterman, R. L., Asymmetric-Synthesis Using Diisopropyl Tartrate Modified (E)-Crotylboronates and (Z)-Crotylboronates - Preparation of the Chiral Crotylboronates and Reactions with Achiral Aldehydes. *Journal of the American Chemical Society* **1990**, 112, (17), 6339-6348.

59. Righi, G.; Rumboldt, G.; Bonini, C., Stereoselective preparation of syn alpha-hydroxy-beta-amino ester units via regioselective opening of alpha,beta-epoxy esters: Enantioselective synthesis of taxol C-13 side chain and cyclohexylnorstatine. *Journal of Organic Chemistry* **1996**, 61, (10), 3557-3560.

60. Medina, E.; VidalFerran, A.; Moyano, A.; Pericas, M. A.; Riera, A., Enantioselective synthesis of N-Boc-1-naphthylglycine. *Tetrahedron-Asymmetry* **1997**, 8, (10), 1581-1586.

61. Schomaker, J. M.; Pulgam, V. R.; Borhan, B., Synthesis of diastereomerically and

enantiomerically pure 2,3-disubstituted tetrahydrofurans using a sulfoxonium ylide. *Journal of the American Chemical Society* **2004**, 126, (42), 13600-13601.

62. Taber, D. F.; Storck, P. H., Synthesis of (-)-tetrodotoxin: Preparation of an advanced cyclohexenone intermediate. *Journal of Organic Chemistry* **2003**, 68, (20), 7768-7771.

63. Minami, N.; Ko, S. S.; Kishi, Y., Stereocontrolled Synthesis of D-Pentitols, 2-Amino-2-Deoxy-D-Pentitols, and 2-Deoxy-D-Pentitols from D-Glyceraldehyde Acetonide. *Journal of the American Chemical Society* **1982**, 104, (4), 1109-1111.

64. Baker, R.; Swain, C. J.; Head, J. C., The Chemistry of Spiroacetals - an Enantiospecific Synthesis of the Spiroacetal Moiety of Milbemycins Alpha-7 and Alpha-8. *Journal of the Chemical Society-Chemical Communications* **1986**, (11), 874-876.

65. Nicolaou, K. C.; Webber, S. E., Stereocontrolled Total Synthesis of Lipoxins-B. *Synthesis-Stuttgart* **1986**, (6), 453-461.

66. Borne, R. F.; Forrester, M. L.; Waters, I. W., Conformational Analogs of Antihypertensive Agents Related to Guanethidine. *Journal of Medicinal Chemistry* **1977**, 20, (6), 771-776.

67. Takeuchi, R.; Akiyama, Y., Iridium complex-catalyzed carbonylation of allylic phosphates. *Journal of Organometallic Chemistry* **2002**, 651, (1-2), 137-145.

68. Yamada, S.; Shiraishi, M.; Ohmori, M.; Takayama, H., Facile and Stereoselective Synthesis of 25-Hydroxyvitamin-D-2. *Tetrahedron Letters* **1984**, 25, (31), 3347-3350.

69. Cho, C. S.; Uemura, S., Palladium-Catalyzed Cross-Coupling of Aryl and Alkenyl Boronic Acids with Alkenes Via Oxidative Addition of a Carbon-Boron Bond to Palladium(0). *Journal of Organometallic Chemistry* **1994**, 465, (1-2), 85-92.

70. Daub, G. W.; Edwards, J. P.; Okada, C. R.; Allen, J. W.; Maxey, C. T.; Wells, M. S.; Goldstein, A. S.; Dibley, M. J.; Wang, C. J.; Ostercamp, D. P.; Chung, S.; Cunningham, P. S.; Berliner, M. A., Acyclic stereoselection in the ortho ester Claisen rearrangement. *Journal of Organic Chemistry* **1997**, 62, (7), 1976-1985.

71. Hashimoto, M.; Kan, T.; Nozaki, K.; Yanagiya, M.; Shirahama, H.; Matsumoto, T., Total Syntheses of (+)-Thyrsiferol, (+)-Thyrsiferyl 2 α -Acetate, and (+)-Venustatriol. *Journal of Organic Chemistry* **1990**, 55, (17), 5088-5107.

72. Kuroda, H.; Hanaki, E.; Izawa, H.; Kano, M.; Itahashi, H., A convenient method for the preparation of alpha-vinylfurans by phosphine-initiated reactions of various

substituted enynes bearing a carbonyl group with aldehydes. *Tetrahedron* **2004**, 60, (8), 1913-1920.

73. Lipshutz, B. H.; Ellsworth, E. L.; Dimock, S. H.; Smith, R. A. J., New Methodology for Conjugate Additions of Allylic Ligands to Alpha,Beta-Unsaturated Ketones - Synthetic and Spectroscopic Studies. *Journal of the American Chemical Society* **1990**, 112, (11), 4404-4410.

74. Grummitt, O.; Splitter, J., Reactions of Terminally Substituted 1,3-Butadienes with Sulfur Dioxide. *Journal of the American Chemical Society* **1952**, 74, (15), 3924-3929.

75. Righi, G.; Ronconi, S.; Bonini, C., A study on the "non-chelation controlled" organometallic addition to trans alpha,beta-epoxy aldehydes - A straightforward stereoselective synthesis of the Abbot amino dihydroxyethylene dipeptide isoster. *European Journal of Organic Chemistry* **2002**, (9), 1573-1577.

76. Yamaguchi, M.; Nobayashi, Y.; Hirao, I., A Ring-Opening Reaction of Oxetanes with Lithium Acetylides Promoted by Boron-Trifluoride Etherate. *Tetrahedron* **1984**, 40, (21), 4261-4266.

77. Molinaro, C.; Jamison, T. F., Nickel-catalyzed reductive coupling of alkynes and epoxides. *Journal of the American Chemical Society* **2003**, 125, (27), 8076-8077.

78. Bailey, W. F.; Gavaskar, K. V., Anionic Cyclization of Olefinic Alkylolithiums - Ring-Closure of Terminally Substituted 5-Hexenylolithiums. *Tetrahedron* **1994**, 50, (20), 5957-5970.

79. Patil, N. T.; Lutete, L. M.; Wu, H. Y.; Pahadi, N. K.; Gridnev, I. D.; Yamamoto, Y., Palladium-catalyzed intramolecular asymmetric hydroamination, hydroalkoxylation, and hydrocarbonation of alkynes. *Journal of Organic Chemistry* **2006**, 71, (11), 4270-4279.

80. Hudson, C. M.; Marzabadi, M. R.; Moeller, K. D.; New, D. G., Intramolecular Anodic Olefin Coupling Reactions - a Useful Method for Carbon-Carbon Bond Formation. *Journal of the American Chemical Society* **1991**, 113, (19), 7372-7385.

81. Narayan, R. S.; Borhan, B., Synthesis of the proposed structure of mucoxin via regio- and stereoselective tetrahydrofuran ring-forming strategies. *Journal of Organic Chemistry* **2006**, 71, (4), 1416-1429.

Chapter V

Absolute Configurations of 1,n Glycols: A Non-empirical Approach for Remote Stereochemical Determination

V.1 Background

1,n-Glycol functionalities are widely present in natural products and usually represent a challenge for determination of their absolute configurations. NMR analysis¹⁻⁷ is extensively used for determining the configurations of 1,2- and 1,3-glycols by analyzing the nucleus couplings or NOE of their cyclic derivatives such as acetonides. However, this technique only provides information regarding relative stereochemistry of the two hydroxyl groups if no other information is given. In addition, for acyclic long chain diols separated by more than four carbons, the NMR method is not helpful due to weak nucleus couplings and undistinguishable NMR signals at the chiral centers.

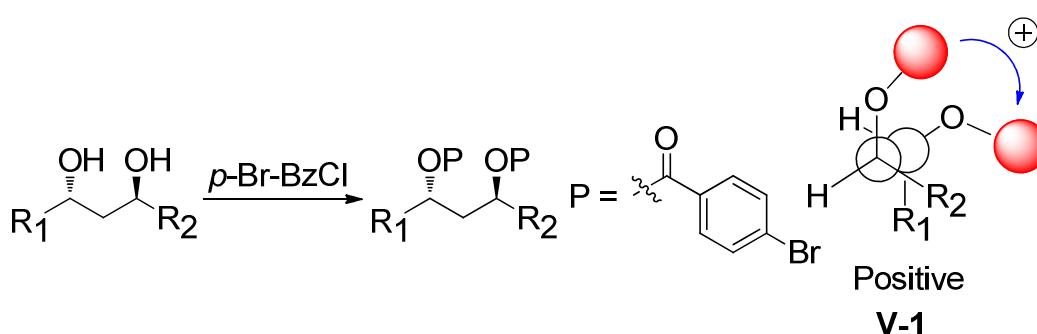


Figure V-1. Stereochemical determination of 1,3-*syn* diols using ECCD method.

ECCD study of dibenzoates⁸⁻¹³ (Figure III-2, Figure V-1) or cyclic derivatives¹⁴⁻²⁰ (Figure V-2, Figure III-4, Figure III-5) of diols is another method used to address the absolute configurations of 1,2- and 1,3-glycols.⁸ As shown in Figure V-1, chiral

1,3-diols could be derivatized as dibenzoates in a similar way as discussed before in Figure II-2. The most highly populated rotamer is believed to be **V-1** leading to a positive ECCD spectrum. In this way, the chirality of 1,3-diols could be determined in a nonempirical fashion. However, this method only worked well for *anti* diols and was not suitable for *syn* diols. Recently, Rosini and coworkers reported the stereochemical determination of 1,2- and 1,3- diols by converting them into cyclic di(1-naphthyl)ketals (Figure V-2) which exhibited couplet effect resulting from the 1B transition of naphthalene chromophores.²¹ The resultant CD couplet could be used to assign the absolute configuration of diols.

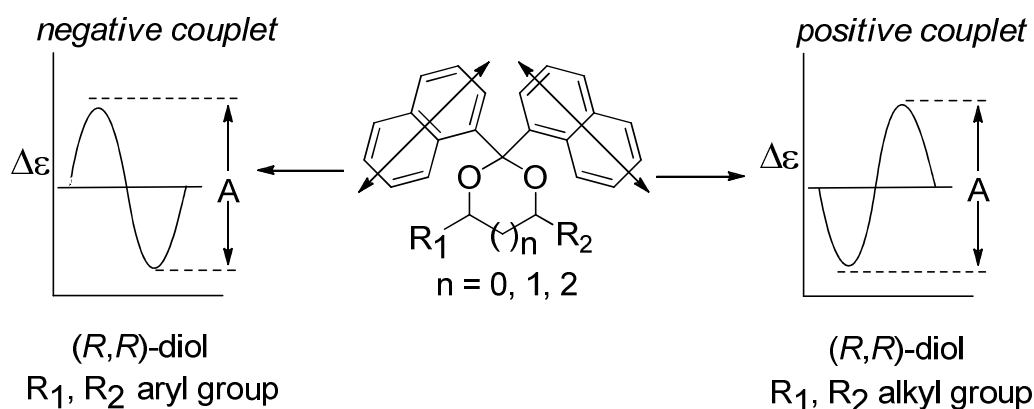


Figure V-2. Rosini's method for stereochemical determination of short chain diols.

However, for the dibenzoate approach weak or zero exciton coupling was usually observed when the chiral centers are distant to each other. For instance, 1,5-dibenzoate in solution did not give observable CD signal. This is attributed to two factors: first, the highly flexible skeleton could lead to energetically indiscriminable rotomers in which the two chromophores orient either clockwise or counterclockwise without significant energetic preference. Second, the long distance between chiral centers would lead to weak exciton couplings. For the cycloketal

approach, an apparent limitation is that the cycloketal cannot be efficiently formed when a long chain diol is involved and the flexible skeleton of long chain diol could give rise to multiple conformations making the resultant CD couplet unpredictable.

A successful study overcoming these difficulties is Molinski's elegant approach²²,²³ which involves making liposomal porphyrin esters of 1,n-glycols ($n = 5,7,9$) with certain chain lengths. The bulky porphyrin esters were pre-aligned in a consistent fashion as a result of the structural alignment of the lipids that make the liposome, rendering steady CD signals. However, this method is only applicable for diols separated with odd number of carbons and the ECCD amplitude falls with increasing chain length which limits its application in substrates with longer chains. A more general and facile protocol addressing the absolute configurations of long chain diols with various chain lengths still remains to be developed.

During our effort centered on the determination of absolute configurations for chiral molecules, we developed a highly fluorinated porphyrin tweezer (Zn-TPFP **II-25**)^{24, 25} which can bind strongly with hydroxyl groups owing to its strong Lewis acidity and was successfully used to determine the absolute stereochemistry of *vicinal* diols bearing two chiral centers via ECCD. We decided to probe the application of this method in the long-range stereochemical determination of 1,n-glycols in which two chiral centers are remote from each other.

The major challenge for the ECCD study of chiral centers remote from each other in acyclic molecules is their highly flexible skeleton, which usually leads to multiple conformations in isotropic solutions complicating the configurational analysis. We

envisaged that the strong complexation of a bulky porphyrin tweezer with diols would form a rigid macrocyclic assembly and reduce the number of conformations facilitating the stereochemical differentiation process and giving rise to predictable ECCD spectra. In this section, we describe an efficient method for the rapid and facile determination of absolute stereochemistry of 1,n ($n = 2-12, 16$) glycols bearing two chiral centers.

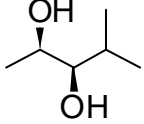
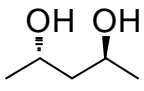
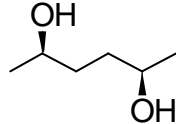
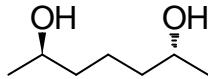
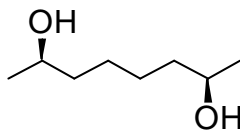
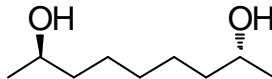
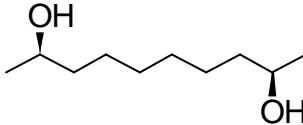
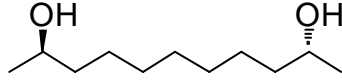
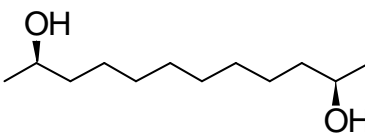
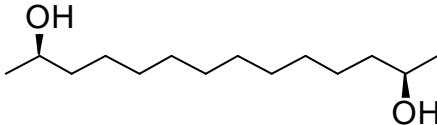
V.2 ECCD Study of 1,n-Glycols

V.2.1 ECCD study of 1,n-glycols using Zn-TPFP tweezer **II-25**

Chiral 1,n-glycols (**II-4~II-11**) were readily accessible through Jacobsen's Hydrolytic Kinetic Resolution (HKR)²⁶⁻²⁸ of terminal diepoxides, followed by ring opening of the chiral diepoxides by LAH. Detailed discussion of the synthesis of 1,n-glycols will be detailed in section V.3. The chiral diols with good optical purity (> 95% ee) were then submitted to ECCD measurement with Zn-TPFP tweezer **II-25**.

As expected, these chiral diols bound well with Zn-TPFP tweezer **II-25** in hexane at 0 °C to generate a supramolecular complex and produce an ECCD signal arising from porphyrin Soret band. A general trend could be discerned that *R,R* chiral diols exhibited positive ECCD spectra upon complexation with tweezer **II-25** (Table V-1). However, several complications were noticed. First, the 1,3-diol (**V-3**) rendered a positive ECCD signal which is opposite to the inferred trend. Second, complicated ECCD curves were obtained for 1,6-diol (2*R*,7*R*-octane diol **V-6**, Figure V-3a) and 1,12-diol (2*R*,13*R*-tetradecane diol **V-11**, Figure V-3b). We observed a switch of

Table V-1. ECCD data of 1,n-glycols in hexane bound with tweezer **II-25**^a

	1,n-Glycols	ECCD Sign	λ nm, ($\Delta\epsilon$)	A
III-15 ^b 2S,3S		<i>pos</i>	425 (+128) 413 (-96)	+224
V-3 2S,4S		<i>pos</i>	424 (+81) 412 (-71)	+152
V-4 2R,5R		<i>pos</i>	424 (+205) 413 (-163)	+368
V-5 2R,6R		<i>pos</i>	424 (+174) 413 (-135)	+309
V-6 2R,7R		<i>neg</i>	426 (-70) 418 (+53)	-123 ^a
V-7 2R,8R		<i>pos</i>	423 (+237) 413 (-199)	+436
V-8 2R,9R		<i>pos</i>	426 (+146) 415 (-140)	+286
V-9 2R,10R		<i>pos</i>	423 (+172) 414 (-130)	+302
V-10 2R,11R		<i>pos</i>	425 (+314) 415 (-177)	+491
V-11 2R,13R		-	430 (-91) 423 (+506) 414 (-171)	-

^a tweezer:substrate ratio - 1:5, ^b tweezer:substrate ratio - 1:40, 2 μ M tweezer concentration at 0 °C was used for all measurements.

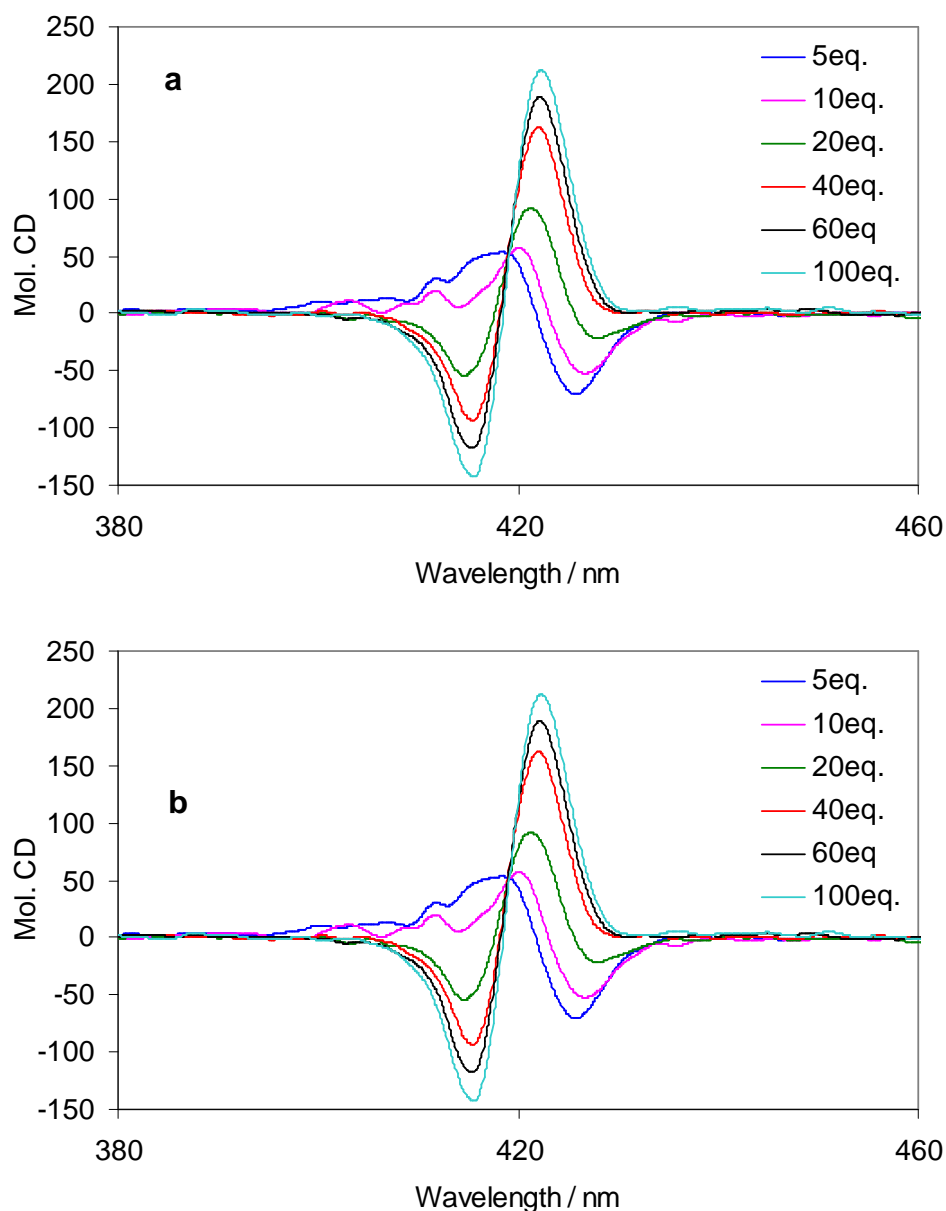


Figure V-3. ECCD spectra of tweezer **II-25** (2 μ M in hexane) with **V-6** (graph **a**) and **V-11** (graph **b**) at different equivalents.

sign from negative to positive for 1,6-diol upon going from 5 to 40 eq. of 1,6-diol which became stronger at even higher amounts of the diol. For the 1,12-diol, three peaks were seen when 5–100 eq. of chiral guest was mixed with the tweezer solution. These strange behaviors implied the possible presence of multiple competing ECCD

active conformations, however their UV-vis profiles (Figure V-4) did not reflect this speculation and essentially shared the same features as other diols.

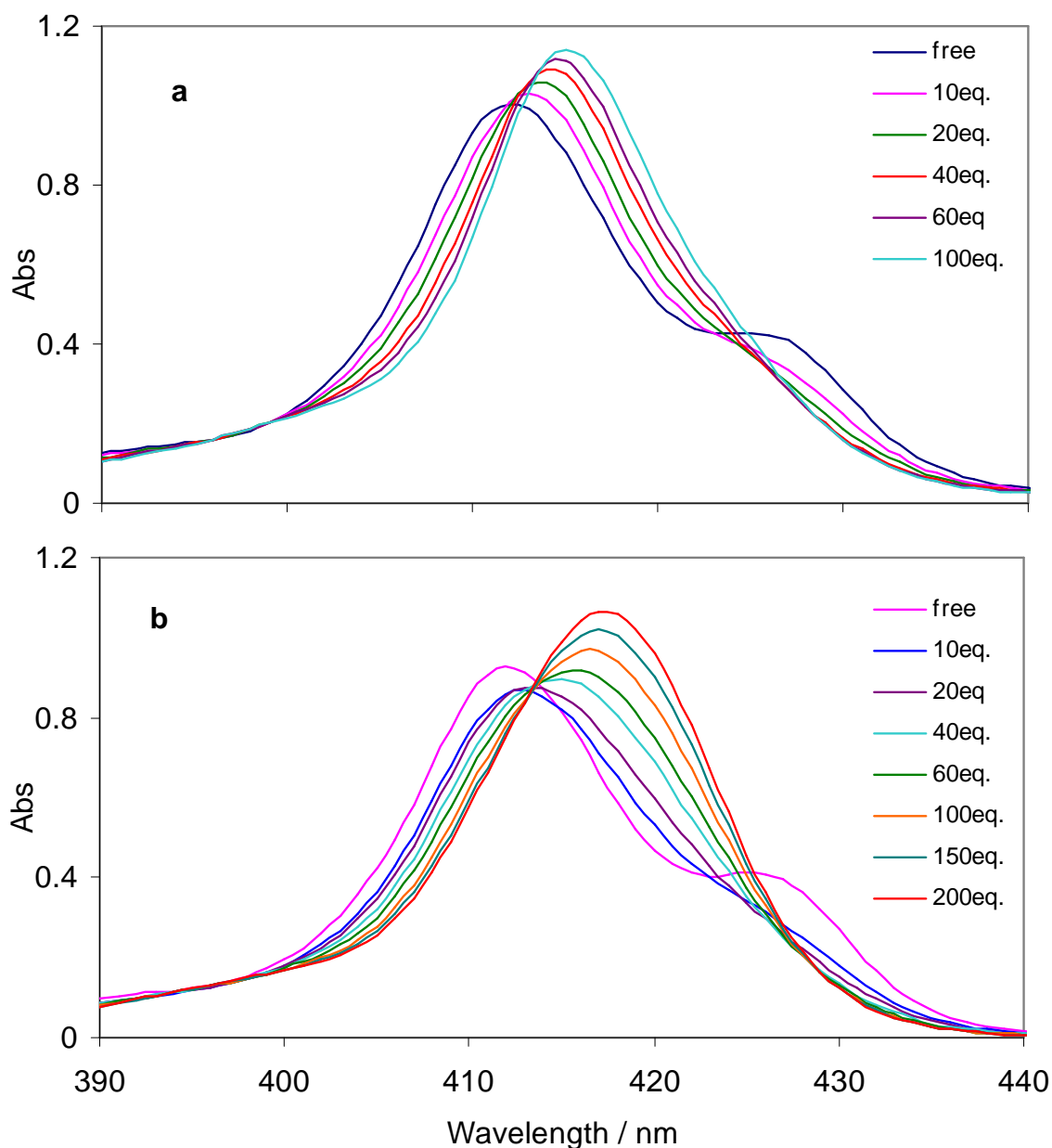


Figure V-4. UV-Vis spectra change upon titration of tweezer **II-25** (1 μ M in hexane) with **V-6** (graph **a**) and **V-11** (graph **b**) at different equivalents (only selected curves are shown for clarity).

Changing temperature did not solve this issue as similar complicated ECCD curves were still observed with diminished amplitude at higher temperature (25 $^{\circ}$ C, Figure

V-5a) or increased amplitude at lower temperature (-10 °C, Figure V-5b). In a different solvent such as methylcyclohexane, fairly poor CD signal was detected. More polar solvents (CH_2Cl_2 , CHCl_3) led to no ECCD as observed for other classes of chiral molecules studied previously.

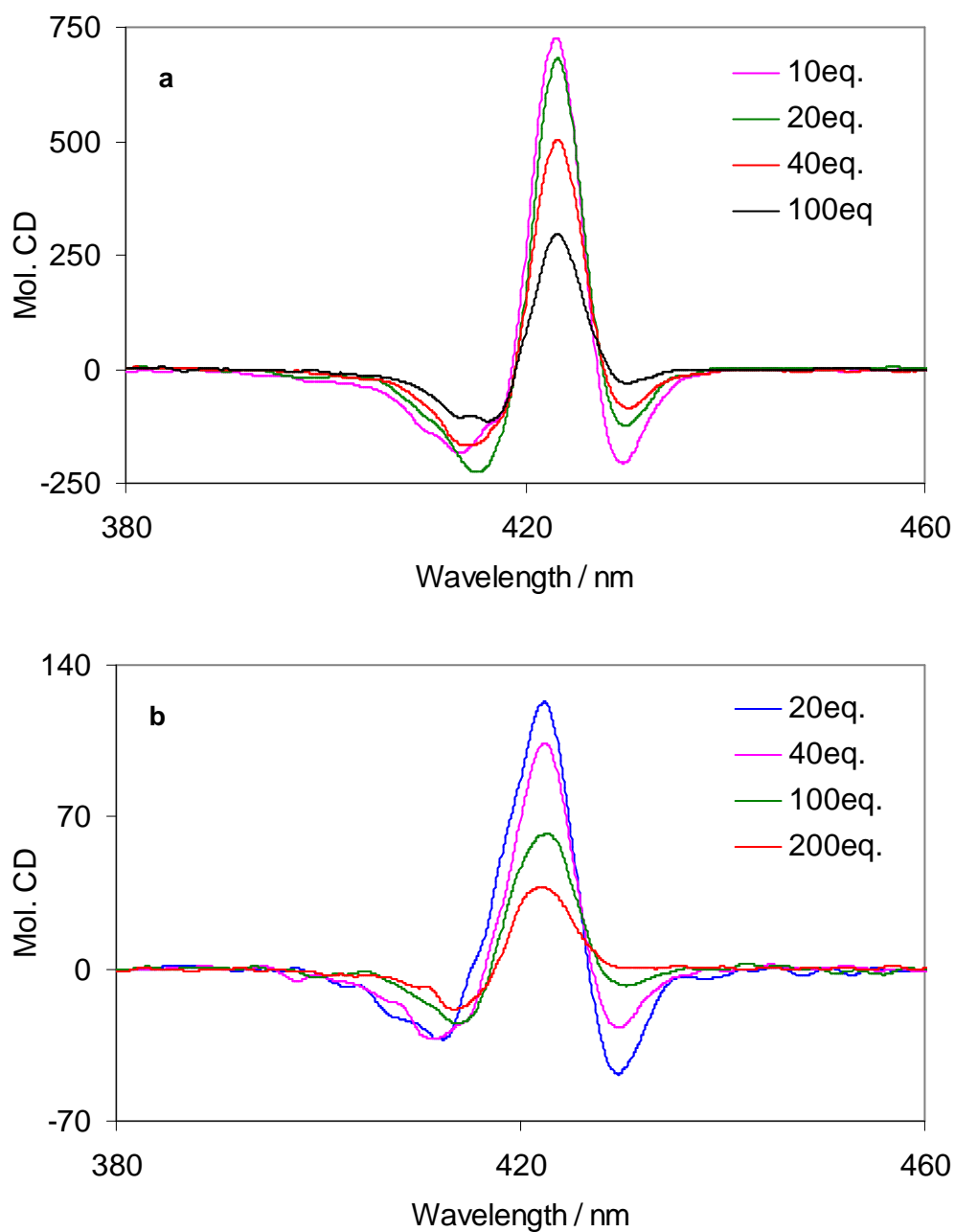


Figure V-5. ECCD spectra of tweezer **II-25** (2 μM in hexane) with 1,12-diol **V-11** at -10 °C (graph **a**) and 25 °C (graph **b**) at different equivalents.

V.2.2 ECCD study of 1,n-glycols using a reengineered tweezer

Reengineering of the porphyrin tweezer focused on minimizing ECCD silent conformations and enhancing the CD active alignment of two chromophores to obtain

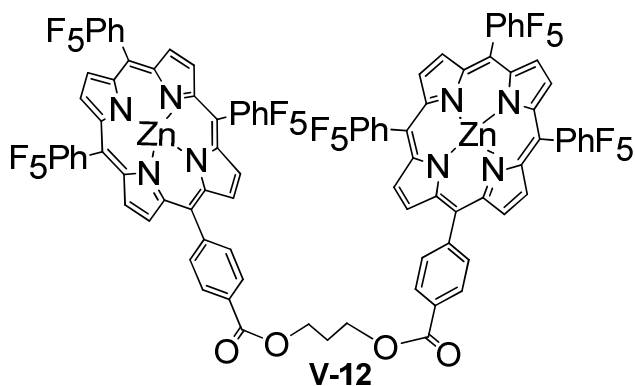


Figure V-6. Zn-TPFP porphyrin tweezer **V-12**.

consistent signals. We decided to keep the Zn-TPFP moiety since binding affinity was not an issue. The 1,5-pentylene linker was replaced by 1,3-propylene to reduce the conformations induced by the flexible linker while keeping appropriate elasticity for accommodation of a large chiral guest.

In Utaka's report²⁹ about a chiral porphyrin tweezer linked through a fairly rigid macrocyclic spacer (Figure V-7), he observed that binding of short chain terminal diamines (2-4 carbons) is detrimental for the ECCD active conformation and using guests with more than six carbons also diminishes the CD amplitude. Therefore, further

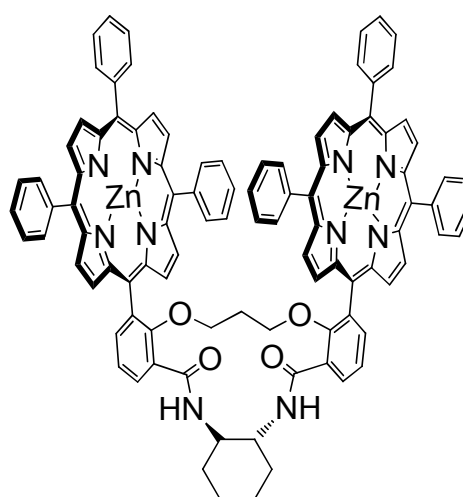


Figure V-7. Utaka's porphyrin tweezer.

rigidifying the linker was considered not beneficial since it might lead to selective recognition for guests only with certain chain lengths. This seemingly simple modification is crucial to accomplishing our goal. It was hypothesized that the resultant porphyrin tweezer **V-12** will prefer approaching long alkyl chain of the guest diol in a ‘side-on’ fashion from both sides instead of a ‘head-on’ fashion from both ends since the latter approach is not energetically favored with a shortened porphyrin linker especially for accommodating very long chain substrates. We believe this distinct binding mechanism would suppress the complications and yield consistent and predictable ECCD results.

Zn-TPFP tweezer **V-12** with the propylene linker was then synthesized ($\lambda_{\text{max}} = 415$ nm, $\epsilon = 670,000 \text{ cm}^{-1} \text{ M}^{-1}$ in hexane) following the similar procedures described for **II-25** in Chapter 2. Gratifyingly, it rendered surprisingly strong and consistent ECCD signals upon binding with diols (Table V-2). Complexation of tweezer **V-12** with 1,6-diol and 1,12-diol bearing *R,R*-configuration consistently yielded positive bisignate CD curves when 5–100 eq. of diol was added (Figure V-8, Figure V-9). 40 eq. was chosen as optimal amount of chiral guests for CD measurements with tweezer **V-12** since most substrates exhibited the strongest signals at this concentration. Due to low solubility of diol **V-13** (precipitation of diol was observed under standard CD experiment conditions), a mixed solvent (5% CH_2Cl_2 / hexane) at slightly elevated temperature (5 °C) was utilized. The relatively low CD amplitude of **V-13** is ascribed to competitive binding of CH_2Cl_2 solvent which is normal for this class of substrates (diols are ECCD silent with **V-12** in polar coordinating solvents such as

CH₂Cl₂, CHCl₃, CH₃CN, THF, and Et₂O). Notably, this tweezer also works well with non-symmetric diol **V-15** implying wide applicability of current method.

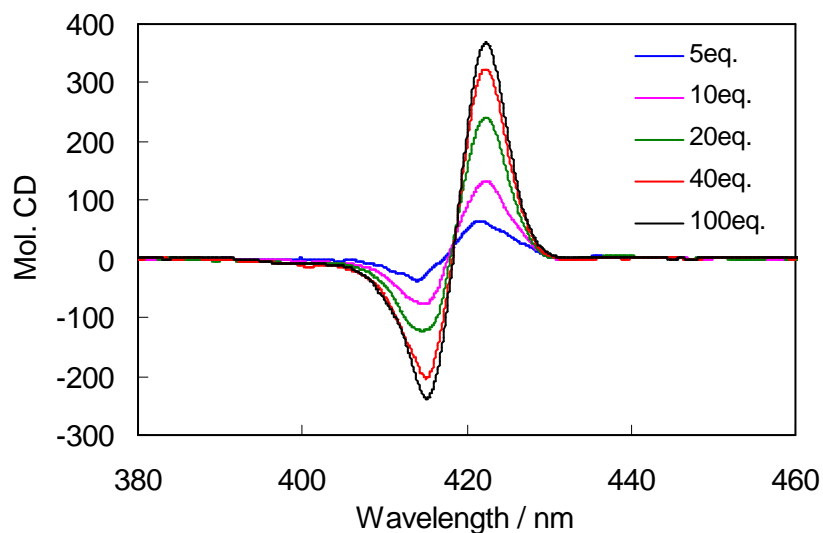


Figure V-8. CD titration for 1,6-diol with tweezer **V-12**; consistent positive signals were obtained at 5–100 eq. of **V-6**.

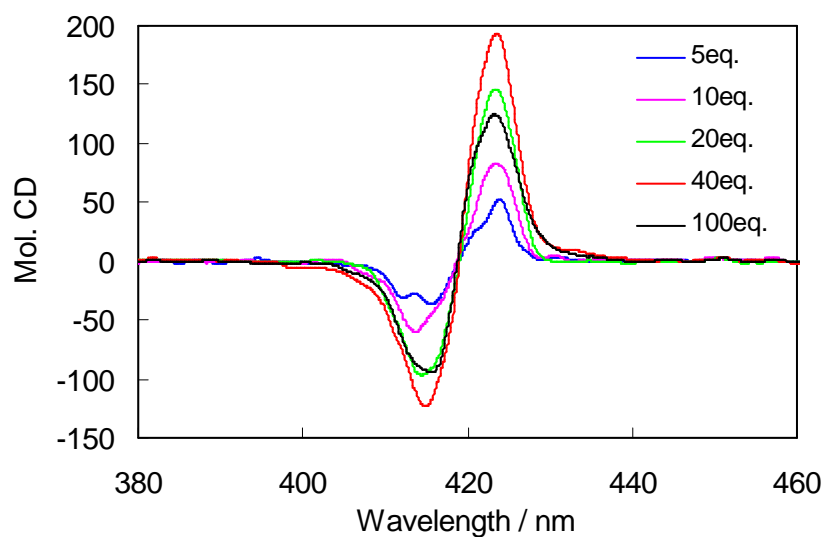


Figure V-9. CD titration for 1,12-diol with tweezer **V-12**; consistent positive signals were obtained at 5–100 eq. of **V-11**.

Table V-2. ECCD data of 1,n-glycols in hexane bound with tweezer **V-12**^a

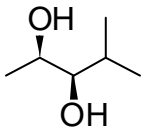
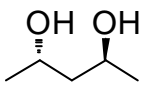
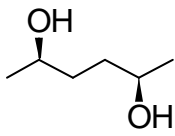
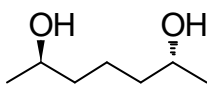
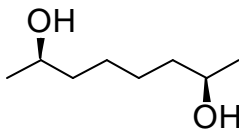
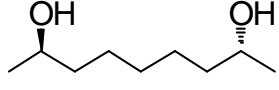
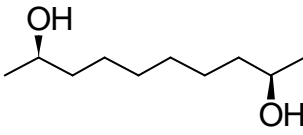
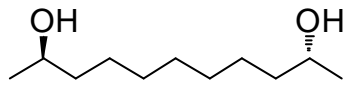
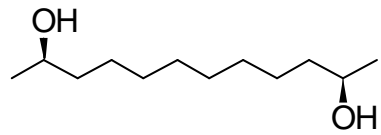
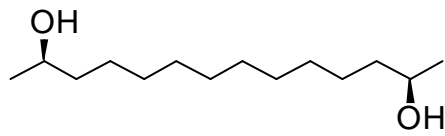
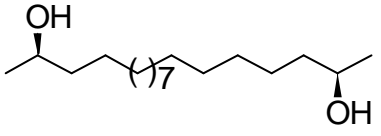
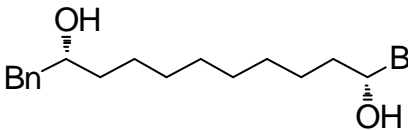
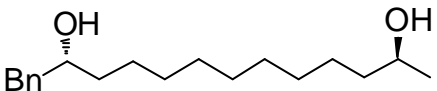
	1,n-Glycols	ECCD Sign	λ nm, ($\Delta\epsilon$)	A
III-15 ^b 2S,3S		<i>pos</i>	425 (+102) 413 (-77)	+179
V-3 2S,4S		<i>neg</i>	423 (-36) 412 (+37)	-73
V-4 2R,5R		<i>pos</i>	424 (+72) 414 (-66)	+138
V-5 2R,6R		<i>pos</i>	423 (+136) 414 (-100)	+236
V-6 2R,7R		<i>pos</i>	422 (+322) 415 (-203)	+525
V-7 2R,8R		<i>pos</i>	423 (+152) 414 (-142)	+294
V-8 2R,9R		<i>pos</i>	426 (+156) 416 (-197)	+353
V-9 2R,10R		<i>pos</i>	424 (+400) 415 (-351)	+751
V-10 2R,11R		<i>pos</i>	427 (+408) 416 (-326)	+734
V-11 2R,13R		<i>pos</i>	424 (+193) 415 (-123)	+316
V-13 2R,17R		<i>pos</i>	421 (+33) 414 (-22)	+55

Table V-2-continued. ECCD data of 1,n-glycols in hexane with tweezer **V-12**^a

	1,n-Glycols	ECCD Sign	λ nm, ($\Delta\epsilon$)	A
V-14 2S,11S		<i>neg</i>	427 (-97) 416 (+117)	-214
V-15 2R,13R		<i>neg</i>	423 (-76) 415 (+62)	-138

^a tweezer:substrate ratio - 1: 40, ^b tweezer:substrate ratio - 1: 100,

^c tweezer:substrate ratio - 1: 60 in 5% CH₂Cl₂ / hexane at 5 °C, 2.5 μ M tweezer concentration at 0 °C was used for all measurements unless otherwise

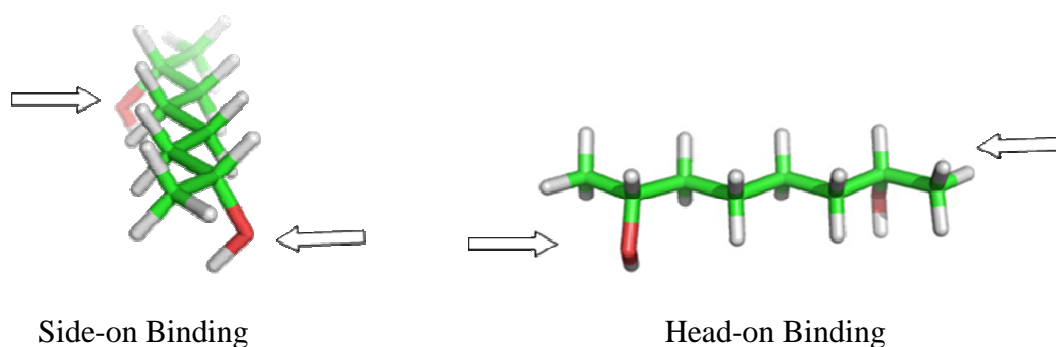


Figure V-10. Side-on binding and head-on binding models.

As shown in Table V-2, fairly high ECCD amplitudes were generally observed for long chain diols. Diols **V-9** and **V-10** exhibited much stronger ECCD signals than their shorter analogs **2-9**. This is straightforward evidence pointing to ‘side-on’ approach (Figure V-10) since in ‘head-on’ binding conformation (Figure V-10) one would expect CD signals to deteriorate dramatically while binding with long chain substrates due to larger interchromophoric distance and consequent weaker interaction of electronic transition dipole moments within porphyrins. Compared to ‘head-on’

binding, the ‘side-on’ approach would consistently ensure a shorter interplanar distance of chromophores as well as stronger interactions between the electronic transitions within the two porphyrin chromophores which explains the unusually strong ECCD signals observed for substrates containing long alkyl chains.

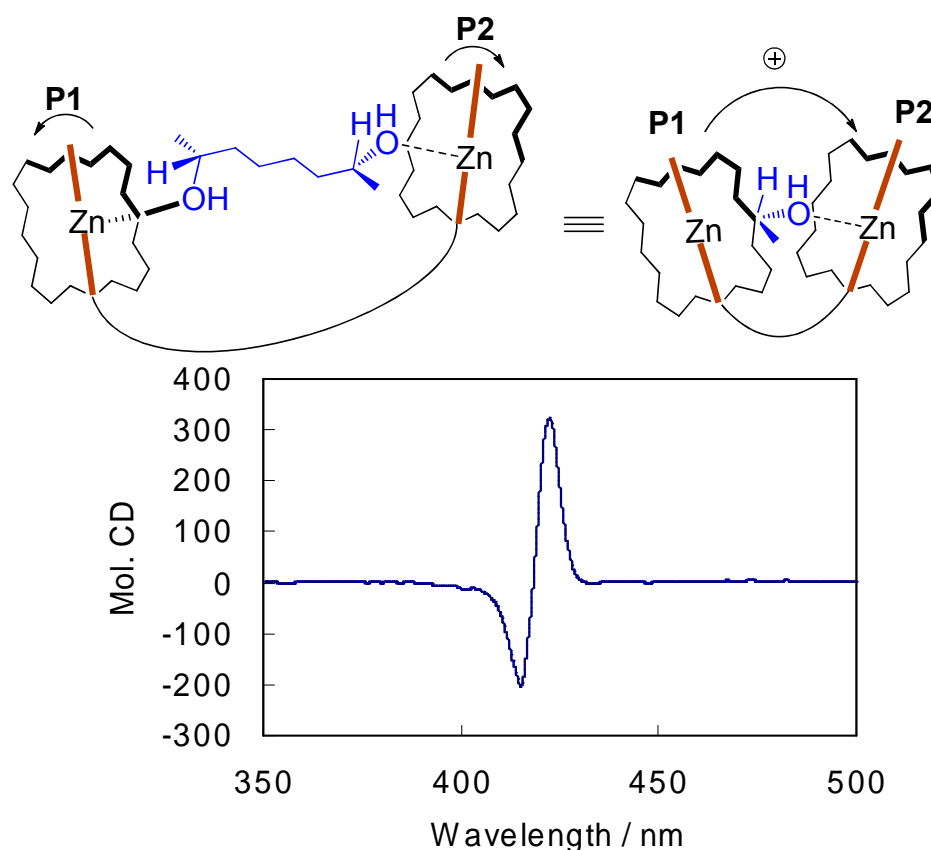


Figure V-11. Proposed complexation pattern for 1,n-diols ($n = \text{even}$) with tweezer **V-12**; Positive ECCD was obtained for **V-6**.

The correlation between diol chirality and the sign of ECCD is illustrated in Figure V-11. Binding interactions invariably occur between the two chiral hydroxyl groups and the metallo centers of porphyrins. It is assumed that *both porphyrins approach the two hydroxyl groups opposite to the largest substituent* (methyl group in this case). As a result, the methyl group is *anti* to the bound porphyrins and is not

involved in the steric differentiation process. The remaining two substituents on the chiral carbon (H and alkyl chain) would be the steric discriminants facing the bulky porphyrin. Therefore, the conformation of the long alkyl chain is important for elucidating the stereodifferentiation mechanism.

Straight chain mono alcohols are known to prefer *trans* all staggered conformations.³⁰

This conformation should also be favored in long chain diols as shown in Figure V-12. To

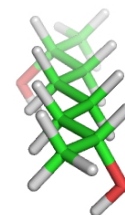


Figure V-12. *trans* –all staggered conformation of **V-6**.

confirm this conformational preference, single crystals of diol **V-11** was grown by slowly

evaporating the CH₃Cl / hexane solvent. To our great delight, high quality single crystals were obtained. This is a bit surprising since such flexible acyclic molecules usually tend to form layered flakes and is hard to afford crystal with good quality. The subsequent X-ray diffraction analysis revealed another surprising result. The diol **V-11** keeps a *trans* all staggered conformation with a well-aligned straight skeleton (Figure V-13). We believe that two intermolecular H-bonds of each OH group in the unit cell account for the surprisingly well-aligned conformation for such a flexible long chain molecule. This finding supports our hypothesis that when strong complexation (H-bonding or metal-ligand coordination) exists the flexible molecular skeleton could be rigidified and aligned to minimize the number of conformations thus facilitating CD measurements.

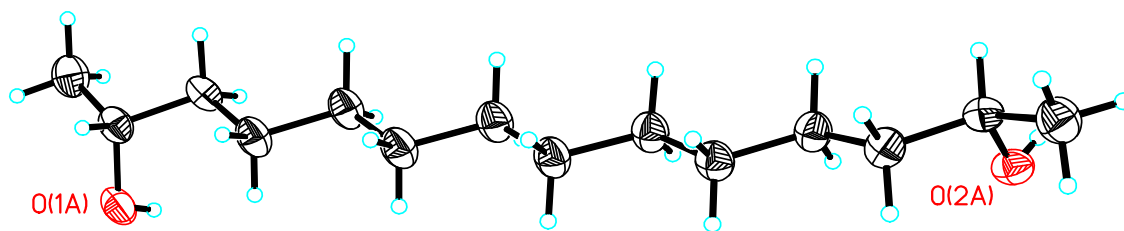


Figure V-13. Crystal structure of 1,12-diol **V-11**.

For diols with even number of carbons, the *trans* all staggered conformation combined with the proposed complexation pattern would position the two porphyrins (**P1**, **P2**) *anti* to each other as shown in Figure V-11. Consequently, **P1** would rotate counterclockwise toward the smaller H atom away from the larger alkyl chain and similarly **P2** would rotate clockwise to minimize the steric repulsion with the bulky alkyl chain. Overall, a clockwise (positive) helicity of **P1** relative to **P2** is generated for *R,R* diols leading to positive ECCD spectrum which is indeed observed.

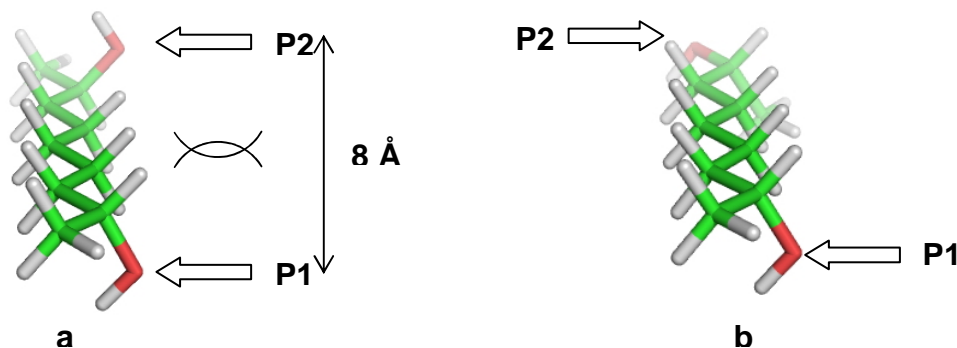


Figure V-14. *trans* all staggered conformations of 1,7-diol **V-7**.

For diols with odd number of carbons, the most stable *trans* all staggered conformation of the diol (Figure V-14 graph **a**) would lead to steric clash of bulky **P1** and **P2** when they approach the OH groups in a manner *anti* to the terminal methyl groups since they would have to approach from the same side of the diol alkyl chain. A simple comparison of molecular sizes of the host and guest could provide straightforward insight about this issue. The linear distance between OH groups in

1,7-diol (**V-7**) is 8 Å (Figure V-14, measured in PC SpartanPro) and the diameter of a monomeric TFPF porphyrin is 18 Å (Figure V-15, measured in PC Spartan). Consequently, when **P1** binds one of the two OH groups in **V-7**, it will completely block one side of the diol preventing the complexation of the incoming **P2** from the same side due to steric crash between two huge porphyrins. However, we did observe a very strong ECCD signal ($A = + 367$) of substrate **V-7** indicating the formation of stable ECCD active complex through ditopic binding between OH groups and zinc porphyrin tweezer. As such, we proposed that the second most stable *trans* all staggered conformation was preferred (Figure V-14 graph **b**) under CD experiment conditions. In this conformation, **P1** and **P2** porphyrins could approach and bind OH groups from opposite sides of diols chain effectively avoiding the crash of bulky porphyrins. Consequently, a stable complex is formed with short interplanar distance accounting for the observed strong ECCD.

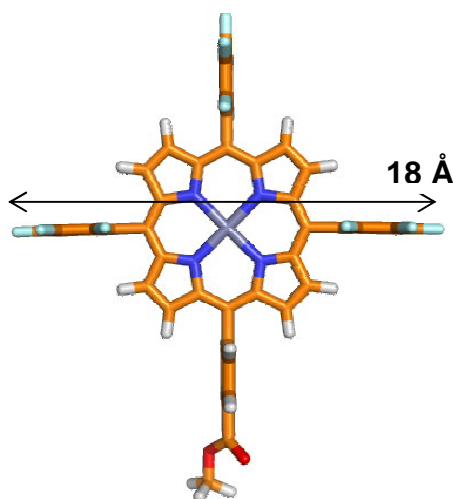


Figure V-15. 3D structure of zinc TFPF porphyrin monoester.

To confirm the preference of this proposed conformation, X-ray analysis was also conducted by growing and analyzing single crystal of 1,9-diol **V-9** (Figure V-16).

We were glad to see that both conformations shown in Figure V-14 were observed in a single unit cell with equal population thus suggesting that the *anti* diol conformation is energetically accessible. Again, the long alkyl chain was well-aligned as a straight chain with the help of intermolecular H-bonds. According to this observation, it is reasonable to propose that in solution the odd-numbered diols could adopt the second most stable *trans* all staggered conformation (Figure V-14 graph **b**) while binding with the bulky porphyrin tweezer.

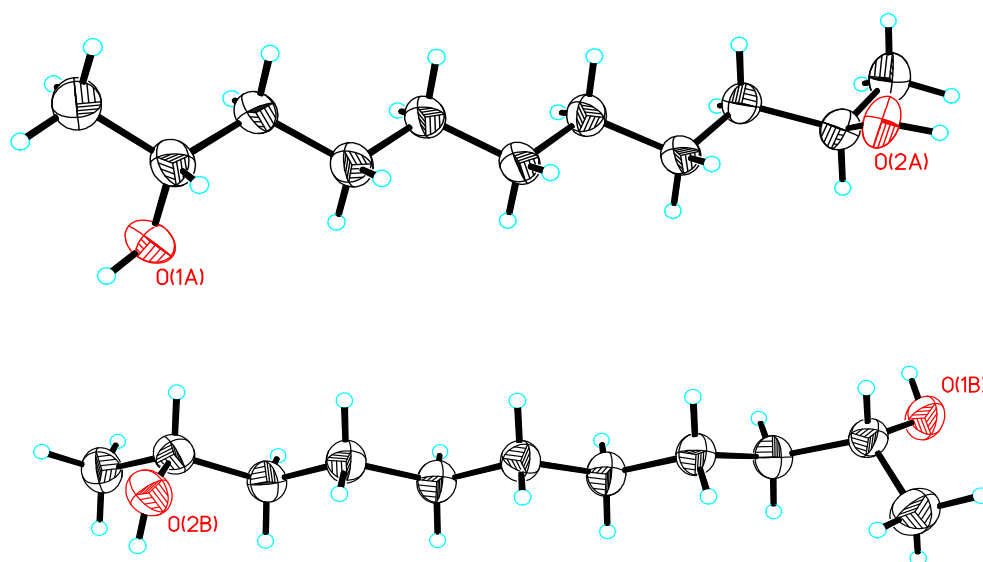


Figure V-16. Crystal structures of 1,9-diol **V-9** (two conformations present in one asymmetric unit cell resemble the conformations of diol **V-7** in Figure V-14).

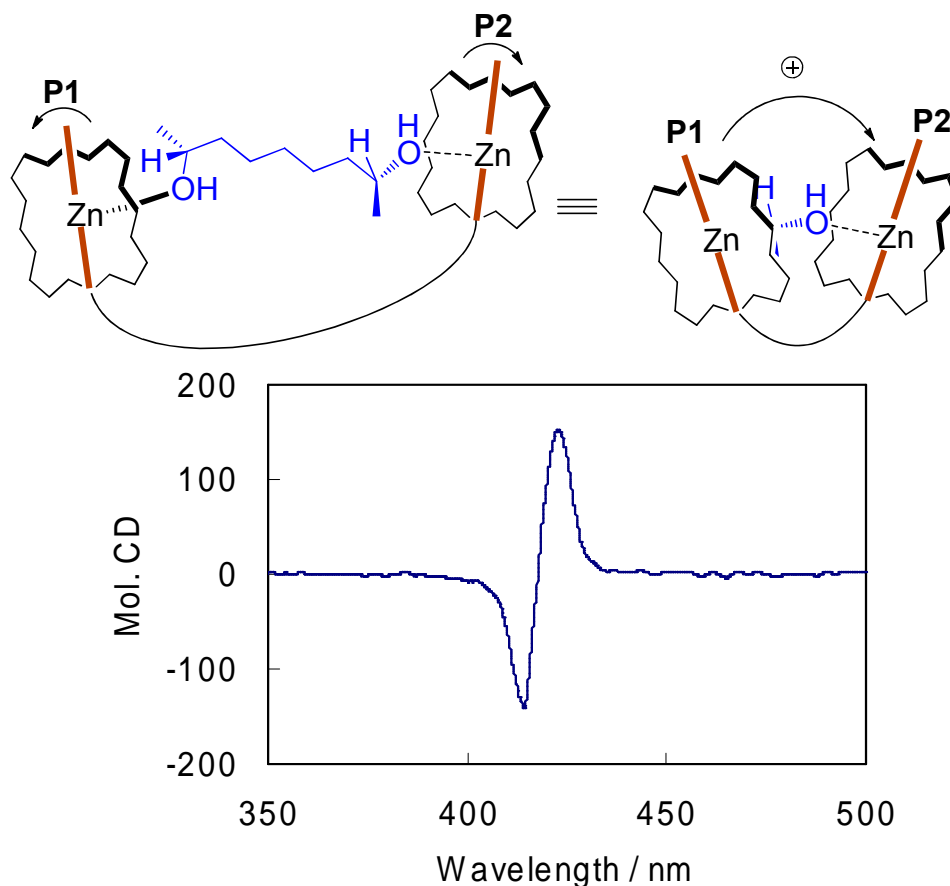


Figure V-17. Proposed complexation for 1,*n*-diols (*n* = odd) with tweezer **V-12**; Positive ECCD was obtained for **V-7**.

Based on the above discussion, in the diol-tweezer complex **P1** and **P2** are still *anti* to each other avoiding steric clash as depicted in Figure V-17. Steric differentiation experienced by **P1** between the H atom and the alkyl chain drives this porphyrin to rotate counterclockwise toward the smaller H atom. Similarly, clockwise rotation of **P2** is expected. Thus, a positive helical arrangement of porphyrins is produced for *R,R* substrates; this is verified by experimental results in Table V-2. Since **P1** and **P2** rotate opposite to each other, each stereocenter would reinforce the same overall helicity of bound tweezer.

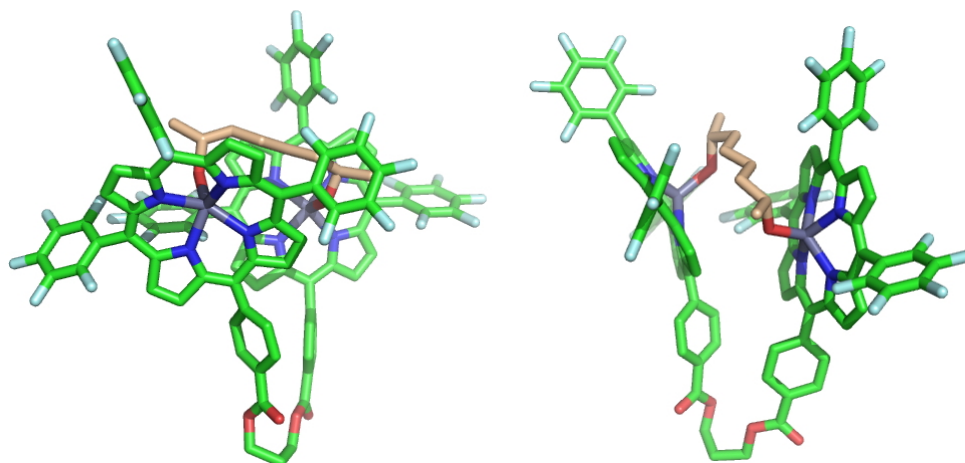


Figure V-18. Front view (left) and side view (right) of the 1,6-diol-tweezer **V-12** complex (hydrogen atoms were omitted for clarity).

These rationales were substantiated by conformational search at molecular mechanics level which showed a clear preference for positive helicity for the *R,R* supramolecular assembly among the low energy conformers examined. Conformational search also unambiguously revealed the slipped cofacial geometry of porphyrin tweezer (Figure V-18 ~ V-20). The conformations of diols revealed in the minimized structures agreed well with proposed *trans*- all staggered conformations

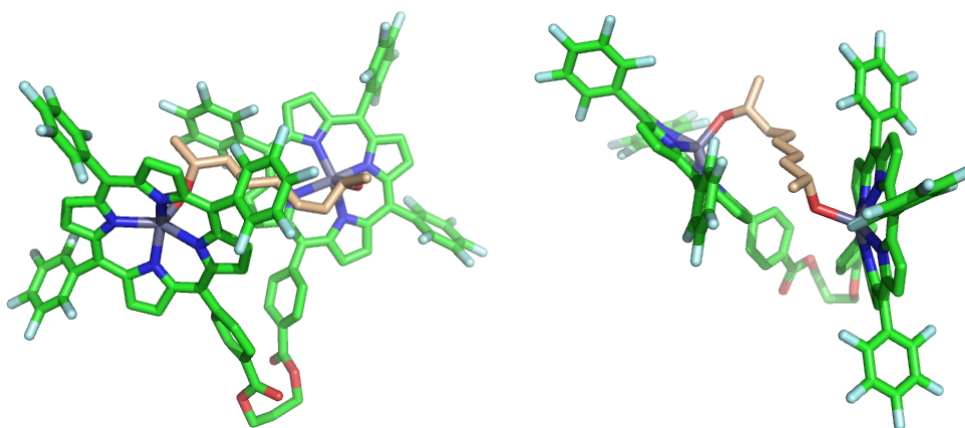


Figure V-19. Front view (left) and side view (right) of the 1,7-diol-tweezer **V-12** complex (hydrogen atoms were omitted for clarity).

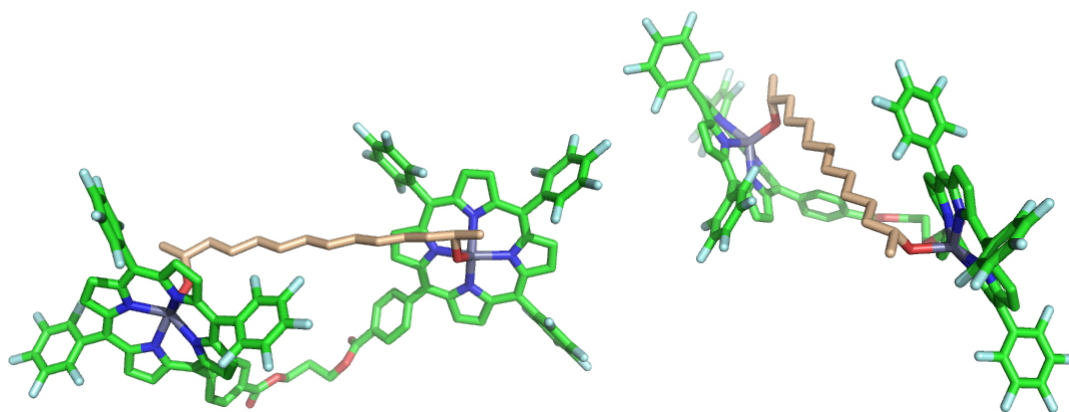


Figure V-20. Front view (left) and side view (right) of the 1,12-diol-tweezer **V-12** complex (hydrogen atoms were omitted for clarity).

and the crystal structures. The center-to-center distance (Zn1-Zn2) of the tweezer host increased accordingly with the increase of diol chain length (ca. 7 Å in **V-12** / **V-6** complex and 16 Å in **V-12** / **V-11** complex). However, the interplanar distance changed only slightly while extending the guest molecular skeleton (ca. 6 Å in **V-12** / **V-6** complex and 7 Å in **V-12** / **V-11** complex) which is in line with the unusually strong CD signals primarily due to intimate chromophoric interaction in side-on binding process. The independence of CD amplitudes on substrate chain length is of particular importance since most bischromophoric derivation methods inevitably suffer from significant dependence of CD signal strength on distance between chiral centers which limits application in long range stereochemical determination.

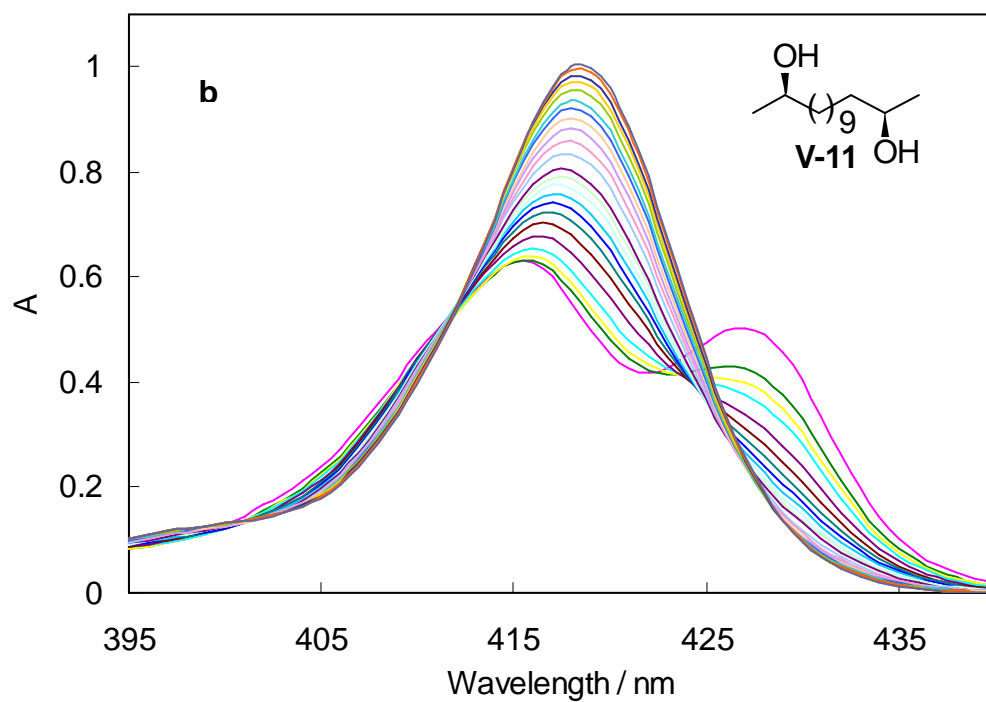
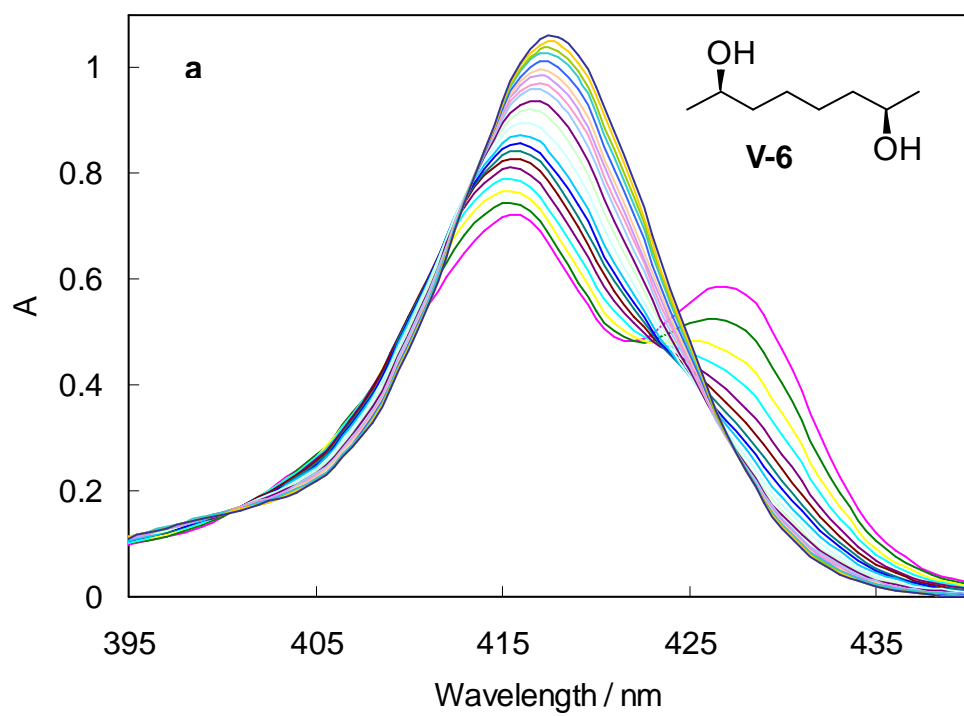


Figure V-21. UV-Vis spectra change upon titration of tweezer **V-12** (1 μM in hexane) with **V-6** (10 mM in DCM, graph **a**) and **V-11** (10 mM in DCM, graph **b**).

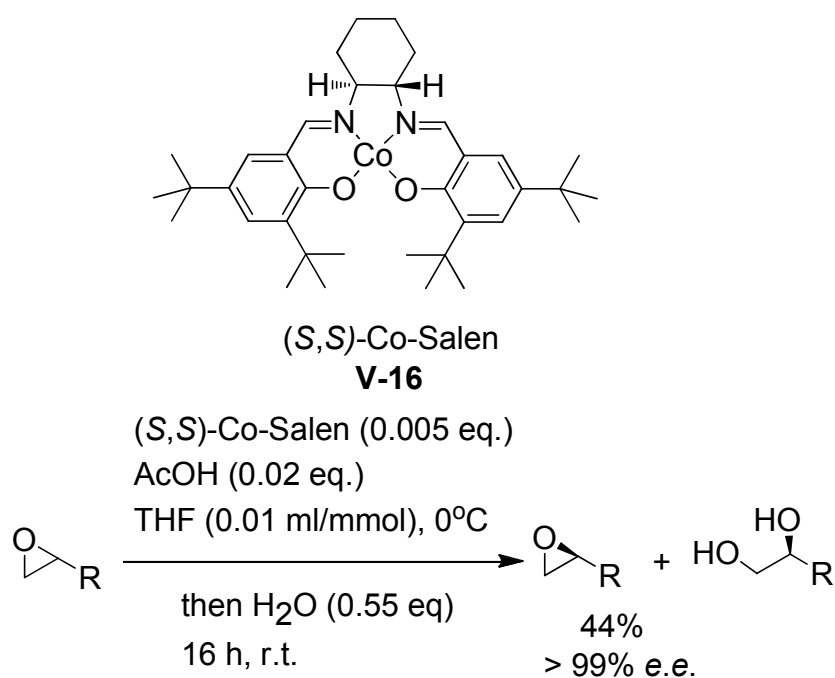
UV-vis profile of complexed tweezer **V-12** with diols further validated the unique side-on approach. It has been recognized that the shift of λ_{max} for zinc porphyrin tweezer complex is the outcome of two opposing effects;^{24, 31} the bathochromic shift resulting from donor-acceptor interaction and hypsochromic shift when the two chromophores are brought close by guest molecules upon coordination. The nucleophilicity of diol homologues **V-3~V-11** is similar, so is the strength of donor-acceptor interaction. Therefore, red-shifts of λ_{max} would reflect the distance between two porphyrin chromophores. UV-vis titration of tweezer **V-12** with 1,6-diol in hexane revealed a small redshift (2.4 nm) of λ_{max} of porphyrin Soret band (Figure V-21a). Extending the diol chain to 1,12 diol only led to slight increase of λ_{max} shift (3 nm redshift, Figure V-21b). Similar UV experiments of these two diols with tweezer **II-25** revealed much larger redshifts, 4.7 nm and 6 nm respectively. The binding constants for diol-tweezer **V-12** derived from UV-vis-titration experiments are very close ($3.37 \times 10^3 \text{ M}^{-1}$ for 1,6-diol and $3.69 \times 10^3 \text{ M}^{-1}$ for 1,12-diol), suggestive of similar strength of donor-accepter interactions. Most importantly, the significantly smaller bathochromic shifts of λ_{max} with tweezer **V-12** and their nearly negligible difference ($\Delta\lambda_{\text{max}} = 0.6 \text{ nm}$) suggests small interchromophoric distance and its insensitivity towards increase of diol chain length are in accordance with the observed strong CD signals and the molecular modeling results that point to the side-on complexation pattern. The large redshifts with tweezer **II-12** is not induced by the slightly longer linker since the tweezer bearing 9 methylene linker rendered similar red-shifts (5.4 nm for **V-6** and 6.7 nm for **V-11**) as

II-12 in UV titrations. This tweezer also encountered the same problems as **1** during ECCD study of diol **V-6** and **V-11**. In an earlier report on the complexation of terminal (1,2- to 1,12-) diamines with zinc TPP tweezer bearing 1,5-pentylene linker, Huang et.al. observed 6.9 nm redshift of porphyrin Soret band while binding with 1,6-hexanediamine and 9.2 nm redshift with 1,12-dodecanediamine. These diamines proved to bind tweezer in a head-on manner since ^1H NMR analysis of diamine/tweezer complex manifested *parallel no-offset disposition* of two porphyrin rings which did not allow side-on binding.³² As a result, the red-shift of porphyrin Soret band is a rigorous measurement of chain length of complexed diamines. The red-shift values are larger compared to those of diols due to much stronger donor-acceptor interaction. But the difference of these two redshifts ($\Delta\lambda_{\text{max}} = 2.3$ nm) is comparable to 1.3 nm difference observed for two diols bound with tweezer **II-25** indicating the preference of the latter for head-on binding. The similar ^1H NMR analysis is not suitable for our tweezer system since Zn-TPFP tweezer **V-12**-diol complex is not ECCD active at NMR concentrations and aggregates significantly, hence structural information obtained from NMR cannot represent the true ECCD active conformation at μM concentration (see section III.2.4 for details). All these arguments are consistent with our scenarios above. We are certain that this distinct binding mechanism would enable the determination of absolute configurations for even longer chain diols.

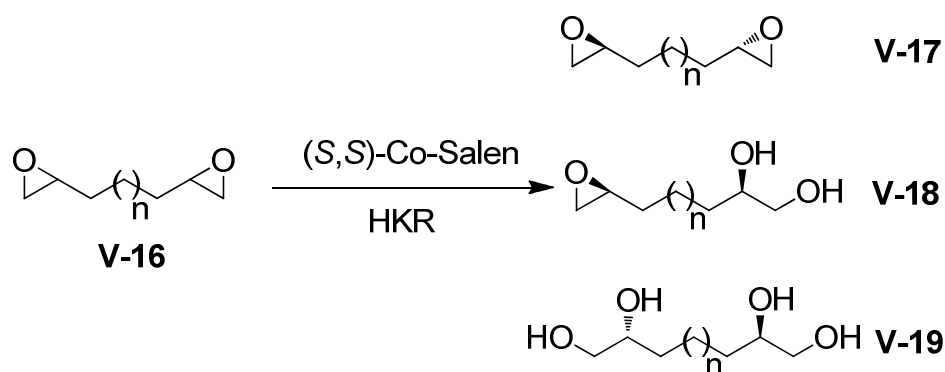
In conclusion, we established a new supramolecular host system with unique chirality recognition process which could serve as a rapid, reliable and highly

sensitive chirality sensor for 1,n-glycols using ECCD protocol over remarkably long atomic distances (19 Å for diol **V-13**). To the best of our knowledge, this is the first general method addressing the absolute stereochemical determination of acyclic 1,n-glycols with varying chain lengths in a nonempirical way. The current study also significantly bettered our understanding of the chirality recognition process involving porphyrin tweezers and provided important guidelines for developing new chirality sensors. Further application of this method in complex diol molecules has revealed promising results and deserve continuous attention.

V.3 Synthesis of chiral 1,n-glycols

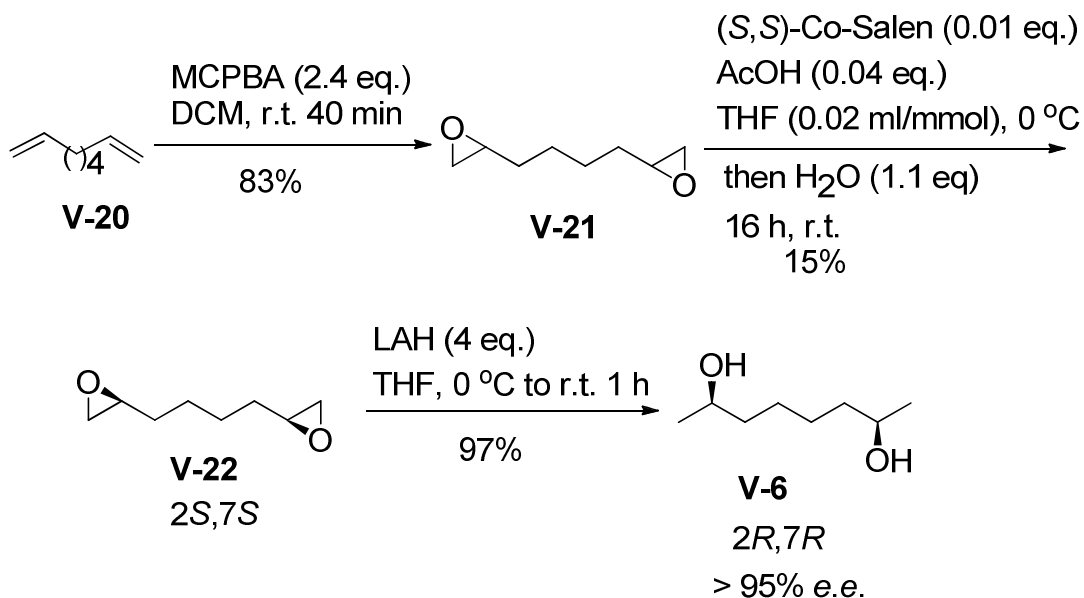


Scheme V-1. Jacobsen hydrolytic kinetic resolution (HKR).



Scheme V-2. Jacobsen hydrolytic kinetic resolution (HKR) for bisepoxides.

A rapid approach to chiral 1,n-glycols is through regioselective ring opening of chiral bisepoxides, which can be prepared by Jacobsen hydrolytic kinetic resolution (HKR).^{26, 28} As shown in Scheme V-1, HKR provides rapid access to chiral terminal diols or epoxides from racemic epoxides. This method is extremely efficient in terms of yield, enantiomeric purity, and turn-over number. This reaction is easily scalable and the chiral salen catalyst can be recovered without losing activity.

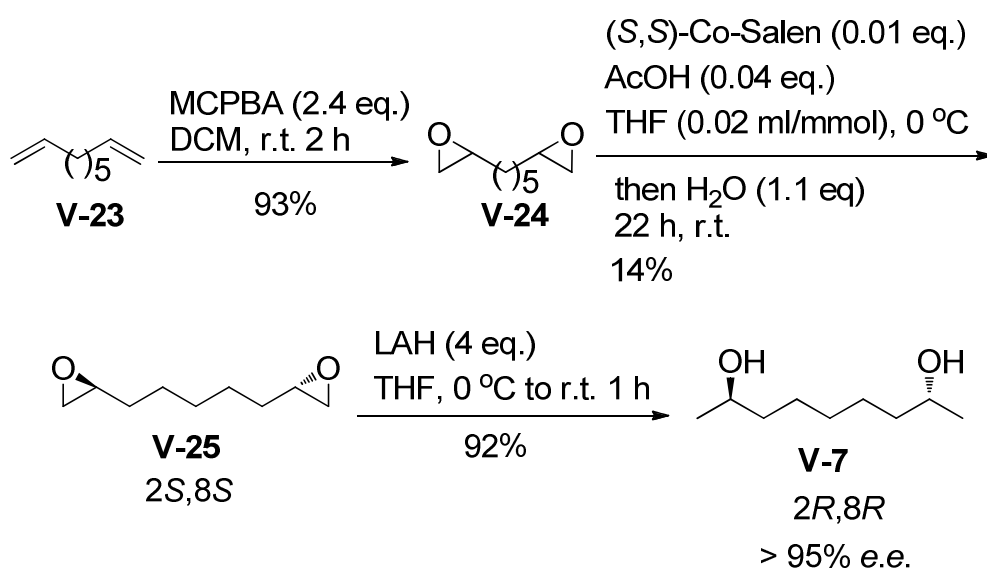


Scheme V-3. The example for synthesis of even-numbered chiral diol V-6.

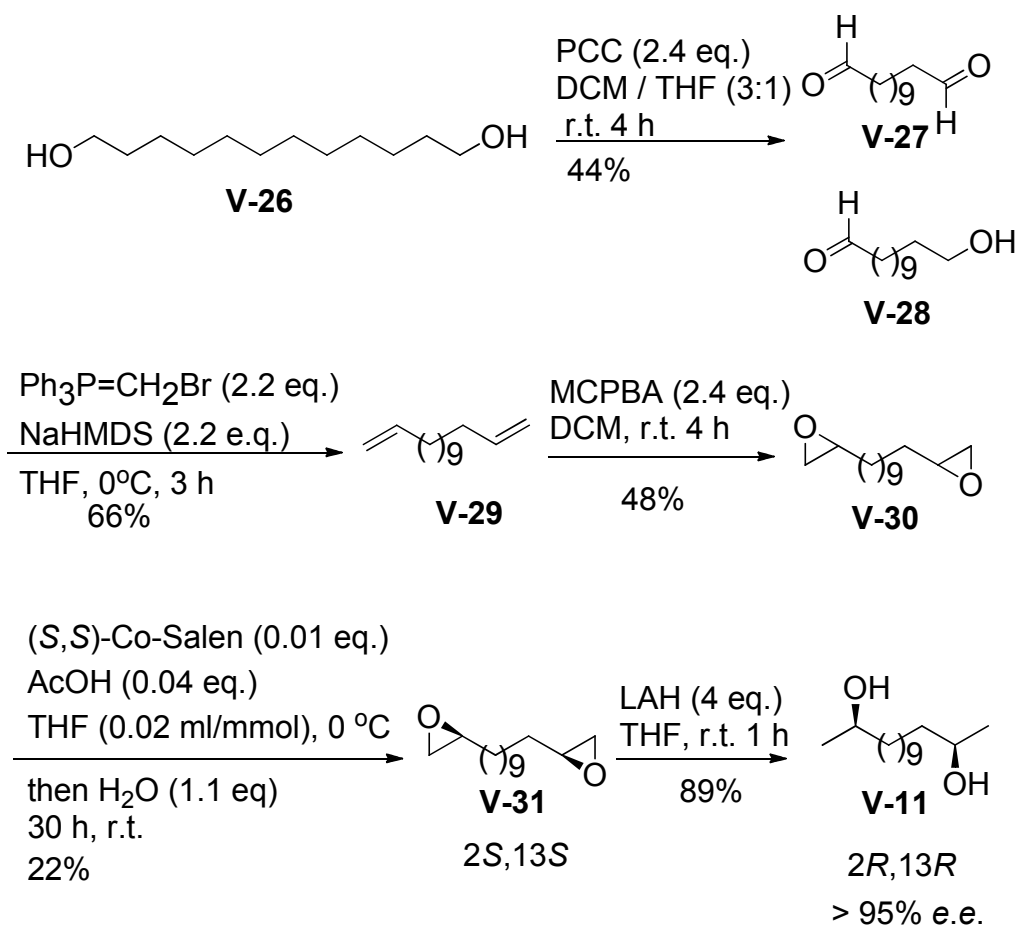
To obtain chiral bisepoxides, we can simply run the HKR of racemic bisepoxides while doubling the amount of chiral catalyst, AcOH and H₂O (Scheme V-2).^{27, 33} In

theory, three products can be produced and they are readily separated by column chromatography. Following this procedure, both even-numbered diols (Scheme V-3) and odd-numbered diols (Scheme V-4) can be made from commercially available terminal dienes with decent yields and very good selectivity. One should note that the maximum yield for HKR of bisepoxide is 25%. ^1H NMR analysis of *R*-MPA esters of ring opened diols afforded the optical purity (usually higher than 95% e.e.) of kinetically resolved chiral bisepoxide as well as the diols.

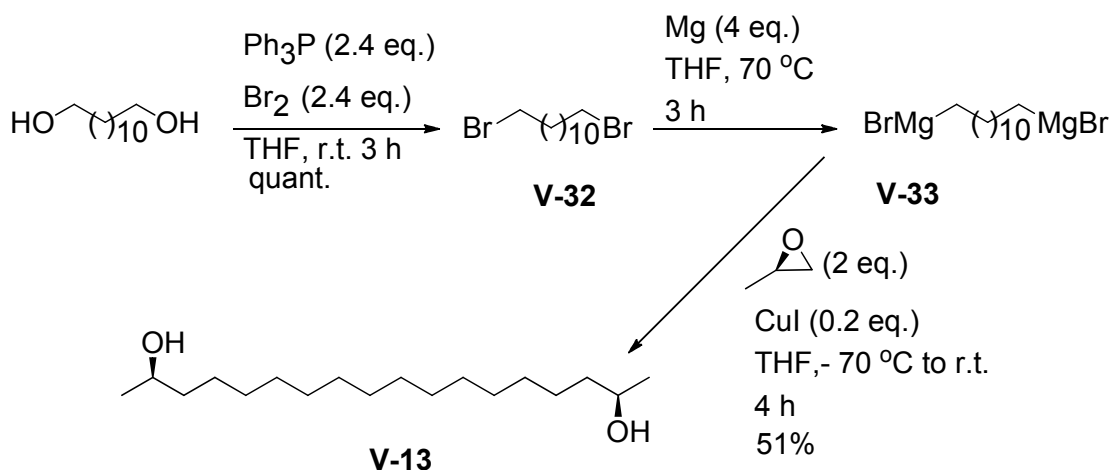
Long chain terminal dienes which are not available were synthesized from PCC oxidation of terminal diols followed by Wittig olefination (Scheme V-5). The conversion of terminal diol into terminal dialdehyde via PCC oxidation suffered from low yield especially for long chain substrate due to poor solubility of diol. Mixed solvent ($\text{CH}_2\text{Cl}_2/\text{THF}$) has to be used to increase solubility and get acceptable yield. Complete conversion is difficult to achieve even under extended reaction time (10 h). Monoaldehyde and a small amount of starting material were always obtained.



Scheme V-4. The example for synthesis of odd-numbered chiral diol **V-7**



Scheme V-5. Synthesis of long chain chiral diol **V-11**.

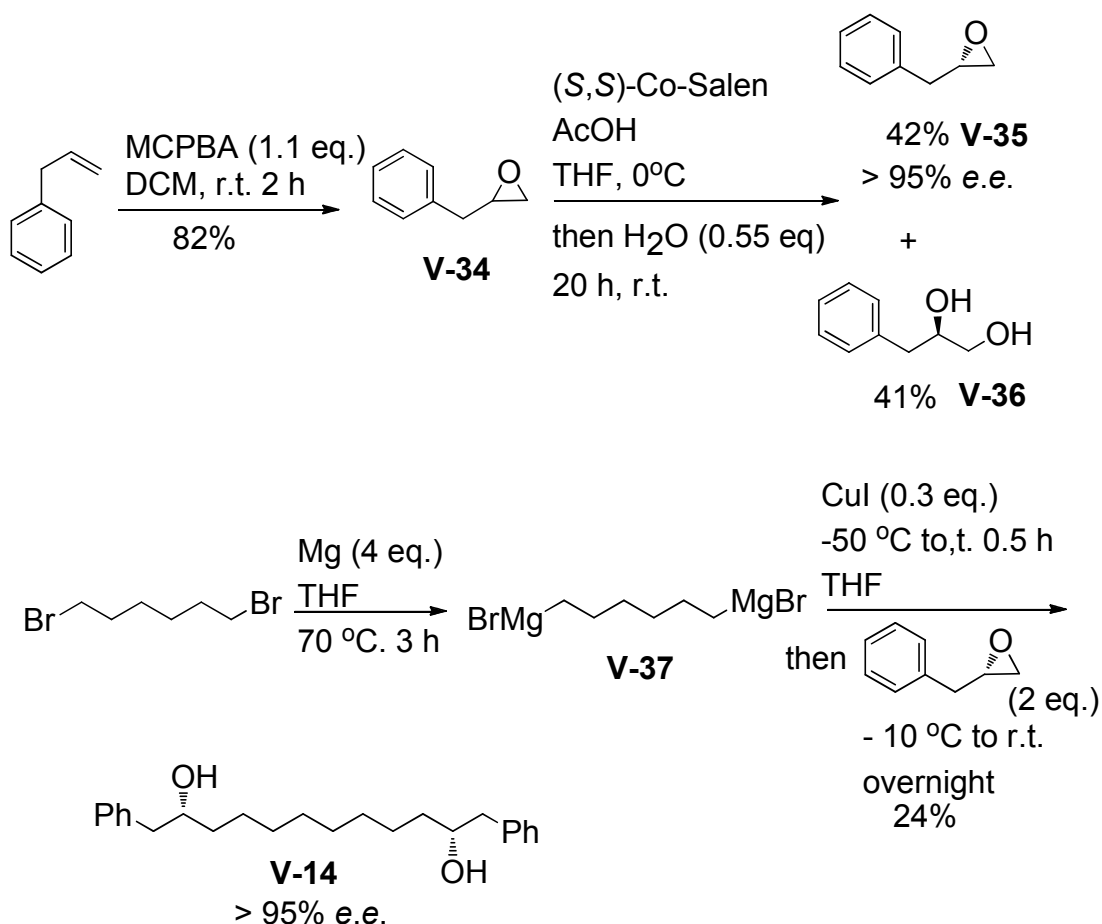


Scheme V-6. Synthesis of long chain chiral diol **V-11** using bis-Grignard reagent.

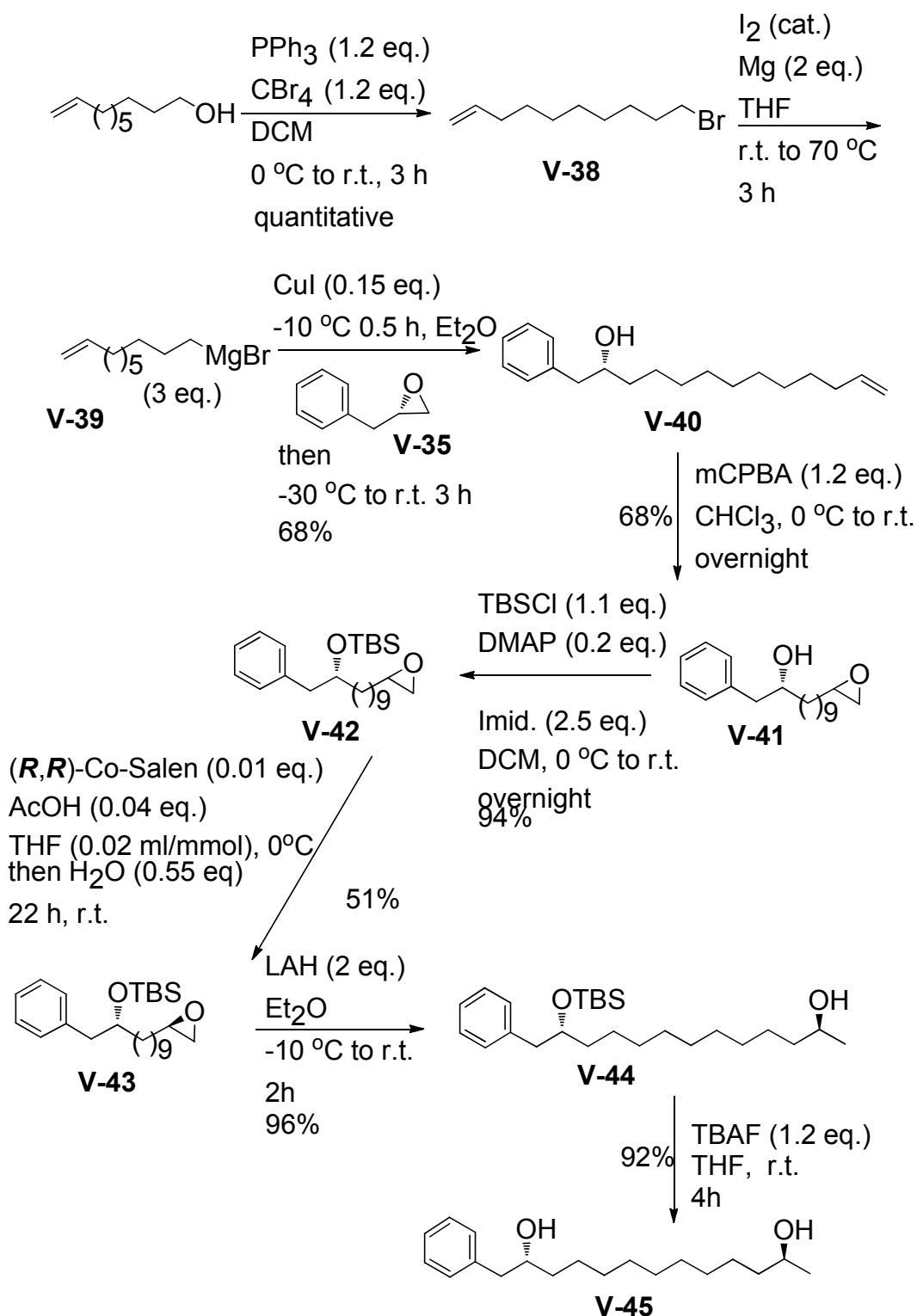
An important reason we pursued the bisepoxide approach is that the chiral bisepoxide presumably can be opened by organometallic species like Grignard or

cuprate reagents leading to a variety of chiral diols with different terminal alkyl groups. However, a couple of attempts to open the bisepoxide with Grignard reagents (vinyl magnesium bromide, phenyl magnesium bromide, cyclohexyl magnesium chloride) with and without CuI did not yield satisfactory results. A mixture was obtained containing ring opening product by MgBr_2 .

An alternative way to prepare the desired chiral diols is through ring opening of chiral monoepoxide with bis-Grignard reagent. As illustrated in Scheme V-6, 1,12-dibromododecane can be obtained in quantitative yield. Following Grignard formation and ring opening of 2*R*-propyleneoxide afforded chiral 1,12-diol with good overall yield and optical purity.



Scheme V-7. Synthesis of long chain chiral diol **V-14** using bis-Grignard reagent.



Scheme V-8. Synthesis of long chain chiral diol **V-11**.

Chiral epoxide **V-35** was then prepared through HKR and underwent nucleophilic ring opening by **V-37** to yield 1,10-diol **V-14** (Scheme V-7). Clearly, employing this

approach we can quickly access chiral diols with different terminal alkyl groups. The procedures described above (Scheme V-4~Scheme V-7) are suitable for rapidly making diols with the same terminal alkyl groups. To further demonstrate the efficiency of our newly developed porphyrin tweezer **V-12**, diols with different terminal alkyl groups were also synthesized though in theory we were confident that the new tweezer should function equally well with these substrates.

As depicted in Scheme V-8, ring opening of chiral epoxide **V-35** by freshly prepared Grignard reagent **V-39** and HKR of newly formed epoxide **V-42** introduced the desired two chiral centers. This white solid **V-45** exhibited prominent ECCD couplet upon complexation with Zn-TPFP tweezer **V-12** in hexane at 0 °C confirming the efficiency of the new chirality sensor.

V.4 A case study of chirality sensing using tweezer **V-12**

Recently, Curran and coworkers reported the stereochemical determination of diol moiety (C3 and C14) in natural product Petrocortyne A (Figure V-22).³⁴ They synthesized a mixture of all four isomers with different fluororous tags, and separated each isomer in its pure form using fluororous HPLC. By analyzing the ¹H NMR of corresponding Mosher esters and comparing the optical rotations, Curran confirmed that the absolute configuration (3*R*,14*S*, **V-46**) proposed by Jung³⁵ was correct. This immediately drew our attention since this natural product containing two chiral OH groups separated by 12 carbons can be a good candidate to test our porphyrin tweezer system.

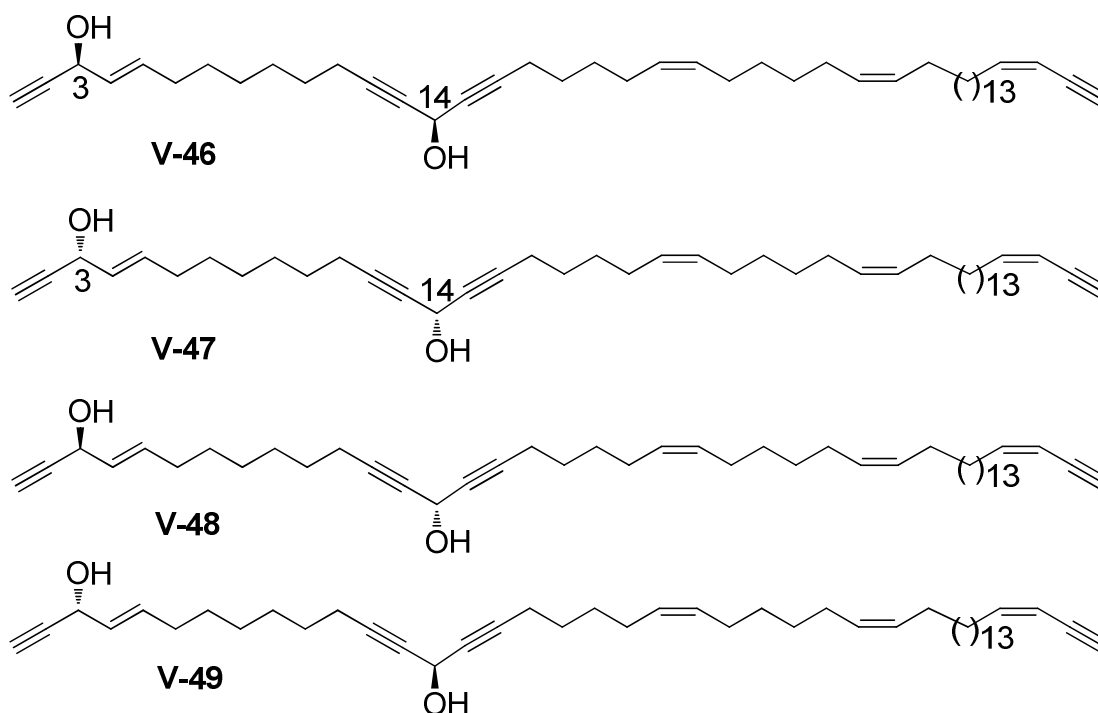
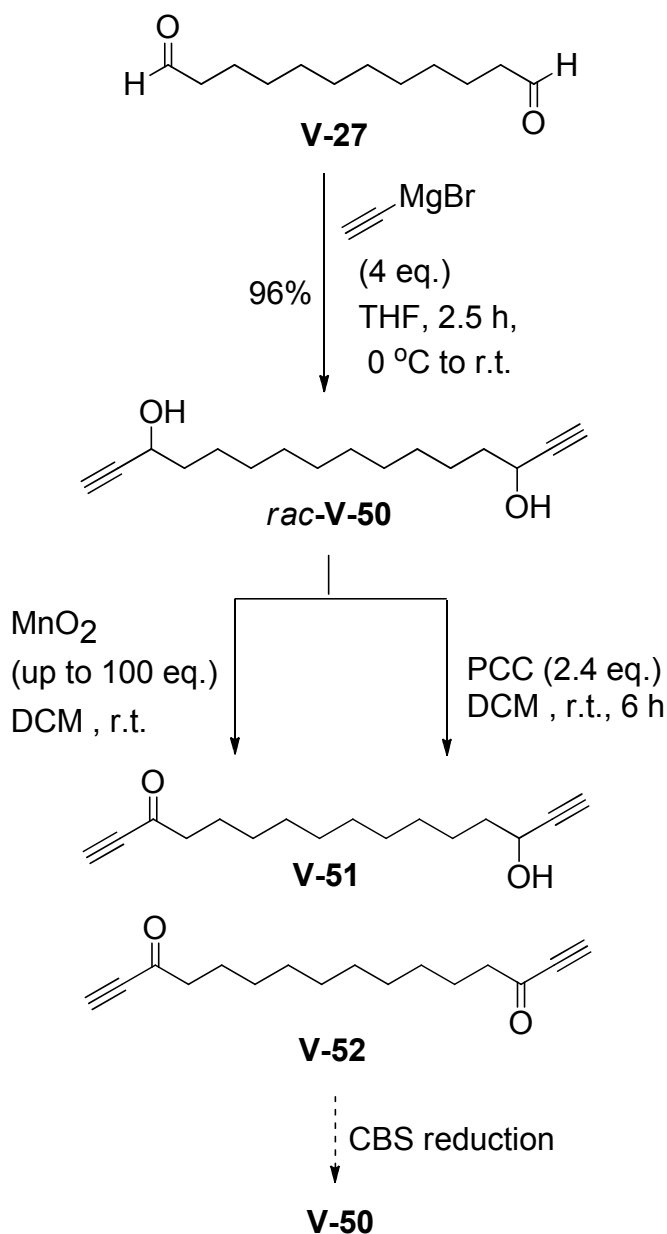


Figure V-22. Petrocortyne A and its isomers.

Professor Curran kindly provided two of the four isomers, around 1 mg each with unlabeled stereochemistry. We quickly ran the ECCD measurements of both samples with Zn-TPFP tweezer **V-12** in hexane. Initial runs revealed weak negative ECCD spectra for both substrates when over 40 eq. of diol was employed indicating that one of the isomers might be **V47**. However, upon scrutiny of the ECCD measurements, we observed an interesting *dynamic* behavior of ECCD signals for both substrates. At certain ratios of substrate versus tweezer, a bisignate CD couplet could be observed. However, the CD couplet was not stable and it would change shape or even disappeared after some time. A steady and consistent ECCD signal was not obtained. Thus, we could not draw a definite conclusion about the absolute configurations of the two samples simply based on overall negative ECCD signals.

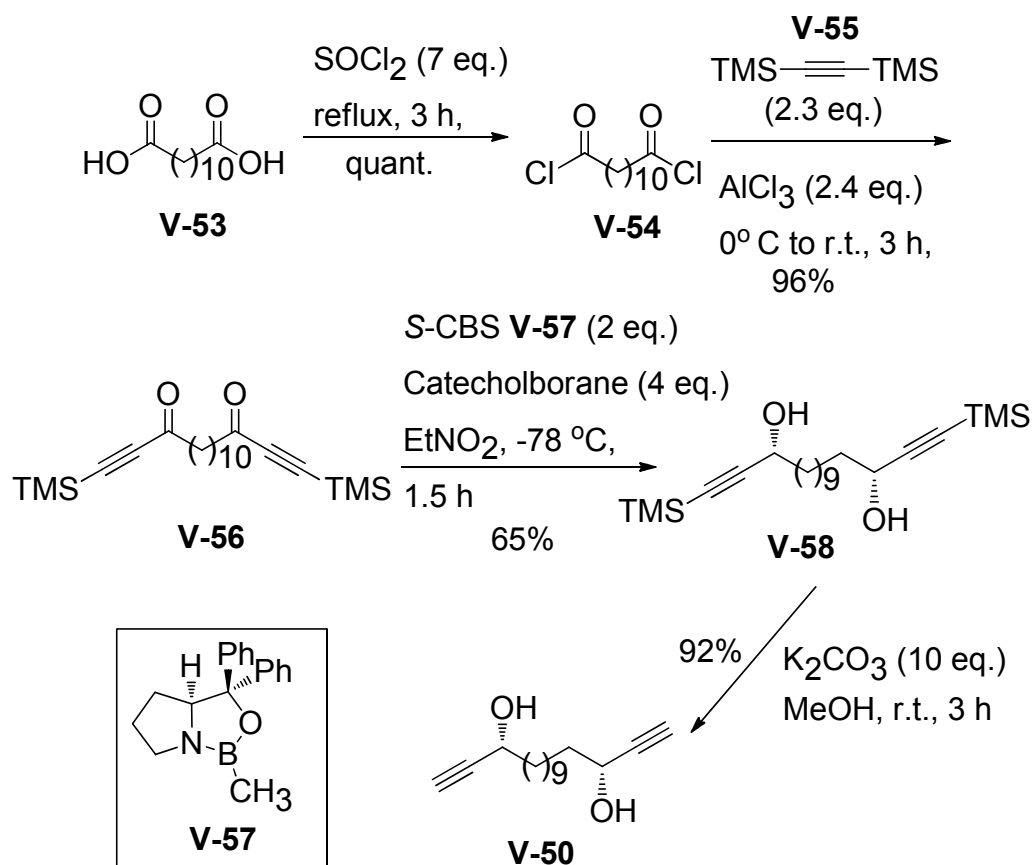


Scheme V-9. Synthesis of bis-ynone **V-52** from oxidation.

We speculated that this dynamic behavior was due to the bulkiness of the extremely long side-chain or the weak nucleophilicity of OH groups at double-propargylic position. Considering the minute amount of these samples, direct elaboration of the big molecules is not advised. To figure out the possible cause, the synthesis of a simplified model compound **V-50** or its enantiomer was planned. As shown in

Scheme V-9 the synthesis of racemic 1,12-diol went smoothly but the subsequent oxidation ran into problems and only a small amount of desired bis-ynone **V-52** was observed on TLC along with a large amount of mono-ynone **V-51** and starting material. The isolated yield of **V-52** was low, thus a different route (Scheme V-10) was undertaken.

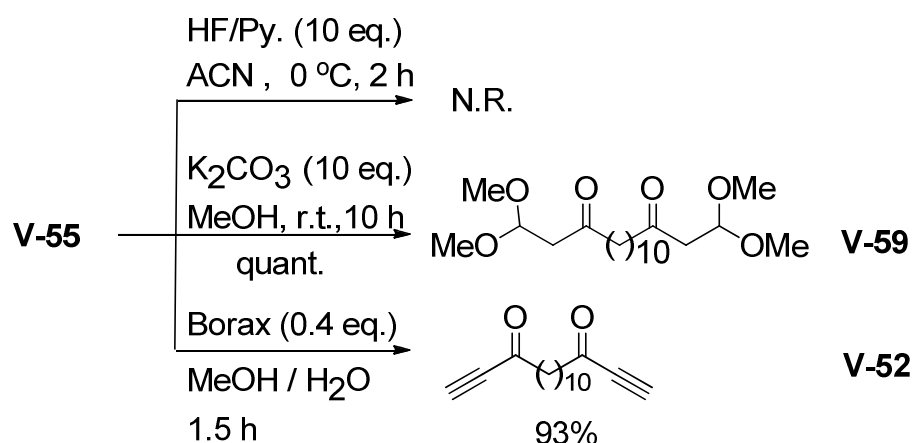
The dicarboxylic acid **V-53** was converted into acyl chloride **V-54** followed by Friedel-Crafts acylation with bisTMS acetylene to afford bis-ynone **V-56** with excellent overall yield. Direct asymmetric reduction of the bis-ynone using (*S*)-CBS reagent in CH_3NO_2 and subsequent desilylation yielded diol **V-50**. The absolute configuration of diol **V-58** was assigned based on the empirical observation of similar CBS reduction of TMS acetylene substituted ynones.^{36, 37} The ECCD study of diol



Scheme V-10. Synthesis of diol **V-50**.

V-58 and **V-50** rendered weak negative CD couplets for both cases at 40 eq. or 100 eq. but again with dynamic behavior. At same equivalent of chiral diol, the negative CD couplet disappeared and appeared again randomly. Unfortunately, the enantiomeric purity of diol **V-50** was low based on ^1H NMR analysis of bis-MPA ester due to the poor selectivity of CBS reduction. Literature search revealed that the presence of terminal silyl group within ynone could make the CBS reduction tricky.³⁶ Therefore, removal of TMS group from **V-58** before CBS reduction was attempted (Scheme V-11).

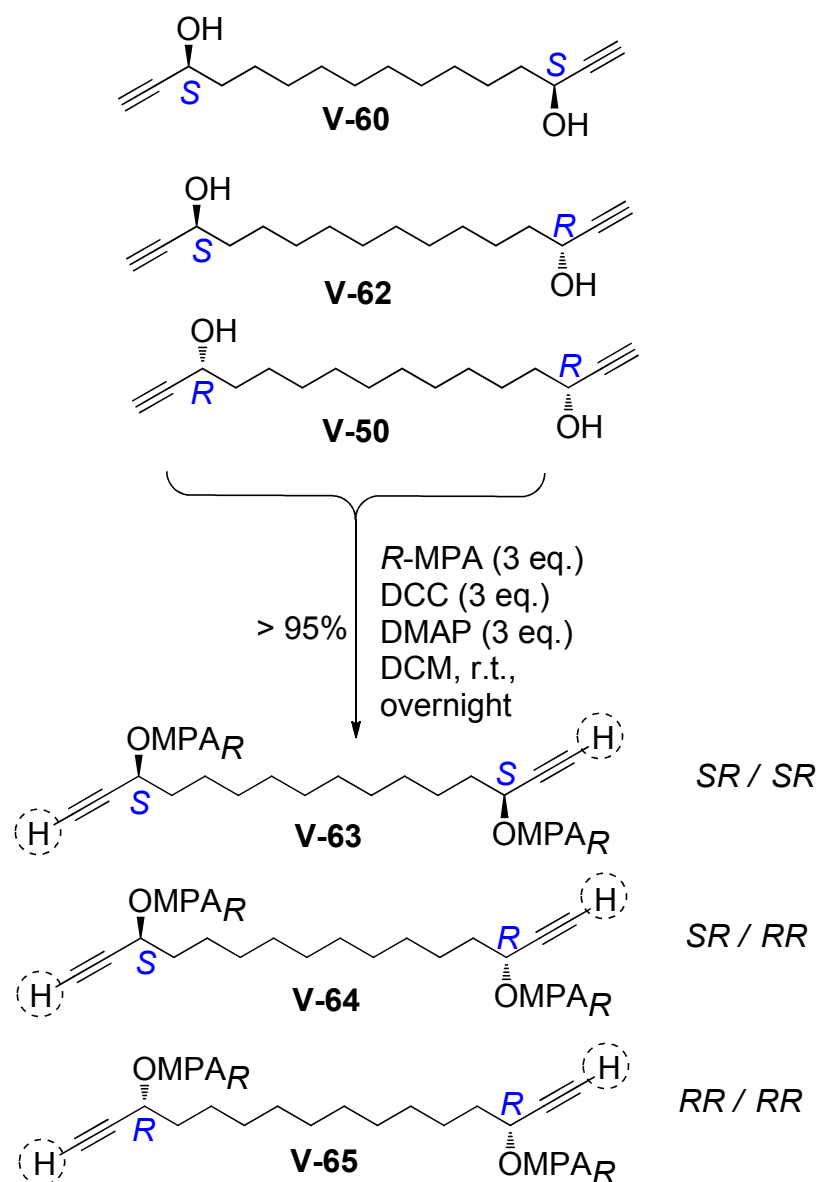
HF / pyridine proved to be inefficient and the commonly used K_2CO_3 / MeOH combination generated an interesting product **V-59** in quantitative yield by double



Scheme V-11. Synthesis of bis-ynone **V-52**.

Michael addition of ynone with MeOH. Catalytic amount of Borax in MeOH and H_2O proved to be efficient in removing the TMS groups. Ynone **V-52** acquired this way was submitted to CBS reduction (Scheme V-12). EtNO_2 was still chosen as solvent since it demonstrated surprisingly acceleration effect in CBS reduction of ynones and allenyl ketones compared to commonly used toluene and DCM and also afforded improved enantioselectivity.³⁸ The reduced diol **V-60** has improved optical

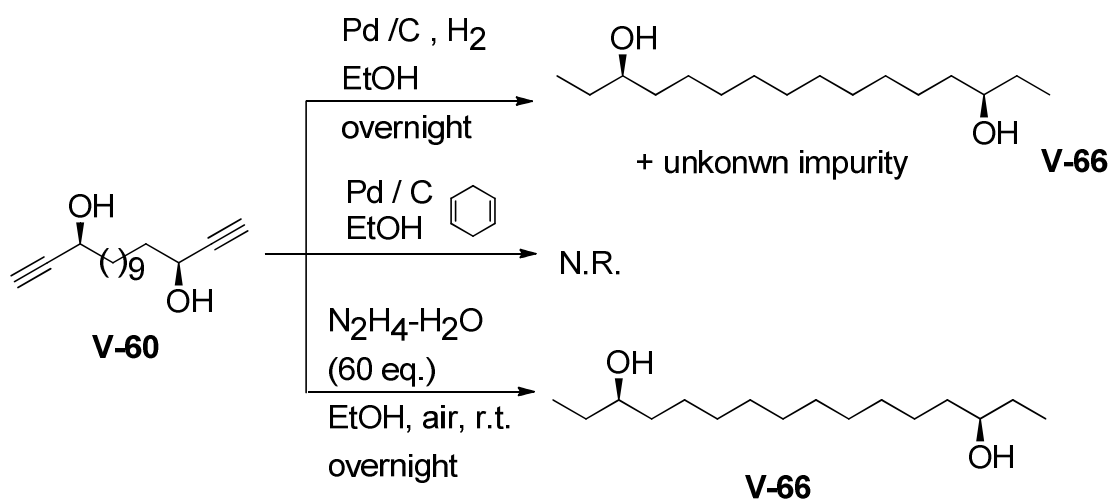
was indeed observed in the *R*-MPA ester of race-**V-50**. The possible presence of *meso*-diol **V-62** does not affect this ratio. Therefore, the ratio of H_{SR} vs. H_{RR} can be used for analyzing the optical purity of this type of chiral diols.



Scheme V-14. Determination of optical purity for bis-ynol.

ECCD study of diol **V-60** revealed a dynamic spectrum as a stable ECCD signal was difficult to be attained. Since sterics is not an issue in this case, this finding supported our concern that the weak nucleophilicity of propargylic alcohol may result

in weak binding between diol and zinc tweezer generating unstable host-guest complex and yielding dynamic ECCD spectra. To finally confirm this concern, we decided to hydrogenate diol **V-60** converting it into saturated diol **V-66** (Scheme V-15). With increased nucleophilicity of hydroxyl groups, diol **V-66** supposed to exhibited stable and consistent ECCD signals during CD titration of tweezer at varying equivalents. Typical hydrogenation procedure (Pd / C / H₂) afforded desired diol contaminated with unknown impurity which was hard to be removed by column chromatography. Since we were looking for a procedure that could be also applied to the reduction of Petracortyne A isomers, we needed a procedure that could cleanly reduce the acetylene moiety without the need of drastic purification steps considering the minute amount of sample available. The transhydrogenation did not afford any product.



Scheme V-15. Reduction of bisynol **V-60**.

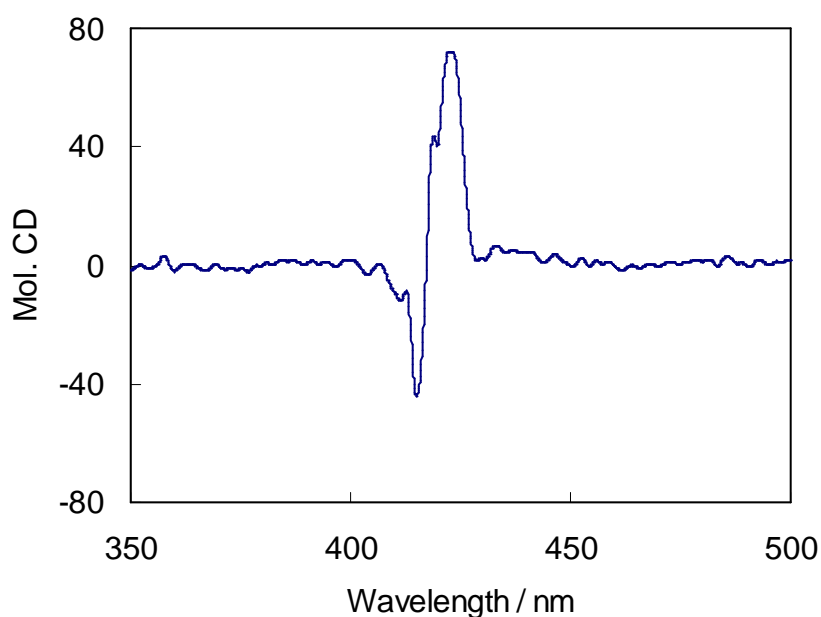
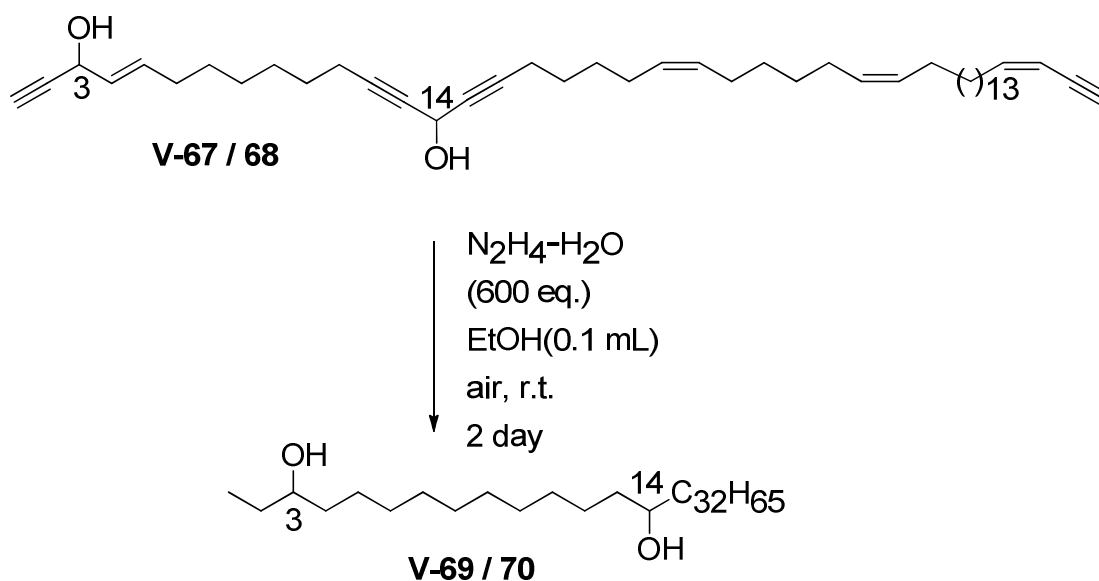


Figure V-23. ECCD spectra of diol **V-66** with tweezer **V-12** in hexane at 0 °C.

Reduction of the propargylic alcohol with the combination of hydrazine / air / $\text{Cu}(\text{OAc})_2$ / EtOH at room temperature proved to be efficient.⁴⁰⁻⁴² This procedure afforded clean **V-66** in quantitative yield when the reaction was conducted at 8.1 mg scale. Subsequent ECCD measurement of **V-66** showed intense and steady ECCD signal ($A = +116$ at 20 eq. of diol, Figure V-23), thus suggesting that the dynamic spectral behavior observed with chiral propargylic alcohols in CD was due to the weak nucleophilicity of OH groups especially when the hydroxyl group is at double-propargylic position as seen in Petrocortyne A isomers.



Scheme V-16. Reduction of Petrocortyne A isomer.

Apparently, reducing the double and triple bonds in Petrocortyne A isomers is necessary for efficient binding with tweezer **V-12** and obtaining steady CD signals. Before reducing the Petrocortyne A samples, we tested the reducing efficiency of hydrazine / air system at minute scale by carrying out the reduction of **V-60** at 180 μg scale with 200 eq. of hydrazine. $\text{Cu}(\text{OAc})_2$ was removed from system since we wanted to eliminate the risk of epimerizing the chiral alcohol and hydrazine / air was also reported effective for the reduction.⁴³ After 2 days of reduction, the crude product obtained also led to observable ECCD spectrum indicating that the reduction was effective. Thus, we went ahead to run the reduction of both Petrocortyne A isomers (**V-69 / 70**) at 180 μg scale with 600 eq. of hydrazine for two days (Scheme V-16). The formation of small amount of solid was suggestive for the generation of product since the starting materials was liquid. However, a satisfactory ^1H NMR was difficult to obtain using 500 MHz NMR machine due to minute amount of product. A NMR equipped with microprobe may be suitable for NMR analysis.

The ECCD measurements of the crude product were still attempted. Unfortunately, no observable ECCD was detected. Considering the large molecular size (47 saturated carbons), the poor solubility of the reduced products probably will not allow the CD measurement in nonpolar solvent such as hexane. A variety of solvents (MCH, isooctane, toluene, CH_2Cl_2 /hexane, CH_2Cl_2 , $\text{CH}_2\text{ClCH}_2\text{Cl}$, CHCl_3 , *tert*-butylether, CH_3CN , CH_3NO_2) were screened along with varying temperatures (-10~25 °C), however, no satisfactory results were obtained. To conclude, the attempt for determination of absolute configuration for Petracortyne A isomers using porphyrin tweezer **V-12** system was not successful due to the weak nucleophilicity of propargylic alcohols, the low solubility of reduced diols, and probably the large size of one side chain containing 32 carbons. However, the efforts dedicated to this work may provide useful insights in the stereochemical determination of long chain diols using modified porphyrin tweezer system.

Experimental Procedures

Materials and general instrumentations:

Anhydrous CH_2Cl_2 was dried and redistilled over CaH_2 . The solvents used for CD measurements were purchased from Aldrich and were spectra grade. All reactions were performed in dried glassware under nitrogen. Column chromatography was performed using SiliCycle silica gel (230-400 mesh). ^1H NMR and ^{13}C NMR spectra were obtained on a Varian Inova 300 MHz or 500Hz instrument and are reported in parts per million (ppm) relative to the solvent resonances (δ), with coupling constants (J) in Hertz (Hz). IR studies were performed on a Nicolet FT-IR 42 instrument. UV/Vis spectra were recorded on a Perkin-Elmer Lambda 40 spectrophotometer, and are reported as λ_{max} [nm]. CD spectra were recorded on a JASCO J-810 spectropolarimeter, equipped with a temperature controller (Neslab 111) for low temperature studies, and were reported as $\lambda[\text{nm}]$ ($\Delta\epsilon_{\text{max}}$ [$\text{L mol}^{-1} \text{cm}^{-1}$]). Optical rotations were recorded at 20 °C on a Perkin Elemer 341 Polarimeter ($\lambda = 589$ nm, 1 dm cell). Chiral GC analyses were performed on a Hewlett Packard 6890 gas chromatograph equipped with a Supelco Gamma Dex 225 column (0.25 mm \times 30 m) using helium as carrier gas. HRMS analyses were performed on a Q-TOF Ultima system using electrospray ionization in positive mode.

General procedure for CD measurement:

Zinc porphyrin tweezer **II-25** (2 μL of a 1 mM solution in anhydrous CH_2Cl_2) was added to hexane (1 mL) in a 1.0 cm cell to obtain a 2 μM tweezer **II-25** solution.

The background spectrum was recorded from 350 nm to 550 nm with a scan rate of 100 nm/min at 0 °C. Chiral diol (1 to 20 µL of a 10 mM solution in anhydrous CH₂Cl₂) was added into the prepared tweezer solution to afford the host/guest complex. The CD spectra were measured immediately (minimum of 4 accumulations). The resultant ECCD spectra recorded in millidegrees were normalized based on the tweezer concentration to obtain the molecular CD (Mol CD).

Determination of binding constant

The solution of Zn-porphyrin tweezer (1 mM in hexane) was titrated with guest molecule (10 mM in DCM) at different equivalents and the UV-vis spectra were recorded. The addition of the chiral substrate continued until no visible change in the spectra was observed. Upon formation of the chiral complex the Soret band of the porphyrin tweezers underwent red-shifts through an isosbestic point. The change of absorption at certain wavelength as a function of the substrate concentration yields an exponential saturation curve which can be fitted through the following non-linear least square equation previously reported by Shoji⁴⁴ to derive the binding constant.

$$f = L \{ (1 + kx + ka) - [L^2(1 + kx + ka)^2 - 4axk^2L^2]^{1/2} \} / 2ka$$

where: L - Δ abs at the point of saturation; x - chiral substrate equivalents; k - calculated K_a ; a - concentration of porphyrin tweezer.

Crystallographic data of diol V-11

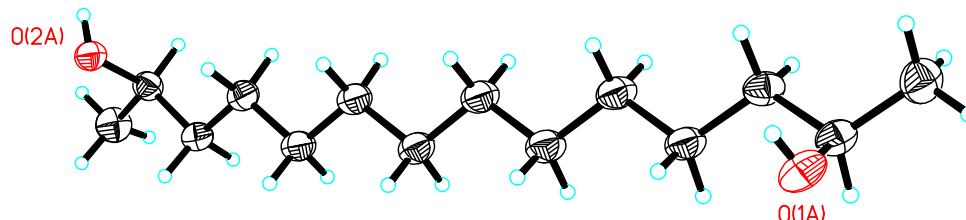


Figure V-S1. Crystal structure of diol **V-11**,

Table V-S1. Crystal data and structure refinement for diol **V-11**.

Identification code	Diol V-11
Empirical formula	C ₁₄ H _{30.50} O _{2.25}
Formula weight	234.88
Temperature	173(2) K
Wavelength	0.71073 Å
Crystal system	Triclinic
Space group	P 1
Unit cell dimension	$a = 9.4357(8) \text{ Å}$ $\alpha = 88.3600(10)^\circ$. $b = 10.0619(8) \text{ Å}$ $\beta = 76.6840(10)^\circ$. $c = 17.2986(13) \text{ Å}$ $\gamma = 71.8240(10)^\circ$.
Volume	1516.8(2) Å ³
Z	4
Density (calculated)	1.029 Mg/m ³
Absorption coefficient	0.067 mm ⁻¹

Table V-S1-continued. Crystal data and structure refinement for diol **V-11**.

F(000)	530
Crystal size	1.08 x 0.20 x 0.18 mm ³
Theta range for data collection	1.21 to 32.04°.
Index ranges	-12<= <i>h</i> <=12, -14<= <i>k</i> <=14, -25<= <i>l</i> <=24
Reflections collected	31513
Independent reflections	14753 [R(int) = 0.0283]
Completeness to theta = 25.00°	99.8 %
Absorption correction	Semi-empirical from equivalents
Max. and min. transmission	0.9881 and 0.9311
Refinement method	Full-matrix least-squares on F ²
Data / restraints / parameters	14753 / 3 / 1074
Goodness-of-fit on F ²	0.983
Final R indices [I>2sigma(I)]	R1 = 0.0433, wR2 = 0.0965
R indices (all data)	R1 = 0.0728, wR2 = 0.1106
Absolute structure parameter	0.6(6)
Largest diff. peak and hole	0.202 and -0.191 e.Å ⁻³

Table V-S1-continued. Crystal data and structure refinement for diol **V-11**.

F(000)	530
Crystal size	1.08 x 0.20 x 0.18 mm ³
Theta range for data collection	1.21 to 32.04°.
Index ranges	-12<= <i>h</i> <=12, -14<= <i>k</i> <=14, -25<= <i>l</i> <=24
Reflections collected	31513
Independent reflections	14753 [R(int) = 0.0283]
Completeness to theta = 25.00°	99.8 %
Absorption correction	Semi-empirical from equivalents
Max. and min. transmission	0.9881 and 0.9311
Refinement method	Full-matrix least-squares on F ²
Data / restraints / parameters	14753 / 3 / 1074
Goodness-of-fit on F ²	0.983
Final R indices [I>2sigma(I)]	R1 = 0.0433, wR2 = 0.0965
R indices (all data)	R1 = 0.0728, wR2 = 0.1106
Absolute structure parameter	0.6(6)
Largest diff. peak and hole	0.202 and -0.191 e.Å ⁻³

Table V-S2-continued. Crystal data and structure refinement for diol **V-9**.

	$c = 28.9411(4) \text{ \AA}$ $\gamma = 90^\circ$.
Volume	$2456.15(6) \text{ \AA}^3$
Z	8
Density (calculated)	1.018 Mg/m^3
Absorption coefficient	0.067 mm^{-1}
F(000)	848
Crystal size	$0.22 \times 0.16 \times 0.12 \text{ mm}^3$
Theta range for data collection	1.41 to 25.31° .
Index ranges	$-8 \leq h \leq 9$, $-13 \leq k \leq 12$, $-34 \leq l \leq 34$
Reflections collected	14442
Independent reflections	4434 [$R(\text{int}) = 0.0363$]
Completeness to $\theta = 25.31^\circ$	99.8 %
Absorption correction	Semi-empirical from equivalents
Max. and min. transmission	0.9922 and 0.9851
Refinement method	Full-matrix least-squares on F^2
Data / restraints / parameters	4434 / 0 / 243
Goodness-of-fit on F^2	1.016
Final R indices [$I > 2\sigma(I)$]	$R1 = 0.0393$, $wR2 = 0.0808$
R indices (all data)	$R1 = 0.0555$, $wR2 = 0.0919$
Absolute structure parameter	$-0.3(11)$
Largest diff. peak and hole	0.110 and $-0.167 \text{ e.\AA}^{-3}$

Computational method

Monte Carlo conformational search of diol-tweezer complex was performed by Spartan V 5.1.3 with SYBYL as force field. The O–Zn distance was constrained at 2.2 Å to avoid dissociation of the complex. After 1500-1900 fully optimized steps, conformers with 10 kcal / mol were collected for analysis. For all three diols (**V-6**, **V-7**, **V-11**) complexed with Zn-TPFP tweezer **V-12**, the most stable conformers consistently indicated clockwise helicity as proposed (Figure V-16~V-18). The side-on approach was also clearly revealed in these optimized structures.

Synthesis of chiral diols

Compound **V-3** is commercially available from Acros. Diols **V-4~V-10** were synthesized from hydrolytic kinetic resolution of corresponding racemic terminal diepoxides and following ring opening by LAH.

Typical procedure for synthesis of chiral diols using Jacobsen hydrolytic kinetic resolutions^{27, 28} described for the synthesis of V-6:

1,2:7,8-Diepoxyoctane (V-21)

To a solution of 1,7-octanediene (5.0 g, 45.5 mmol) in CH₂Cl₂ (100 mL) at 0 °C was added *m*-CPBA (70%, 13.4 g, 54.5 mmol). The suspension was stirred at room temperature for 2 h monitored by TLC until completion. The reaction was quenched

and washed by saturated NaHCO₃ solution (4 × 80 mL) followed by brine (100 mL). The organic layers were then dried (Na₂SO₄) and concentrated. The oil residue was purified by flash chromatography (5-20% EtOAc / hexane) to afford the 1,2:7,8-diepoxyoctane (5.32 g, 83%) as a colorless oil. ¹H NMR (CDCl₃, 300 MHz) δ 1.52 (s, br, 8H), 2.44 (dd, 2H, *J*' = 5.1 Hz, *J*'' = 2.7 Hz), 2.73 (t, 2H, *J* = 5.1 Hz), 2.88 (s, br, 2H); ¹³C NMR (CDCl₃, 75 MHz) δ 25.5, 32.1, 46.6, 51.8.⁴⁵

(1,2*S*:7*S*,8)-Diepoxyoctane (V-22)

1,2:7,8-Diepoxyo-heptane (3.68 g, 25.94 mmol), (*S,S*)-Salen-Co catalyst (157 mg, 0.0259 mmol, 0.01 eq.), THF (0.26 mL) and HOAc (62 mg, 1.04 mmol, 0.04 eq.) were added sequentially to a 50 mL round bottom flask rendering a dark red-brown solution. The mixture was cooled in ice-bath and H₂O (514 mg, 28.53 mmol, 1.1 eq.) was added in one portion. The reaction mixture was stirred for 20 h and then purified by flash chromatography (10-30% EtOAc / hexane) to afford the (1,2*S*:7*S*,8)-diepoxyoctane (552 mg, 15%) as a colorless oil. $[\alpha]_D^{20} = -22.3$, (*c* = 2.0, CHCl₃); ¹H NMR (CDCl₃, 300 MHz) δ 1.52 (s, br, 8H), 2.44 (dd, 2H, *J*' = 5.1 Hz, *J*'' = 2.7 Hz), 2.73 (t, 2H, *J* = 5.1 Hz), 2.88 (s, br, 2H); ¹³C NMR (CDCl₃, 75 MHz) δ 25.5, 32.1, 46.6, 51.8.

(2*R*,7*R*)-Octanediol (V-6)

To a solution of (1,2*S*:7*S*,8)-diepoxyoctane (205 mg, 1.44 mmol) in dry THF (10 mL)

at 0 °C was added LAH (219 mg, 5.77 mmol, 4.0 eq.). The mixture was stirred for 1 h until completion, then was quenched with Et₂O (20 mL), H₂O (1 mL), and H₂SO₄ (1 mL). After filtration through celite, the organic layer was dried and concentrated. Purification by flash chromatography (30-50% EtOAc / hexane) to afford (2*R*,7*R*)-octanediol (203 mg, 97%) as a colorless oil. $[\alpha]_D^{20} = -17.5$, ($c = 0.72$, CHCl₃); $ee = 95\%$ (NMR analysis of *R*-MPA diester); ¹H NMR (CDCl₃, 300 MHz) δ 1.14 (d, 6H, $J = 6.3$ Hz), 1.35 (m, 8H), 1.71 (s, 2H), 3.75 (m, 2H); ¹³C NMR (CDCl₃, 75 MHz) δ 23.4, 25.6, 39.1, 67.8.⁴⁵

REFERENCES

References

1. Rychnovsky, S. D.; Rogers, B.; Yang, G., Analysis of 2 C-13 Nmr Correlations for Determining the Stereochemistry of 1,3-Diol Acetonides. *Journal of Organic Chemistry* **1993**, 58, (13), 3511-3515.
2. Matsumori, N.; Kaneno, D.; Murata, M.; Nakamura, H.; Tachibana, K., Stereochemical determination of acyclic structures based on carbon-proton spin-coupling constants. A method of configuration analysis for natural products. *Journal of Organic Chemistry* **1999**, 64, (3), 866-876.
3. Kobayashi, Y.; Lee, J.; Tezuka, K.; Kishi, Y., Toward creation of a universal NMR database for the stereochemical assignment of acyclic compounds: The case of two contiguous propionate units. *Organic Letters* **1999**, 1, (13), 2177-2180.
4. Kobayashi, Y.; Tan, C. H.; Kishi, Y., Toward creation of a universal NMR database for stereochemical assignment: Complete structure of the desertomycin/oasomycin class of natural products. *Journal of the American Chemical Society* **2001**, 123, (9), 2076-2078.
5. Kobayashi, Y.; Hayashi, N.; Kishi, Y., Toward the creation of NMR Databases in chiral solvents: Bidentate chiral NMR solvents for assignment of the absolute configuration of acyclic secondary alcohols. *Organic Letters* **2002**, 4, (3), 411-414.
6. Higashibayashi, S.; Czechtizky, W.; Kobayashi, Y.; Kishi, Y., Universal NMR databases for contiguous polyols. *Journal of the American Chemical Society* **2003**, 125, (47), 14379-14393.
7. Freire, M.; Seco, J. M.; Quinoa, E.; Riguera, R., The prediction of the absolute stereochemistry of primary and secondary 1,2-diols by H-1 NMR spectroscopy: Principles and applications. *Chemistry-a European Journal* **2005**, 11, (19), 5509-5522.
8. Harada, N.; Saito, A.; Ono, H.; Gawronski, J.; Gawronska, K.; Sugioka, T.; Uda, H.; Kuriki, T., A CD Method for Determination of the Absolute Stereochemistry of Acyclic Glycols .1. Application of the CD Exciton Chirality Method to Acyclic 1,3-Dibenzoate Systems. *Journal of the American Chemical Society* **1991**, 113, (10), 3842-3850.
9. Harada, N.; Nakanishi, K., *Circular Dichroic Spectroscopy: Exciton Coupling in Organic Stereochemistry*. University Science Books: Mill Valley, CA., 1983.

10. Wiesler, W. T.; Nakanishi, K., Relative and Absolute Configurational Assignments of Acyclic Polyols by Circular-Dichroism .1. Rationale for a Simple Procedure Based on the Exciton Chirality Method. *Journal of the American Chemical Society* **1989**, 111, (26), 9205-9213.
11. Wiesler, W. T.; Nakanishi, K., A Simple Spectroscopic Method for Assigning Relative and Absolute-Configuration in Acyclic 1,2,3-Triols. *Journal of the American Chemical Society* **1989**, 111, (9), 3446-3447.
12. Wiesler, W. T.; Nakanishi, K., Relative and Absolute Configurational Assignments of Acyclic Polyols by Circular-Dichroism .2. Determination of Nondegenerate Exciton Coupling Interactions by Assignment of Prochiral Aryloxymethylene Protons for H-1-Nmr Conformational-Analysis. *Journal of the American Chemical Society* **1990**, 112, (14), 5574-5583.
13. Zhao, N.; Zhou, P.; Berova, N.; Nakanishi, K., Combined synthetic CD strategy for the preparation and configurational assignments of model acyclic 1,3-polyols with a 1,2-diol terminal. *Chirality* **1995**, 7, (8), 636-651.
14. Di Bari, L.; Pescitelli, G.; Pratelli, C.; Pini, D.; Salvadori, P., Determination of absolute configuration of acyclic 1,2-diols with Mo-2(OAc)(4). 1. Snatzke's method revisited. *Journal of Organic Chemistry* **2001**, 66, (14), 4819-4825.
15. Rosini, C.; Scamuzzi, S.; Pisani-Facati, M.; Salvadori, P., A General, Multitechnique Approach to the Stereochemical Characterization of 1,2-Diarylethane-1,2-diol. *Journal of Organic Chemistry* **1995**, 60, 8289.
16. Rosini, C.; Scamuzzi, S.; Uccellobarretta, G.; Salvadori, P., Synthesis and Stereochemical Characterization of Some Optically-Active 1,2-Dinaphthylethane-1,2-Diols. *Journal of Organic Chemistry* **1994**, 59, (24), 7395-7400.
17. Snatzke, G.; Wagner, U.; Wolff, H. P., Circular-Dichroism .75. Cottonogenic Derivatives of Chiral Bidentate Ligands with the Complex [Mo₂(O₂cch₃)₄]. *Tetrahedron* **1981**, 37, (2), 349-361.
18. Superchi, S.; Casarini, D.; Laurita, A.; Bavoso, A.; Rosini, C., Induction of a preferred twist in a biphenyl core by stereogenic centers: A novel approach to the absolute configuration of 1,2-and 1,3-diols. *Angewandte Chemie-International Edition* **2001**, 40, (2), 451-454.
19. Superchi, S.; Casarini, D.; Summa, C.; Rosini, C., A general and nonempirical approach to the determination of the absolute configuration of 1-aryl-1,2-diols.

Journal of Organic Chemistry **2004**, 69, (5), 1685-1694.

20. Superchi, S.; Donnoli, M. I.; Rosini, C., Determination of the Absolute Configuration of 1-Arylethane-1,2-diols by a Nonempirical Analysis of the CD Spectra of Their 4-Biphenylboronates. *Org. Lett.* **1999**, 1, 2093-2096.

21. Tartaglia, S.; Pace, F.; Scafato, P.; Rosini, C., A new case of induced helical chirality in a bichromophoric system: absolute configuration of transparent and flexible diols from the analysis of the electronic circular dichroism spectra of the corresponding di(1-naphthyl)ketals. *Organic Letters* **2008**, 10, (16), 3421-3424.

22. MacMillan, J. B.; Linington, R. G.; Andersen, R. J.; Molinski, T. F., Stereochemical assignment in acyclic lipids across long distance by circular dichroism: Absolute stereochemistry of the aglycone of caminoside A. *Angewandte Chemie-International Edition* **2004**, 43, (44), 5946-5951.

23. MacMillan, J. B.; Molinski, T. F., Long-range stereo-relay: Relative and absolute configuration of 1,n-glycols from circular dichroism of liposomal porphyrin esters. *Journal of the American Chemical Society* **2004**, 126, (32), 9944-9945.

24. Li, X. Y.; Tanasova, M.; Vasileiou, C.; Borhan, B., Fluorinated porphyrin tweezer: A powerful reporter of absolute configuration for erythro and threo diols, amino alcohols, and diamines. *Journal of the American Chemical Society* **2008**, 130, (6), 1885-1893.

25. Li, X. Y.; Borhan, B., Prompt determination of absolute configuration for epoxy alcohols via exciton chirality protocol. *Journal of the American Chemical Society* **2008**, 130, (48), 16126-16127.

26. Tokunaga, M.; Larrow, J. F.; Kakiuchi, F.; Jacobsen, E. N., Asymmetric catalysis with water: Efficient kinetic resolution of terminal epoxides by means of catalytic hydrolysis. *Science* **1997**, 277, (5328), 936-938.

27. Chow, S.; Kitching, W., Hydrolytic kinetic resolution of mono- and bisepoxides as a key step in the synthesis of insect pheromones. *Chemical Communications* **2001**, (11), 1040-1041.

28. Schaus, S. E.; Brandes, B. D.; Larrow, J. F.; Tokunaga, M.; Hansen, K. B.; Gould, A. E.; Furrow, M. E.; Jacobsen, E. N., Highly selective hydrolytic kinetic resolution of terminal epoxides catalyzed by chiral (salen)Co-III complexes. Practical synthesis of enantioenriched terminal epoxides and 1,2-diols. *Journal of the American Chemical Society* **2002**, 124, (7), 1307-1315.

29. Ema, T.; Misawa, S.; Nemugaki, S.; Sakai, T.; Utaka, M., New optically active

- diporphyrin having a chiral cyclophane as a spacer. *Chemistry Letters* **1997**, (6), 487-488.
30. Izumi, H.; Yamagami, S.; Futamura, S.; Nafie, L. A.; Dukor, R. K., Direct observation of odd-even effect for chiral alkyl alcohols in solution using vibrational circular dichroism spectroscopy. *Journal of the American Chemical Society* **2004**, 126, (1), 194-198.
31. Kurtan, T.; Nesnas, N.; Li, Y. Q.; Huang, X. F.; Nakanishi, K.; Berova, N., Chiral recognition by CD-sensitive dimeric zinc porphyrin host. 1. Chiroptical protocol for absolute configurational assignments of monoalcohols and primary monoamines. *Journal of the American Chemical Society* **2001**, 123, (25), 5962-5973.
32. Huang, X. F.; Rickman, B. H.; Borhan, B.; Berova, N.; Nakanishi, K., Zinc porphyrin tweezer in host-guest complexation: Determination of absolute configurations of diamines, amino acids, and amino alcohols by circular dichroism. *Journal of the American Chemical Society* **1998**, 120, (24), 6185-6186.
33. Chow, S.; Kitching, W., Hydrolytic kinetic resolution of terminal mono- and bis-epoxides in the synthesis of insect pheromones: routes to (-)-(R)- and (+)-(S)-10-methyldodecyl acetate, (-)-(R)-10-methyl-2-tridecanone, (-)-(R)-(Z)-undec-6-en-2-ol (Nostrenol), (-)-(1R,7R)-1,7-dimethylnonyl propanoate, (-)-(6R,12R)-6,12-dimethylpentadecan-2-one, (-)-(2S,11S)-2,11-diacetoxytridecane and (+)-(2S,12S)-2,12-diacetoxytridecane. *Tetrahedron-Asymmetry* **2002**, 13, (7), 779-793.
34. Curran, D. P.; Sui, B., A "Shortcut" Mosher Ester Method To Assign Configurations of Stereocenters in Nearly Symmetric Environments. Fluorous Mixture Synthesis and Structure Assignment of Petrocortyne A. *Journal of the American Chemical Society* **2009**, 131, (15), 5411-+.
35. Kim, J. S.; Lim, Y. J.; Im, K. S.; Jung, J. H.; Shim, C. J.; Lee, C. O.; Hong, J.; Lee, H., Cytotoxic polyacetylenes from the marine sponge *Petrosia* sp. *Journal of Natural Products* **1999**, 62, (4), 554-559.
36. Helal, C. J.; Magriotis, P. A.; Corey, E. J., Direct catalytic enantioselective reduction of achiral alpha,beta-ynones. Strong remote steric effects across the C-C triple bond. *Journal of the American Chemical Society* **1996**, 118, (44), 10938-10939.
37. Corey, E. J.; Helal, C. J., Aminoacrylic compounds. Part 31 - Reduction of carbonyl compounds with chiral oxazaborolidine catalysts: A new paradigm for enantioselective catalysis and a powerful new synthetic method. *Angewandte Chemie-International Edition* **1998**, 37, (15), 1987-2012.
38. Yu, C. M.; Kim, C.; Kweon, J. H., Enantioselective synthesis of allenyl carbinols

by the CBS reduction in nitroethane: dramatic solvent effect for reactivity and enantioselectivity. *Chemical Communications* **2004**, (21), 2494-2495.

39. Parker, K. A.; Ledebøer, M. W., Asymmetric reduction. A convenient method for the reduction of alkynyl ketones. *Journal of Organic Chemistry* **1996**, 61, (9), 3214-3217.

40. Braude, E. A.; Linstead, R. P.; Mitchell, P. W. D.; Wooldridge, K. R. H., Hydrogen Transfer .8. Metal-Catalysed Transfer-Hydrogenation of Miscellaneous Acceptors. *Journal of the Chemical Society* **1954**, (OCT), 3595-3598.

41. Braude, E. A.; Linstead, R. P.; Mitchell, P. W. D., Hydrogen Transfer .6. Metal-Catalysed Transfer-Hydrogenation of Ethylenic Compounds. *Journal of the Chemical Society* **1954**, (OCT), 3578-3585.

42. Felix, A. M.; Heimer, E. P.; Lambros, T. J.; Tzougraki, C.; Meienhofer, J., Rapid Removal of Protecting Groups from Peptides by Catalytic Transfer Hydrogenation with 1,4-Cyclohexadiene. *Journal of Organic Chemistry* **1978**, 43, (21), 4194-4196.

43. Roush, W. R.; Hoong, L. K.; Palmer, M. A. J.; Straub, J. A.; Palkowitz, A. D., Asymmetric-Synthesis Using Tartrate Ester Modified Allylboronates .2. Single and Double Asymmetric Reactions with Alkoxy-Substituted Aldehydes. *Journal of Organic Chemistry* **1990**, 55, (13), 4117-4126.

44. Shoji, Y.; Tashiro, K.; Aida, T., Sensing of chiral fullerenes by a cyclic host with an asymmetrically distorted pi-electronic component. *Journal of the American Chemical Society* **2006**, 128, (33), 10690-10691.

45. van As, B. A. C.; van Buijtenen, J.; Mes, T.; Palmans, A. R. A.; Meijer, E. W., Iterative tandem catalysis of secondary diols and diesters to chiral polyesters. *Chemistry-a European Journal* **2007**, 13, (29), 8325-8332.

Chapter VI

Determination of Absolute Configurations of Chiral Aziridines using Zn TFPF Tweezer

VI.1 Background

Chiral aziridines are useful building blocks for rapid access to nitrogen-containing molecules and heterocycles that are important to pharmaceutical and biologically related fields. In the past decade, substantial amount of efforts have been dedicated to the asymmetric synthesis of chiral aziridines¹⁻³ as well as the ring-opening reactions.^{1, 4, 5} A lot of advances have been made to develop enantioselective aziridination pathways. However, preparation of chiral aziridines does not share the popular platform as seen for synthesizing epoxy alcohols. An efficient synthesis for this class of compounds from achiral sources is still in great need. The stereochemical determination of chiral aziridines relies on the empirical mnemonics established for different systems. Unlike the well developed asymmetric epoxidations of olefin double bond which could afford epoxy alcohols straightforwardly and provide well-recognized mnemonics facilitating the empirical assignment of chirality for products, there is no direct access to chiral aziridinol from olefin and hence no simple mnemonic available for its chirality assignment. Comparing the optical rotations of ring opened products with reported values is also frequently used. The empirical nature of both methods is a big intrinsic limitation and the latter approach also suffers from extra synthetic work with sensitive

molecules. Furthermore, the necessary transformations and derivatizations are inefficient and time consuming. A general non-empirical expedient protocol addressing the absolute stereochemistry of chiral aziridines has not emerged.

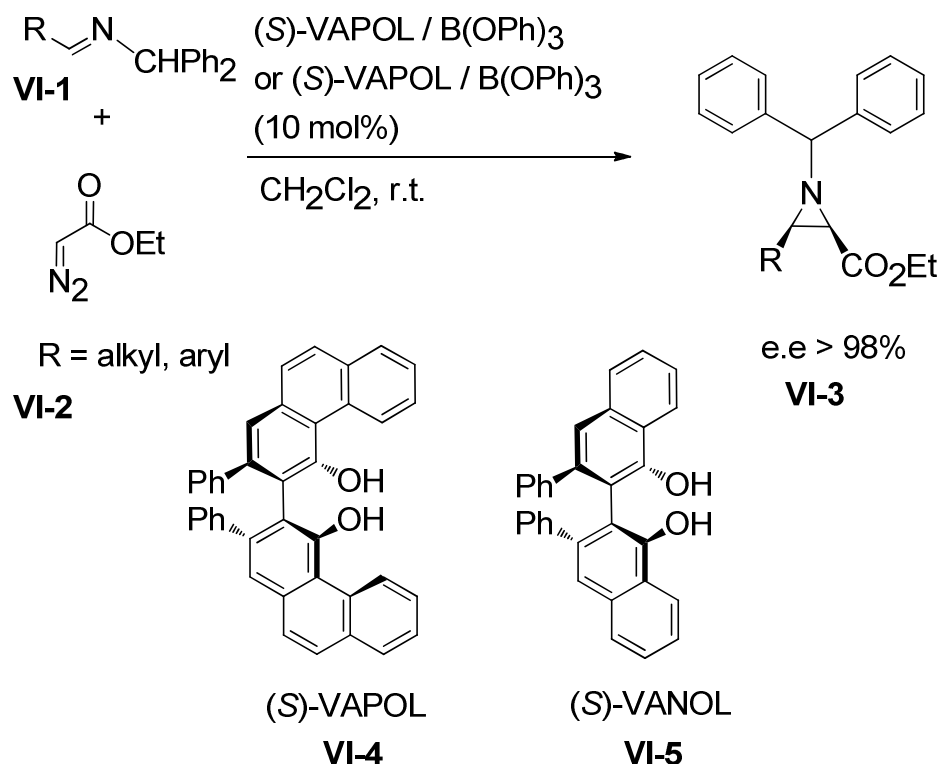
VI.2 ECCD Study of Chiral Aziridines

VI.2.1 ECCD study of *cis* chiral aziridinols using tweezer II-25

Previously, we described the rapid determination of absolute configurations for chiral 2,3-epoxy alcohols with a variety of substitution patterns using the zinc TFPF tweezer linked by a 1,5-pentylene linker (**II-25**) via ECCD protocol. A natural extension of this work would be the ECCD study of the nitrogen-containing analog of epoxy alcohols, namely the aziridinols. Similar to the epoxy alcohols, there is no direct method to determine the absolute stereochemistry of aziridinols. We are hoping that current ECCD study could provide some important insights or even an effective solution for this deficiency.

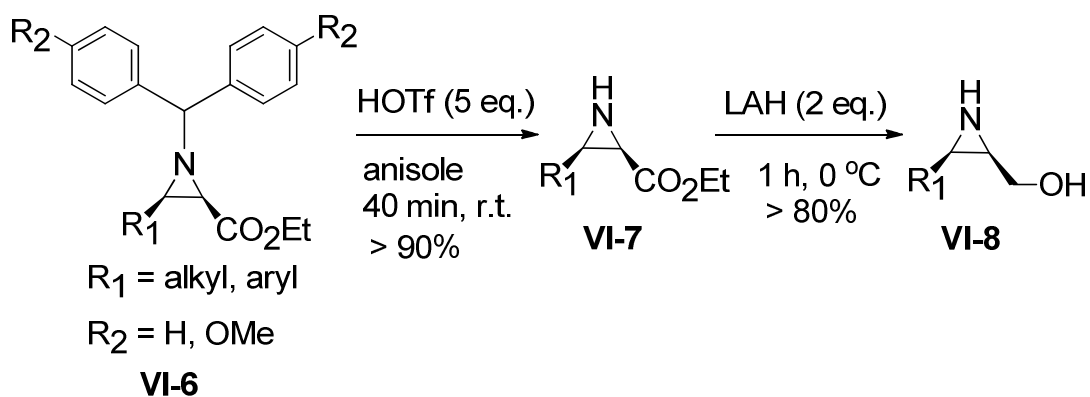
Professor Wulff and coworkers have developed an efficient catalytic asymmetric aziridination method which could yield *cis* chiral N-benzhydryl aziridine 2-carboxylic esters in excellent enantioselectivity (Scheme VI-1).⁶⁻⁸ The absolute stereochemistry of the products from the Wulff aziridination is assigned based on the proposed mnemonic and is confirmed by converting the aziridine esters to known amino esters or amino alcohols and comparing the optical rotations with reported values. As discussed before, the empirical nature of mnemonic for chirality assignment has its intrinsic limitations. Conversion of the aziridine esters to

aziridinols and binding with zinc TPFP tweezer was planned in hope of developing a method to determine the chirality of aziridines rapidly in a non-empirical fashion. As depicted in Scheme VI-2, the N-protected aziridine esters can be easily transformed into free aziridinols without loss of optical purity.⁹



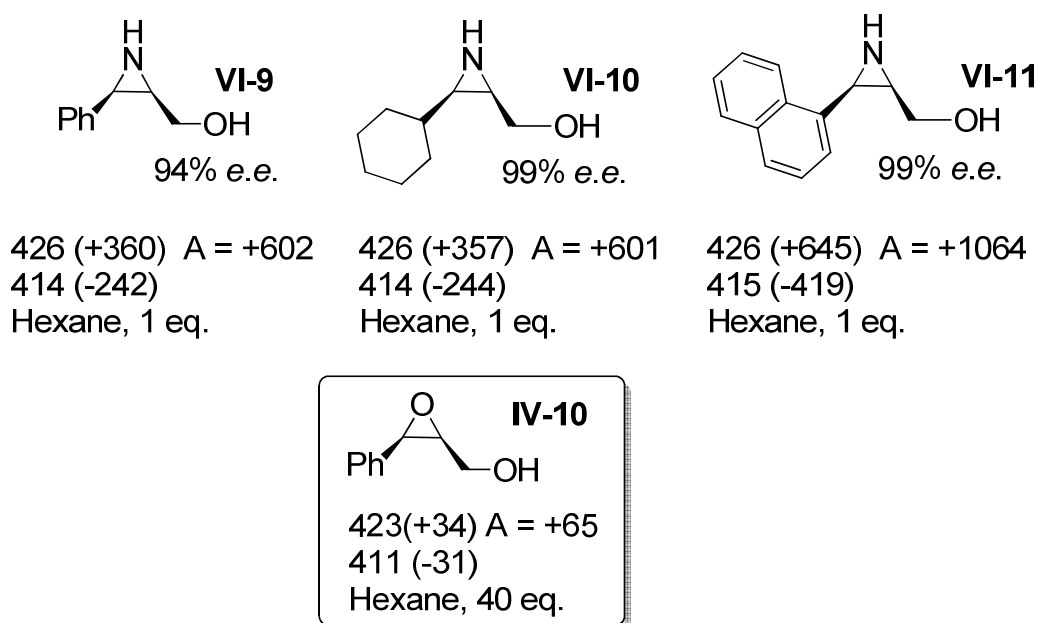
Scheme VI-1. Wulff catalytic asymmetric aziridination using VAPOL / VANOL.

We envision that free aziridinols would bind Zn TPFP tweezer in a similar manner to that of epoxy alcohols considering their structure similarity. Consequently, the stereodifferentiation process in the tweezer-aziridinol supramolecular complex is expected to be the same as in the epoxy alcohol case. Therefore, the sign of resultant ECCD should have consistent correlation with the chirality of aziridinols.



Scheme VI-2. Synthesis of free aziridinol from N-benzhydryl aziridine esters

To our delight, extremely strong ECCD signals were observed when only 1 eq. of free aziridinol was mixed with Zn-TPFP tweezer **II-25** (2 μM) in hexane at 0 °C as shown in Scheme VI-3. The remarkably higher amplitudes of aziridinols over epoxy alcohols are due to the stronger nucleophilicity of aziridinic nitrogen over the epoxidic oxygen. It is noted that the amino group could bind the zinc porphyrin 200 times stronger than hydroxyl group (see Table III-2).



Scheme VI-3. ECCD data of free aziridinols with tweezer **II-25** (2 μM) in hexane at 0 °C

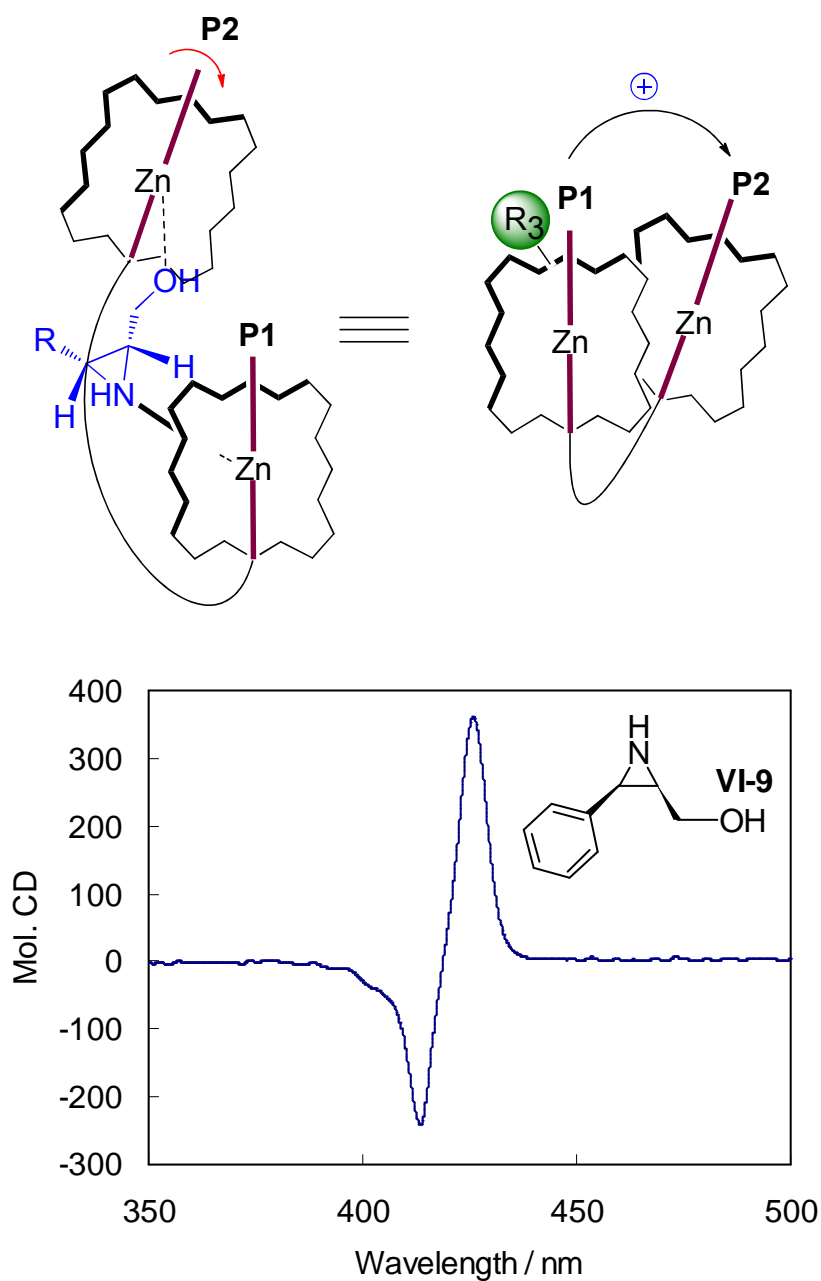


Figure VI-1. Proposed binding mode between tweezer **II-25** and *cis*-aziridinol. Positive ECCD was obtained for *cis*- (2*R*,3*R*) substrate **VI-9**.

More importantly, a consistent trend was observed with 2*R*,3*R*-substrates (**VI-9**~**VI-11**), which rendered positive ECCD spectra. This is in excellent agreement with the observation of *cis* 2*S*,3*R* epoxy alcohols (**IV-10**) which also yielded positive bisignate couplet upon complexation with Zn-TPFP tweezer (note

that the chirality annotation of C2 is different in aziridinols **VI-9~VI-11** based on priority rule, but absolute configuration remains the same as *cis* 2*S*,3*R* epoxide **IV-10**). This agreement proved our hypothesis that chiral aziridinols and epoxy alcohols share the same stereodifferentiation process in the supramolecular assembly.

The proposed complexation pattern was shown in Figure VI-1. The porphyrin **P1** would bind to the lone pair of aziridinic nitrogen and face two hydrogens, thus no stereodifferentiation would occur. The **P2** porphyrin bound with terminal hydroxyl group would rotate clockwise as indicated by the arrow to minimize the steric repulsion with bulky R group at C3 position. Overall, a clockwise chiral twist is generated between the two porphyrin chromophores while binding with *cis*- (2*R*,3*R*) substrates which leads to a positive CD couplet. In this binding pattern, the **P1** and **P2** are on opposite sides of the aziridine ring to avoid steric clash with each other. This is consistent with the complexation mode of *cis* epoxy alcohols. The another invertmer in which the lone pair of nitrogen is *syn* to the terminal hydroxyl group, the two bound porphyrins would bump into each other while approaching the substrate and is energetically disfavored. Consequently, only one of the two invertmers would be preferred for complexation of tweezer with the *cis* free aziridinols. Therefore, pyramidalization of the trivalent nitrogen does not affect the binding pattern for unprotected aziridinols and well defined binding models should be easily derived after carefully examining the preferred position of nitrogen lone pair during complexation.

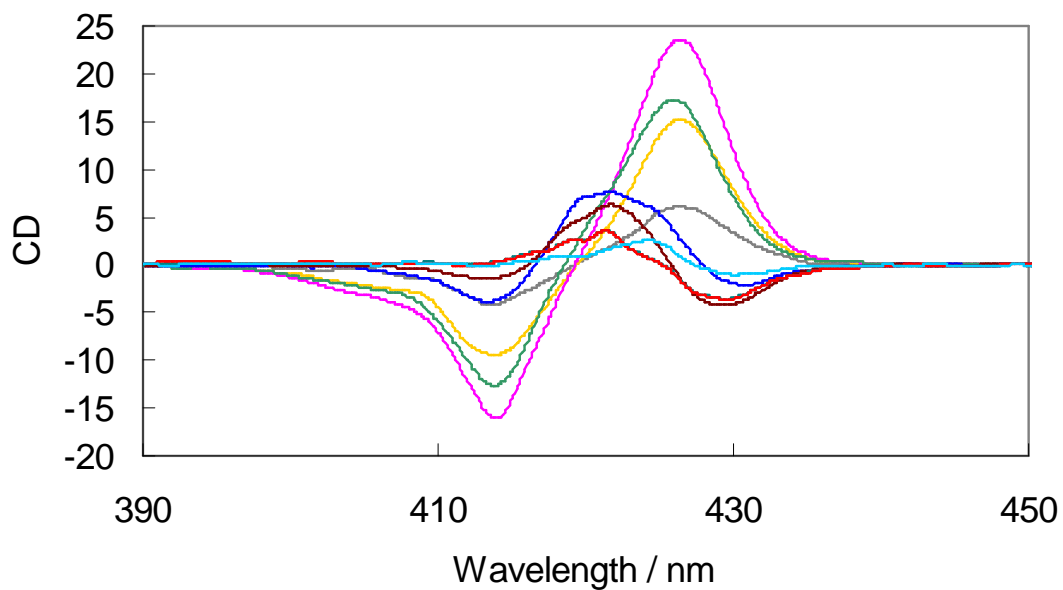


Figure VI-2. CD profile of tweezer **II-25**-aziridinol **VI-10** complex in hexane (1 μ M tweezer).

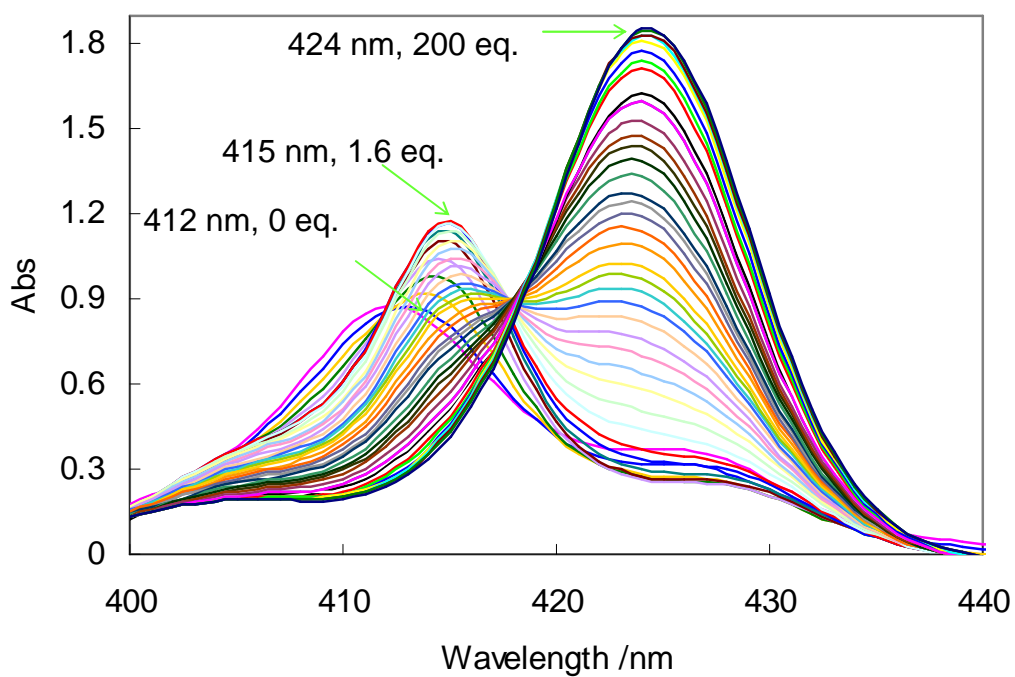


Figure VI-3. UV-vis profile of tweezer **II-25**-aziridinol **VI-10** complex in hexane (1 μ M tweezer).

Further scrutiny of the ECCD titration curves of compound **VI-10** (Figure VI-2) disclosed an interesting fact that the CD amplitude first increased with increasing

concentration of **VI-10** and peaked at 1 eq. of **VI-10**, then started decreasing, leading to complicated CD curve after over 5 eq. of **VI-10** was added. These changes indicated multiple binding processes and interconversion of different bound conformations during the titration.

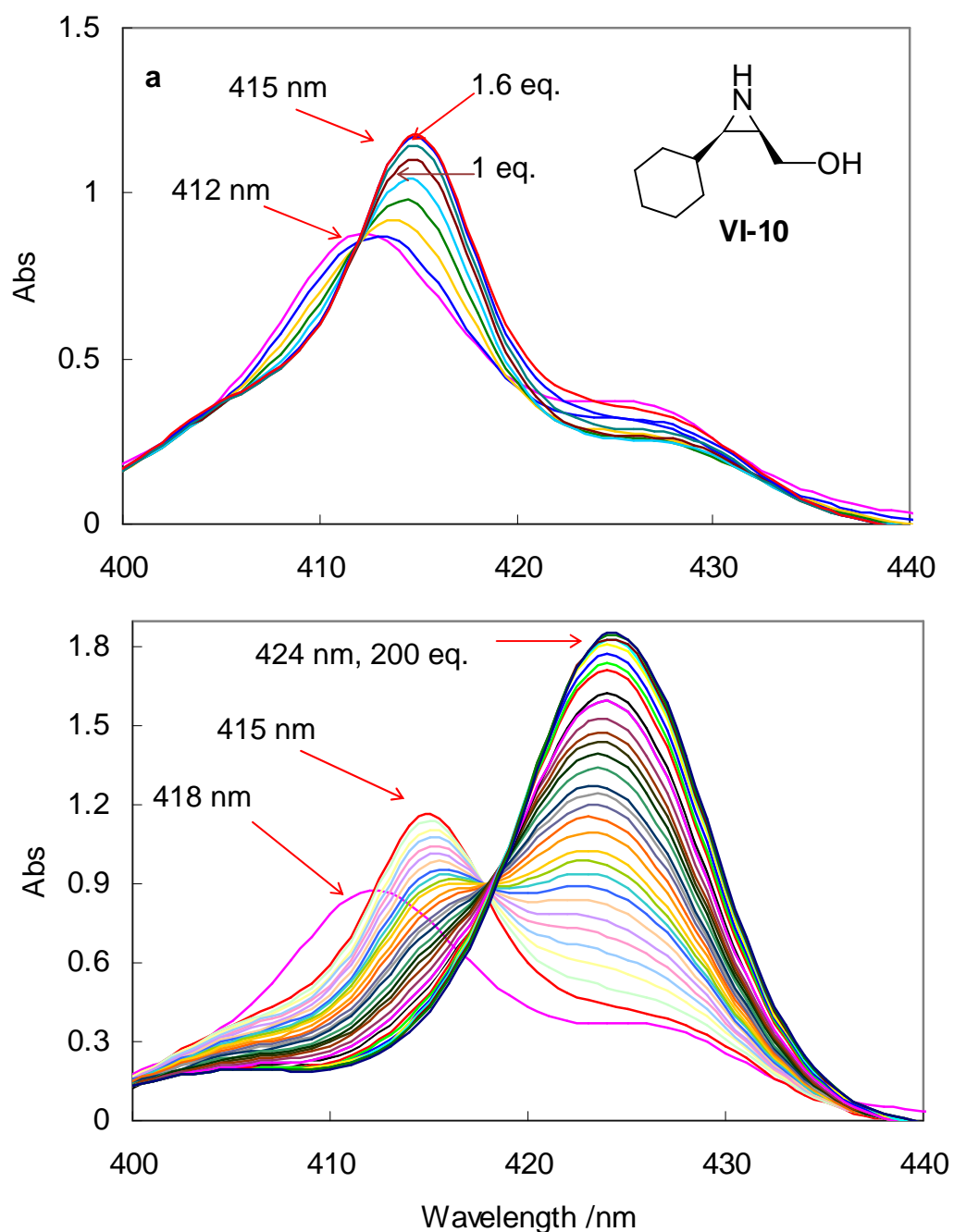
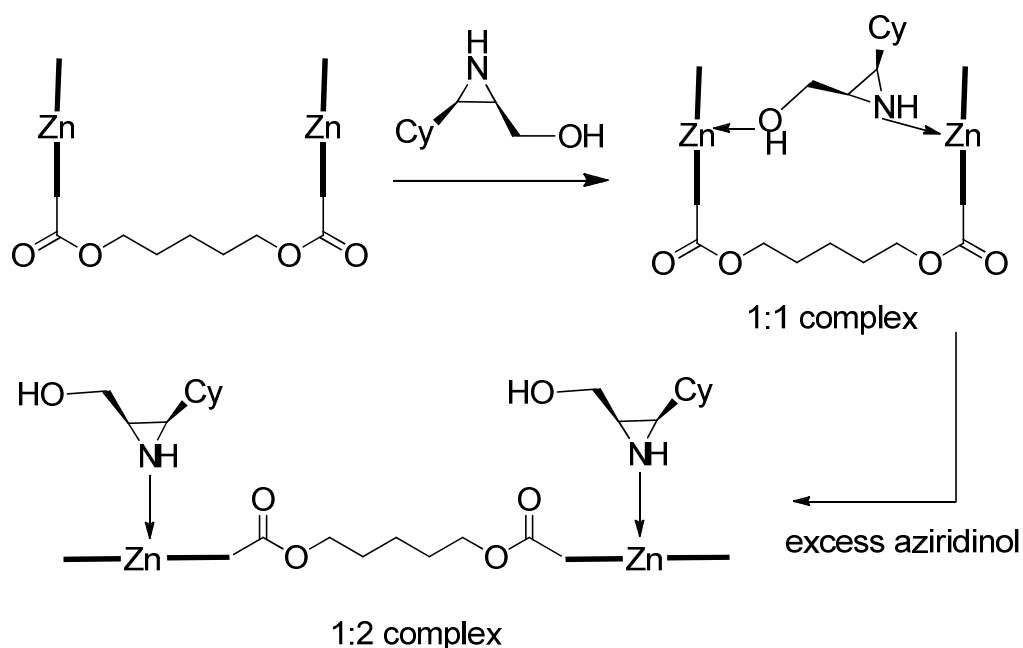


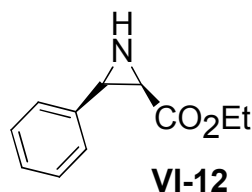
Figure VI-4. UV-vis profile of tweezer **II-25**-aziridinol **VI-10** complex in hexane (1 μM tweezer) at 0~1.6 eq. (graph **a**) and 2~200 eq. (graph **b**).

To probe the multiple binding processes, UV titration of Zn TFPF tweezer **II-25** using **VI-10** in hexane was conducted. As illustrated in Figure VI-3 and Figure VI-4, two isobestic points were obtained at 412 nm and 418 nm respectively, suggesting two binding processes. The first process (leading to the absorption at 415 nm) occurred when 0-1.6 eq. of guest **VI-10** was added and can be attributed to the 1:1 complexation of the aziridinol with Zn-TFPF tweezer (Scheme VI-4). Further addition of the aziridinol leads to the breakup of the ECCD active 1:1 complex (binding of aziridine nitrogen to zincated porphyrin is stronger than that of an alcohol) so that each porphyrin is bound to a nitrogen atom forming ECCD inactive 1:2 complex corresponding to the absorption at 424 nm (Scheme VI-4). The distance between two porphyrins was then maximized leading to a 12 nm red-shift, which is nearly the same red-shift as observed upon binding of a monoamine to the porphyrin. As a result, the ECCD amplitude would diminish when excess aziridinols were added.

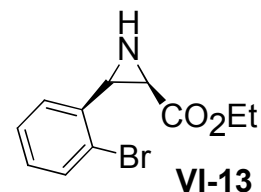


Scheme VI-4. Binding process of tweezer **II-25** with aziridinol **VI-10**.

Interestingly, free aziridine esters **VI-12** and **VI-13** also yielded observable ECCD signals upon complexation with Zn TFPF tweezer in hexane.



423(+ 40) A = +74
418 (- 34)
Hexane, 40 eq.



422(+ 33) A = +57
418 (- 24)
Hexane, 10 eq.

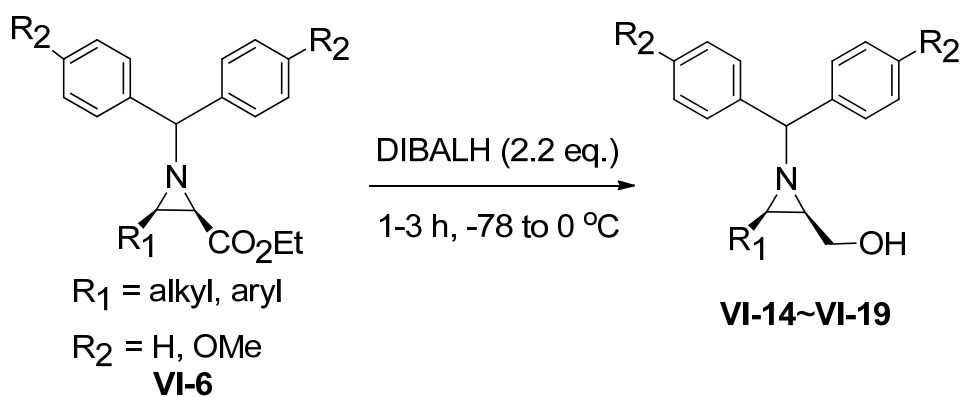
Scheme VI-5. ECCD data of free aziridine

The sign of the CD couplets are the same as those observed with esters with tweezer **II-25** in hexane at 0 °C.

aziridinols bearing the same configuration implying the same binding mechanism involved in the chirality recognition process. Obviously, the carbonyl in the ester group participated in the binding interaction with zincated tweezer. This is due to the strong Lewis acidity of zinc TFPF tweezer since usually ester carbonyl is a weak Lewis base and usually does not participate in the binding interaction with zincated porphyrins. Cooperative binding is believed to contribute to the participation of ester group considering the strong binding of aziridine nitrogen since other substrates such as hydroxyl esters do not lead to a substrate / tweezer complex. We propose that further increase in the Lewis acidity of porphyrin tweezer host will lead to observable ECCD spectra with aziridine esters and thus eliminating the need for reduction of ester to hydroxyl group or removal of the nitrogen protecting group.

Considering the fact that many aziridines are N-protected during organic synthesis, we sought to examine N-protected aziridinols for the ECCD study. The *cis* N-benzhydryl protected aziridinols (**VI-14~VI-19**) were first screened since the protected aziridine esters are readily available from Wulff aziridination and simple

reduction by DIBAL or LAH could afford aziridinols in good yields (Scheme VI-6).



Scheme VI-6. Reduction of N-benzhydryl aziridine esters to aziridinols.

To our surprise, substrates **VI-14~VI-19** all exhibited ECCD couplets upon complexation with zinc TPFP tweezer (2 μM in hexane) despite the presence of the fairly bulky benzhydryl group. These signals were steady and consistent during the CD titration process when over 40 eq. of substrate was added (Figure VI-5). An

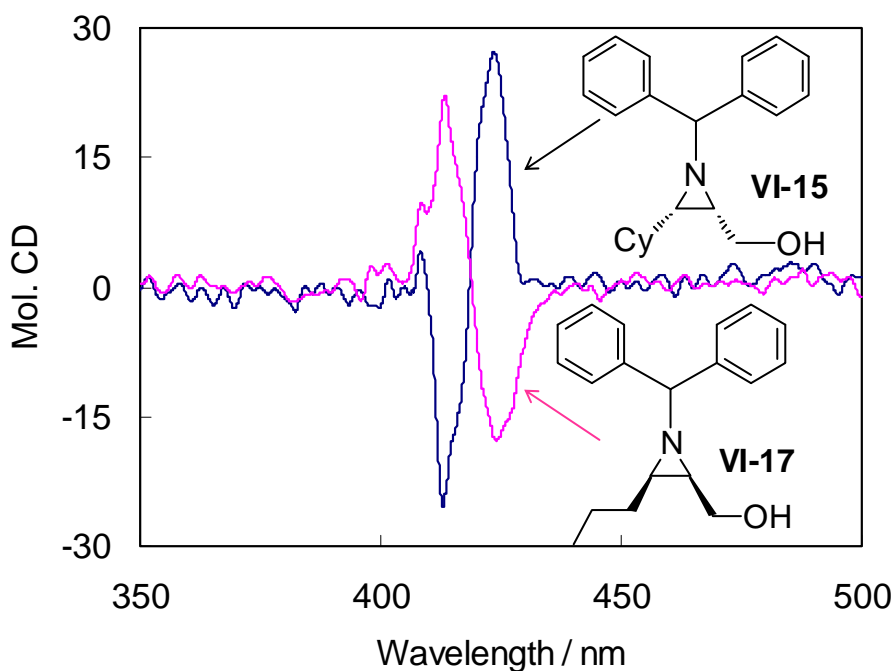
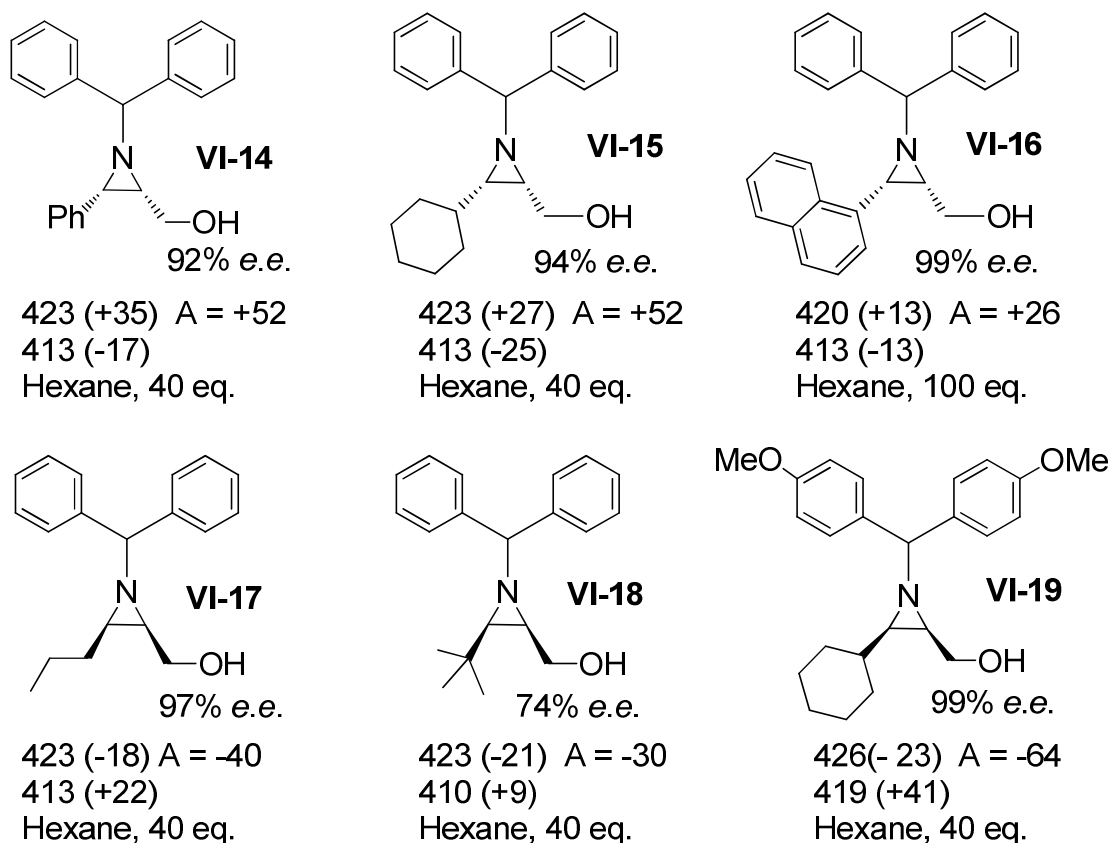


Figure VI-5. ECCD spectra of N-benzhydryl aziridinols **VI-15** and **VI-17** (40 eq.) with tweezer **II-25** (2 μM) in hexane at 0 $^\circ\text{C}$.



Scheme VI-7. ECCD data of N-benzhydryl aziridinols with tweezer **II-25** (2 μ M) in hexane at 0 °C

apparent trend can be seen from Scheme VI-7 that positive signals were detected for 2*S*,3*S* substrates aziridinols (**VI-14~VI-16**) and negative spectra were acquired for substrates (**VI-17~VI-19**) bearing 2*R*,3*R* configuration. This trend is exactly opposite to that of unprotected aziridinols discussed above (Scheme VI-3). The discrepancy disclosed here is presumably due to the bulky benzhydryl group, which would probably force a preferential pyramidalization of the aziridinic nitrogen atom and change the binding pattern of aziridinols toward zinc porphyrin resulting in a different stereodifferentiation mechanism.

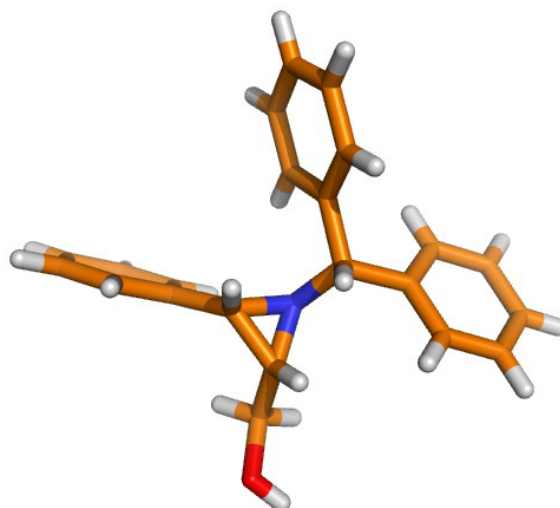


Figure VI-6. Crystal structure of **VI-14**.

To gain further insight of this distinct binding interaction, we obtained the single crystals of compound **VI-14** by slow evaporation of its solution in CH_2Cl_2 . The crystal structure depicted in Figure VI-5 clearly showed a single invertmer in which the benzhydryl group is *anti* to the phenyl and terminal hydroxyl group. In this manner, the bulky benzhydryl group is situated away from the aziridine substituents, thus minimizing the steric interactions. The preferred geometry depicted in Figure VI-6 would leave the lone pair on nitrogen *syn* to the OH group which is opposite to the *anti* relationship between OH group and the bound lone pair on the aziridinic nitrogen we proposed for unprotected aziridinols (Figure VI-7). Though the crystal structure implied that the two porphyrins might approach the chiral aziridinols in the same side, we still think it is not favorable since that would lead to the serious clash of two huge porphyrins.

An *anti* approach was proposed in Figure VI-8. After **P2** porphyrin binds with the

nitrogen lone pair, **P1** porphyrin would approach the OH group *anti* to **P2** with the C1-C2 bond rotated as to avoid the clash of the two porphyrins. The weaker ECCD signals are most probably due to the more strained binding of the protected aziridinols as compared to the less sterically encumbered binding arrangement anticipated for the unprotected aziridinols (see Figure VI-7). Considering the distinct geometry of N-BzH aziridinols, it is reasonable to speculate that **P1** approaches the smallest group (H) on C2, consistent to that proposed for other porphyrin tweezer complexes. Another major difference between models in Figure VI-7 and Figure VI-8 is that

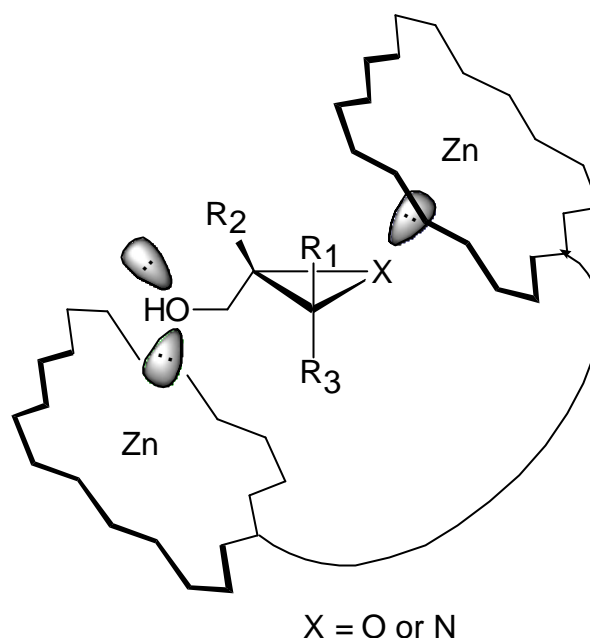


Figure VI-7. Proposed binding mode for epoxy alcohol and free aziridinol.

unlike the epoxyl alcohol model in which the epoxidic oxygen points down toward the tweezer linker, the aziridine nitrogen would prefer pointing to the upper region of the binding pocket to avoid the unfavorable steric interaction between bulky benzhydryl group and tweezer linker.

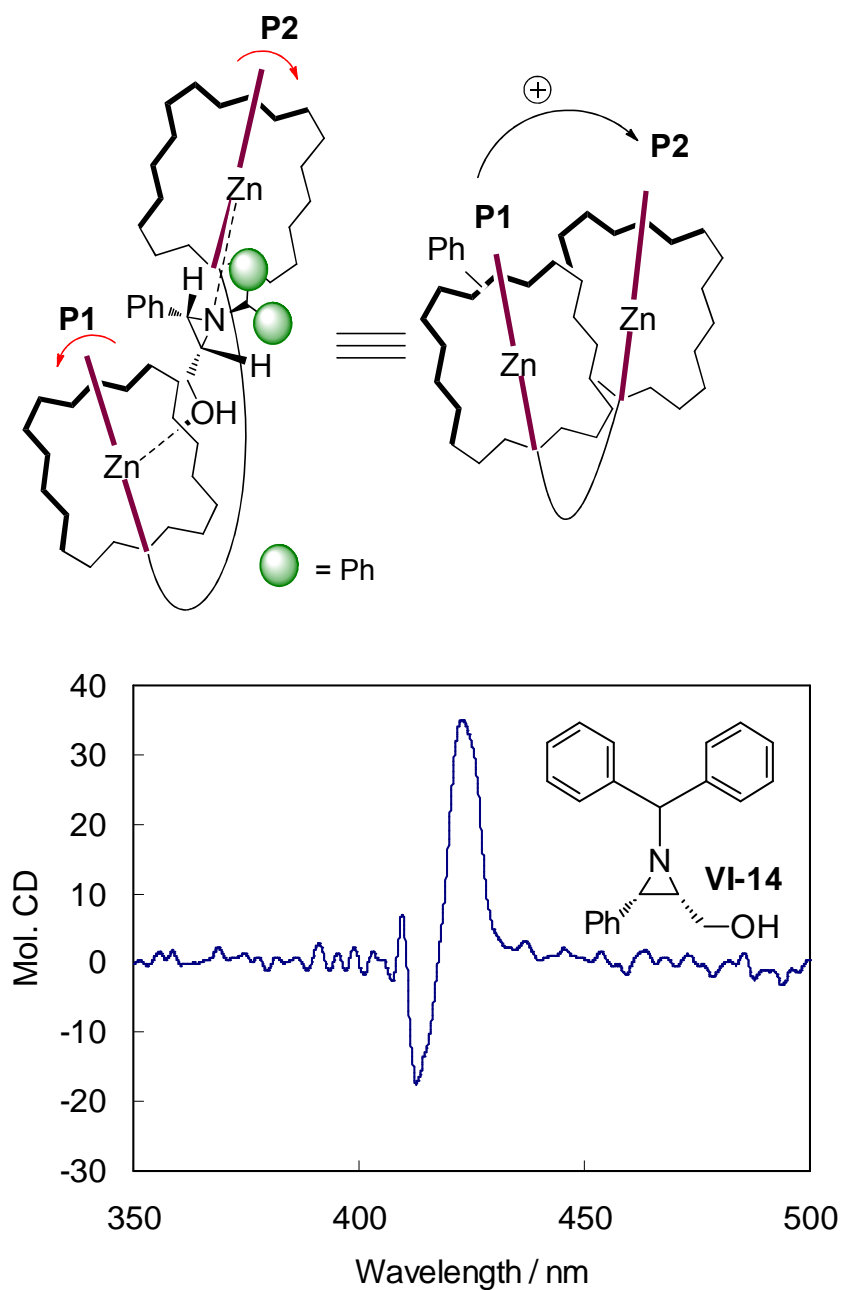


Figure VI-8. Proposed binding model for N-benzhydryl aziridinol with tweezer; Positive EEC spectrum was obtained for N-benzhydryl aziridinol **VI-14** (40 eq.) with tweezer **II-25** (2 μ M) in hexane at 0 $^{\circ}$ C.

As to the stereodifferentiation, **P1** is facing H at C3 and bulky benzhydryl group at nitrogen, and apparently it would prefer rotating toward the much smaller H group

as the arrow indicates. **P2** which is *anti* to the benzhydryl after complexation would rotate away from the large phenyl group at C3. Overall, a clockwise helicity of the porphyrin tweezer complex is expected and is actually detected as positive CD couplet during CD measurements.

ECCD study of N-benzhydryl aziridine esters (**VI-6**) was also performed, however no observable ECCD signals were detected for the substrates examined. Unlike the case of free aziridine esters which could benefit from the strong cooperative binding of aziridinic nitrogen, the bulky benzhydryl group introduced large steric interactions which lowered the binding affinity of aziridinic nitrogen toward porphyrin tweezer. Consequently, the cooperative binding is significantly diminished and the overall binding interaction is much weaker compared to free aziridine esters. Therefore, for N-benzhydryl aziridines reduction of ester into alcohol is necessary to acquire enough binding affinity for forming stable ECCD active complex and yielding observable CD signals.

When extremely bulky protecting group (BUDAM) is used, we observed different result. Substrate **VI-8** bearing *2R,3R* configuration rendered intense positive ECCD spectrum (Figure VI-9) upon mixing with tweezer **II-25** in hexane at 0 °C. This observation is opposite to the trend revealed from Scheme VI-7 for N-benzhydryl aziridinols suggesting a different binding mechanism caused by the sterically demanding BUDAM group. Further investigation is necessary to probe this interesting result.

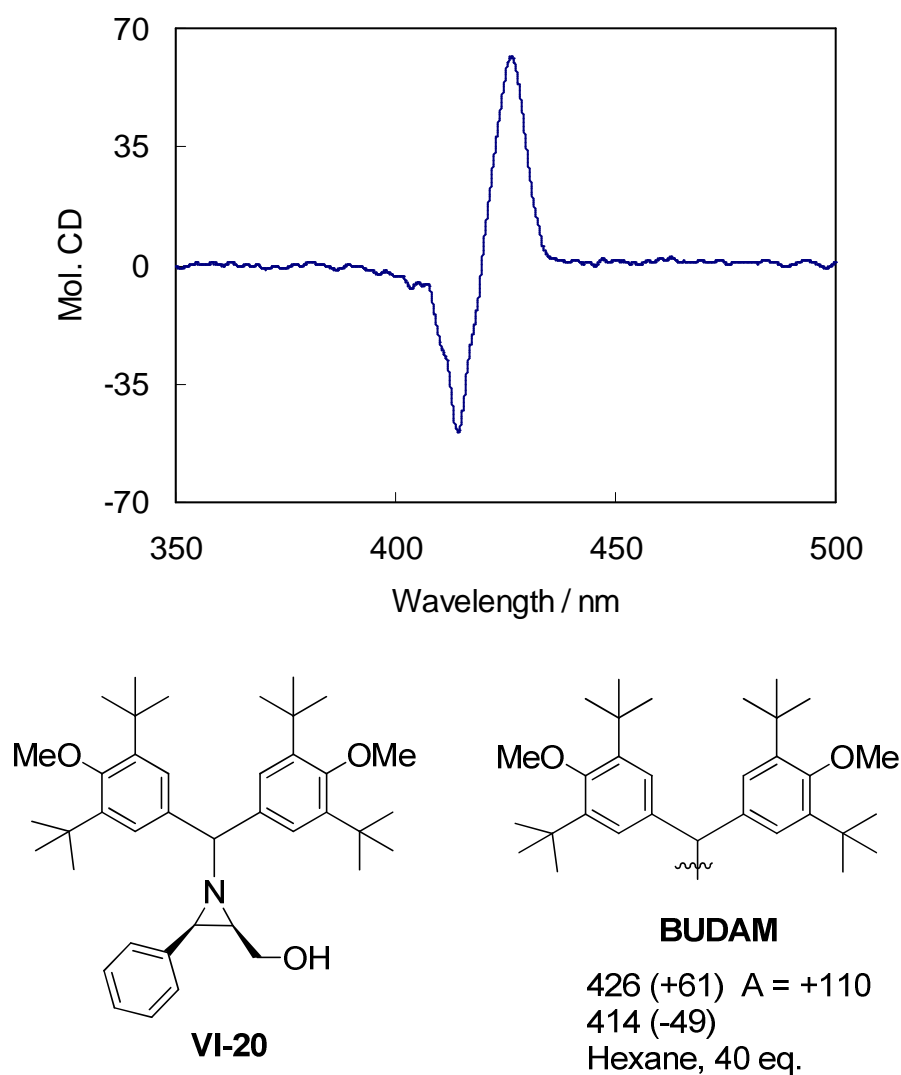
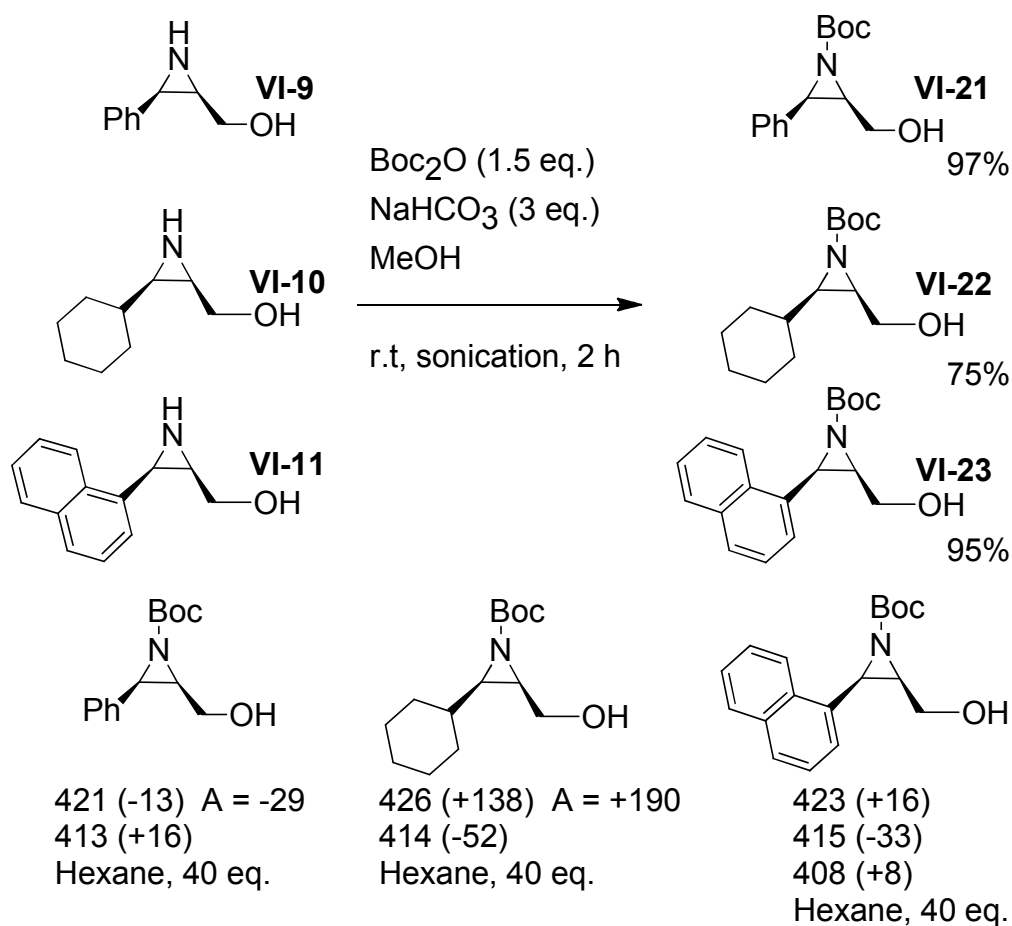


Figure VI-9. ECCD of aziridinol **VI-20** with tweezer **II-25** (2 μ M) in hexane at 0 °C.

Another commonly used protecting group for aziridines is Boc. We prepared three Boc protected aziridinols from unprotected aziridinols using sonification condition⁹ in MeOH (Scheme VI-8) and conducted ECCD experiments. Unfortunately, the obtained ECCD data are inconsistent as shown in Scheme VI-8. The absolute configurations of the three substrates are the same. But **VI-21** gave negative CD couplet while **VI-22** yielded intense positive ECCD signal. Substrate **VI-23** exhibited 3 peaks upon complexation with tweezer **II-25**. This inconsistency

is probably due to the weak binding between tweezer and carbonyl oxygen of the carbamate group. Enhancing the binding interaction by using more Lewis acidic porphyrin tweezer may solve this issue.



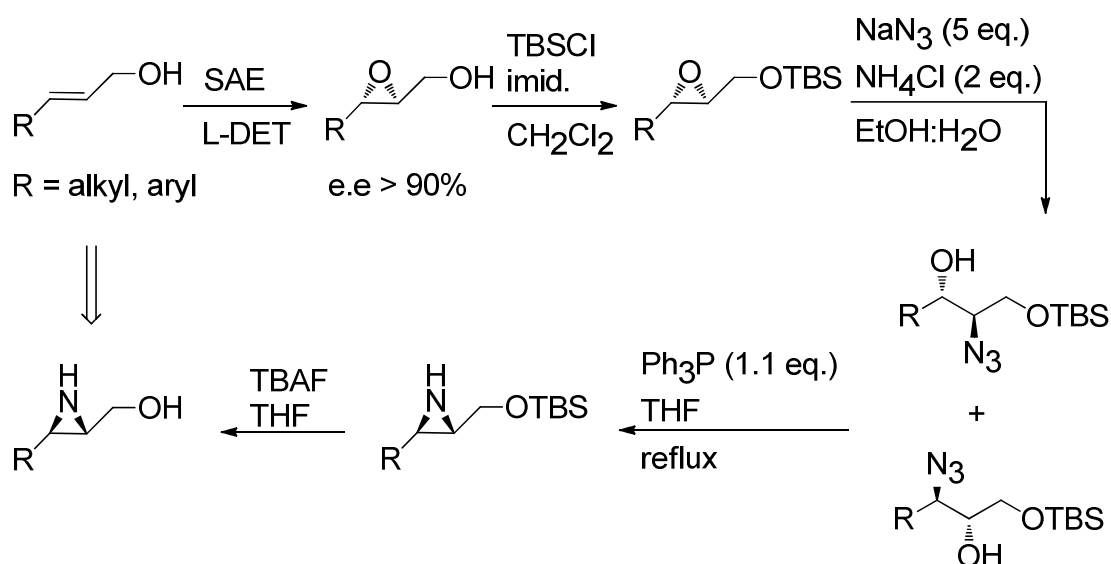
Scheme VI-8. Synthesis of N-Boc-protected aziridinols and their ECCD data with tweezer **II-25** (2 μ M) in hexane 0 °C.

VI.2.2 ECCD study of *trans* chiral aziridines using tweezer **II-25**

Next, we tested our host system with *trans* aziridinols. We prepared *trans*-aziridinols indirectly from chiral epoxy alcohols as shown in Scheme VI-9.

The chiral epoxy alcohol was synthesized using SAE condition and following TBS

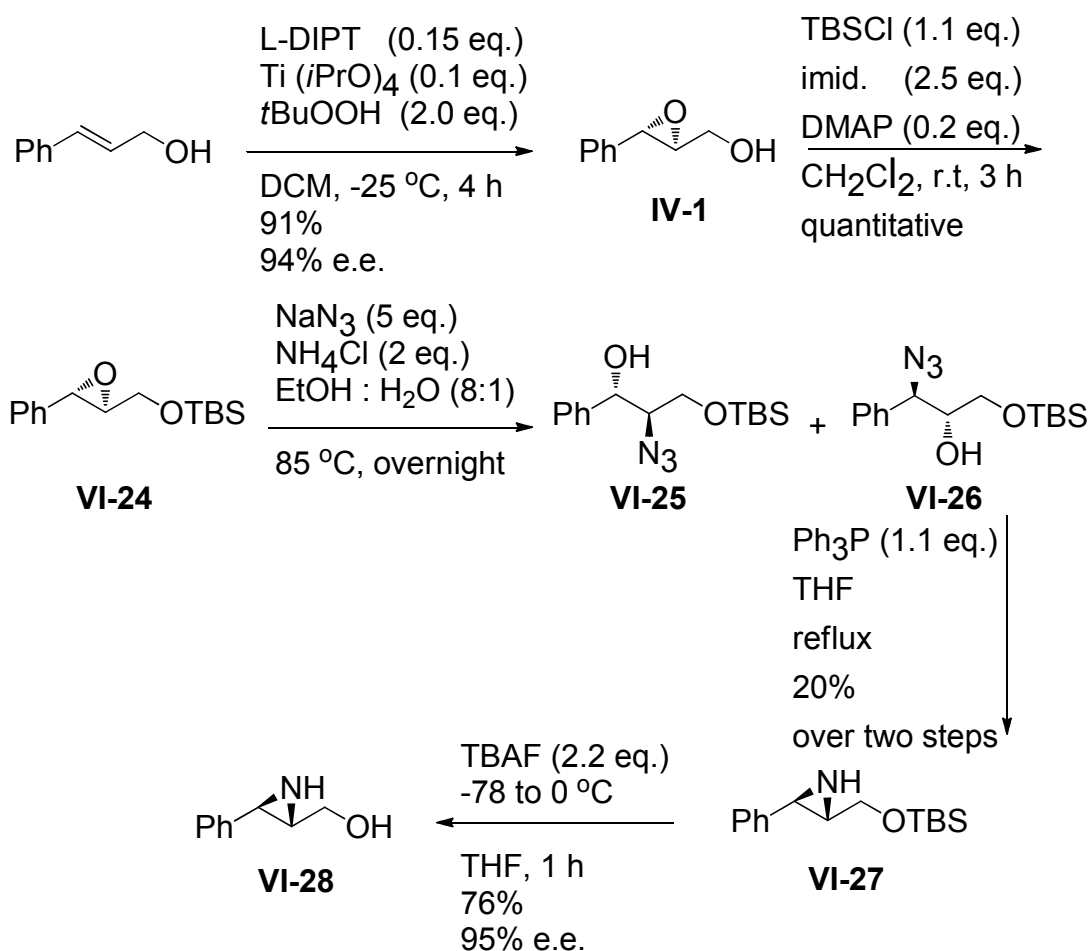
protection afforded the protected epoxide, which readily underwent ring opening by NaN_3 to yield a mixture of azido alcohol regioisomers. Reductive ring closing mediated by Ph_3P in refluxing THF led to OTBS protected aziridine which upon desilylation by TBAF furnished the desired *trans* chiral aziridinols in good optical purity. It is anticipated that the *trans* aziridinols should behave the same as *trans* epoxy alcohols due to structural similarity and render predictable signals in ECCD measurements.



Scheme VI-9. Synthetic route for *trans* chiral aziridinol.

Chiral aziridinol **VI-28** was obtained via the route described in Scheme VI-10. The ring opening reaction was conducted in EtOH / H_2O at 85 °C. Other solvent systems such as $\text{MeOCH}_2\text{CH}_2\text{OH}$ / H_2O was also tested using racemic substrates and afforded the same products. Temperature above 90 °C was detrimental since the TBS group fell off. The reductive ring closing of the crude mixture of azido

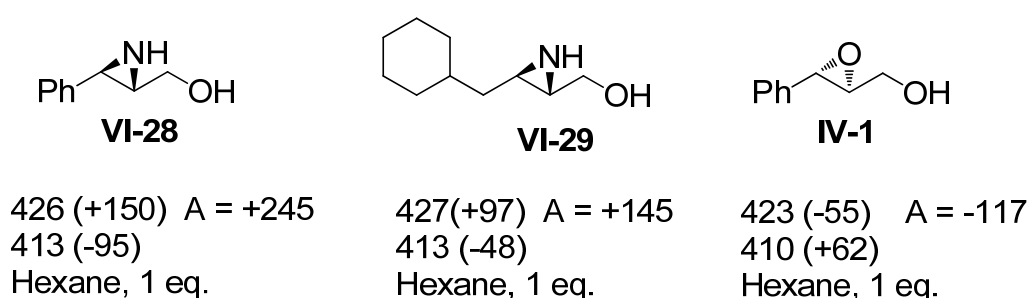
alcohols by Ph_3P produced low yields. The purification of azido alcohols by column chromatography may be necessary to improve the yield. During the synthesis of *trans* unprotected aziridinol **VI-29**, purification of azidols by column chromatography did lead to an improved ring closing yield (67%)



Scheme VI-10. Synthesis of *trans* chiral aziridinol **VI-28**.

Subsequent ECCD study with Zn TPFP tweezer **II-25** in hexane revealed positive CD signals for the two substrates (**VI-28**, **VI-29**) bearing *2S,3R* configuration. This observation agrees well with the *trans* epoxy alcohol case in which *2R,3R* chiral

epoxy alcohols exhibited positive ECCD couplet upon mixing with Zn TFPF tweezer **II-25** in hexane (see Table IV-1 in chapter IV). So, the same binding mechanism is operative in both cases considering their structural similarity. Similar to the *cis* case, *trans* aziridinol demonstrated much stronger binding affinity toward zinc porphyrin tweezer than its epoxy alcohol analog by yielding more intense CD signal when only 1 eq. of substrate was added.



Scheme VI-11. ECCD data of *trans* aziridinols (1 eq.) with tweezer **II-25** (2 μ M) in hexane 0 °C

The stereodifferentiation process is similar to the epoxy alcohol case and was shown in Figure VI-10. The two porphyrins would approach from opposite sides of aziridine ring to avoid clashing. **P1** senses the steric bias between the bulky R_1 at C3 position and the small hydrogen at the C2 position. As a result, the **P1** porphyrin would rotate away from bulky R_1 to minimize steric interaction. The resultant counterclockwise helicity of the complex gave rise to a negative ECCD signal corresponding to the *2R,3S* substrate. Accordingly, for *2S,3R trans* aziridinols positive CD couplet was expected and indeed obtained as shown for **VI-28** (Figure VI-11).

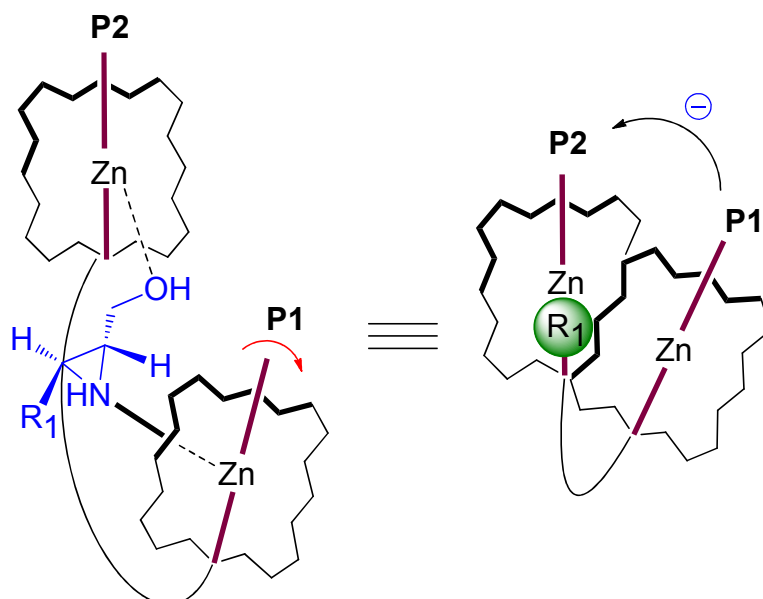


Figure VI-10. Proposed binding mode between tweezer **II-25** and *trans* (2*R*,3*S*) unprotected aziridinol.

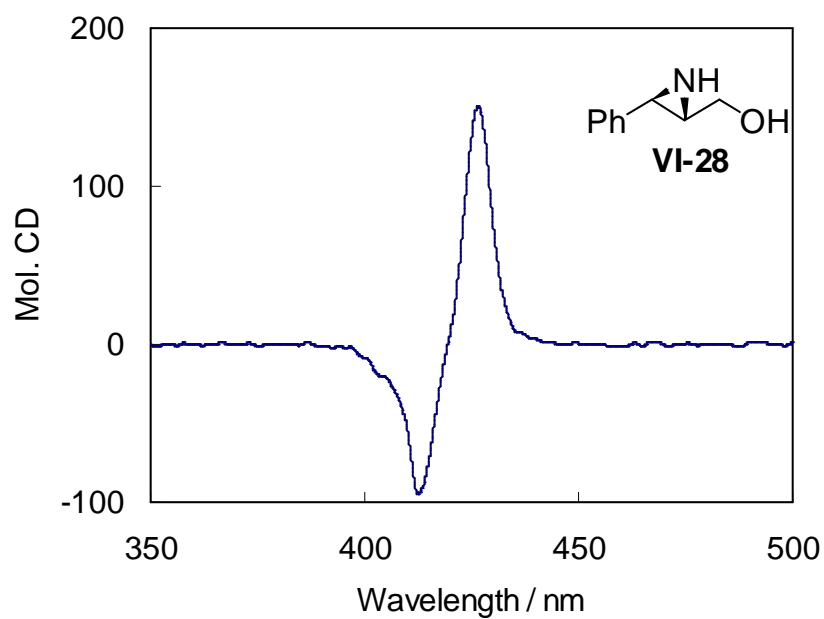


Figure VI-11. Positive EECDD was obtained for *trans* (2*S*,3*R*) substrate **VI-28** (1 eq.) with tweezer **II-25** (2 μ M) in hexane at 0 °C.

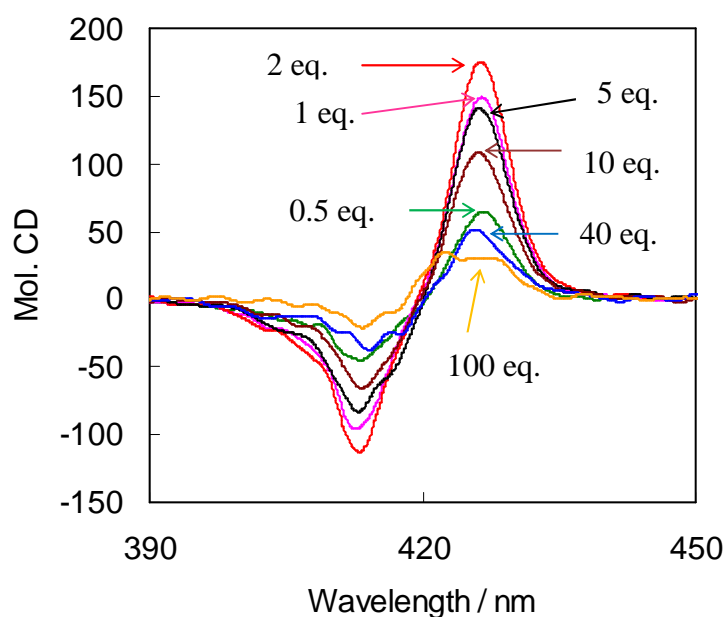
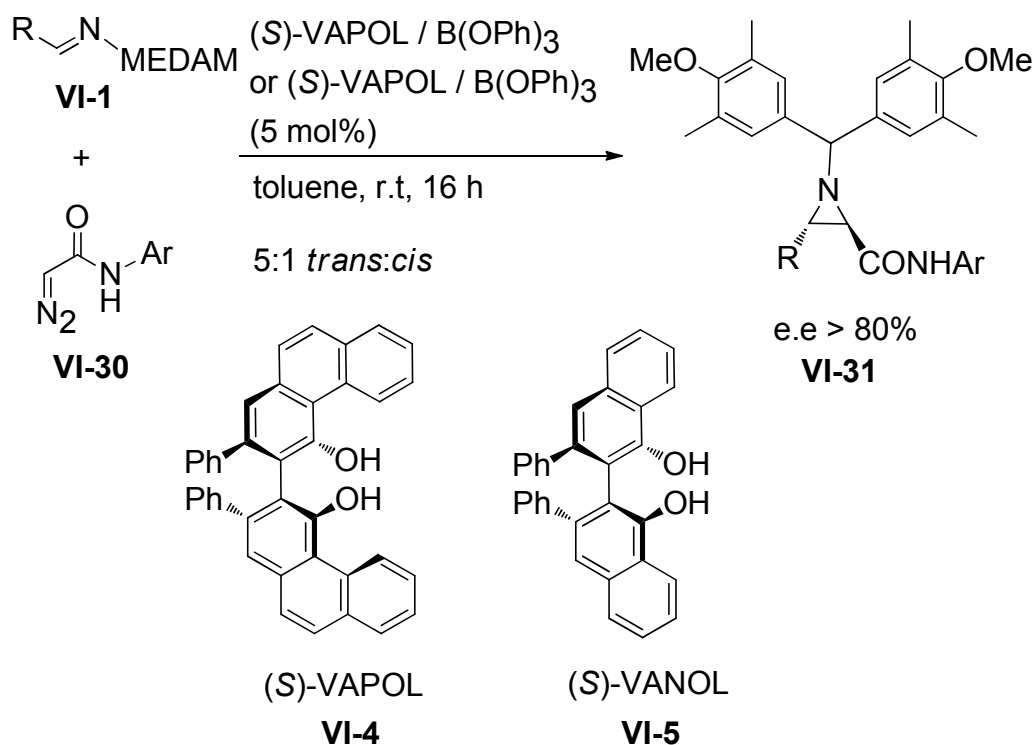


Figure VI-12. ECCD spectra of tweezer **II-25** (2 μ M in hexane) with *trans* (*2S,3R*) substrate **VI-28** at 0 °C at different equivalents.

Close inspection of the CD titration process between aziridinol **VI-28** and tweezer **II-25** revealed a dynamic change of ECCD amplitude (Figure VI-12). The amplitude kept increasing while starting titration at 0.1 eq. of aziridinol and maximized at 2 eq. of substrate. Further addition of guest molecule led to dramatic decrease of CD amplitude. Up to 5 fold decrease of signal strength was detected after 100 eq. of **VI-28** was introduced. This dynamic behavior is attributed to the competitive binding of aziridinic nitrogen with hydroxyl group when more guest molecules are added. It corresponds to the two step binding process that was illustrated in Scheme VI-4 for unprotected *cis* aziridinol. Therefore, when unprotected aziridinol was used for ECCD study with Zn-TPFP porphyrin tweezer, one should avoid the use of large excess of substrate since it tends to give inferior CD signals. One or two equivalents is considered as the optimal amount.



Scheme VI-12. Catalytic asymmetric synthesis of *trans* aziridines.

Recently, Prof. Wulff's lab¹⁰ has had great success in *trans*-aziridination with the same chiral catalysts (VAPOL / VANOL) while using primary diazoamides instead of diazoesters as carbene source (Scheme VI-12). This modification led to good *trans* selectivity as well as enantioselectivity. Reduction of the resultant aziridine amides for ECCD study is not recommended since it requires harsher conditions compared to the reduction of aziridine esters and would risk opening the aziridine ring. However, the stronger nucleophilicity of amide functionality over ester could be beneficial because it could enable the direct complexation of the zinc porphyrin tweezer with aziridine nitrogen protected. A number of chiral aziridine amides protected with MEDAM were kindly provided by Mr. Aman Desai (Professor Wulff group) and we conducted ECCD measurements with zinc porphyrin tweezer **II-25** in hexane at 0 °C.

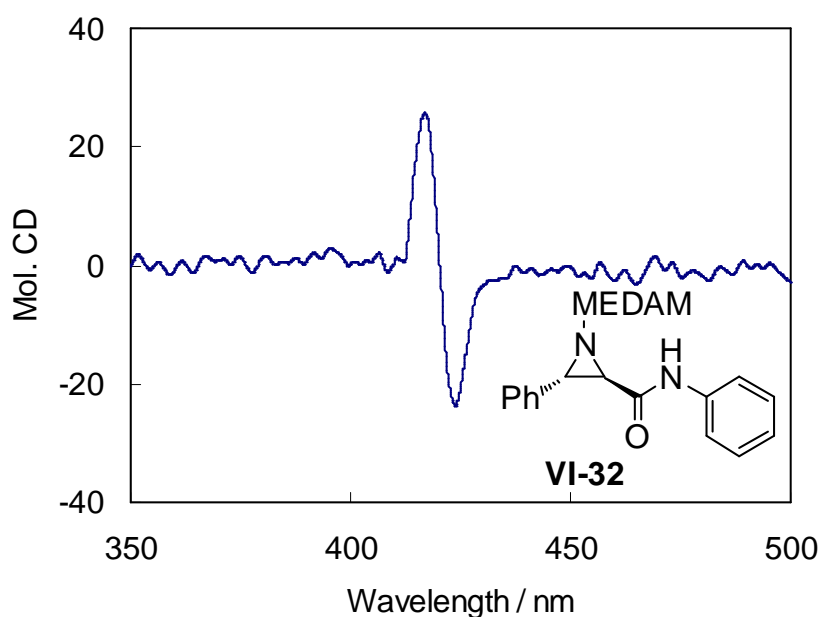


Figure VI-13. ECCD spectrum of *trans*-(2*R*,3*S*) amide **VI-32** (5 eq.) with tweezer **II-25** (2 μ M) in hexane at 0 °C.

As expected, the aziridine amides bound well with zinc tweezer **II-25** and exhibited consistent CD signals during titration of tweezer at different equivalents. Amide **VI-32** yielded the bisignate CD curve as shown in Figure VI-13, but three Cotton effects were seen for amides **VI-33** and **VI-34** (Figure VI-14 and Figure VI-15) at varying equivalents. We speculate that this complication is caused by the weaker nucleophilicity of amide carbonyl compared to that of **VI-32**. However, it is instructive that the correlation of the first Cotton effect with the substrate chirality is still consistent. For amides with 2*R*,3*S* configuration (**VI-32** and **VI-33**), the first

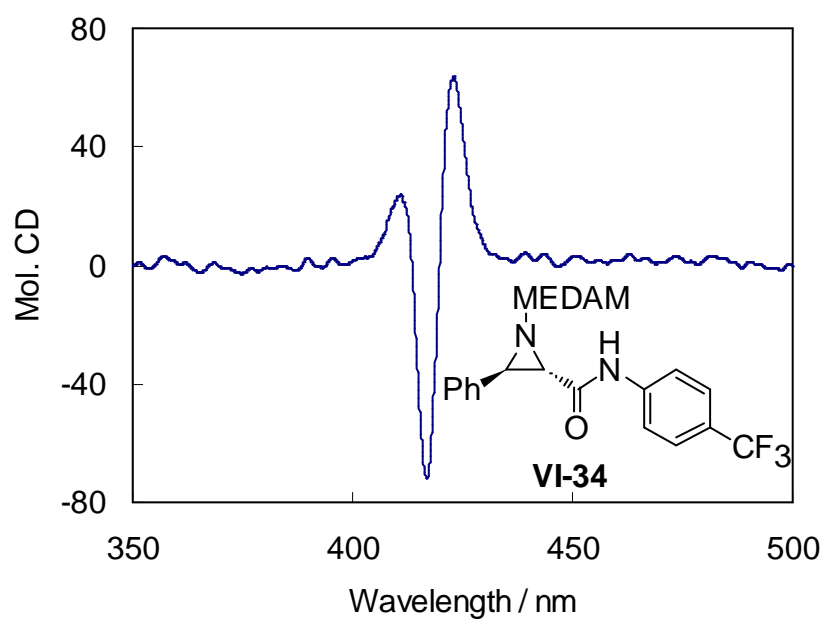


Figure VI-14. ECCD spectrum of *trans*-(2*S*,3*R*) amide **VI-33** (20 eq.) with tweezer **II-25** (2 μ M) in hexane at 0 °C

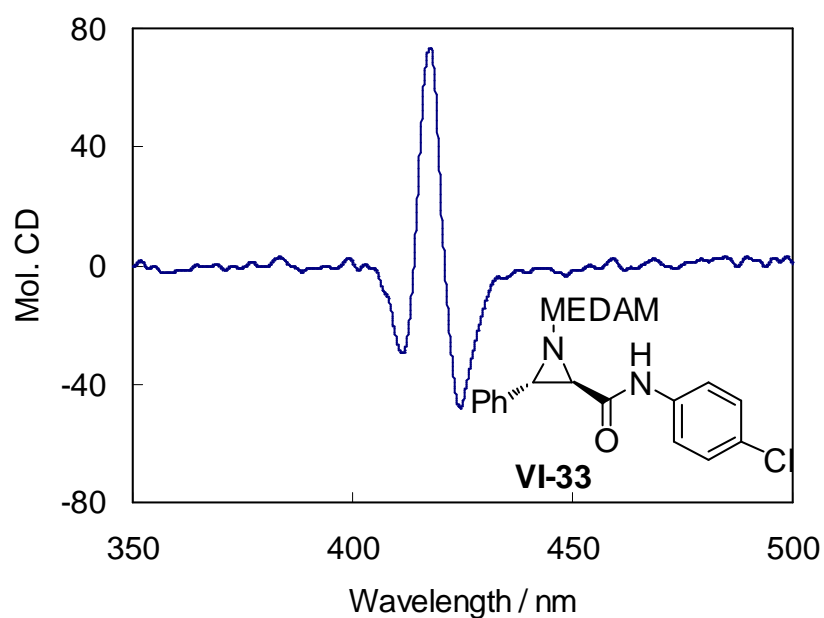
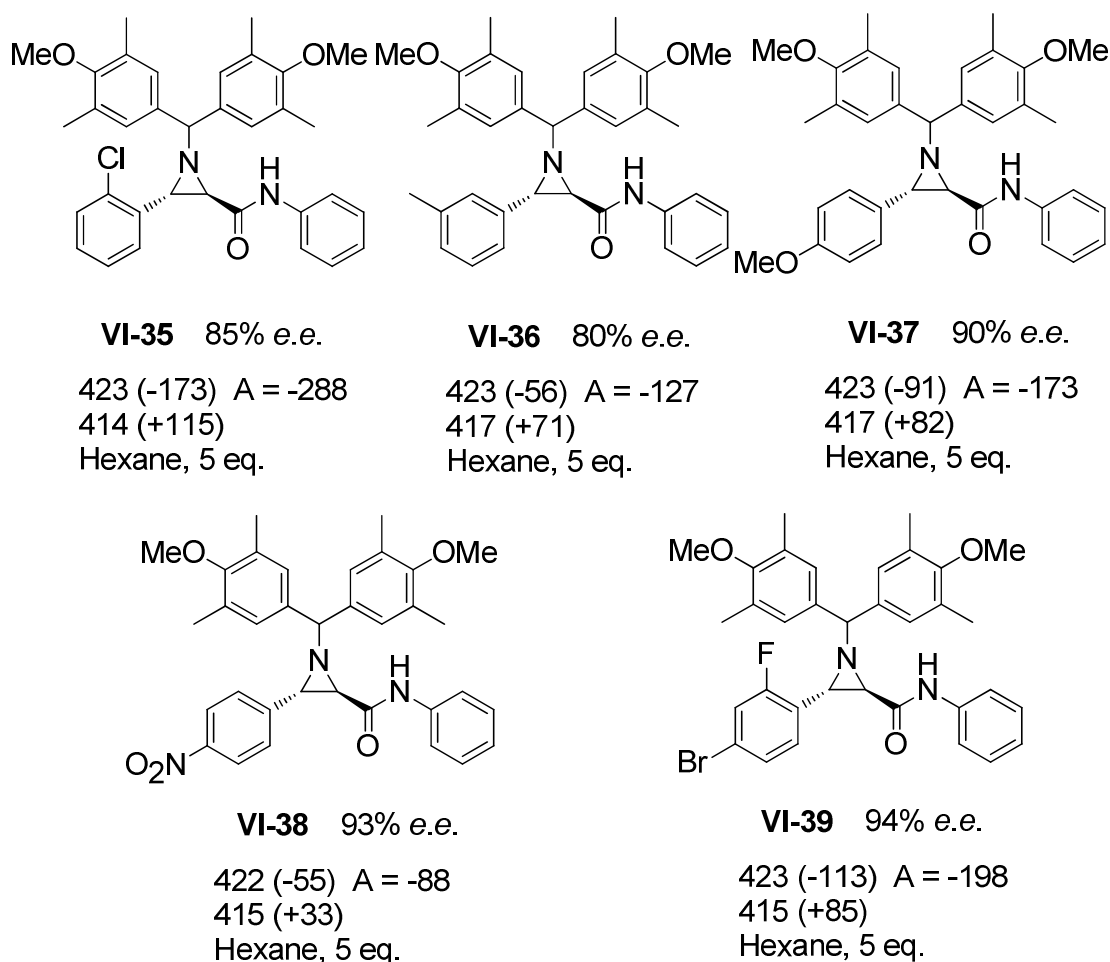


Figure VI-15. ECCD spectrum of *trans*-(2*R*,3*S*) amide **VI-34** (5 eq.) with tweezer **II-25** (2 μ M) in hexane at 0 °C

Cotton effect is negative. Accordingly, positive first Cotton effect was seen for amide **VI-34** with *2S,3R* configuration (Figure VI-14). Amides **VI-35~VI-39** bearing the same N-aryl substituent as **VI-32** were then submitted for ECCD study. As shown in Scheme VI-13, all the substrates with (*2R,3S*) configuration yielded smooth and strong negative bisignate CD couplets after complexation with tweezer **II-25**.



Scheme VI-13. ECCD data of *trans*- (*2R,3S*) amides (5 eq.) with tweezer **II-25** (2 μ M) in hexane at 0 °C.

The prominent CD signals are in sharp contrast to the ECCD silence of

N-benzhydryl aziridine esters proving that the improved binding affinity of amide substrate plays a crucial role for the formation of stable ECCD active complex. As anticipated, there is no need to convert the amide functionality since the acquired signals are fairly intense. The electronic property of the substituent at C3 position clearly affected the ECCD amplitude. In the presence of electron rich 4-MeO-phenyl group (**VI-37**), the CD amplitude is as high as -173 at 5 eq. of guest molecule. The introduction of electron poor 4-NO₂-phenyl group (**VI-38**) led to the reduction of CD amplitude by 2 fold ($A = -88$). The substitution pattern of aryl ring at C3 position also affected the ECDD signal. The *ortho* substitution (**VI-35**, **VI-39**) favors stereodifferentiation process by yielding much stronger CD couplet despite the fact that in both molecules the electron density of the aryl ring is lower compared to **VI-36**, and **VI-37**. This is probably due to the increased sterics in the presence of *ortho* substituted group since it is closer to the chiral center and consequently leads to a larger steric bias detected by porphyrin tweezer.

Interpretation of the binding process requires consideration of several factors. First, unlike the unprotected aziridinols, the pyramidalization of aziridinic nitrogen cannot be neglected due to the presence of bulky MEDAM group. This pyramidalization would determine the orientation of the electron lone pair as well as the approach fashion of the zinc porphyrin tweezer. Secondly, the bulky MEDAM group probably would force the aziridinic nitrogen to point toward the upper region of the binding pocket due to potential unfavorable steric interaction between MEDAM and tweezer linker.

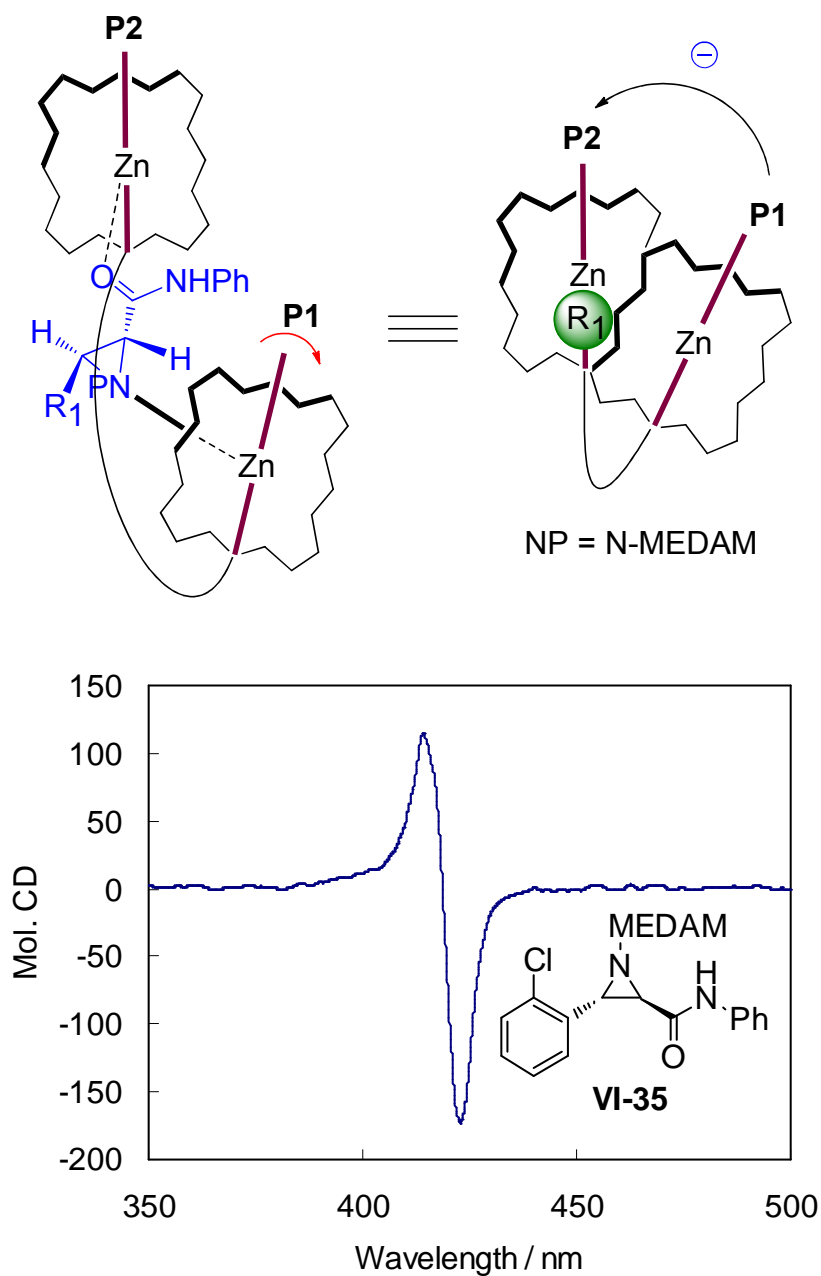


Figure VI-16. Proposed binding mode between tweezer **II-25** and *trans* (2*R*,3*S*) N-MEDAM aziridine amide; Negative ECCD was obtained for *trans* (2*R*,3*S*) substrate **VI-35** (5 eq.) with tweezer **II-25** (2 μ M) in hexane at 0 °C.

It is interesting to point out that the correlation of observed ECCD sign and substrate chirality is the same as that for unprotected *trans* aziridine amide as shown

in Figure VI-16. This correlation is also the same as that for *trans* epoxy alcohols as well as unprotected *trans* aziridinols. Further investigation is needed to elicit more specific proof for the complexation pattern.

In conclusion, Zn-TPFP tweezer demonstrated its efficiency in absolute stereochemical determination for chiral aziridines. The chirality of aziridinols can be unequivocally assigned based on the similar binding mechanism revealed for the epoxy alcohols owing to their structural similarity to epoxy alcohols. This method is more sensitive for unprotected aziridinols than epoxy alcohols because of the stronger binding interaction of aziridinic nitrogen. N-Benzhydryl protected aziridinols are surprisingly ECCD active exhibiting consistent CD couplets upon complexation with zinc porphyrin tweezer. A distinct binding mechanism was proposed. N-Boc protected aziridinols rendered inconsistent behavior during ECCD study and employment of new porphyrin tweezer with further improved Lewis acidity may help resolve this issue. N-MEDAM protected *trans* aziridine amides can be directly used for ECCD measurements owing to the strong nucleophilicity of amide functionality. Prominent ECCD spectra were acquired for aziridine amides and an interesting trend was disclosed. This study revealed fairly encouraging results. More importantly, it furthered our understanding to the chiral recognition behavior involving porphyrin tweezer system and provided valuable insights for the development of novel chirality sensors. An offshoot of this study would be the ECCD study of other nitrogen containing heterocycles such as pyrrolidines which are frequently encountered in organic synthesis. We are confident that the hydroxyl pyrrolidines could bind well

with zinc porphyrin tweezer and systematic ECCD study of this class of compounds is necessary.

Experimental Procedures

Materials and general instrumentations:

Anhydrous CH_2Cl_2 was dried and redistilled over CaH_2 . The solvents used for CD measurements were purchased from Aldrich and were spectra grade. All reactions were performed in dried glassware under nitrogen. Column chromatography was performed using SiliCycle silica gel (230-400 mesh). ^1H NMR and ^{13}C NMR spectra were obtained on a Varian Inova 300 MHz instrument and are reported in parts per million (ppm) relative to the solvent resonances (δ), with coupling constants (J) in Hertz (Hz). IR studies were performed on a Nicolet FT-IR 42 instrument. UV/Vis spectra were recorded on a Perkin-Elmer Lambda 40 spectrophotometer, and are reported as λ_{max} [nm]. CD spectra were recorded on a JASCO J-810 spectropolarimeter, equipped with a temperature controller (Neslab 111) for low temperature studies, and were reported as $\lambda[\text{nm}]$ ($\Delta\epsilon_{\text{max}}$ [$\text{L mol}^{-1} \text{cm}^{-1}$]). Optical rotations were recorded at 20 °C on a Perkin Elmer 341 Polarimeter ($\lambda = 589 \text{ nm}$, 1 dm cell). Chiral GC analyses were performed on a Hewlett Packard 6890 gas chromatograph equipped with a Supelco Gamma Dex 225 column (0.25 mm \times 30 m) using helium as carrier gas. HRMS analyses were performed on a Q-TOF Ultima system using electrospray ionization in positive mode.

General procedure for CD measurement:

Zinc porphyrin tweezer **II-25** (2 μL of a 1 mM solution in anhydrous CH_2Cl_2) was added to hexane (1 mL) in a 1.0 cm cell to obtain a 2 μM tweezer **II-25** solution.

The background spectrum was recorded from 350 nm to 550 nm with a scan rate of 100 nm/min at 0 °C. Chiral epoxy alcohol (1 to 20 μ L of a 10 mM solution in anhydrous CH_2Cl_2) was added into the prepared tweezer solution to afford the host/guest complex. The CD spectra were measured immediately (minimum of 4 accumulations). The resultant ECCD spectra recorded in millidegrees were normalized based on the tweezer concentration to obtain the molecular CD (Mol CD).

All aziridine esters were kindly provided by Professor Wulff.

To a solution of phenyl substituted free aziridine ester (58.9 mg, 0.308 mmol) in dry Et_2O (5 mL) at 0 °C, was added LAH (23.4 mg, 0.616 mmol). The mixture was stirred at 0 °C for 2 h and quenched by careful addition of Et_2O (10 mL), H_2O (1 mL), and 2 M NaOH (1 mL). The solution was stirred for 30 min and then filtered through celite. After thorough washing of the filter cake with Et_2O , the filtrate was dried over Na_2SO_4 and concentrated under reduced pressure. Flash chromatography (5% MeOH / EtOAc) afforded **1** as white solid (36.1 mg, 78%). ^1H NMR (CDCl_3 , 300 MHz) δ 1.67 (br, s, 1H), 2.65 (q, 1H, $J' = 6.6$ Hz, $J'' = 6.0$ Hz), 3.25 (dd, 1H, $J' = 11.7$ Hz, $J'' = 6.9$ Hz), 3.41 (dd, 2H, $J' = 12.0$ Hz, $J'' = 6.0$ Hz), 7.31 (m, 5H).¹¹

REFERENCES

References

1. Tanner, D., Chiral Aziridines - Their Synthesis and Use in Stereoselective Transformations. *Angewandte Chemie-International Edition in English* **1994**, 33, (6), 599-619.
2. Muller, P.; Fruit, C., Enantioselective catalytic aziridinations and asymmetric nitrene insertions into CH bonds. *Chemical Reviews* **2003**, 103, (8), 2905-2919.
3. Vilaivan, T.; Bhanthumnavin, W.; Sritana-Anant, Y., Recent advances in catalytic asymmetric addition to imines and related C=N systems. *Current Organic Chemistry* **2005**, 9, (14), 1315-1392.
4. Pineschi, M., Asymmetric ring-opening of epoxides and aziridines with carbon nucleophiles. *European Journal of Organic Chemistry* **2006**, (22), 4979-4988.
5. McCoull, W.; Davis, F. A., Recent synthetic applications of chiral aziridines. *Synthesis-Stuttgart* **2000**, (10), 1347-1365.
6. Antilla, J. C.; Wulff, W. D., Catalytic asymmetric aziridination with a chiral VAPOL-boron Lewis acid. *Journal of the American Chemical Society* **1999**, 121, (21), 5099-5100.
7. Zhang, Y.; Desai, A.; Lu, Z. J.; Hu, G.; Ding, Z. S.; Wulff, W. D., Catalytic asymmetric aziridination with borate catalysts derived from VANOL and VAPOL ligands: Scope and mechanistic studies. *Chemistry-a European Journal* **2008**, 14, (12), 3785-3803.
8. Zhang, Y.; Lu, Z. J.; Wulff, W. D., Catalytic Asymmetric Aziridination with Catalysts Derived from VAPOL and VANOL. *Synlett* **2009**, (17), 2715-2739.
9. Lu, Z. J.; Zhang, Y.; Wulff, W. D., Direct access to N-H-aziridines from asymmetric catalytic aziridination with borate catalysts derived from vaulted binaphthol and vaulted biphenanthrol ligands. *Journal of the American Chemical Society* **2007**, 129, (22), 7185-7194.
10. Desai, A.; Wulff, W. D., In 2009.
11. Gennari, C.; Vulpetti, A.; Pain, G., Highly enantio- and diastereoselective boron aldol reactions of alpha-heterosubstituted thioacetates with aldehydes and silyl imines. *Tetrahedron* **1997**, 53, (16), 5909-5924.

Chapter VII

Elucidating the Absolute Configurations for Functionalities in Complex Molecules using TFPF Tweezer: The Case Study in Natural Products

VII.1 Background

In previous chapters, we described development of new porphyrin tweezers (**II-25** and **V-12**) and their successful applications in absolute stereochemical determination of a variety of organic molecules bearing nitrogen- or oxygen-containing functionalities. In most cases, prominent ECCD signals were observed and consistent trends were derived for assigning the chirality of substrates in a nonempirical fashion. However, the compounds examined are mostly simple molecules with two functionalities which serve as binding sites. In this chapter, we challenged the newly developed chirality sensor (**II-25**) with a number of complex molecules bearing multiple chiral centers and heteroatom functionalities to interrogate its efficiency in elucidating the absolute stereochemistry of functionalities within complex molecules. The results would provide valuable guidelines for chirality sensing by porphyrin tweezer hosts.

VII.2 ECCD Study of Steroids

Steroids are good candidates for ECCD study of complex molecules since the functionalities are geometrically fixed in the rigid molecular skeleton, thus providing

well-defined binding sites and facilitating the investigation of stereodifferentiation process. The relevant ECCD study would also yield important insights about the stereochemical determination of chiral functionalities in *cyclic* substrates, which are complementary to the studies discussed in previous chapters for acyclic substrates.

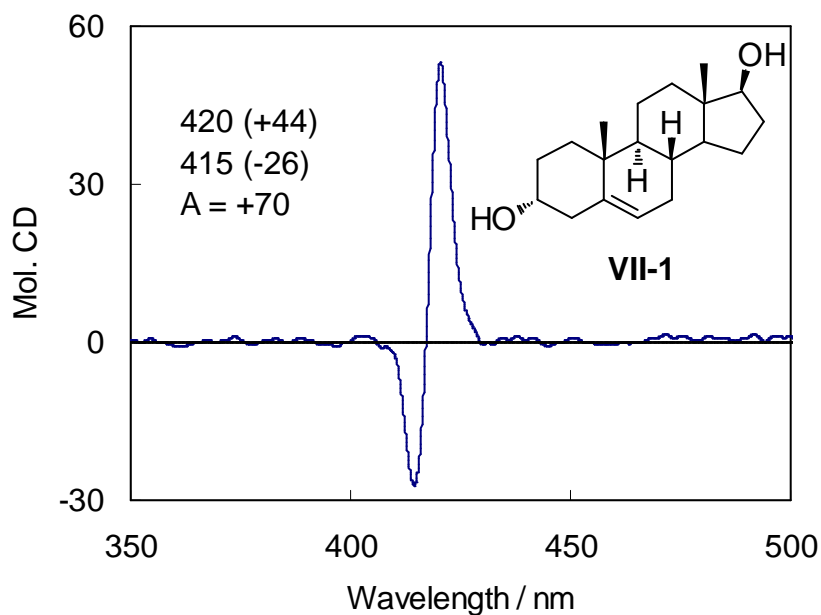


Figure VII-1. ECCD spectra of **VII-1** (20 eq.) with tweezer **II-25** (2 μ M) in MCH at 0 °C.

Several steroidal diols were the subjects of our ECCD study. All the substrates gave strong CD couplets upon binding with Zn-TPFP tweezer **II-25** in methylcyclohexane at 0 °C. 3 α ,17 β -Androstene diol **VII-1** rendered steady positive ECCD signals (Figure VII-1) suggesting that the two OH groups bound tweezer host well to form ECCD active complex despite the long distance (ca. 10 Å) between the two binding sites. The UV-vis profile of tweezer-steroid complex in Figure VII-2 demonstrated a clear isosbestic point, signifying the conversion of free unbound

tweezer to complexed tweezer. Nonlinear least square analysis of the change in absorption yielded a binding constant of $8.65 \times 10^3 \text{ M}^{-1}$ for binding of **VII-1** with fluorinated tweezer **II-25** in MCH. This value is close to the binding affinity ($\sim 10^4 \text{ M}^{-1}$) of vicinal diols with tweezer **II-25** in MCH showing that the porphyrin tweezer can accommodate this sterically demanding molecule fairly well and demonstrate good binding affinity.

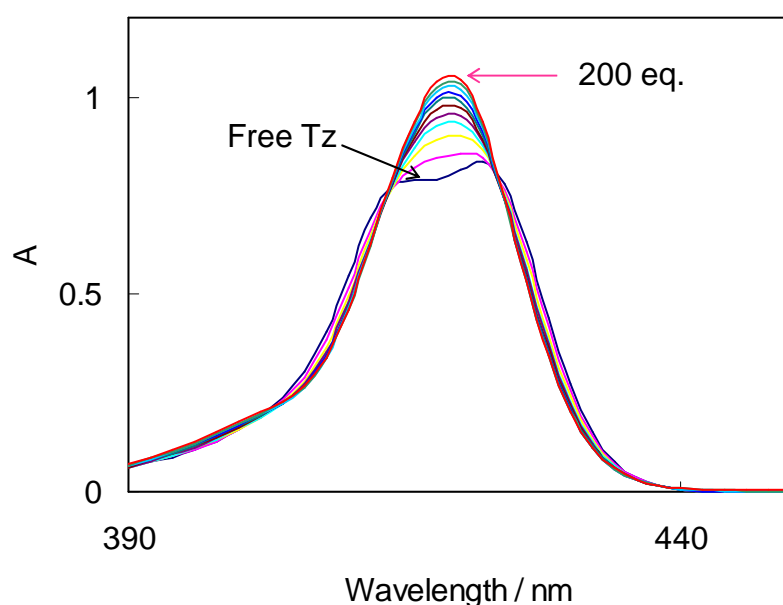


Figure VII-2. UV-Vis spectra change upon titration of tweezer **VII-25** ($1 \mu\text{M}$ in MCH) with **VII-1** (10 mM in DCM).

5β -Pregnane- 3α - 20α -diol **VII-2** and pregnene- 3β - 20α -diol **VII-3** were also examined with tweezer **II-25** and highly encouraging results were obtained. The former led to positive ECCD spectra and the latter returned intense negative ECCD signals (Figure VII-3). Therefore, the porphyrin tweezer can sense the change of stereochemistry of hydroxyl group at C3 position.

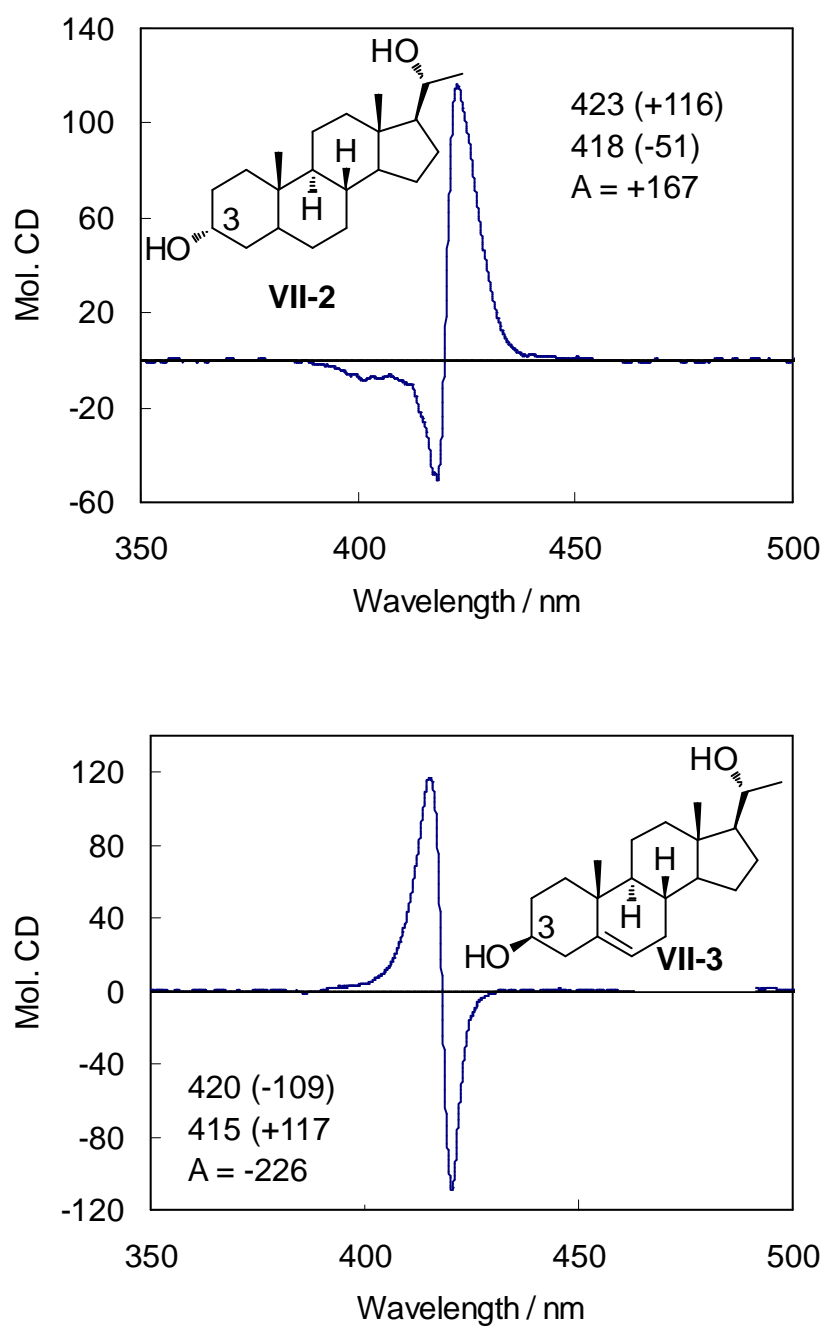


Figure VII-3. ECCD spectra of **VII-2** (40 eq.) and **VII-3** (40 eq.) with tweezer **II-25** (2 μ M) in MCH at 0 $^{\circ}$ C.

After careful analysis of these data, we tentatively proposed that the major function of zinc porphyrin tweezer here is to introduce the strong chromophores and the

relative orientation of the two porphyrin chromophores upon complexation is dictated by the relative orientation of the two OH groups. Each porphyrin would still feel the steric bias at the chiral centers, but the overall helicity of the resultant supramolecular complex was mainly governed by the relative orientation of functionalities that bind to porphyrins. According to this proposal, the interpretation of the signs for observed ECCD signals is illustrated in Figure VII-4.

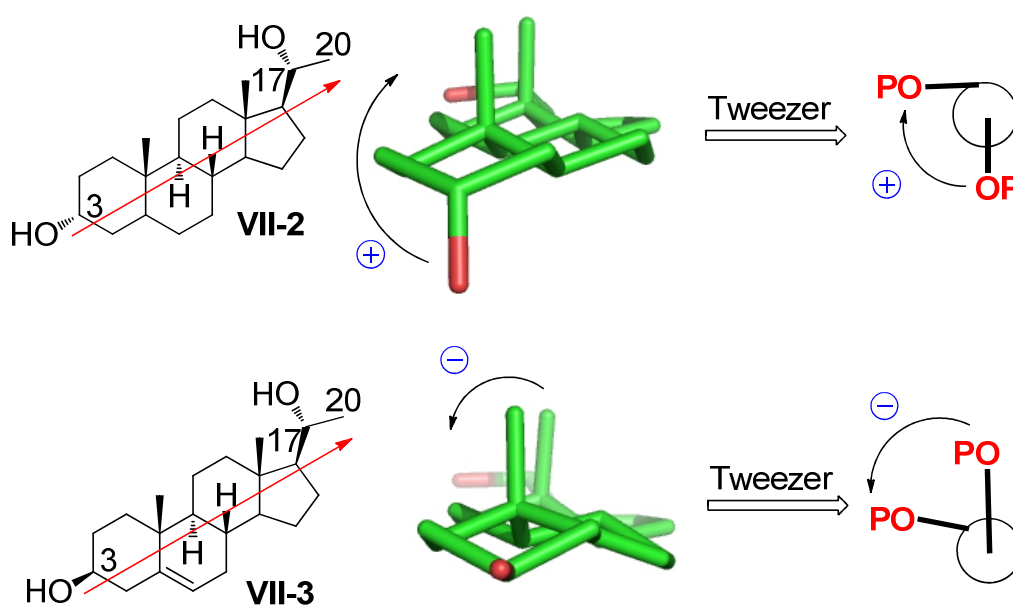


Figure VII-4. Interpretation of ECCD sign for **VII-2**-tweezer (top) and **VII-3**-tweezer (bottom) complex. The red arrow across the molecule indicated the perspective for looking at the relative orientation of hydroxyl groups.

The relative orientation of two porphyrin chromophores is dictated by the relative orientation of two bound hydroxyl groups. In case of **VII-2**, the two hydroxyl groups are oriented clockwise to each other considering the approach of the tweezer from the least sterically hindered face of the steroid. Therefore, a clockwise helicity of the two porphyrin chromophores is produced and manifested as positive CD

couplet. In case of **VII-3**, the counter clockwise orientation of two hydroxyl groups led to counter clockwise helicity of porphyrin chromophores resulting in a negative ECCD signal. The different helicity of the two cases are induced by the change of chirality at C3 position. As such, the observed ECCD signals could be used to determine the stereochemistry at C3 position for similar substrates. Applying this rule, we may explain the positive CD couplet observed for **VII-1** (Figure VII-5) and the negative ECCD signal for substrate **VII-4** (Figure VII-6).

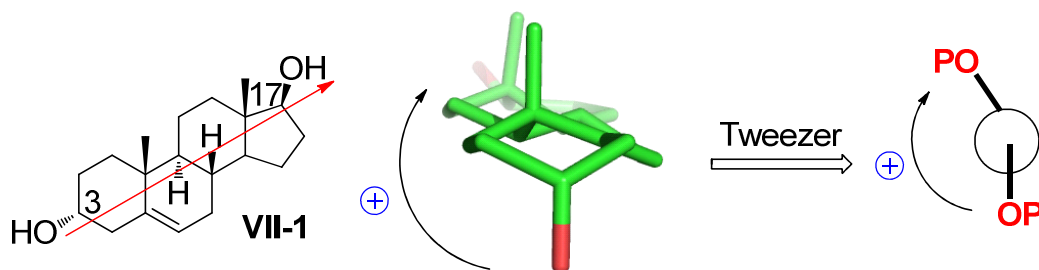


Figure VII-5. Interpretation of the ECCD sign for **VII-1**-tweezer complex.

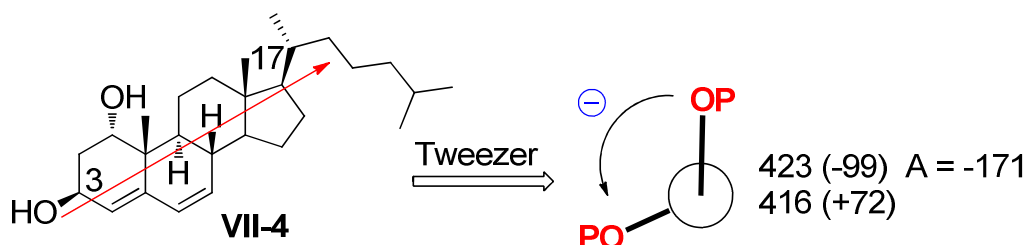


Figure VII-6. Complexation of **VII-4** (40 eq.) with tweezer **II-25** (2 μ M) in MCH at 0 °C led to negative ECCD signal.

The above analysis resembles the ECCD study of steroidal diols via bischromophoric derivatizations with porphyrins (Figure VII-7).^{1, 2} In those cases, figuring out the preferential orientation of porphyrin chromophores is crucial to apply the exciton chirality rule in the derivatized steroid compounds and it is usually a

complicated issue.^{2, 3} Our proposed analysis above for correlating the substrate chirality to the observed ECCD signal with porphyrin tweezer system is a simple speculation at this point and should be used with caution. Further interrogation of this proposal is still necessary.

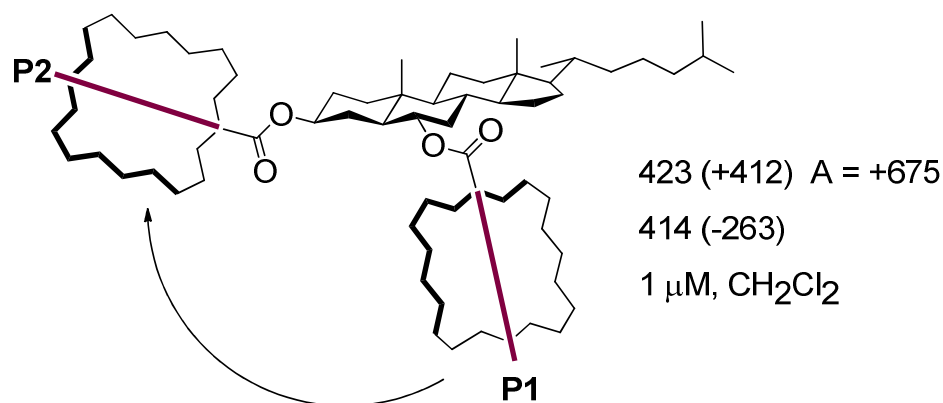


Figure VII-7. Exciton chirality of steroidal diol that is derivatized with porphyrins.

Steroids containing both hydroxyl and ketone functionality are not suitable for stereochemical determination via bischromophoric derivatization since only one hydroxyl group is available for chromophoric derivatization. However, using Zn-TPFP tweezer **II-25**, we may introduce two chromophores via metal-ligand coordination and conduct exciton chirality analysis to elucidate the stereochemistry of the substrate. Several steroidal hydroxyl ketones were tested with TPFP tweezer **II-25** and the results are shown in Figure VII-8. To our delight, all the hydroxy ketones bound well with the porphyrin tweezer and generated intense ECCD signals. The correlation of substrate chirality with the sign of observed ECCD signal follows the same rule that was proposed for steroidal diols. For instance, the relative

orientation of hydroxyl group and ketone in 16,17-dehydro-pregnenolone **VII-5** would result in counter clockwise helicity of bound porphyrins upon complexation with the tweezer, thus leading to the observed negative ECCD spectrum.

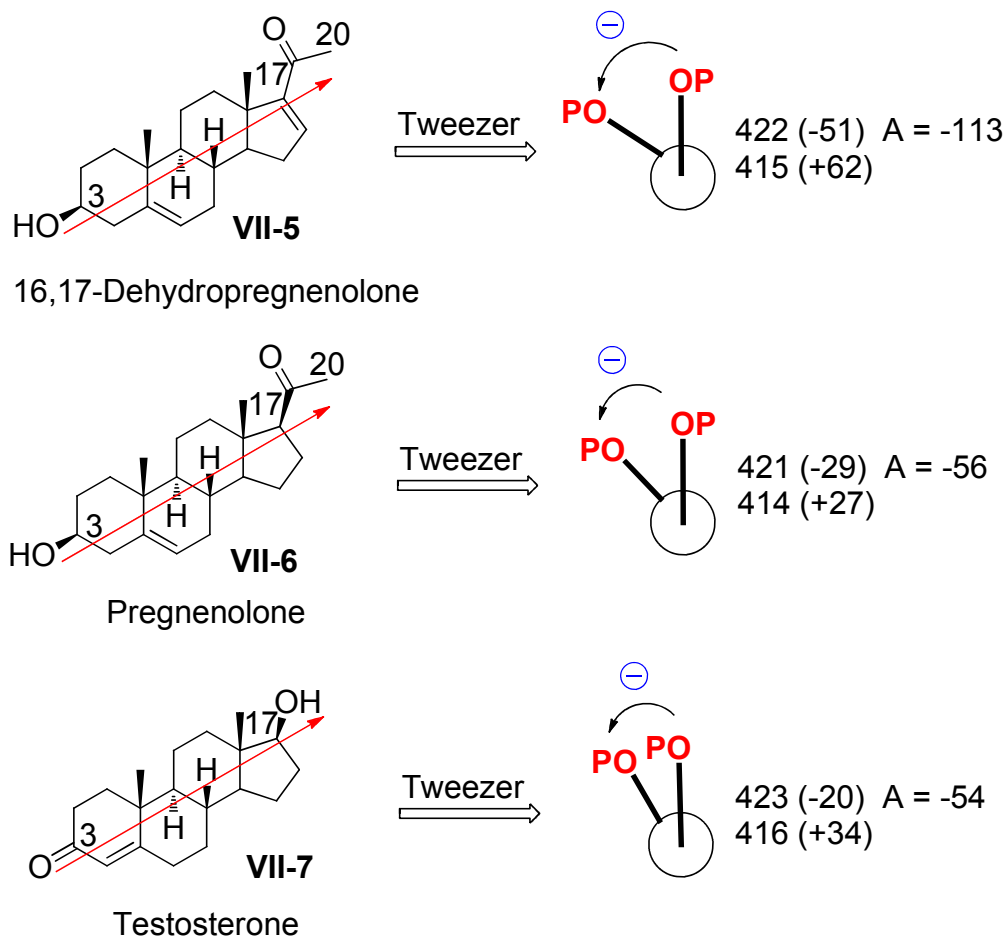


Figure VII-8. ECCD data for **VII-5~VII-7** (40 eq.) with tweezer **II-25** (2 μ M) in MCH at 0 $^{\circ}$ C. The red arrow across the molecule indicates the perspective for looking at the relative orientation of functional groups.

Steroid **VII-8** (11 α -hydroxy progesterone) also exhibited fairly strong positive ECCD signal upon mixing with tweezer. But the presence of three functionalities in **VII-8** implies three possible ditopic binding modes with tweezer. Binding between the two ketone moieties at C3 and C20 positions can be first ruled out since

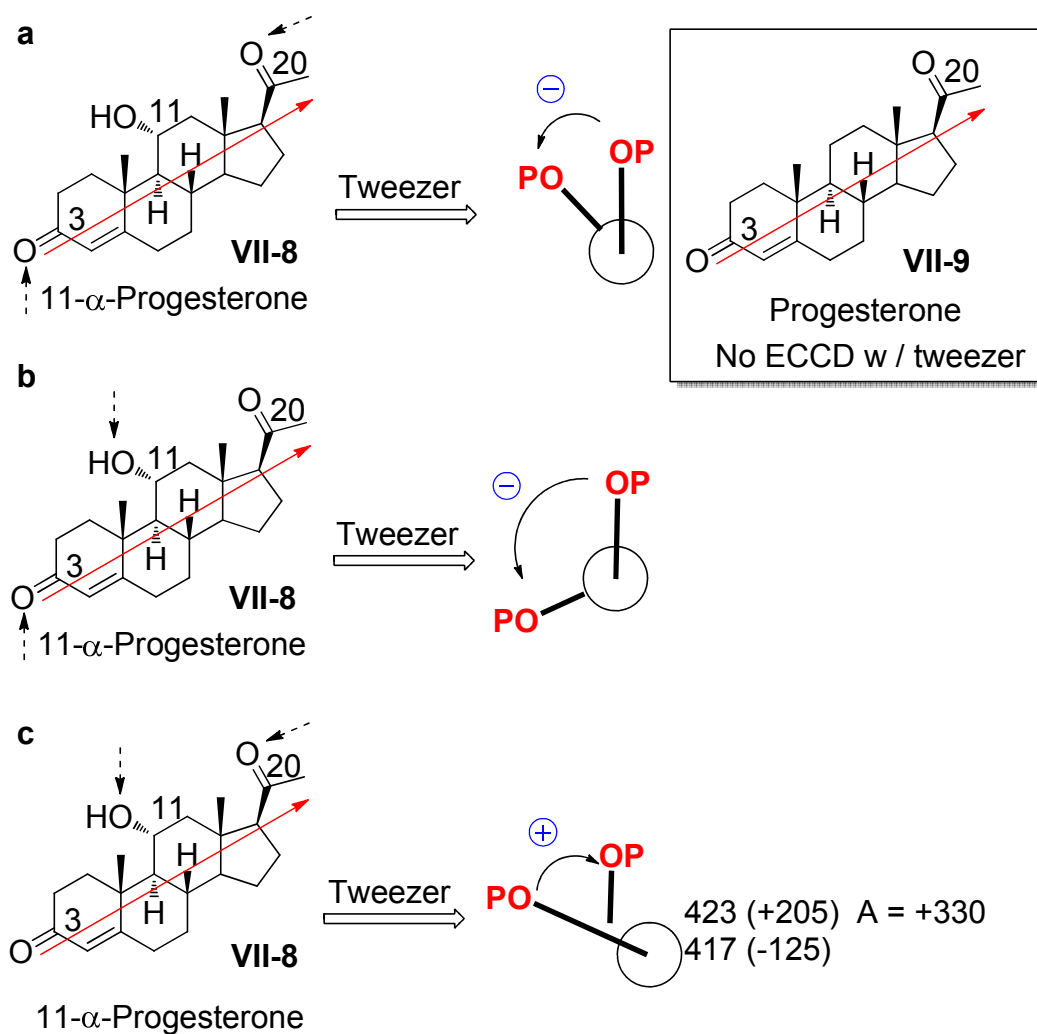
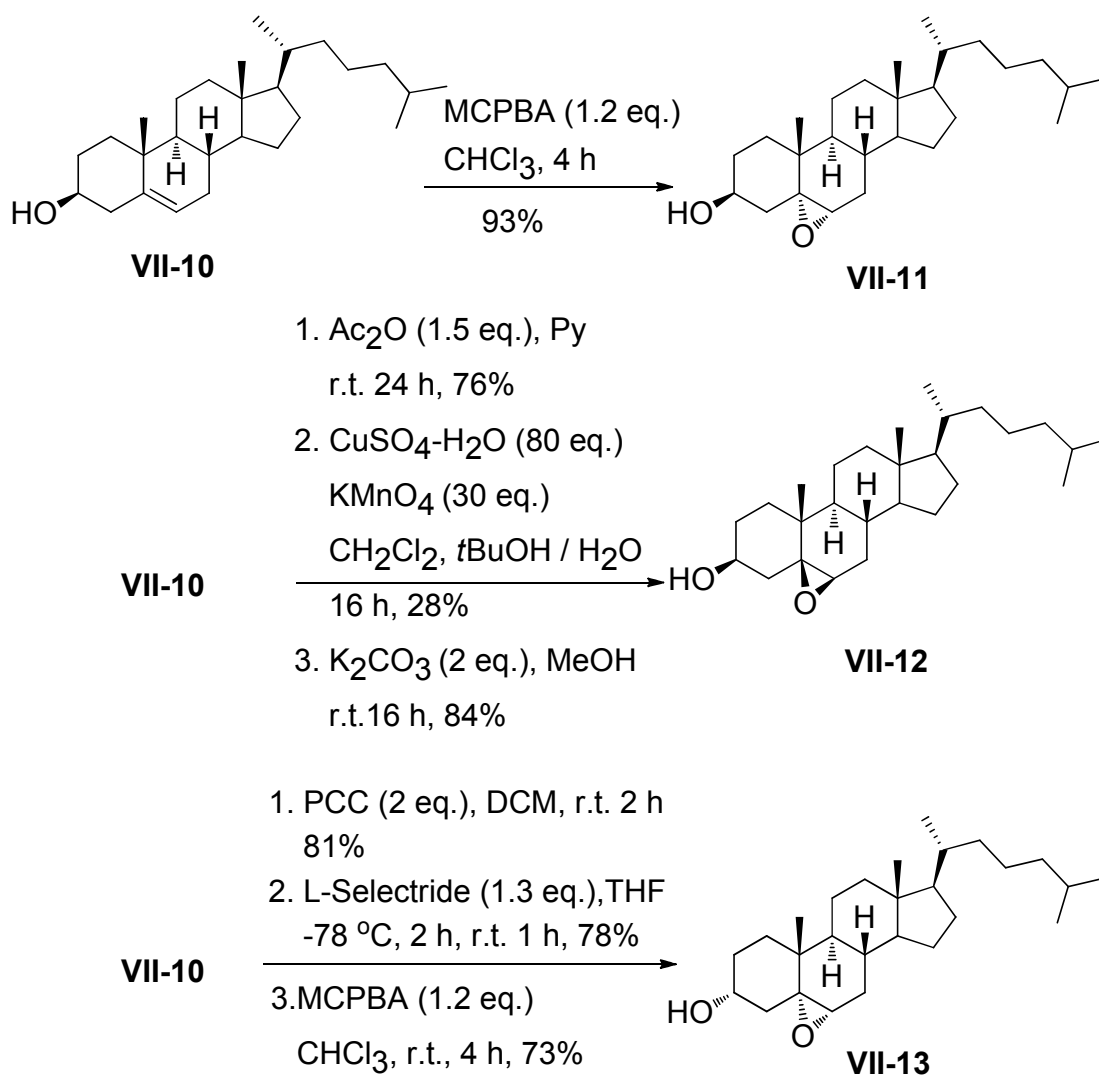


Figure VII-9. Three possible binding modes of **VII-8** with tweezer **II-25** (dashed arrows indicated the functionalities bound to porphyrins). Mode **c** is preferred and leads to positive ECCD signal in MCH at 0 °C. The red arrow across the molecule indicated the perspective for looking at the relative orientation of functional groups.

progesterone **VII-9** mixed with tweezer **II-25** is not ECCD active (Figure VII-9a). Another mode of ditopic binding between hydroxyl group at C11 position and ketone group at C3 position is shown in Figure VII-9b. This binding mode would give rise to a counter clockwise exciton chirality and negative ECCD curve. This is opposite to the observed ECCD spectrum and thus can be also excluded. The third binding

mode, which occurs between hydroxyl group at C11 position and ketone group at C20 position leads to the positive exciton chirality as illustrated in Figure VII-9c. The short distance between the two functionalities in VII-8 may account for the much higher CD amplitude compared to steroids VII-5~VII-7.



Scheme VII-1. Synthesis of steroids VII-11~VII-13 from cholesterol.

The success in determining the stereochemistry of acyclic epoxy alcohols (chapter 4) prompted us to further challenge the Zn-TPFP tweezer II-25 with steroids containing epoxy alcohol moiety. Again, conventional bischromophoric

derivatization method is unable to determine the stereochemistry of such compounds.

As shown in Scheme VII-1, three substrates were prepared from cholesterol **VII-10**.⁴,

5

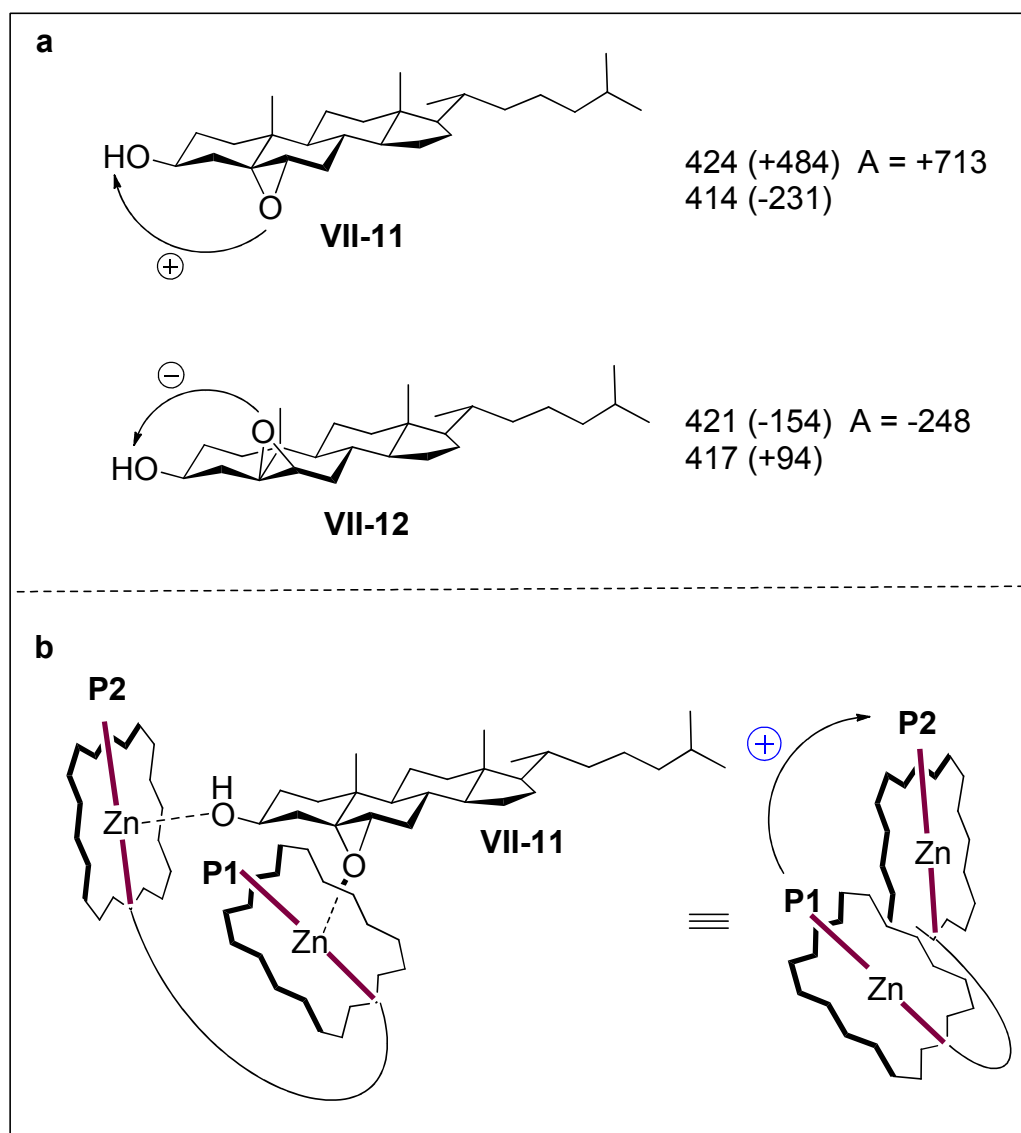


Figure VII-10. (a) ECCD data of **VII-11**, **VII-12** (40 eq.) with tweezer **II-25** (2 μ M) in MCH at 0 °C. (b) Exciton chirality induced by complexation of **VII-11** with tweezer.

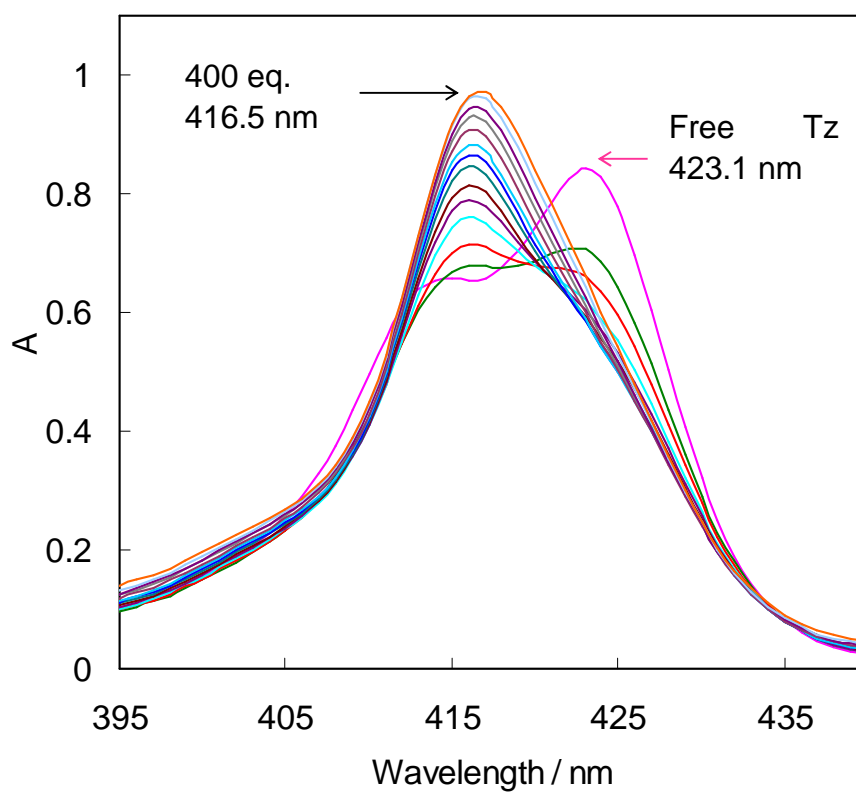
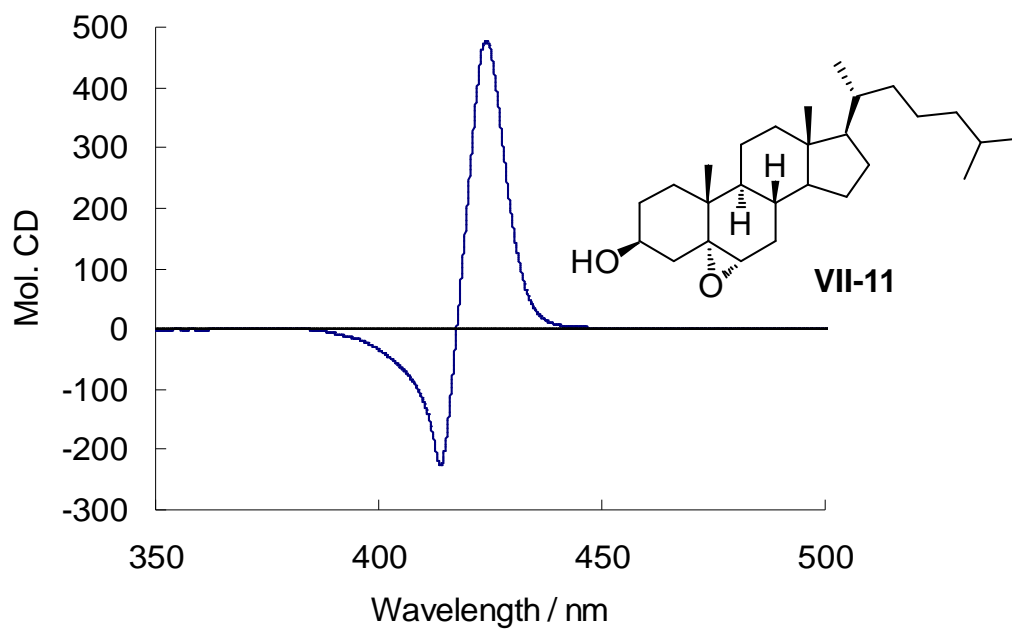


Figure VII-11. (a) ECCD spectra of **VII-11** (40 eq.) with tweezer **II-25** (2 μM) in MCH at 0 $^{\circ}\text{C}$; (b) UV-Vis spectra change upon titration of tweezer **VII-25** (1 μM in MCH) with **VII-11** (10 mM in DCM)

Compound **VII-11** rendered extremely strong positive ECCD signal upon binding with porphyrin tweezer in MCH (Figure VII-10a, Figure VII-11a). UV-vis titration of porphyrin tweezer with **VII-11** in MCH (Figure 11b) revealed a binding constant of $2.8 \times 10^5 \text{ M}^{-1}$. This binding constant is even higher than that of diols with tweezer **II-25**, accounting for the strong Cotton effect. Interpretation of the positive ECCD sign is depicted in Figure VII-10b. After complexation, the clockwise relative orientation between epoxide ring and hydroxyl group results in a positive

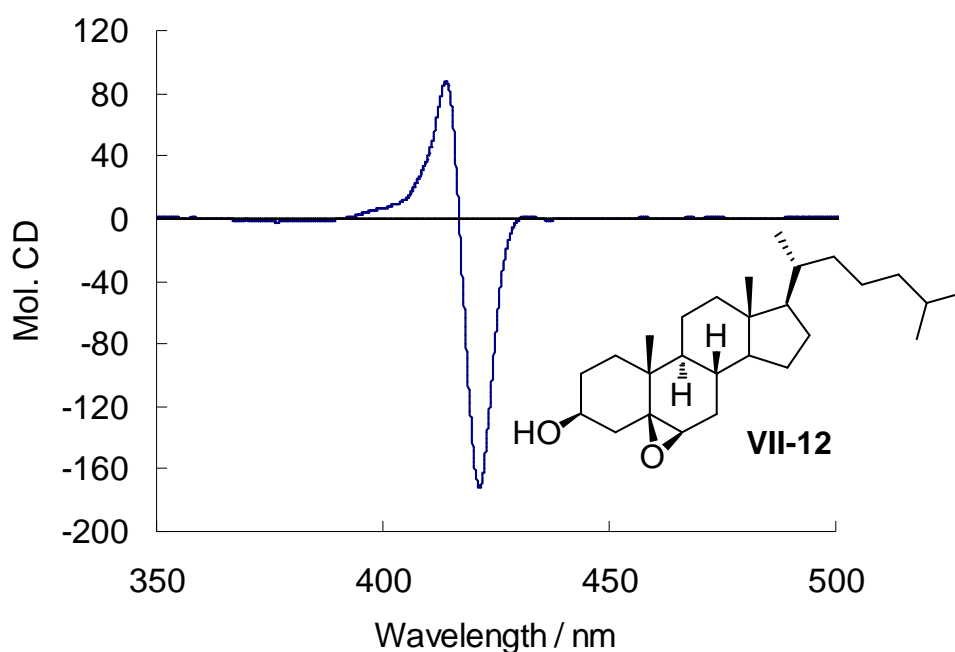


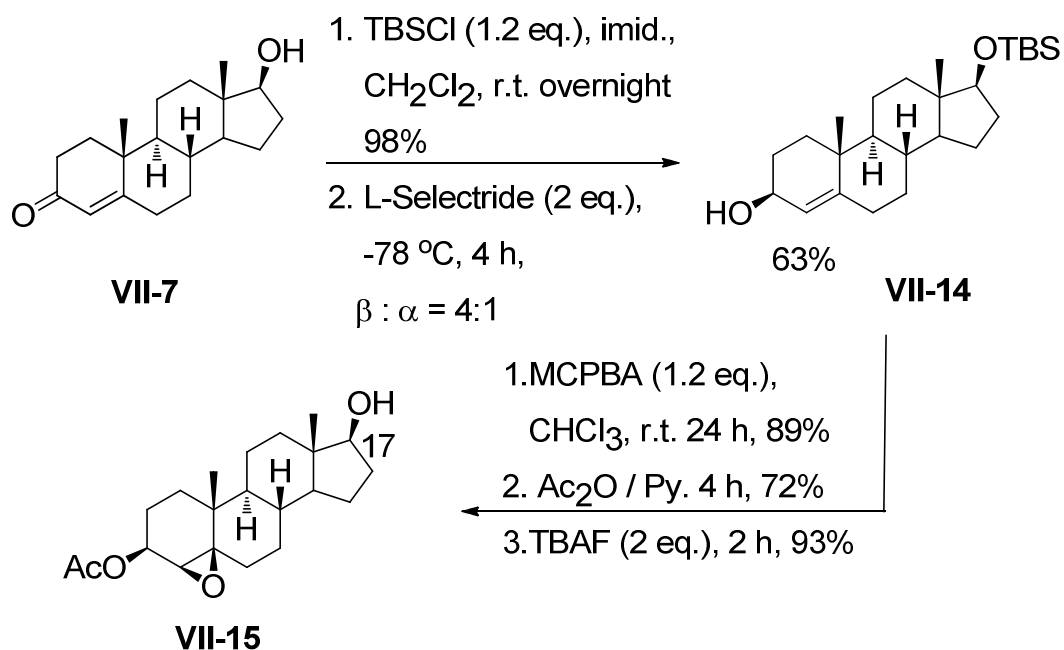
Figure VII-12. ECCD spectra of **VII-12** (40 eq.) with tweezer **II-25** (2 μM) in MCH at 0 °C.

helicity of bound porphyrin chromophores as indicated by the curved arrow. A positive ECCD couplet is then generated. The high rigidity of the epoxy alcohol

functionalities in the steroid minimizes the number of conformations available to the tweezer complex and contributes to the unusually high CD amplitude. Changing the orientation of the epoxide ring from $5\alpha,6\alpha$ in **VII-11** to $5\beta,6\beta$ in **VII-12** led to the switch of the ECCD sign (Figure VII-12) since the relative orientation of the epoxide ring and hydroxyl group changed from clockwise to counter clockwise (Figure VII-10a) signifying the switch of exciton chirality while bound with porphyrin tweezer.

To our surprise, substrate **VII-13** was not ECCD active under standard conditions. The NMR analysis of **VII-13** at dilute and concentrated concentrations indicated the presence of intramolecular hydrogen bonding between OH group and epoxidic oxygen since the OH proton at 2.97 ppm did not shift and remained a sharp doublet ($J = 8.7 \text{ Hz}$) after the sample concentration was increased 10 times. This hydrogen bonding probably competed with the metal ligand interaction between substrate and zinc porphyrin tweezer and suppressed the formation of an ECCD active complex. Similar NMR analysis of **VII-11** and **VII-12** did not reveal the existence of intramolecular hydrogen bonding.

Another steroidal epoxy alcohol **VII-15** was synthesized from testosterone **VII-7** (Scheme VII-2). ECCD experiment with tweezer **II-25** demonstrated intense positive Cotton effect. The positive sign of CD spectrum is attributed to the clockwise relative orientation between epoxide ring and hydroxyl group at C17 position (Figure VII-13).



Scheme VII-2. Synthesis of steroid **VII-15** from testosterone.

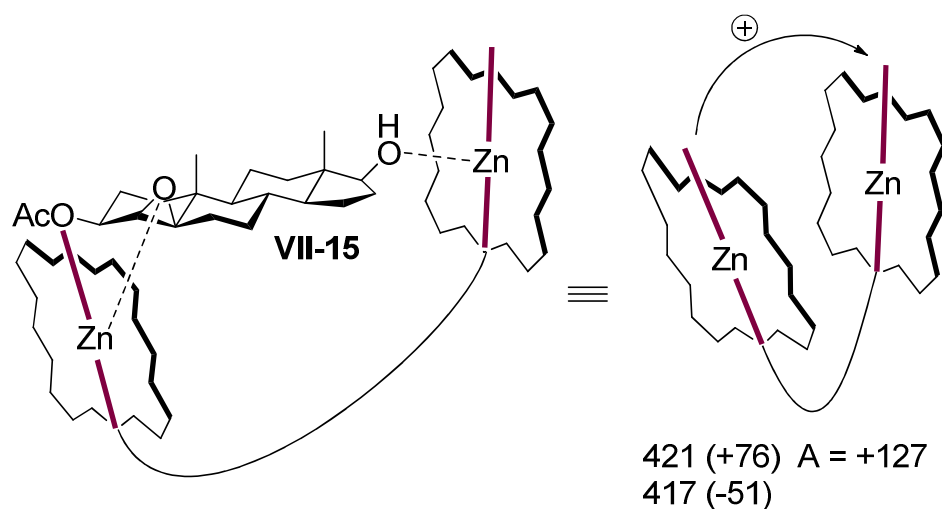
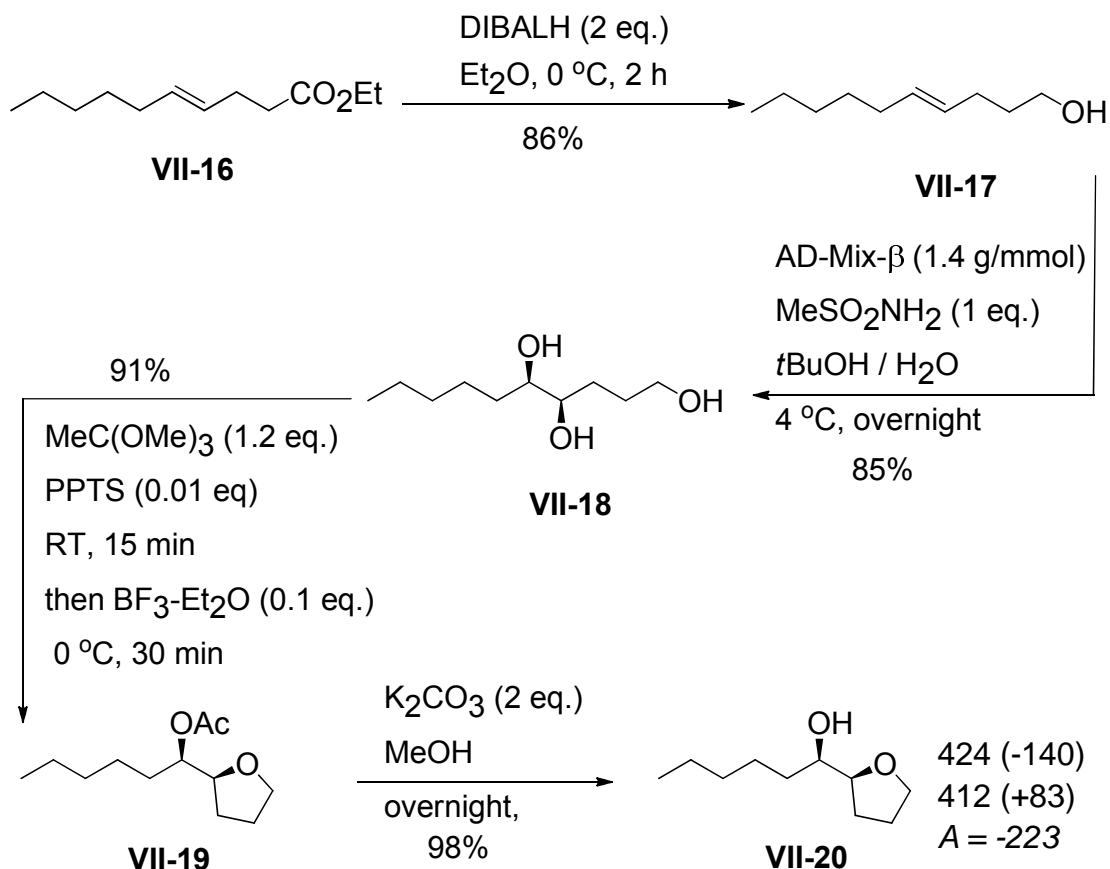


Figure VII-13. Exciton chirality induced by complexation of **VII-15** (40 eq.) with tweezer **II-25** (2 μM) in MCH at 0 $^\circ\text{C}$. Positive helicity was observed.

The significantly increased sterics going from small molecules to bulky steroid compounds did not comprise the binding interaction between porphyrin host and chiral guest. The highly Lewis acidic zinc porphyrin tweezer can bind the

oxygen-containing functionalities well and sense the change in stereochemistry for one of the bound functionalities. The presence of multiple chiral centers did not interfere with the chirality assignment. Though the correlation of substrate chirality and observed ECCD signal is based on speculations and deserves further investigation, these results are promising and demonstrate the efficiency of Zn-TPFP tweezer for stereochemical determination of complex molecules.

VII.3 ECCD Study of Hydroxyl Tetrahydrofurans



Scheme VII-3. Synthesis of **VII-20**.

Tetrahydrofuran (THF) rings are widely present in biologically active molecules

and tremendous progress have been made in past decades for rapid construction of THF rings. However, absolute configurational analysis of this class of compounds is difficult. Previously, we described the rapid determination of absolute configurations for chiral 2,3-epoxy alcohols with a variety of substitution patterns using the Zn-TPFP tweezer (**II-25**) via ECCD protocol. Considering the similar nucleophilicity of epoxidic oxygen and THF ring oxygen, we believe that the hydroxyl THF rings could bind Zn-TPFP tweezer well. If a consistent trend can be revealed from systematic ECCD study of hydroxyl THF rings with TPFP tweezer, we may provide an efficient way for stereochemical determination of this type of molecules.

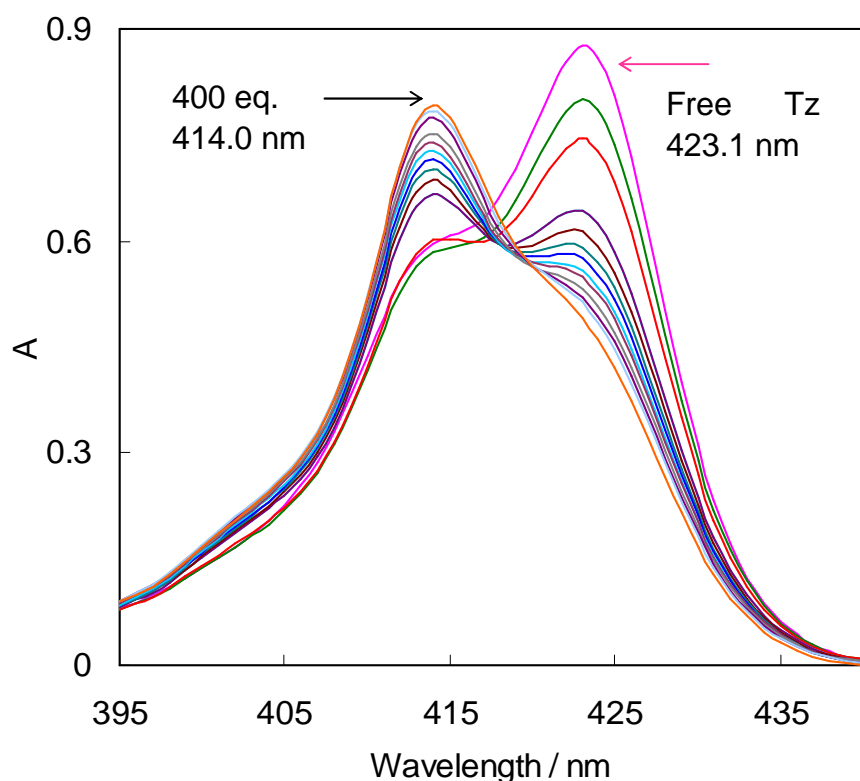
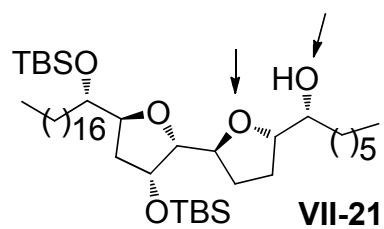


Figure VII-14. UV-Vis spectra change upon titration of tweezer **VII-25** (1 μ M in MCH) with **VII-20** (10 mM in DCM)

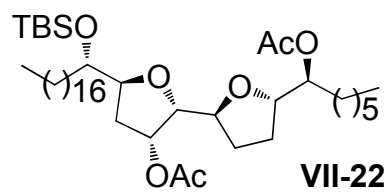
Compound **VII-20** was readily accessed using the triol cyclization method that was

developed in our lab (Scheme VII-3).⁶ As expected, this substrates exhibited intense ECCD while complexing with Zn-TPFP tweezer **II-25** in MCH (Figure VII-14). This observation encouraged us to further examine a number of substrates containing bisTHF rings, synthesized by Dr. Jun Yan in our lab. Interestingly, all the compounds are ECCD active, the data are summarized in Figure VII-15. Compounds **VII-23** and **VII-24** are enantiomers and exhibited enantiomeric CD signals suggesting the capability of the porphyrin tweezer for absolute configurational analysis of this class of substrates. Though a conclusive binding mechanism for the complicated bisTHF ring system is yet to be investigated, we tentatively propose that the binding interaction occurs between the zinc tweezer and the oxygen-containing functionalities which are indicated by arrows.

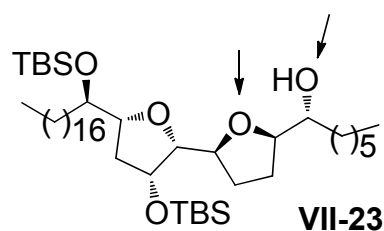
Apparently, to gain further insights about the binding mechanism more stereo isomers should be examined. The preliminary data offers important clues and implies that the stereochemical determination for functionalities in complex molecules using Zn-TPFP tweezer **II-25** is feasible. Though only oxygen-containing functionalities were demonstrated in this chapter, the nitrogen-containing analogs should also be suitable for ECCD study using the porphyrin tweezer and stronger signals are expected due to the much higher binding affinity of nitrogen toward zinc porphyrins.



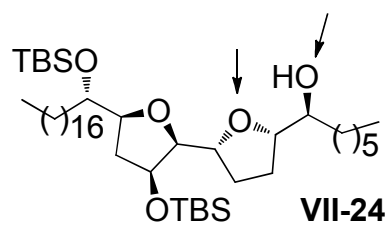
421 (+78) $A = +137$
415 (-59)



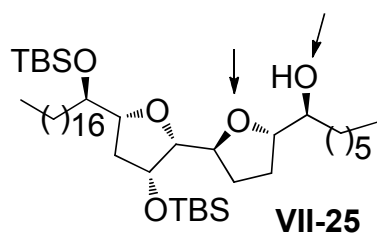
421 (-19) $A = -45$
414 (+26)



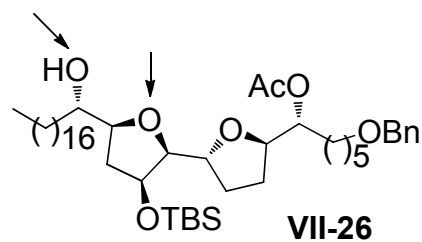
423 (-14) $A = -36$
416 (+22)



422 (+22) $A = +33$
417 (-11)



420 (+80) $A = +130$
415 (-50)



424 (-182) $A = -274$
415(+92)

Figure VII-15. ECCD data of **VII-21~VII-26** (40 eq.) with tweezer **II-25** (2 μ M) in MCH at 0 °C.

Experimental Procedures

Materials and general instrumentations:

Anhydrous CH_2Cl_2 was dried and redistilled over CaH_2 . The solvents used for CD measurements were purchased from Aldrich and were spectra grade. All reactions were performed in dried glassware under nitrogen. Column chromatography was performed using SiliCycle silica gel (230-400 mesh). ^1H NMR and ^{13}C NMR spectra were obtained on a Varian Inova 300 MHz or 500Hz instrument and are reported in parts per million (ppm) relative to the solvent resonances (δ), with coupling constants (J) in Hertz (Hz). IR studies were performed on a Nicolet FT-IR 42 instrument. UV/Vis spectra were recorded on a Perkin-Elmer Lambda 40 spectrophotometer, and are reported as λ_{max} [nm]. CD spectra were recorded on a JASCO J-810 spectropolarimeter, equipped with a temperature controller (Neslab 111) for low temperature studies, and were reported as $\lambda[\text{nm}]$ ($\Delta\epsilon_{\text{max}}$ [$\text{L mol}^{-1} \text{cm}^{-1}$]). Optical rotations were recorded at 20 °C on a Perkin Elemer 341 Polarimeter ($\lambda = 589$ nm, 1 dm cell). Chiral GC analyses were performed on a Hewlett Packard 6890 gas chromatograph equipped with a Supelco Gamma Dex 225 column (0.25 mm \times 30 m) using helium as carrier gas. HRMS analyses were performed on a Q-TOF Ultima system using electrospray ionization in positive mode.

General procedure for CD measurement:

Zinc porphyrin tweezer **II-25** (2 μL of a 1 mM solution in anhydrous CH_2Cl_2) was added to hexane (1 mL) in a 1.0 cm cell to obtain a 2 μM tweezer **II-25** solution.

The background spectrum was recorded from 350 nm to 550 nm with a scan rate of 100 nm/min at 0 °C. Chiral diol (1 to 20 μ L of a 10 mM solution in anhydrous CH_2Cl_2) was added into the prepared tweezer solution to afford the host/guest complex. The CD spectra were measured immediately (minimum of 4 accumulations). The resultant ECCD spectra recorded in millidegrees were normalized based on the tweezer concentration to obtain the molecular CD (Mol CD).

Determination of binding constant

The solution of Zn-porphyrin tweezer (1 mM in hexane) was titrated with guest molecule (10 mM in DCM) at different equivalents and the UV-vis spectra were recorded. The addition of the chiral substrate continued until no visible change in the spectra was observed. Upon formation of the chiral complex the Soret band of the porphyrin tweezers underwent red-shifts through an isosbestic point. The change of absorption at certain wavelength as a function of the substrate concentration yields an exponential saturation curve which can be fitted through the non-linear least square equation previously reported by Shoji⁷ to derive the binding constant.

Compound **VII-4** was kindly provided by Professor William Reusch.

To a solution of cholesterol (1.0 g, 2.59 mmol) in CHCl_3 (100 mL), was added MCPBA (483 mg, 2.8 mmol). The mixture was stirred at room temperature for 4 h

under N₂ and quenched by addition of saturated Na₂SO₃ (30 mL). The aqueous layer was separated and extracted with CHCl₃ (3 × 30 mL). Combined organic extracts were washed with saturated NaHCO₃ and H₂O, dried over Na₂SO₄, and concentrated under reduced pressure. Recrystallization from acetone afforded **VII-11** as white solid (968 mg, 93%). ¹H NMR (CDCl₃, 300 MHz) δ 0.58 (s, 3H), 0.82-1.94 (m, 45H), 2.05 (t, 1H, *J* = 12.0 Hz), 2.88 (d, 1H, *J* = 4.5Hz), 3.88 (m, 1H). ¹³C NMR (CDCl₃, 75 MHz) δ 11.8, 15.9, 18.6, 20.6, 22.5, 22.8, 23.8, 24.0, 27.96, 28.04, 28.8, 29.9, 31.0, 32.4, 34.8, 35.7, 36.1, 39.4, 39.5, 39.8, 42.3, 42.5, 55.8, 56.8, 59.3, 65.7, 68.7.⁴

REFERENCES

References

1. Matile, S.; Berova, N.; Nakanishi, K.; Novkova, S.; Philipova, I.; Blagoev, B., Porphyrins - Powerful Chromophores for Structural Studies by Exciton-Coupled Circular-Dichroism. *Journal of the American Chemical Society* **1995**, 117, (26), 7021-7022.
2. Matile, S.; Berova, N.; Nakanishi, K.; Fleischhauer, J.; Woody, R. W., Structural studies by exciton coupled circular dichroism over a large distance: Porphyrin derivatives of steroids, dimeric steroids, and brevetoxin B. *Journal of the American Chemical Society* **1996**, 118, (22), 5198-5206.
3. Pescitelli, G.; Gabriel, S.; Wang, Y. K.; Fleischhauer, J.; Woody, R. W.; Berova, N., Theoretical analysis of the porphyrin-porphyrin exciton interaction in circular dichroism spectra of dimeric tetraarylporphyrins. *Journal of the American Chemical Society* **2003**, 125, (25), 7613-7628.
4. Ma, E.; Kim, H.; Kim, E., Epoxidation and reduction of cholesterol, 1,4,6-cholestatrien-3-one and 4,6-cholestadien-3 beta-ol. *Steroids* **2005**, 70, (4), 245-250.
5. McCarthy, F. O.; Chopra, J.; Ford, A.; Hogan, S. A.; Kerry, J. P.; O'Brien, N. M.; Ryan, E.; Maguire, A. R., Synthesis, isolation and characterisation of beta-sitosterol and beta-sitosterol oxide derivatives. *Organic & Biomolecular Chemistry* **2005**, 3, (16), 3059-3065.
6. Zheng, T.; Narayan, R. S.; Schomaker, J. M.; Borhan, B., One-pot regio- and stereoselective cyclization of 1,2,n-triols. *Journal of the American Chemical Society* **2005**, 127, (19), 6946-6947.
7. Shoji, Y.; Tashiro, K.; Aida, T., Sensing of chiral fullerenes by a cyclic host with an asymmetrically distorted pi-electronic component. *Journal of the American Chemical Society* **2006**, 128, (33), 10690-10691.